P2X$_4$ receptor in human macrophages: role in ATP-evoked calcium responses and cytokine production

Janice Anastasia Layhadi

A Thesis Presented for the Degree of Doctor of Philosophy to the University of East Anglia

Faculty of Science, School of Biological Science

UEA

University of East Anglia

Declaration

I certify that the work contained in the thesis submitted by me for the degree of Doctor of Philosophy is my original work except where due reference is made to other authors, and has not been previously submitted by me for a degree at this or any other university.

In line with the regulations for the degree of Doctor of Philosophy, I have submitted a thesis that has a word count of approximately 65,000 words, including footnotes and bibliography, but excluding appendices of approximately 600 words.

Abstract

$P2X_4$ is a ligand-gated cation channel that is widely expressed amongst immune cells, especially in monocytes and macrophages. Despite its expression profile, the functional role of $P2X_4$ in human macrophages has not been elucidated. This study aimed to (i) investigate the contribution of $P2X_4$ towards ATP-evoked Ca^{2+} responses and (ii) determine the role of $P2X_4$ towards cytokine production in human macrophages. Here, human THP-1-differentiated macrophages (TDM) and primary monocyte-derived macrophages (MDMs) were utilized as human macrophage models to investigate the contribution of $P2X_4$ by means of Ca^{2+} measurements, mRNA expression analysis and cytokine secretion assays. A side-by-side comparison study of MDM generated through stimulation with either GM-CSF (GM-MDM) or M-CSF (M-MDM) illustrated that $P2X_4$ has a bigger contribution towards ATP-evoked Ca^{2+} responses in GM-MDM cells. In GM-MDM cells, $P2Y_{11}$ and $P2Y_{13}$ activation both contributed towards the amplitude and sustained phase of response, while $P2X_4$, but not $P2X_1$ or $P2X_7$, activation contributed towards the sustained phase of ATP-evoked Ca^{2+} response. Employment of a cytokine and chemokine mRNA profiler array in GM-MDM revealed that 100 μM ATP induced transforming growth factor-β2 (TGF-β2) and C-X-C motif chemokine 5 (CXCL5). Selective antagonism of $P2X_4$ with PSB-12062 positively modulated ATP-mediated induction of TGF-β2 gene expression while it inhibited ATP-mediated induction of CXCL5 gene expression. Although the effect on TGF-β2 was not translated at a protein level, PSB-12062 inhibited ATP-mediated induction of CXCL5 protein synthesis and secretion. Reciprocally, positive allosteric modulation of $P2X_4$ with ivermectin augmented ATP-mediated CXCL5 secretion. Inhibition of $P2X_7$, $P2Y_{11}$ or $P2Y_{13}$ had no effect on CXCL5 secretion. Altogether, we have identified a role for $P2X_4$ activation in determining the duration of ATP-evoked intracellular Ca^{2+} response and stimulating induction and secretion of CXCL5 in human primary macrophage.

Table of Contents

List of Figures

CHAPTER 5

CHAPTER 6

APPENDICES

List of Tables

Abbreviations

Listed below are the meanings of some commonly used abbreviations throughout this thesis:

AC	Adenylate cyclase
ADP	Adenosine diphosphate
AMP	Adenosine monophosphate
ATP	Adenosine triphosphate
bp	Base pairs
BzATP	3'-O-(4-Benzoyl)benzoyl ATP
Ca^{2+}	Calcium ions
CD14	Cluster differentiation 14
CD39	Cluster differentiation 39
CXCL5	C-X-C chemokine 5
DAG	Diacyl glycerol
EC_{50}	Concentration of an agonist giving half-maximal response
GM-MDM	GM-CSF differentiation monocyte-derived macrophages
HKG	Housekeeping Genes
IC_{50}	Concentration of an inhibitor/antagonist where response is reduced by half
IL-1β	Interleukin-1β
IL-12	Interleukin-12
IP3	Inositol triphosphate
KD	Knockdown
LDH	Lactate dehydrogenase
α,β-MeATP	α,β-methylene adenosine triphosphate
mRNA	Messenger ribonucleic acid
M-MDM	M-CSF differentiated monocyte-derived macrophages
OSM	Oncostatin M
PBMC	Peripheral blood mononuclear cells
PMA	Phorbol 12-myristate 13-acetate
PLC	Phospholipase C
qRT-PCR	Quantitative real-time polymerase chain reaction
RT	Reverse transcription
RT-PCR	Reverse transcription polymerase chain reaction

SBS	Salt buffered saline
Tg	Thapsigargin
TGF-β	Transforming growth factor β
TGF-β2	Transforming growth factor β2

Acknowledgements

I would like to thank my family, especially my sister and my mum, for their endless support through the difficult times during my PhD and for always believing in me. I would like to also thank my one and only soul mate, Lawrence, for always being there – night and day – listening to my complaints and for always having faith and trust in me. You practically live in the lab with me with the amount of times you've had to drop me to and pick me up from work, even on weekends. Thanks for keeping up with me and never ever complaining.

I would like to thank my supervisors, Dr Jeremy Turner and Professor David Crossman, for their endless guidance and support. Most importantly, I would like to thank my primary supervisor Dr Samuel Fountain for his continuous guidance, support and patience. More than anyone else, Sam, you pushed me, sometimes even with a little insensitivity to my workload, but that made me realize my true capabilities and I thank you for that. I would also like to thank the entire Fountain Lab, Seema Ali, David Richards and Izzuddin Ahmad. We've had some very memorable times together and I will miss you all. Seema, I can't imagine how much harder my PhD would have been without you there – our late nights together, gossiping and moaning times, and our endless brown bread session and coffee/tea breaks to de-stress. One of the hardest parts of leaving the lab would undoubtedly be losing out on these activities with you (and watching the awesome videos!).

This PhD has been a thoroughly great experience with many ups and downs. Though I won't do it again, I am glad to have met so many amazing people and to have made some of the most precious friendships in my life.

Chapter 1: Introduction

1.1   Innate immune system

The immune system is a complex network involving various cellular and molecular components with specialized roles in defending the host against foreign materials. It can be categorized into two fundamentally different responses: the innate 'natural' response and the acquired 'adaptive' response. The innate response provide immediate host defense through involvement of various cells in combination with its molecular components such as complement, cytokines and acute phase proteins (Delves and Roitt, 2000). Cells involved in the innate response include natural killer cells, phagocytic cells such as neutrophils, monocytes and macrophages and cells that release inflammatory mediators such as basophils, eosinophils and mast cells. Though rapid in its actions, innate response can damage normal tissues due to the lack of specificity. On the other hand, acquired responses often take several days to weeks to develop and involve a series of key reactions such as antigen-specific responses achieved through activity of T- and B-lymphocytes in driving effector responses (Parkin and Cohen, 2001).

The innate immune response is initiated upon the recognition of danger signals by pattern recognition receptors (PRRs) found either on the cell surface or internally in host immune cells (Mogensen, 2009). These danger signals include pathogen-associated molecular patterns (PAMPs) such as foreign microbial challenge, or damage-associated molecular patterns (DAMPs) resulting from cellular damage or death (Mogensen, 2009, Janeway et al., 2001). The recognition of PAMPs and DAMPs by PRRs initiate a cascade of responses within the host that leads to the activation of intracellular signaling pathways such as kinases, transcription factors and adaptor molecules. These ultimately activate gene expression and synthesis of a broad range of molecules such as cytokines, chemokines, cell adhesion molecules and immunoreceptors, all of which are important in initiating early host response against infection and provide an important link towards adaptive immune response (Janeway et al., 2001, Mogensen, 2009). The first part of this chapter will focus on one type of cell crucial for the immune system, macrophages – their origin, different phenotypes resulting from polarization as well as their functions. This will be followed by an introduction on calcium signaling and the purinergic receptors, specifically how they relate to macrophages. Finally, the aims of the project will be discussed.

1.2   Macrophages

1.2.1 Development and Differentiation Theories

Since first introduced by Metchnikoff in 1892 as large phagocytic cells 'macrophages', the origin and differentiation of macrophages have been studied and debated significantly. Various theories have been proposed regarding their origin however, two theories raised major attention: the reticuloendothelial system (RES) proposed by Aschoff (1924) and one described much later, the mononuclear phagocyte system developed by van Furth et al. (1972).

1.2.1.1 Reticuloendothelial system (RES) theory

The RES theory detailed that macrophages belong to a system of reticulum cells, categorized as a single cell system of local tissue origin and properties (Aschoff, 1924). Studies using lithium carmine allowed the categorization of reticulum cells into reticuloendothelial (phagocytic endothelia) and histocytes (tissue macrophages). This concept was widely accepted initially until the end of 1960s, following several contradicting issues. First, Aschoff had no confirmation from his own research to back up the statement that all reticulum cells were related in terms of origin. Following 20 years of research by a different group, it was identified that histocytes and reticulum cells differed significantly in terms of cell morphology, function and origin (Akazaki, 1962, Takahashi et al., 1996). The second issue was that the proposal of the RES theory relied heavily on the use of lithium carmine which Aschoff believed to be taken up by reticulum cells through phagocytosis. However, studies by Lewis et al., (1931) illustrated that all living cells can take up materials by pinocytosis and de Duve (1969) demonstrated the ability of lithium carmine to accumulate in large lysosomal granules of reticulum cells which appeared to be mistaken for any evidence of phagocytosis observed in macrophages. These evidences, together with advances in technology post 1960s, allowed further confirmation that macrophages were in fact distinct from reticulum cells and endothelial cells.

1.2.1.2 Mononuclear phagocyte system (MPS) theory

The second and more accepted theory of macrophage origin and differentiation was described by van Furth in 1972. The MPS theory defined that all macrophages, including those appearing in inflammatory foci and those residing in tissues under normal quiescent conditions, are derived from monocytes. These monocytes are

differentiated from promonocytes and monoblasts originating in the bone marrow (Figure 1.1) (Takahashi et al., 1996). In addition to this, van Furth also described that all macrophages have no proliferative capacity and to be short-lived terminal cells of the MPS. Since the establishment of MPS theory however, various conflicting data have been raised. First, phylogenetic observations of macrophages illustrated that they emerge before the development of monocytic cells contradicting the idea that all macrophages are derived from monocytes (Dzierzak and Medvinsky, 1995, Takahashi et al., 1996). Secondly, studies by several groups challenged the idea that all macrophages are short-lived and non-dividing. In a study of parabiosis by Parwaresch and Wacker (1984), they found that half of peritoneal macrophages can survive by cell division while a study by Volkman (1976) identified that tissue macrophages such as peritoneal and pulmonary alveolar can survive a long time by self-renewal, without a supply of circulating monocytes. These findings illustrated that while monocyte-derived macrophages can last in peripheral tissues for approximately two weeks, tissue macrophages (i.e. Kupffer cells) can last up to five weeks. Therefore, although MPS theory has helped to define the differentiation of monocytic cells into macrophages in the context of inflammatory lesions, it is still unclear if under quiescent state, all tissue macrophages are derived from monocytes alone. Despite these contradictions, MPS remain to be the leading theory describing the origin of macrophages.
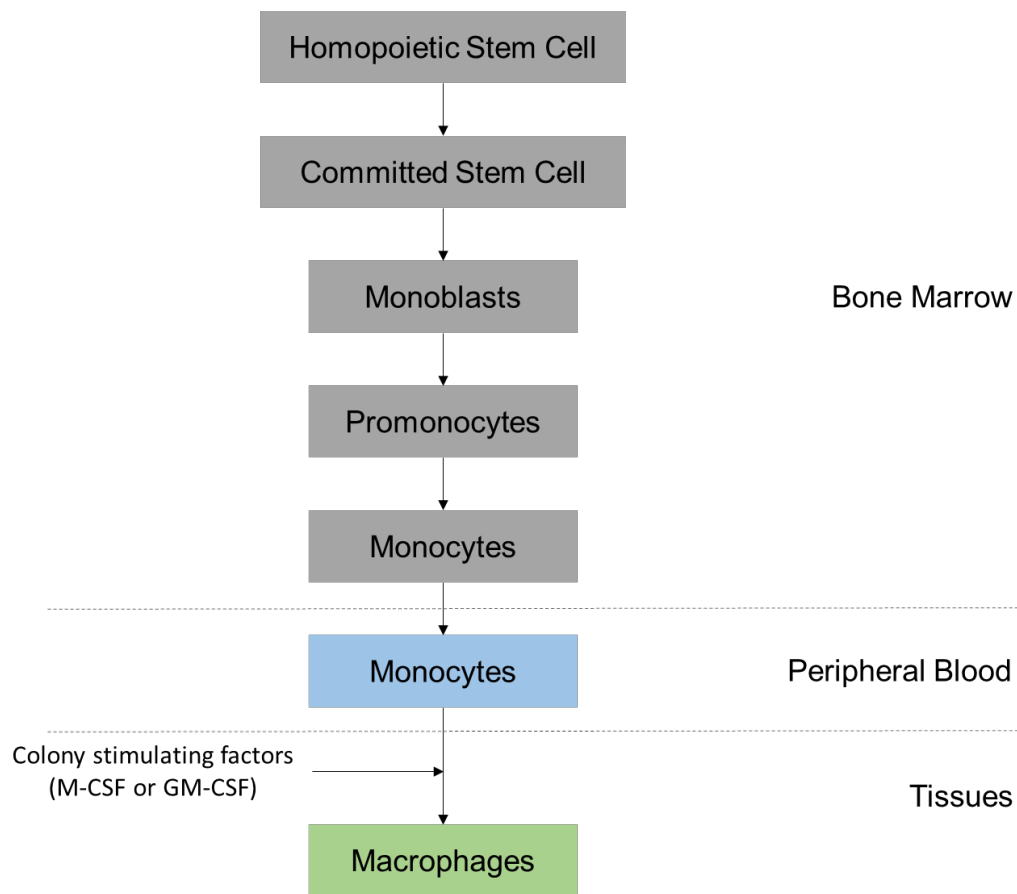
Figure 1.1. **The mononuclear phagocyte system (MPS).** Illustration describing suggested origin of macrophages from monocytes as described by van Furth (1972). This model describes that monocytes are differentiated from promonocytes and monoblasts that originate within the bone marrow. These monocytes can then differentiate into macrophages with the help of colony stimulating factors such as macrophage colony-stimulating factor (M-CSF) or granulocyte macrophage-colony stimulating factor (GM-CSF). Adapted from van Furth (1980).

1.2.2 Macrophage subpopulations and development

Two major macrophage populations have been described in literature, participating at different stages of inflammation: tissue-resident macrophages and monocyte-derived macrophages (Daems et al., 1976, Davies and Taylor, 2015, Lahmar et al., 2016). Although the majority of our knowledge on the development of macrophages comes from research in mouse models, the human embryonic hematopoietic system is thought to be organized in a similar manner to mice (Tavian and Peault, 2005). Initially, tissue-resident macrophages are thought to solely be derived from circulating monocytes, which are supplied by bone marrow hematopoietic stem cells (HSC) (Geissmann et al., 2010). However, further studies illustrated that in humans, macrophages could arise in the embryo through a process independent of the bone marrow progenitors. The current knowledge describes that macrophages in fetal and adult tissues are derived from three possible sources which includes the yolk sac, the fetal liver and the bone marrow. The bone marrow is thought to give rise to tissue resident bone marrow derived macrophages and inflammatory bone marrow monocyte-derived macrophages.

1.2.2.1   Tissue-resident macrophage

Tissue-resident macrophages are heterogeneous cells, which represents up to 10-15% of total cell number in steady-state conditions (Italiani and Boraschi, 2014). They are found in every tissue of an adult mammal and display unique location-specific phenotypes and gene expression profiles. Macrophages have been described to play critical roles in innate immune system as well as development and homeostasis of the tissue in which they reside (Haldar and Murphy, 2014). Specialization of macrophages in different microenvironments means that they are defined with different names according to their location within tissue (Table 1.1). Examples of this include: microglia (CNS), osteoclasts (bone), alveolar (lung), histocytes (connective tissue), Kupffer cells (liver) and Langerhans cells (skin) (Italiani and Boraschi, 2014). Although displaying highly different transcriptional profiles, macrophages of different tissue origin possess similar basic functions such as phagocytosis, antigen presentation and wound-healing, all of which will be described in greater detail in section 1.2.3 (Gautier et al., 2012). It is thought that unlike monocyte-derived macrophages, tissue-resident macrophages in most tissues do not require an ongoing supply from circulating monocytes and instead, they can be maintained through a self-renewal process. In steady-state conditions, tissue-resident macrophages can proliferate at low levels; however, in situations where macrophages are depleted or during an inflammatory challenge, this

proliferation rate greatly increase (Hashimoto et al., 2013, Sieweke and Allen, 2013). Despite much effort to increase understanding on tissue-resident macrophage development, it is still poorly understood and awaits further work.

1.2.2.2　　　Monocyte-derived macrophages

In response to an inflammatory reaction, an increase in effector cell number is observed within the tissue. These effector cells are also known as monocyte-derived macrophages (Italiani and Boraschi, 2014). The increase in monocyte-derived macrophages at inflammatory sites is usually a result of the drastic loss of resident macrophages due to tissue adherence, emigration and death (Barth et al., 1995, Italiani and Boraschi, 2014). Hence, two strategies are recruited as a mechanism to cope with the reduced number of effector cells within tissues. The first includes blood monocytes recruitment into tissue, which is driven by resident macrophages in combination with other cells within the tissue. These recruited monocytes are a source of inflammatory macrophages or also known as monocyte derived macrophages. The second mechanism is to increase the number of tissue resident macrophages proliferation, which is achieved through the enhancement of their self-renewal properties (Italiani and Boraschi, 2014).

Macrophages (Tissue)	Function
Microglia (Brain)	Brain development, immune surveillance and synaptic modelling
Osteoclasts (Bone)	Bone remodelling and resorption
Heart macrophages (Heart and Vasculature)	Surveillance
Kupffer cells (Liver)	Removal of toxins, iron recycling and erythrocyte clearance, lipid metabolism, clearance of cell debris from blood
Alveolar macrophages (Lung)	Surfactant clearance, Surveillance
Adipose tissue macrophages (Adipose tissue)	Metabolism and Adipogenesis
Bone marrow macrophages (Bone Marrow)	Reservoir of monocytes
Intestinal macrophages (Gut)	Tolerance to microbiota, maintaining homeostasis and defense against pathogens
Langerhans cells (Skin)	Immune surveillance
Red Pulp macrophages (Spleen)	Capture of microbes from blood and erythrocyte clearance
Inflammatory macrophages / M1 phenotype (All tissues)	Defence against pathogens and protection against dangerous stimuli
Healing macrophages / M2 phenotype (All tissues)	Angiogenesis

Table 1.1 Types of tissue-resident macrophages depending on their localization and their specialized function. Different names are allocated for the different macrophages depending on tissue locations. Despite having specialized functions within the tissues, these macrophages in general possess similarities in their function which will be described in greater detail in section 1.2.1.3. Adapted from Italiani and Boraschi (2014).

1.2.3 Macrophage Function

Macrophages are a heterogeneous population of cells widely and ubiquitously distributed throughout various tissues and organs of vertebrates. They possess different cell morphology and variable functions depending on which tissue they reside in, as described in Table 1.1. In addition to specific roles of tissue-resident macrophages, they share a series of common functions that include phagocytosis, immune surveillance, antigen presentation, cytokine secretion and wound healing (Arango Duque and Descoteaux, 2014). Each of these functions will be discussed further below.

1.2.3.1   Phagocytosis

Macrophages are specialized cells involved in phagocytosis within the immune system – a process that involves the internalization of large particles such as pathogens, apoptotic cells and debris into phagosomes. Phagocytosis is considered the first step in triggering host defense and inflammation and is required for the removal of enormous numbers of apoptotic cells (Aderem, 2003). The removal of particles through phagocytosis is thought to involve four basic steps: 1) pathogen is recognized by receptors present on the surface of macrophages, 2) signaling pathway is activated resulting in polymerization of actin, 3) actin-rich membrane is extended to reach out to particles and pull them towards the center of the cell, and finally 4) phagosomes mature into phagolysosome (Aderem, 2003). Phagolysosome is an acidic and hydrolytic compartment that can kill and digests pathogens in preparation for antigen presentation.

1.2.3.2   Immune Surveillance and Initiation of Inflammation

Macrophages are key immune cells involved in maintaining homeostasis and performing immune surveillance. In quiescent state, macrophages secrete very low levels of pro-inflammatory mediators, which is insufficient to initiate inflammation. However, upon exposure to pro-inflammatory mediators (i.e. cytokines, interferons), microbial products and DAMPs, macrophages acquire a pro-inflammatory phenotype resulting in the secretion of a vast array of mediators and cytokines (Arango Duque and Descoteaux, 2014). These cytokines include IL-1, IL-6, IL-12, TNF-α and inducible nitric oxide synthase (Figure 1.2). In addition to this, macrophages also produce chemoattractants (i.e. chemokines) that can recruit additional leukocytes to participate in the resolution of inflammation (Arango Duque and Descoteaux, 2014).

Monocyte

LPS, TNF,
IFN-γ, GM-CSF

IL-4, IL-13

LPS, IL-1Ra

IL-10, TGF-β

M1

M2a

M2b

M2c

Cytokines
Chemokines

TNF, IL-1β, IL-6, IL-12, IL-23
CCL2-5, 8-11

IL-10, TGF-β, IL-1Ra
CCL17, 22, 24

TNF, IL-1β, IL-6, IL-10
CCL1

IL-10, TGF-β

Function

↑ Th1 responses
↑ Antimicrobial properties

↑ Th2 responses
↑ Wound healing and tissue repair
↑ Immunosuppression
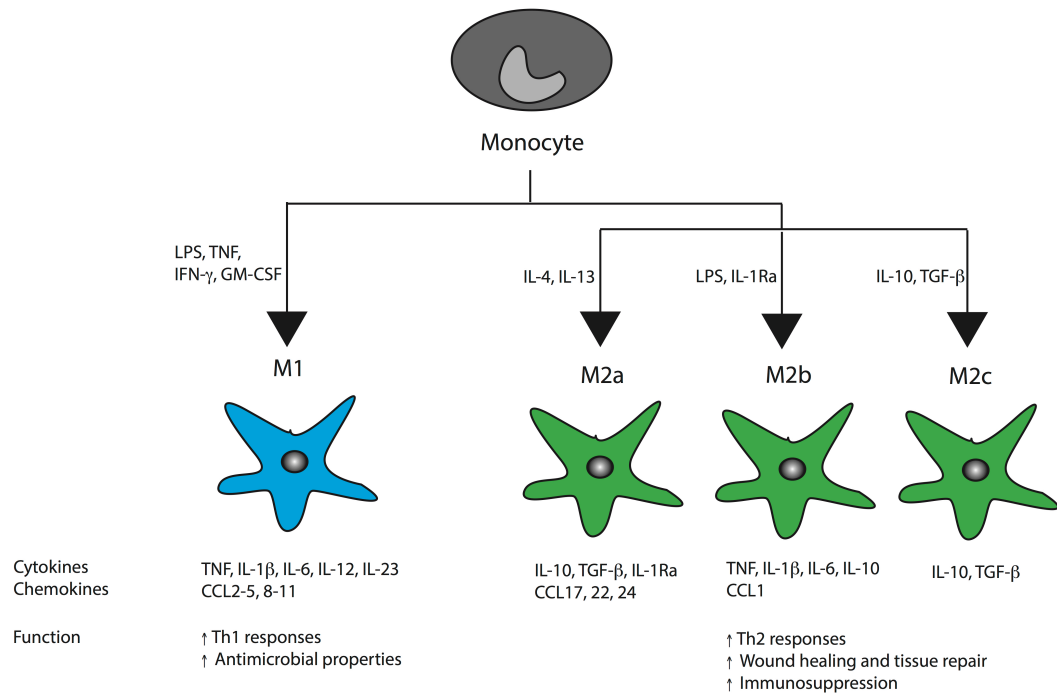
Figure 1.2. **Monocytes can differentiate to become phenotypically distinct macrophages.** Upon exposure to different stimuli, monocytes differentiate into either pro-inflammatory (M1), or anti-inflammatory (M2) macrophages. These stimuli include microbial substances as well as biochemical signals present in the microenvironment. Macrophage polarization depends on the presence of various cytokines, which are provided by lymphocytes, and other non-immune cells. Following polarization towards M1/M2, macrophages secrete vast array of cytokines and chemokines that can either promote inflammation or wound healing/tissue repair. Adapted from Duque and Descoteaux (2014).

1.2.3.3   Antigen Presentation

In the innate immune system, some immune cells can act as professional antigen-presenting cells (APCs) with a main role in presenting antigen to T cells to induce their activation during inflammatory responses. To activate T cells, APC must first degrade native proteins into peptides which can then be fed onto major histocompatibility complex (MHC) molecules. Two MHC molecules exist: class 1 for CD8-expressing T cells and class II for CD4-expressing T cells (Sprent, 1995). Once on the surface, the peptide-bound MHC molecules on APC are recognized by T cells via specific $\alpha\beta$ T-cell receptors. These are then able to manifest effector function of activated T cells within the adaptive immune system.

The taking up and presentation of antigen is a process that links together the innate and adaptive immune system and is therefore considered one of the most crucial features of tissue macrophages (Ley, 2014). Many studies have revealed the ability of tissue-resident macrophages in participating as APCs. This includes a recent study by Morris et al. (2013) illustrating the ability of adipose tissue macrophages as APCs to regulate adipose tissue $CD4^+$ T cells in mice. In addition to this, it has also been speculated that inflammatory monocyte-derived cells with M1-like functional phenotype act as APC that activate/polarize effector Th_1 and Th_{17} cells upon generation of IL-12 and IL-23, respectively. In a similar manner, M2-like tissue macrophages are likely to be involved in the polarization of iT_{reg} cells, while their role in Th_2 polarization is not as clearly understood (Ley, 2014, Mills and Ley, 2014).

1.2.3.4   Cytokine Secretion

Cytokines are a group of small proteins that play an important role in cell signaling. They are produced mainly by macrophages and lymphocytes, although other cells such as endothelial cells, epithelial cells and adipocytes are also capable of cytokine production (Arango Duque and Descoteaux, 2014). In macrophages, cytokines are crucial in determining their polarization and mediating their transition from innate to adaptive immunity (Unanue et al., 1976). Depending on the origin and the microenvironment that they reside in, macrophages can be categorized into several subsets which include either 'classically' M1 or 'alternatively' M2 activated. Each of the two subsets of macrophages secretes different cytokines: pro-inflammatory (M1) or anti-inflammatory (M2) (Figure 1.2). The release of cytokines involves an orchestrated pathway that is spatiotemporally regulated. The

dysregulation of cytokine secretion is often implicated with disease states that range from allergy to chronic inflammation (Arango Duque and Descoteaux, 2014).

1.2.3.5 Wound healing

One of the more interesting roles of macrophage in the immune system is their ability to promote wound healing. In fact, macrophages play such an important role in this process that Mosser & Edwards (2008) attempted to classify macrophages into three categories based on their homeostatic function: host defence, immune regulation and wound healing. *In vitro* studies revealed that macrophages can transition from a pro-inflammatory phenotype towards an anti-inflammatory or reparative phenotype (Fadok et al., 1998). This transition is a requisite for the switch from inflammation to proliferation in the wound healing process (Fadok et al., 1998). Although it was initially assumed that IL-4/IL-13 are the canonical factors responsible for the generation of anti-inflammatory macrophage phenotype, recent studies suggest that it may involve an IL-4/IL-13 independent pathway (Daley et al., 2010). It is speculated that this alternative pathway involves the activation of TLRs which induces the activation of adenosine 2A receptor giving rise to an M2 phenotype.

Macrophages play a key role in wound healing as they retain the ability to remove neutrophils, which are often abundant in early wounds (Koh and DiPietro, 2011). This is an essential process as excessive number of neutrophils can negatively influence repair, causing damage to normal tissue (Dovi et al., 2003). Removal of neutrophils from sites of injuries by macrophages can be performed in several ways: 1) inducing apoptosis in neutrophils (Meszaros et al., 2000), and 2) recognizing and ingesting apoptotic neutrophils through phagocytosis to resolve wound inflammation (Khanna et al., 2010, Meszaros et al., 1999). This latter mechanism of removal is thought to drive phenotypic change of macrophages from pro-inflammatory to the reparative phenotype (Fadok et al., 1998).

1.2.4 Macrophage polarization and functional phenotypes

Macrophages are remarkably plastic and flexible cells that are able to alter their physiological characteristics following the exposure to varying environmental cues, hence giving rise to different populations of cells with distinct functions. The process describing perturbation of macrophages with endogenous danger signals (such as debris of necrotic cells or ATP) and exogenous agents (such as cytokines, microbes or microbial products) is known as macrophage activation or polarization. The polarization of macrophages is a crucial process involved in the outcome of many diseases and various macrophage taxonomy has been described in an attempt to classify the different populations of macrophages. Two taxonomy have been discussed thoroughly within the literature: 1) the M1/M2 classification which imitate the Th cell nomenclature (Martinez and Gordon, 2014) and 2) classification by Mosser and Edwards (2008) based on macrophage functions (wound healing, host-defense and immune regulation). Here, only the M1/M2 classifications of macrophage phenotype will be described in greater detail.

1.2.4.1 M1

In vitro, macrophages are activated towards an M1 functional program upon exposure to infectious microorganism such as the Gram-negative product lipopolysaccharide (Suresh and Sodhi, 1991) and by inflammation-related cytokines TNF-α or IFN-γ (Arango Duque and Descoteaux, 2014) (Figure 1.3). A few of the main characteristics of M1 macrophages, also known as classically-activated macrophages, include their participation as inducers in Th1 responses, their ability to mediate resistance against intracellular parasites and finally, their ability to produce effector molecules (i.e. nitric oxide, reactive oxygen species and inflammatory cytokines (IL-1β, TNF, IL-6, IL-8 and IL-12)). *In vitro,* they are characterized by an IL-12^{hi}IL-23^{hi}IL-10^{lo} phenotype (Gordon and Taylor, 2005). For this reason, M1 macrophages are described as pro-inflammatory accompanied with killing/inhibitory functional capacity. It is thought that monocyte-derived macrophages from circulating inflammatory monocytes tend to polarize towards M1 phenotype although they can polarize towards both M1 or M2 phenotype, depending on tissue condition (Figure 1.3) (Davies et al., 2011, Hashimoto et al., 2013).

1.2.4.2   M2

In contrast to M1 macrophages, M2 macrophages are described as anti-inflammatory, involved in healing/growth promoting functions (Mills, 2012, Mills et al., 2000). The activation of M2 macrophage phenotype *in vitro* can be categorized further into M2a (alternative inflammation), M2b and M2c (deactivation) macrophages, depending on their stimuli exposure. Exposure towards Th_2-related cytokines IL-4 or IL-13 leads to the polarization towards M2a which expresses a series of chemokines to promote the local increase of Th_2 cells, basophils and eosinophils. Polarization towards M2b phenotype are achieved by a combination of immune complexes, LPS, apoptotic cells and IL-1Rα, all of which results in the secretion of anti-inflammatory cytokines such as IL-10 as well as pro-inflammatory cytokines TNF and IL-6. Finally, exposure to anti-inflammatory molecules such as IL-10, TGF-β and glucocorticoids leads to the polarization towards M2c, which causes the secretion of immunosuppressive cytokines such as IL-10 and TGF-β (Figure 1.2). Cytokines secreted by M2c macrophages have the ability to promote the development of Th_2 lymphocytes and T_{regs}, making them competent cells to protect organs from injury resulting from inflammatory insults (Gordon, 2003, Martinez et al., 2008). Further characteristics of M2 macrophages *in vitro* involved their high expression level of mannose, scavenger and galactose-type receptors, their ability to take part in polarized Th_2 responses and finally, possessing an IL-12^{lo}IL-23^{lo}IL-10^{hi}TGF-β^{hi} phenotype (Italiani and Boraschi, 2014).

1.2.4.3   Current hypothesis on macrophage polarization

Although activation of macrophages towards M1 and M2 phenotype has been described in greater detail *in vitro,* it is still unclear whether this phenotypic and functional evolution occurs *in vivo*. Studies in mice revealed that the switch from M1 to M2 macrophages in the context of inflammatory response allows macrophages to perform different activities at the different stages of the process. However, whether M1 and M2 macrophages belong to two phenotypically distinct populations performing different functions, or whether they are the same cells that shift from one phenotype to another depending on microenvironment signals, remain a controversy (Italiani and Boraschi, 2014).

Three hypotheses have been generated to attempt to explain this issue. The first described that different subsets of monocytes or macrophages can adopt different functional phenotype, with monocyte-derived macrophages in tissues adopting M1

phenotype and tissue-resident macrophages adopting a cytoprotective and reparative M2 macrophage phenotype (Auffray et al., 2007). The second hypothesis described that an inflammatory reaction involves a sequential recruitment of monocytes into the tissue. Monocytes recruited at the early phase are exposed to signals that polarize them towards M1 phenotype while those recruited at a late phase are exposed to signals polarizing them towards an M2 phenotype (Arnold et al., 2007). Finally, the third hypothesis described that depending on the environmental condition, polarized macrophages can switch from one phenotype to another. This was evident from *in vitro* studies illustrating the ability of polarized M1 macrophages to switch to M2 macrophages in culture (Italiani et al., 2014, Mylonas et al., 2009, Stout et al., 2005). Despite our increasing understanding for macrophage activation and polarization, the current knowledge on the mechanistic basis of macrophage diversity in different tissues or in response to changing environment is still lacking.

1.2.5 Disease implication of macrophages

Tissue damage resulting from infection or injury initiates the recruitment of inflammatory monocytes from the circulation into tissue which then differentiate into macrophages (Geissmann et al., 2010). Due to the nature of the microenvironment of damaged tissue, these recruited macrophages exhibit a pro-inflammatory phenotype and secrete a range of pro-inflammatory factors as well as ROS and NO to activate anti-microbial defense mechanisms (Murray and Wynn, 2011b). Although inflammatory macrophages are beneficial in facilitating the clearance of invading organisms, uncontrolled regulation may result in substantial tissue damage due to excessive cytotoxic activity that is induced by ROS and nitrogen species (Nathan and Ding, 2010). This can potentially lead to the progression of chronic inflammatory and autoimmune diseases (Krausgruber et al., 2011, Sindrilaru et al., 2011). To limit this damage, pro-inflammatory macrophages must undergo apoptosis or switch towards an anti-inflammatory phenotype. Here, the involvement of macrophages in inflammatory disease is described in greater detail.

1.2.5.1 Macrophages in inflammatory disease

Macrophages are known to contribute to the pathogenesis of many chronic inflammatory conditions that include asthma, rheumatoid arthritis, fibrosis and atherosclerosis (Hansson and Hermansson, 2011, Murray and Wynn, 2011b). For example, the inflammatory response in allergic asthma is accompanied by the recruitment of Th_2 lymphocytes, mast cells, eosinophils and macrophages to the lung as well as the presence of a macrophage-like APC within the airway lumen (Julia et al., 2002). Additional studies also revealed that the severity of allergen-induced disease is worsened by IL-4R^{+} macrophages (Ford et al., 2012), while protection is associated with a reduction in IL-4R^{+} macrophages (Moreira et al., 2010). Increased number of IL-4R^{+} macrophages have also been associated with reduced lung function (Melgert et al., 2011).

The role of monocyte-derived macrophage in atherogenesis has been a topic of interest. Recruitment of monocytes into the intima layer of the artery marks the earliest event in atherosclerosis. Following their infiltration to the intima, monocytes differentiate into macrophages, which can ingest lipoproteins transforming them into lipid-rich foam cells and giving rise to the atherosclerotic plaque (Moore et al., 2013, Liu et al., 2014). As the disease progresses, the atherosclerotic plaque can increase in size, becoming vulnerable and eventually rupturing resulting in a heart attack,

stroke or even sudden cardiac arrest (Moore and Tabas, 2011). *In vivo* studies in a mouse model of atherosclerosis identified that targeting chemokines to inhibit monocyte recruitment resulted in the inhibition or reduction of atherogenesis, confirming the essential role of macrophages in atherosclerosis development (Mestas and Ley, 2008). Different subsets of macrophages are observed in atherosclerotic plaques. In the early stages, infiltration of M2 phenotype macrophages was observed, however, as the plaque development progressed, M1 phenotype macrophages increased and eventually become dominant, promoting acute atherothrombotic vascular accident (Leitinger and Schulman, 2013, Moore and Tabas, 2011). Although usually associated with negative impact towards atherosclerosis, macrophages have also been associated with anti-atherosclerotic function. For example, macrophages as professional phagocytes, remove pathogens, small debris and damaged cells from atherosclerotic tissue through the process of phagocytosis (Schrijvers et al., 2007). Additionally, TGF-β secreted by M2 macrophages has been shown to inhibit the recruitment of inflammatory cells and has been associated with protection against atherosclerosis (Mallat et al., 2001).

Upon activation by endogenous danger signals and PAMPs, macrophages are activated and secrete various anti-microbial mediators, inflammatory cytokines and chemokines that include TNFα, IL-1, IL-6 and CCL2 (Wynn and Barron, 2010). If not tightly controlled, these cytokines and chemokines drive inflammatory responses and can exacerbate tissue injury, even leading to abnormal wound healing and ultimately causing scarring, also known as fibrosis (Duffield et al., 2005). Hence, macrophages are primary producers of various cytokines implicated in the pathogenesis of inflammatory conditions.

In addition to chronic inflammatory conditions, macrophages have also been implicated in the pathogenesis of autoimmune diseases. They are regarded as an important source of many key inflammatory cytokines (IL-12, IL-18, IL-23 and TNFα) acting as important drivers of autoimmune inflammation (Murray and Wynn, 2011a). Studies in mice revealed that macrophage production of IL-23 promotes end-stage joint autoimmune inflammation (Wynn et al., 2013). In addition to this, pro-inflammatory phenotype macrophages have also been attributed with the pathogenesis of chronic demyelinating diseases of the central nervous system (CNS) by contributing to axon demyelination in a mouse model of multiple sclerosis

(Ponomarev et al., 2011). Finally, secretion of IL-23 and TNF by CD14^{+} macrophages has been detected in Crohn's disease patients (Kamada et al., 2008).

Although the majority of studies reported macrophages as a contributor towards inflammatory conditions, a few have also reported suppressive roles. The suppressive role of macrophages is evident from a study which illustrated ROS produced by macrophages can limit arthritis in mice through inhibition of T cell activation (Gelderman et al., 2007) and the ability of resident tissue macrophages to maintain homeostasis of the gut through the production of suppressive cytokine IL-10 and antagonizing pro-inflammatory macrophages (Murai et al., 2009, Smith et al., 2009). Taken together, it is apparent that macrophage differentiation in the local environment can affect the pathogenesis of various inflammatory conditions.

1.3 Calcium signaling

Calcium ions (Ca^{2+}) play a vital role in every aspect of cellular life as an intracellular messenger participating in cellular processes which include gene transcription, contraction and differentiation (Bootman, 2012). Cells invest much of their energy to control changes in Ca^{2+} concentration with a gradient maintained between their intracellular (approximately 100 nM free) and extracellular (~1 μM) concentrations (Clapham, 2007). Ca^{2+} concentration gradients in cells are controlled through three methods: 1) chelation, 2) compartmentalization, or 3) extrusion. To control Ca^{2+} levels within a cell, an array of channels, pumps and cytosolic buffers are involved.

In macrophages, Ca^{2+} signaling plays a critical role and regulates various cellular processes such as regulating pro-inflammatory gene expression and cytokine secretion (Desai and Leitinger, 2014). LPS-activated macrophages have been shown to increase cytosolic calcium level, which is crucial for the production of TNF-α (Watanabe et al., 1996) and reduced IL-12 production (Liu et al., 2016). Another important role for Ca^{2+} signaling in macrophages is their contribution towards phagosome maturation, engulfment of apoptotic cells and subsequent anti-inflammatory response as well as their contribution to maintaining leading-edge structure of migrating macrophages (Evans and Falke, 2007; Gronski et al., 2009). Studies have revealed that the process of phagocytosis is also tightly regulated by level of intracellular Ca^{2+} (Nunes and Demaurex, 2010). This was demonstrated in a study by Cuttell et al. (2008) whereby mutations in genes linked to Ca^{2+} flux resulted in defects in the clearance of apoptotic cells.

1.3.1 ON and OFF mechanisms

The Ca^{2+} signalling pathway is a complex network that involves several steps. The activation of signalling pathways requires a stimulus which results the in the activation of an 'ON' mechanism that feed Ca^{2+} into the cytoplasm, stimulating Ca^{2+}-sensitive processes. The final step of the Ca^{2+} signalling pathway involves an 'OFF' mechanism that is made up of pumps and exchangers to extrude Ca^{2+} from the cytoplasm to restore the resting state of a cell (Berridge et al., 2000).

The first stage of the Ca^{2+} network involves the generation of Ca^{2+}-mobilizing signals from both internal and external sources resulting in the activation of the 'ON' mechanism. While internal sources are controlled by channels found on endoplasmic reticulum (ER) or sarcoplasmic reticulum in muscles (SR), external

sources are controlled by channels found within the plasma membrane of cells (Berridge et al., 2000). The entry of Ca^{2+} from extracellular space to the cytoplasm is governed by voltage-operated channels (VOCs) and receptor-operated channels (ROCs) (Berridge et al., 2000). The release of Ca^{2+} from internal stores is a tightly controlled mechanism triggered by a variety of second messengers which include inositol 1,4,5-triphosphate (IP_3), cyclic ADP ribose (cADPr) or, significantly Ca^{2+} itself. The increase in intracellular Ca^{2+} level can act on channels such as IP_3 and ryanodine receptors (RyR), to promote further release of Ca^{2+} from intracellular stores. This process is known as Ca^{2+}-induced Ca^{2+} release (Berridge, 1993). The emptying of internal stores can also then result in the activation of store-operated channels (SOCs) found on the plasma membrane of cells.

The final part of the Ca^{2+} signaling network involves the OFF mechanism in which Ca^{2+} is rapidly removed from the cytoplasm by numerous pumps and exchangers (Blaustein and Lederer, 1999, Pozzan et al., 1994). Removal of Ca^{2+} involves the extrusion of Ca^{2+} out of cells through plasma membrane Ca^{2+}-ATPase (PMCA) pumps and Na^+/Ca^{2+}-exchangers as well as the uptake of Ca^{2+} back into internal stores through sarco-endoplasmic reticulum ATPase (SERCA) (Berridge et al., 2000). The mitochondrion is also responsible for sequestering Ca^{2+} rapidly during the development of Ca^{2+} signal.

1.3.2 Calcium channels in macrophages

Macrophages are non-excitable cells and rely on Ca^{2+} permeable channels that are not gated by voltage. These cell surface receptors in macrophages include ROCs such as purinergic receptor (P2 receptors; discussed in section 1.4), SOCs (Orai channels) and transient receptor potential (TRP) channel (Desai and Leitinger, 2014).

1.3.2.1   Orai channels

Orai channels, also known as CRAC channels, are activated upon the emptying of ER stores (Hogan et al., 2010). Although studies have revealed their regulatory mechanisms, their functional role in macrophage biology remains unclear. Previously, they have been linked with the production of ROS and with the engulfment of apoptotic cells in macrophages. In addition to this, it is also thought that the opening of Orai channels requires the activation of G_q-coupled P2Y receptors which leads to the subsequent depletion of Ca^{2+} stores (Desai and

Leitinger, 2014). This led to the speculation that activation of Orai channels may be critical for the cellular processes downstream of P2Y receptors. However, further work is still required to confirm this hypothesis.

1.3.2.2   TRP channels

TRP channels are a family of cation-selective channels that are gated by temperature, mechanical force, ligands and internal cues such as pH. TRP channels play an important role in macrophages and this is evident from a study which illustrated that a lack of TRPM2 in mice impaired their ability to induce Ca^{2+} influx upon ROS stimulation, resulting in the inability to produce chemokines. These chemokines are crucial for the recruitment of cells and the attenuation of neutrophil infiltration (Yamamoto et al., 2008). In addition to this, TRP channels have been shown to play a role in phagocytosis and chemotaxis with macrophages lacking TRPV2 showing deficiency in triggering of phagocytosis when exposed to zymosan and IgG opsonized particles (Link et al., 2010). Most recently, TRPC1 has been associated with a role in restraining the secretion of IL-1β in response to inflammatory stimuli (Py et al., 2014).

1.4 Purinergic signaling

Adenosine 5-triphosphate (ATP) was identified as a co-transmitter in nerves supplying the gut and bladder in the early 1970s (Burnstock, 1972). This discovery, together with various studies by Drury and Szent-Gyorgyi (1929), Buchthal and Folkow (1948) and Emmelin and Feldberg (1948) relating to purines in heart and peripheral ganglia, allowed the proposal of the purinergic signaling concept by Geoffrey Burnstock in 1972. It is now well accepted that ATP is a cotransmitter in all nerves of the peripheral and central nervous system (Verkhratsky et al., 2009). Purinergic signaling is the extracellular signaling pathway mediated by purine nucleotides and nucleosides and involves the activation of purinergic receptors. These extracellular mediators include purine nucleoside (adenosine), its nucleotides (ATP, adenosine diphosphate (ADP), and adenosine monophosphate (AMP)) and pyrimidine nucleotides (uridine diphosphate (UDP), uridine diphosphate glucose (UDP-Glu) and uridine triphosphate (UTP)), all of which are key extracellular messengers in the central and peripheral nervous system, regulating cell function (Williams, 2002).

1.4.1 Purinergic receptors

In 1978, the discovery of two families of purinergic receptors, P1 and P2 receptors, was made (Burnstock, 1978). While P1 receptors are described to be sensitive to adenosine, P2 receptors are sensitive to ATP and ADP (Verkhratsky et al., 2009). Pharmacological characterization of P2 receptors were reported in 1985 allowing their categorization into ligand-gated ion channel P2X receptors and G protein-coupled P2Y receptors (GPCRs) (Burnstock and Kennedy, 1985). However, it was not until the successful cloning of these receptors in early 1990's that the purinergic signaling hypothesis was finally accepted. Currently, there are 4 subtypes of P1 receptors, 7 subtypes of P2X receptors and 8 subtypes of P2Y receptors. The activation of purinergic receptors leads to various major cellular signaling pathways that are evident by reports demonstrating short-term signaling in neurosecretion, neuromodulation and neurotransmission. In addition to this, their activation also mediates long-term signaling involved in cell proliferation, differentiation and death (Verkhratsky et al., 2009).

1.4.1.1 P1 receptors

P1 receptors all couple to G proteins which have seven putative transmembrane (TM) domains with the NH_2 terminus lying on the extracellular side and the COOH

terminus lying on the cytoplasmic side of the membrane (King and Burnstock, 2002). So far, four subtypes of P1 receptors have been successfully cloned and are denoted as A_1, A_{2A}, A_{2B} and A_3 receptors. While A_1 and A_{2A} receptors possess high affinity for adenosine, A_{2B} and A_3 receptors possess relatively lower affinity for the agonist (Fredholm et al., 2011). In addition to this, A_1 and A_3 receptors are coupled to $G_{i/o}$ proteins while A_{2A} and A_{2B} are coupled to G_s protein (Fredholm et al., 2011). P1 receptors are widely distributed in the mammalian system with A_1 receptors being widely distributed in the CNS, adrenal glands, skeletal muscle and adipose tissue (Dixon et al., 1996, Fredholm et al., 2011), A_{2A} receptors being widely distributed in spleen, immune cells, platelets and the heart (Fredholm et al., 2011), A_{2B} receptors being ubiquitously distributed in the brain (Dixon et al., 1996) and A_3 receptors being widely expressed in rat testis (Meyerhof et al., 1991) and mast cells as well as low levels in the brain (Dixon et al., 1996). *In vitro* and *in vivo* studies have illustrated potent anti-inflammatory function of all adenosine receptors in inflammatory cells. Pro-inflammatory function has also been associated with some adenosine receptors (King and Burnstock, 2002).

1.4.1.2　　P2X receptors

P2X receptors (P2XR) are ligand gated ion channels permeable to sodium, potassium and calcium that open upon the binding of ATP. P2X receptors are found in all vertebrate species (Burnstock, 2007) and in many invertebrate marine species (Fountain and Burnstock, 2009, Fountain, 2013). In vertebrates, they are implicated in various physiological processes, which range from synaptic transmission to inflammation as well as pain and taste. P2XR can be categorized into 7 different subtypes (P2X$_{1-7}$), showing 30 – 50% sequence identity at the amino acid level (Burnstock, 2006). The formation of trimeric P2XR can involve homo- and hetero-multimers. While all P2XR, except for P2X$_6$, can form a functional receptor as a homomultimer, heteromultimers have only been described in a few instances. These include the formation of P2X$_{2/3}$ in nodose ganglia, P2X$_{4/6}$ in CNS neurons and P2X$_{1/5}$ in blood vessels (Burnstock, 2006). The main difference between receptor subtypes lies in their agonist sensitivities as well as their rates of activation and deactivation (Table 1.2) (Coddou et al., 2011). While P2X$_1$ and P2X$_3$ have been shown to be rapidly activating and desensitizing, P2X$_2$ and P2X$_4$ are slowly desensitizing (North, 2002, North, 2016).

1.4.1.3   P2Y receptors

P2Y receptors (P2YR) are a family of metabotropic G-protein coupled receptors, which can be activated by various nucleotides such as ATP, ADP, UTP, UDP and UDP-glucose (Table 1.3) (Burnstock and Knight, 2004). There are 8 subtypes of P2YR which are known as $P2Y_1$, $P2Y_2$, $P2Y_4$, $P2Y_6$, $P2Y_{11}$ – $P2Y_{14}$. P2YR share 21 – 48 % sequence homology, with the greatest similarity observed between $P2Y_{12}$ and $P2Y_{13}$ (Abbracchio et al., 2003, Abbracchio and Burnstock, 1994, Khakh et al., 2001). They are characterized by seven TM spanning regions, an extracellular NH_2- and intracellular COOH-termini and structural diversity of intracellular loops and the C termini which determines the coupling to either $G_{\alpha q/11}$, $G_{\alpha s}$ or $G_{\alpha i}$ proteins (Figure 1.3) (Burnstock and Knight, 2004).

In response to nucleotide activation, recombinant P2YR either activate phospholipase C (PLC) which causes the release of intracellular Ca^{2+} or affect adenylate cyclase (AC) which in turn results in the alteration of cyclic AMP (cAMP) levels (Table 1.3) (Abbracchio et al., 2003). While $P2Y_1$, $P2Y_2$, $P2Y_4$, $P2Y_6$ and $P2Y_{11}$ have been shown to mainly signal through $G_{\alpha q/11}$ activating PLC, $P2Y_{12}$ – $P2Y_{14}$ signal through $G_{\alpha i}$ to inhibit AC (Abbracchio et al., 2006). In addition to being coupled to the $G_{\alpha q/11}$ subunit, $P2Y_{11}$ is also coupled to $G_{\alpha s}$ which leads to the activation of AC and increase in cAMP levels. P2YR has also been suggested to form homomultimeric and heteromultimeric assemblies under certain conditions and it is also known that many cells express multiple subtypes of P2YRs (Abbracchio et al., 2006, Burnstock and Knight, 2004).
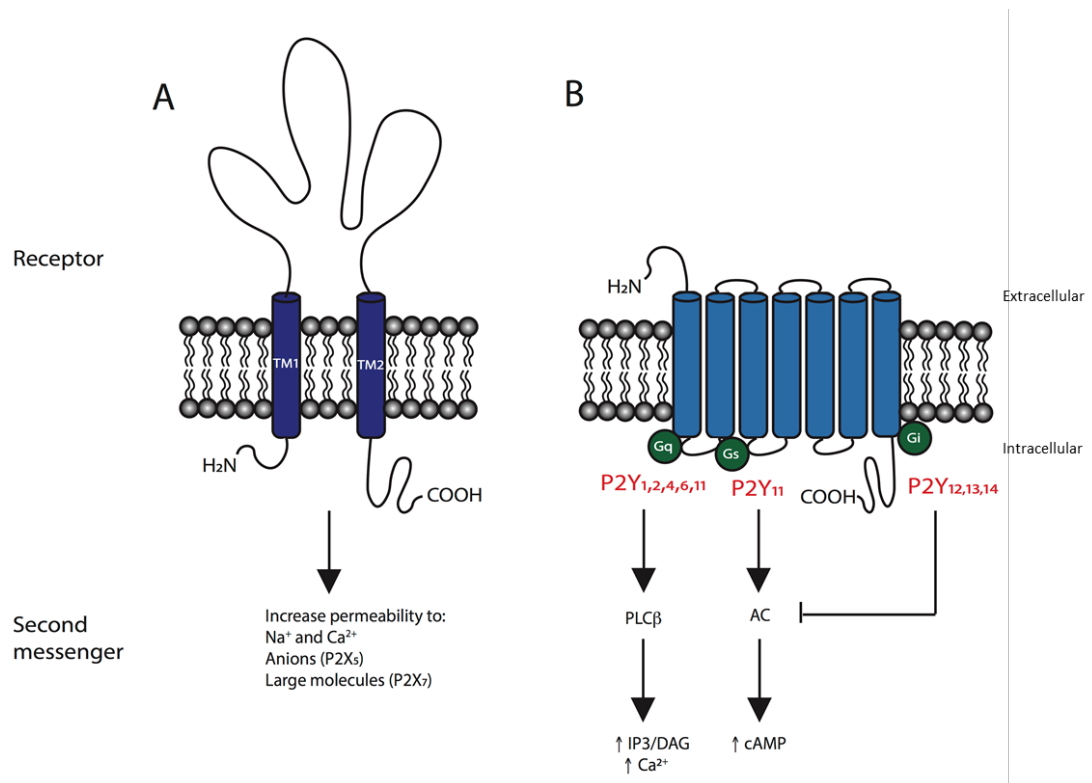
Figure 1.3 Structure of P2 receptors and second messengers associated with their activation. A) Diagram illustrating the transmembrane topology of P2XR protein showing both N-terminus and C-terminus within the cytoplasm. Two putative membrane-spanning segments (TM1 and TM2) traverse the lipid bilayer of the plasma membrane and are connected by a long extracellular loop containing the ATP binding site. B) Illustration of G-protein coupled P2YR. $P2Y_{1,2,4,6}$ are coupled to $G_{\alpha q}$ subunit activating PLCβ and mobilization of intracellular Ca^{2+}. $P2Y_{12,13,14}$ are coupled to the $G_{\alpha i}$ subunit inhibiting adenylyl cyclase (AC). $P2Y_{11}$ is coupled to both $G_{\alpha q}$ and $G_{\alpha s}$ subunit activating Ca^{2+} mobilization and cAMP, respectively. Adapted from Burnstock and King (2004).

P2XR subtype	Downstream signaling pathway	Agonist	Antagonist	Primary distribution
P2X$_1$*	LIC	ATP = $\alpha\beta$-meATP = 2-meSATP	MRS2220, MRS2159, NF449, NF279, Ro-0437626, Suramin, PPADS, TNP-ATP	Platelets, cerebellum, smooth muscle and dorsal horn spinal neurons
P2X$_2$**	LIC	ATP > ATPγS >2-meSATP > $\alpha.\beta$-meATP	RB-2, NF279, NF770, NF776, NF778, PSB-12011, PSB-10211, Suramin, PPADS	CNS, smooth muscle, retina, chromaffin cells, autonomic and sensory ganglia
P2X$_3$*	LIC	2-meSATP > ATP > α,β-meATP	A-317491, NF023, NF279, NF449, RO-85, MRS2159, MRS2257, Suramin, PPADS	Sensory neurons and sympathetic neurons
P2X$_4$**	LIC	ATP > α,β-meATP > BzATP	5-BDBD, BBG, Paroxetine, PSB-12062, BX430, Suramin, PPADS, TNP-ATP	CNS, immune cells, testis, colon
P2X$_5$	LIC	ATP > 2-meSATP > ATPγS	BBG, Suramin, PPADS, TNP-ATP	Skin, gut, bladder, spinal cord
P2X$_6$***	LIC	ATP > 2-meSATP	TNP-ATP, PPADS	CNS and spinal cord
P2X$_7$	LIC	BzATP > ATP	MRS2159, KN-62, BBG, suramin, A438079, AZ11645373, PPADS	Immune cells, pancreas, skin

Table 1.2 Characteristics of P2XR. P2XR have a widespread tissue distribution with each receptor having different agonist sensitivity. *P2X$_1$ and P2X$_3$ are fast desensitizing, **P2X$_2$ and P2X$_4$ are slow desensitizing, ***P2X$_6$ do not form a functional receptor as a homotrimer. LIC: Ligand gated ion channel. Table adapted from Burnstock and Knight (2004).

P2YR subtype	Downstream signaling pathways	Agonist	Antagonist	Primary distribution
P2Y$_1$	GPCR: G$_{\alpha q}$ - PLCβ activation, ↑[Ca^{2+}]i	2-MeSADP > 2-MeSATP = ADP > ATP	MRS2279, MRS2179, MRS2500	Epithelial and endothelial cells, platelets, immune cells and brain
P2Y$_2$	GPCR: G$_{\alpha q}$ and G$_{\alpha i}$ - PLCβ activation, ↑[Ca^{2+}]i	UTP = ATP	Suramin, AR-C118925XX	Epithelial and endothelial cells and immune cells
P2Y$_4$	GPCR: G$_{\alpha q}$ - PLCβ activation, ↑[Ca^{2+}]i	UTP > ATP	ATP (human), Reactive blue 2, PPADS	Endothelial cells, placenta
P2Y$_6$	GPCR: G$_{\alpha q}$ - PLCβ activation, ↑[Ca^{2+}]i	UDP > UTP >> ATP	MRS2578, Reactive blue 2, PPADS, suramin	Epithelial cells, placenta, T cells, thymus
P2Y$_{11}$	GPCR: G$_{\alpha q}$ and G$_{\alpha s}$ - PLCβ activation, AC activation, ↑[Ca^{2+}]i	AR-C67085MX > Bz-ATP > ATP	Suramin, Reactive Blue 2, NF340, NF157	Spleen, intestins, granulocytes
P2Y$_{12}$	GPCR: G$_{\alpha i}$ - inhibition of AC	ADP = 2-MeSADP	PSB-0739, Ticagrelor, Clopidogrel, AR-C69931MX	Platelets, glial and microglial cells of the brain
P2Y$_{13}$	GPCR: G$_{\alpha q}$ and G$_{\alpha i}$ - inhibition of AC, PLCβ activation	ADP = 2-MeSADP > ATP = 2-MeSATP	ARC-69931MX, ARC-67085MX, MRS-2211	brain, bone marrow, spleen and lymph nodes
P2Y$_{14}$	GPCR: G$_{\alpha i}$ - inhibition of AC	UDP-glucose = UDP	N/A	Adipose tissue, stomach, intestine, brain, mast cells

Table 1.3 Characteristics of P2YR. P2YR have a widespread tissue distribution and each receptor are coupled to either G$_{\alpha q}$, G$_{\alpha s}$ or G$_{\alpha i}$ subunit leading to various downstream signaling pathways. GPCR: G protein coupled receptor. Table adapted from Burnstock and Knight (2004).

1.4.2   P2X$_4$ receptors

P2X receptors have been described briefly in section 1.4.1.2. However, as the focus of this thesis is to study P2X$_4$ receptors, a thorough overview discussing pharmacology, structure and composition as well as localization of this receptor will be discussed below.

1.4.2.1   Structure and Composition

All P2X receptor subtypes have been described to consist of intracellular NH$_2$ and COOH termini and form two functional domains, the extracellular domain and the transmembrane (TM) domain. All subunits are made up of two TM-spanning domains, one responsible for channel gating and the other responsible for lining of the ion conducting pore, joined by a large extracellular loop (ectodomain). This ectodomain is known to consist of 10 conserved cysteine residues forming the ATP binding site (North, 2016, Marquez-Klaka et al., 2007) (Figure 1.3). Biophysical characterization of native and recombinant P2XRs informed the hypothesis that these channels form as trimeric homomers or heteromers (Coddou et al., 2011) and whole-cell and single-cell recordings illustrated that three molecules of ATP were required for the activation of the channel (Jiang et al., 2003, Ding and Sachs, 1999, Bean et al., 1990). Evidence that P2XR are organized as either homotrimers or heterotrimers initially came from studies co-expressing slowly desensitizing P2X$_2$ with fast desensitizing P2X$_3$ (Lewis et al., 1995). Immunoprecipitation studies allowed the prediction of 11 different forms of heteromers (Torres et al., 1999) although only six functional P2XR heteromers have been characterized and these include P2X$_{1/4}$ (Nicke et al., 2005) and P2X$_{4/6}$ (Le et al., 1998).

The crystal structure of P2X$_4$ zebrafish by Kawate et al. (2009) confirmed the hypothesis that the receptor forms a trimer and since then, there has been a significant advancement to the understanding of this ligand-gated ion channel. Crystallization studies illustrated each subunit rises from the plasma membrane, resembling the structure of a dolphin surfacing from the ocean, with its tail submerged within the lipid bilayer (Figure 1.4A and B). With this, the body regions of the three subunits intertwine to form one central vertical cavity (Kawate et al., 2009). Upon the binding of ATP, it is thought that the subunits flex together within the ectodomain and separate in the membrane-spanning region to form an open channel state (North, 2002, North, 2016).
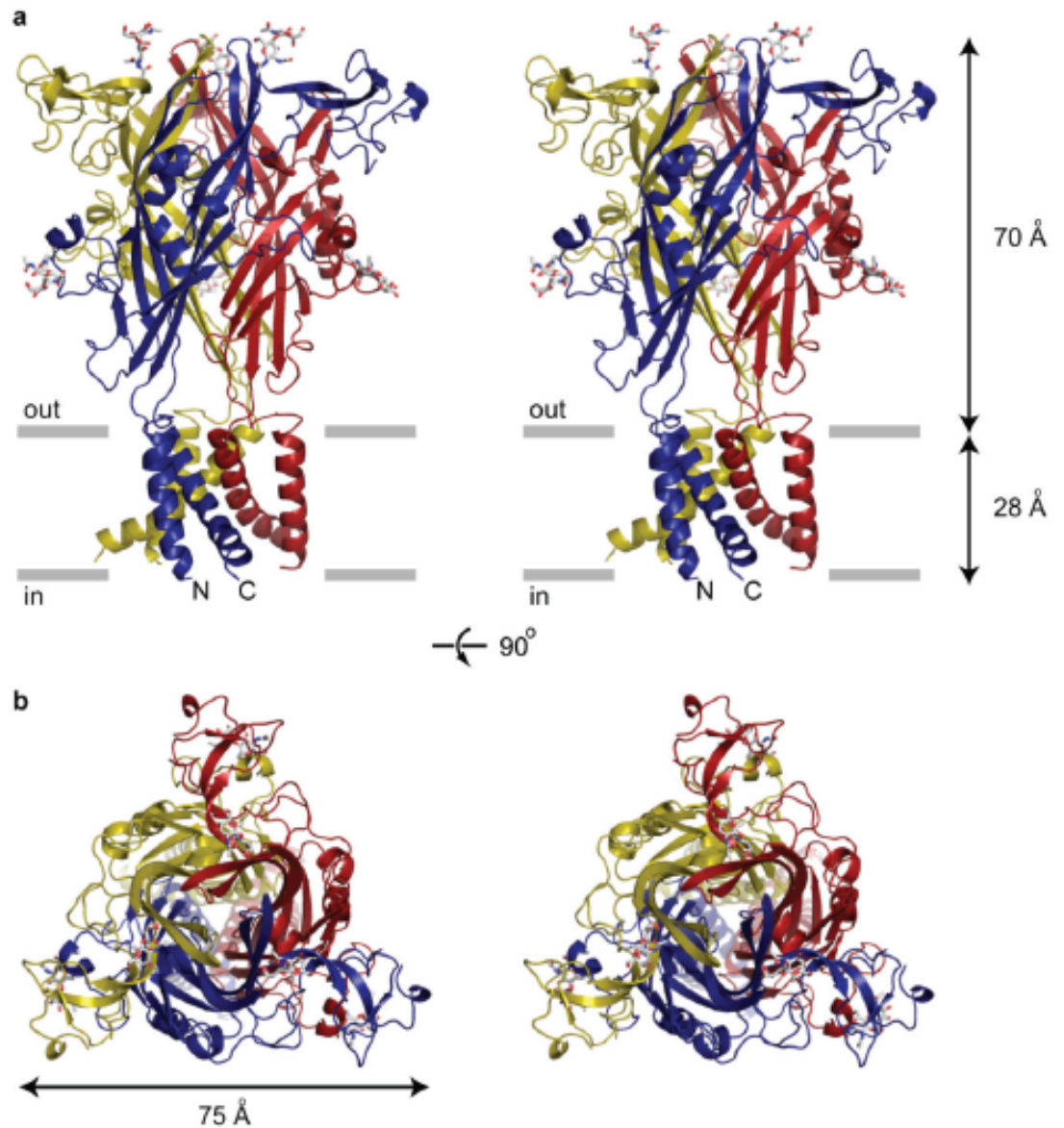
Figure 1.4 Crystal structure of P2X$_4$ receptor. A and B) Stereo-view of homotrimeric zebrafish P2X$_4$ receptor views parallel to the membrane and from the extracellular side of the membrane, respectively. Each trimer subunit is depicted in different colors. Image taken from Kawate et al., 2009.

1.4.2.2 Pharmacology

1.4.2.2.1 Agonist

ATP acts as the main agonist for all homomeric and heteromeric P2XR although activation is done in a receptor-specific manner with EC_{50} values ranging from nanomolar to milimolar concentrations (Coddou et al., 2011). Early electrophysiological studies by Soto et al. (1996a) in rat $P2X_4$ expressed in *Xenopus* oocytes reported the agonist profile as ATP > 2-methylthio-ATP > CTP > α,β-meATP > dATP. The same order of agonists efficacy was demonstrated in human $P2X_4$ expressed in *Xenopus* oocytes (Garcia-Guzman et al., 1997). Reported EC_{50} values for ATP in rat and human $P2X_4$ was illustrated to be 6.9 ± 0.8 μM and 7.4 ± 0.5 μM, respectively (Soto et al., 1996a, Garcia-Guzman et al., 1997). Further characterization of $P2X_4$ orthologues in mammalian HEK293 cells illustrated EC_{50} values for ATP in mouse, human and rat $P2X_4$ to be 2.3 μM, 1.4 μM and 5.5 μM, respectively (Jones et al., 2000).

1.4.2.2.2 Positive modulators

There are currently two well-described positive modulators for $P2X_4$. The first positive modulator is cibacron blue, an isomer of reactive blue 2 that possess an inhibitory action at all P2X receptors, except for $P2X_4$. Application of low concentrations (3 – 30 μM) of cibacron blue has been shown to potentiate rat $P2X_4$ responses in HEK293 cells by increasing the potency of ATP agonist towards $P2X_4$ (Miller et al., 1998).

The second known positive modulator is ivermectin (IVM), a derivative of *Streptomyces avermitilis*. IVM is a member of lipophilic compounds known as avermectins and is used widely in human medicine for the treatment of river blindness, and in veterinary medicine for the treatment of a range of ento- and ecto-parasites (Burkhart, 2000). It has been described to act as positive allosteric modulator of vertebrate $GABA_A$ and nicotinic $\alpha 7$ receptor (Zemkova et al., 2014) and P2XR. Amongst the P2XR, IVM has been shown to be capable of acting as a positive modulator for both $P2X_4$ and $P2X_7$, although $P2X_4$ has been shown to be the most sensitive towards IVM (Khakh et al., 1999). Extracellular application of IVM potentiated $P2X_4$ currents and delayed channel deactivation (Khakh et al., 1999, Fountain and North, 2006) while IVM potentiated only the magnitude of human $P2X_7$ responses while not affecting channel deactivation (Norenberg et al., 2012).

Although IVM binding to invertebrate glutamate-activate chloride channels has been studied (Hibbs and Gouaux, 2011), the IVM binding site on $P2X_4$ remains to be elucidated. It has been speculated by Priel and Silberberg (2004) that IVM is likely to bind to separate sites on $P2X_4$ with a high affinity IVM binding site which results in an increase in maximal current activated by saturating agonist concentration and a second low affinity binding site which causes a delay to the deactivation of the channel.

1.4.2.2.3 Non-selective antagonists of $P2X_4$

The study of $P2X_4$ has been hampered mainly due to the lack of selective antagonists available commercially. Up until recently, researchers had to rely on the use of broad-spectrum antagonists such as suramin, blue brilliant G (BBG) dye and PPADS, as well as other inhibitory methods such as divalent cations, pH and several drugs (anti-depressants and statins). Each of these will be described below.

1.4.2.2.3.1 Broad-spectrum antagonists

Suramin is a broad-spectrum purinergic receptor antagonist that shows very weak activity at mouse, rat and human $P2X_4$ orthologues. Maximal inhibition of currents varies between 11-35% with $pIC_{50} > 4$ displayed for all orthologues (Jones et al., 2000). In addition to this, another broad-spectrum antagonist pyridoxalphosphate-6-azophenyl-2',4'-disulfonic acid (PPADS) has been illustrated to fully inhibit human and mouse, but not rat, $P2X_4$ with pIC_{50} of approximately 5 for both. Lastly, 2',3'-O-(2,4,6-trinitrophenyl) ATP (TNP-ATP) displayed a weak inhibitory action at $P2X_4$ with a competitive nature (Hernandez-Olmos et al., 2012, Balazs et al., 2013a).

1.4.2.2.3.2 Ethanol

The $P2X_4$ has been shown to be the most abundant P2XR subtype in mammalian CNS and the most sensitive towards ATP. Ethanol has been shown to inhibit ATP-gated currents in $P2X_4$ in HEK293 cells through whole-cell patch-clamp (Ostrovskaya et al., 2011). IVM has also been shown to antagonize the inhibitory action of ethanol at $P2X_4$ by interfering with ethanol binding to the channel (Asatryan et al., 2010).

1.4.2.2.3.3 Divalent cations

Several divalent cations have been associated with having an inhibitory effect towards ATP-gated currents in $P2X_4$. Extracellular Zn^{2+} at high concentrations (>100 mM) and Cd^{2+} was shown to inhibit $P2X_4$ currents in a voltage-dependent manner

(Garcia-Guzman et al., 1997). Extracellular Cu^{2+} was also shown to inhibit $P2X_4$ current but in a non-competitive and voltage-independent manner (Acuna-Castillo et al., 2000).

1.4.2.2.3.4   pH

Studies have revealed that extracellular H^+ negatively modulates $P2X_4$ with acidic environments (pH<6) completely abolishing channel activity while a pH above physiological levels potentiates channel activity (Clarke et al., 2000). $P2X_4$ has been shown to be predominantly found within the intracellular lysosomal compartment and the inhibition of channel activity at low pH may be an important physiological regulator for this receptor (Qureshi et al., 2007).

1.4.2.2.3.5   Antidepressants

The majority of research surrounding $P2X_4$ has been focused on neuropathic pain within the CNS. Several clinically used antidepressants such as paroxetine, fluoxetine and clomipramine have been illustrated to have an inhibitory effect towards $P2X_4$ (Nagata et al., 2009). It was hypothesized that these drugs mediate analgesic effects for the treatment of neuropathic pain through $P2X_4$ inhibition. Amongst them, paroxetine has been shown to be the most potent $P2X_4$ inhibitor with a non-competitive nature and a pIC_{50} of 5.7, although it is much more potent as a serotonin reuptake inhibitor (Nagata et al., 2009). In addition to this, the inhibitory effect of paroxetine appears to be non-selective as studies by Dao-Ung et al. (2015) illustrated their ability to block human $P2X_7$. The antidepressant amitriptyline was also studied further but was revealed to inhibit mouse and rat $P2X_4$, but not the human isoform (Sim and North, 2010).

1.4.2.2.3.6   Statins and cholesterol depleting agents

More recently, HMG-CoA reductase inhibitor, fluvastatin has been reported to have an inhibitory activity on heterologously expressed human $P2X_4$ and native $P2X_4$ in human THP-1 monocytes as assessed through intracellular Ca^{2+} measurements (Li and Fountain, 2012). It was speculated that the inhibitory effect of fluvastatin on the $P2X_4$-mediated Ca^{2+} response was due to depletion of cellular cholesterol (Li and Fountain, 2012).

1.4.2.2.4   Selective antagonists

For a long time, researchers had to rely on non-selective P2XR antagonists such as TNP-ATP, BBG) and paroxetine, to study $P2X_4$. However, these agents possess low

affinity for $P2X_4$ and are significantly more potent at other targets (Gum et al., 2012). Recently, growing evidence that highlights the importance of $P2X_4$ in health and disease has triggered interest in the development of selective receptor antagonists. The discovery of selective $P2X_4$ antagonists will, therefore, present a new avenue for scientific research to selectively target $P2X_4$ therapeutically.

1.4.2.2.4.1   5-BDBD

Benzodiazepine derivative 5-BDBD is one of the first selective $P2X_4$ antagonists to be described in the literature that has become commercially available (Fisher et al., 2005). It has been reported as a moderately potent and selective $P2X_4$ antagonist with an IC_{50} value of 0.5 μM in CHO cells. The application of two different concentrations of 5-BDBD resulted in a rightward shift in the ATP dose-response curve indicating that 5-BDBD acts as a competitive antagonist to the $P2X_4$ receptor (Balazs et al., 2013b). However, radio-ligand binding assays illustrated that 5-BDBD was unable to displace $[^{35}S]ATP\gamma S$ binding to $P2X_4$ indicating that rather than acting as a competitive antagonist, it has an allosteric nature towards $P2X_4$ (Muller, 2015).

1.4.2.2.4.2   N-substituted phenoxazine derivative

More recently, two compounds derived from N-substituted phenoxazine were identified as potent and selective allosteric $P2X_4$ antagonists. One of the derivatives is *N*-(Benzyloxycarbonyl)phenoxazine (PSB-12054), a potent antagonist of the human $P2X_4$ receptor (IC_{50} value of 0.189 μM), but less potent towards rat (IC_{50} value of 2.1 μM) and mouse (IC_{50} value of 1.77 μM) $P2X_4$. It has been reported to possess high selectivity for human $P2X_4$ with over 50-fold against $P2X_2$, $P2X_3$ and $P2X_7$ and over 30-fold against $P2X_1$ (Hernandez-Olmos et al., 2012).

The second less potent, but more water-soluble, of the two derivatives is *N*-(p-methylphenylsulfonyl)phenoxazine (PSB-12062). PSB-12062 was shown to have similar potency in all three species: human (IC_{50} value of 1.38 μM), rat (IC_{50} value of 0.928 μM) and mouse (IC_{50} value of 1.76 μM) $P2X_4$ (Hernandez-Olmos et al., 2012). It has been shown to be allosteric in nature with 35-fold selectivity towards $P2X_4$ versus $P2X_1$, $P2X_2$, $P2X_3$, and $P2X_7$ (Hernandez-Olmos et al., 2012). However, PSB-12062 was unable to completely block ATP-induced $P2X_4$-mediated Ca^{2+} influx even when used at high concentrations (>30 μM).

1.4.2.2.4.3   Carbamazepine derivatives

Several carbamazepine derivatives were recently investigated as potential $P2X_4$ receptor antagonists, with N,N-diisopropyl-5H-dibenz[b,f]azepine-5-carboxamide being found to be the most potent towards human $P2X_4$ (IC_{50} of 3.44 μM). However, this compound was found to be less potent at mouse and rat $P2X_4$ (Tian et al., 2014). Despite its potency towards human $P2X_4$, it appeared to lack selectivity against two other P2X subtypes ($P2X_1$ and $P2X_3$) but was selective versus $P2X_2$ and $P2X_7$. Further optimization will be required to improve the selectivity of this compound.

1.4.2.2.4.4   BX430

Phenylurea BX430 (1-(2,6-dibromo-4-isopropyl-phenyl)-3-(3-pyriudyl)urea is a recently discovered $P2X_4$ antagonist. Patch-clamp studies illustrated BX430 to have a sub-micromolar potency with IC_{50} value of 0.54 μM, and 10 – 100 fold selectivity toward $P2X_4$ receptor versus other P2XR subtypes (Ase et al., 2015). Acting through a noncompetitive allosteric route, BX430 has been shown to potently antagonize the zebrafish $P2X_4$ receptor but has no effect on rat and mouse $P2X_4$ orthologs (Ase et al., 2015).

1.4.2.3   Subcellular localization, trafficking and regulation

The subcellular distribution of P2XR subunits are all different because of their varying trafficking properties. While some are localized within the endoplasmic reticulum (ER), others are predominantly found at the cell surface or within endosomes and lysosomes (Robinson and Murrell-Lagnado, 2013). It is thought that the trafficking of receptors to and from the plasma membrane serves as a means to rapidly up- or down-regulate cellular responses mediated by ATP.

1.4.2.3.1   Subcellular Localization

$P2X_4$ have been described to undergo rapid constitutive internalization from the plasma membrane and to be predominantly expressed within late endosomes and intracellular lysosomal compartments (Bobanovic et al., 2002, Qureshi et al., 2007, Robinson and Murrell-Lagnado, 2013, Vacca et al., 2009) (Figure 1.5). They resist degradation within the lysosome by their N-linked glycans which can be found within the intra-luminal loop of the receptor (Boumechache et al., 2009). The localization of $P2X_4$ to endolysosomes was demonstrated in immune and endothelial cells (Bobanovic et al., 2002, Qureshi et al., 2007, Royle et al., 2002). Various studies

have revealed that the constitutive endocytosis of $P2X_4$ receptor is a process that is regulated by clathrin and can be inhibited by a pharmacological compound known as dynasore. The inhibition of $P2X_4$ endocytosis results in the accumulation of P2X4 receptor at the cell membrane of cells (Bobanovic et al., 2002, Boumechache et al., 2009, Qureshi et al., 2007, Royle et al., 2002). Two examples include the contradicting effect of dynasore in cultured microglial cells and bone marrow derived macrophages. *In vitro* studies of microglial cells treated with LPS showed an upregulation of $P2X_4$ expression indicating that they relied on the continuous cycling of the receptors to and from the cell surface. However, treatment of BMDM cells with LPS had a significantly different effect and did not result in an increase in cell surface $P2X_4$ expression. Despite various studies, the regulation of plasma membrane expression of $P2X_4$ is not well understood.
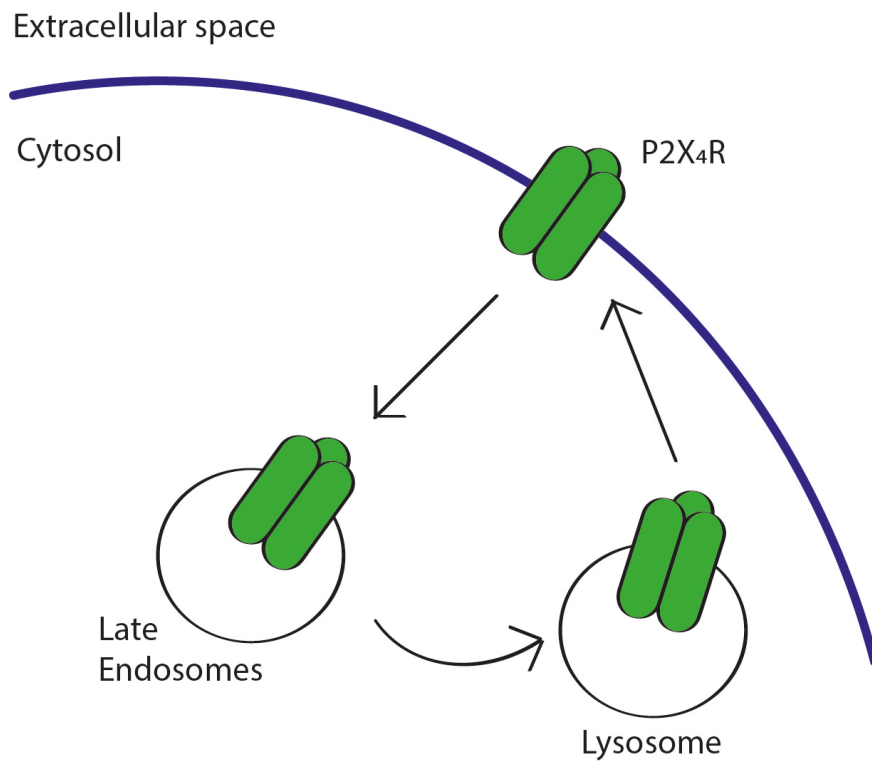
Figure 1.5. Subcellular distribution of P2X$_4$ receptor. P2X$_4$ are constitutively recycled between the plasma membrane and late endosomes and lysosomes. Within the lysosomes, P2X$_4$ remain stable and are not degraded. Endocytosis of P2X$_4$ involves a clathrin- and dynamin-dependent process. Adapted from Robinson and Murrell-Lagnado (2013).

1.4.2.3.2 Receptor Trafficking and Regulation

Trafficking of P2XR is determined by a common motif YXXXK in the C-terminus (Chaumont et al., 2004). $P2X_4$ has two tyrosine-based endocytic motifs found in the C-terminus and one dileucine-like motif within the N terminus (Royle et al., 2005, Royle et al., 2002, Qureshi et al., 2007). Mutations of one of the tyrosine-based endocytic motifs resulted in slowing down of receptor endocytosis while mutation of the leucine motif within the N terminal resulted in failure of receptor targeting to lysosomes (Royle et al., 2005, Royle et al., 2002).

The trafficking of P2XR to and from the cell surface is regulated by their activation in a Ca^{2+}-dependent manner (Robinson and Murrell-Lagnado, 2013). For $P2X_4$ that is predominantly intracellular, enhanced translocation of intracellular receptors to the cell surface as a mechanism of up-regulating receptor function. In macrophages, $P2X_4$ surface expression has been shown to be increased following stimulation that promotes lysosome exocytosis via alkalinazation of lysosomes or increasing cytosolic Ca^{2+} level (Qureshi et al., 2007). In addition to their activation, the trafficking and targeting of P2XR is also regulated by their interactions with other proteins and lipids which can vary from cell to cell (Robinson and Murrell-Lagnado, 2013, Pike, 2004). $P2X_4$ expressed in HEK293 cells have been illustrated to associate with lipid rafts generated using a detergent-free approach (Allsopp et al., 2010). The exact mechanism to which $P2X_4$ target rafts has not been determined.

1.4.2.4 Single nucleotide polymorphism

Single nucleotide polymorphisms (SNPs) are common in the genes encoding human P2XR (Caseley et al., 2014). Although $P2X_7$ present the highest number of polymorphisms and contain a large set of SNPs, reports within the literature identified four nonsynonymous polymorphisms in the human $P2X_4$ gene (Stokes et al., 2011). Genotyping of two Australian cohorts by Stokes et al. (2011) illustrated polymorphism of $P2X_4$ as a potential risk factor for high pulse pressure. It was identified that this SNP caused substitution of tyrosine315 with cysteine in the human $P2X_4$ causing impairment of the receptor function. Electrophysiological analysis revealed that this mutation caused a significant reduction of ATP-induced peak current amplitude when compared to wild-type $P2X_4$ (Stokes et al., 2011). It was speculated that this mutation resulted in the disruption of the agonist binding site of the receptor, hence impairing receptor function.

1.4.2.5　　　　　Expression in immune cells

Amongst the P2XR, $P2X_4$, along with $P2X_7$, are the predominant receptors found within immune cells (Boumechache et al., 2009, de Rivero Vaccari et al., 2012, Jacob et al., 2013). The expression of $P2X_4$ has been described in almost all immune cells including lymphocytes (B, T lymphocytes and NK cells), monocytes/macrophages, mast cells and eosinophils. Despite its widespread distribution in immune cells, no studies have reported the expression of $P2X_4$ in neutrophils. A thorough quantitative mRNA analysis by Wang et al. (2004) identified mRNA expression of $P2X_4$ to be the highest in lymphocytes and monocytes. The high expression of $P2X_4$ in T lymphocytes and B lymphocytes was also elaborated further in studies reported by Di Virgilio et al. (2001) and Sluyter et al. (2001), respectively. mRNA expression of $P2X_4$ was also detected in NK cells by Gorini et al. (2010). Corroborating with reports by Wang et al. (2004), various other studies have also illustrated the expression of $P2X_4$ in monocytes, macrophages and microglia where it plays a role in the release of inflammatory mediators (Ulmann et al., 2010, Tsuda et al., 2003, Raouf et al., 2007, Bowler et al., 2003). Following peripheral nerve injury, the expression of $P2X_4$ on the surface of spinal microglia was described to be upregulated which results in the release of brain-derived neurotrophic factor (BDNF) contributing to chronic neuropathic pain (Tsuda et al., 2003, Trang and Salter, 2012). Whole-cell recordings of mouse peritoneal macrophages further illustrated functional $P2X_4$ through ATP-evoked inward currents (Sim et al., 2007) and co-expression of $P2X_4$ and $P2X_6$ subunits was also identified in subpopulations of rat Kupffer cells (the liver macrophage). All murine and rat macrophage cell lines have been shown to express $P2X_4$ subtypes which have also been demonstrated to be functionally implicated in evoking ATP-mediated increase in cytosolic Ca^{2+} levels (Coutinho-Silva et al., 2005, Bowler et al., 2003). In humans, the expression of $P2X_4$ has been reported in alveolar macrophages (Myrtek et al., 2008) and monocyte derived macrophages (Stokes et al., 2011, de Rivero Vaccari et al., 2012). However, no functional implications through induction of intracellular Ca^{2+} elevation have been demonstrated in alveolar macrophages.

In addition to monocytes, macrophages and lymphocytes, co-expression of $P2X_4$ and $P2X_7$ subunits was identified in rat dendritic cells (Xiang et al., 2006). Human dendritic cells were found to express mRNA for $P2X_4$ (Di Virgilio et al., 2001, Berchtold et al., 1999) and evidence of functional $P2X_4$ was described in immature and mature dendritic cells through Ca^{2+} measurement studies (Ferrari et al., 2000b). Finally, mRNA transcripts for $P2X_4$ have been described in human eosinophils

(Ferrari et al., 2000a, Ferrari et al., 2006, Idzko et al., 2001) and in human lung mast cells (HLMC) (Bradding et al., 2003). Despite reports of $P2X_4$ expression in eosinophils and mast cells, their function remains unexplored.

1.4.3 ATP as DAMP signal to activate purinergic receptors in macrophages

For many years, the main source of ATP acting on purinergic receptors was thought to be damaged or dying cells. However, it is now clear that many healthy cells can release ATP physiologically in response to many factors such as mechanical distortion, hypoxia and other agents (Bodin and Burnstock, 2001). For example, during acute inflammation, there is an increase in ATP release from endothelial cells which can act on cell surface receptors P2XR and P2YR. This extracellular ATP is quickly degraded by a series cell surface enzymes called ectonucleotidases into ADP, AMP and adenosines (Cekic and Linden, 2016). These enzymes can be further categorized into nucleoside triphosphate diphosphohydrolases (NTPDases 1, 2, 3 and 8), nucleotide pyrophosphatases (NPP 1, 2 and 3), alkaline phosphatase and 5' nucleotidase (Yegutkin, 2008, Robson et al., 2006). Ectonucleotidases, ENTPDases, like CD39 degrades ATP into ADP and ADP into AMP while 5' nucleotidase, like CD73, converts AMP into adenosine (Burnstock and Boeynaems, 2014).

Macrophages are thought to be able to respond to extracellular ATP gradients at three basic stages. First, macrophages migrate towards increasing ATP concentration, second, they use the ATP gradients from apoptotic cells as a 'find-me' signal to locate and phagocytose the dying cells. Lastly, in the presence of high concentrations of ATP, macrophages are able to robustly secrete pro-inflammatory cytokines (Desai and Leitinger, 2014). The presence of extracellular ATP has been shown to inhibit macrophage-mediated cytotoxicity of human tumour cells (Cameron, 1984)

1.4.4 Role of P2 receptors in macrophages

P2XR are widely distributed throughout tissues, both excitable and non-excitable, of the mammalian system (Zemkova et al., 2008). Despite their wide distribution, it has been illustrated that the mammalian brain has the highest levels of purines and the greatest variety of purinergic receptors (Buell et al., 1996, Seguela et al., 1996). In other tissues of the mammalian system, the distribution of P2XR has been described to be more variable with $P2X_4$ and $P2X_7$ being the predominant P2XR expressed in immune cells (Buell et al., 1996, Soto et al., 1996b). Tabulated information regarding the distribution of different subtypes of P2XR and P2YR in the

mammalian system is shown in Table 1.2 and 1.3, respectively. Table 1.4 illustrated the roles of P2XR and P2YR in macrophages of the immune system.

Most research in immune cells like macrophages has focused on understanding the role of $P2X_7$ (Table 1.4) (Griffiths et al., 1995, Perregaux and Gabel, 1994). $P2X_7$ has been shown to be expressed in human monocyte-derived macrophages and also in BAC1.2F5 mouse macrophages with their main function being to mediate phospholipase (PL) D activity (el-Moatassim and Dubyak, 1993, Hickman et al., 1994). In RAW 264.7 mouse macrophages, ATP released through stimulation with LPS increased nitric oxide synthase (NOS) expression and production of nitric oxide (NO) and has been shown to induce activation and production of tissue factors that favors thrombosis (Sperlagh et al., 1998, Tonetti et al., 1994). $P2X_7$ has also been shown to be important in mediating phagocytosis where over-expression of $P2X_7$ was observed during phagocytosis of non-opsonized beads and heat-inactivated bacteria (Gu et al., 2012, Gu et al., 2010). Loss of function polymorphisms of $P2X_7$ and $P2X_4$ are associated with reduction in phagocytosis and were seen in patients suffering from macular degeneration (Gu et al., 2013).

Although $P2X_7$ have been illustrated to play a dominant role in macrophages of the immune system, evidence of the involvement of other receptors has slowly accumulated. Studies in the spleen and peritoneal macrophages of mouse J774 allowed the identification of multiple P2XR and P2YR subtypes (Coutinho-Silva et al., 2005). In human alveolar macrophages, mRNA expression of multiple P2XR ($P2X_1$, $P2X_4$, $P2X_5$ and $P2X_7$) and multiple P2YR ($P2Y_2$, $P2Y_4$, $P2Y_6$, $P2Y_{11}$, $P2Y_{13}$ and $P2Y_{14}$) were observed (Myrtek et al., 2008). The potential roles of $P2X_4$ in macrophages, often working together with $P2X_7$, have also been slowly emerging. Examples of this include the possible involvement of $P2X_4$ in the ATP-mediated current of human macrophages as slowly desensitizing ATP-induced currents were abolished in $P2X_4$ knockout mice (Brone et al., 2007). Studies using siRNA against $P2X_4$ illustrated a potential role of $P2X_4$ in regulating $P2X_7$-induced cell death (Kawano et al., 2012a, Kawano et al., 2012b).

In addition to P2XR, P2YR have also been illustrated to be expressed and found to be functional in macrophages of the immune system. Knockout studies showed that $P2Y_2$ and $P2Y_4$ are the dominant P2YR subtypes in mouse peritoneal macrophages (del Rey et al., 2006). Out of the P2YR, involvement of $P2Y_2$ has been studied the most in macrophages. DAMP signals such as nucleotides, are released by apoptotic

cells and promote $P2Y_2$-dependent recruitment of phagocytic macrophages. This recruitment of phagocytic macrophages was shown to be reduced in $P2Y_2$-deficient mice (Elliott et al., 2009).

Purinergic receptors	Potential function
$P2Y_1$, $P2Y_2$, $P2Y_4$, $P2Y_{11}$, $P2X_1$, $P2X_4$, $P2X_7$	Increase in intracellular Ca^{2+}
$P2X_7$	Release of IL-1β Release of cathepsins
$P2X_4$, $P2X_7$	Regulation of autophagy Release of PGE_2
$P2Y_2$, $P2Y_{12}$, $P2X_1$, $P2X_3$	Promotion of chemotaxis and phagocytosis
$P2Y_4$, $P2Y_6$, $P2Y_{11-14}$, $P2X_{1-6}$	Undefined roles

Table 1.4. **Role of purinergic receptors in human macrophages.** Potential roles of P2XR and P2YR in macrophages of the immune system. Adapted from Jacobson et al., 2013.

1.4.4.1 Role of P2 receptors in control of cytokines of immune cells

The production of cytokines in the immune system is a tightly regulated process as dysregulation can act as a contributor to disease pathologies. Studies have revealed that the modulation of P2 receptors can affect production of cytokines.

1.4.4.1.1   P2X receptors

The most well studied P2 receptor that has been associated with cytokine secretion is $P2X_7$. In macrophages, $P2X_7$ have been associated with roles such as mediating pro-inflammatory response achieved through the secretion of IL-1β and bacterial killing. It has been described in several cellular systems that a rise in intracellular Ca^{2+} level promoted by $P2X_7$ activation is required for IL-1β posttranslational processing (Brough et al., 2003, Gudipaty et al., 2003). The involvement of $P2X_7$ in IL-1β secretion is evident from studies illustrating that high ATP concentrations (>1 mM) is an effective stimuli for posttranslational processing of IL-1β and that this high agonist concentration is a requirement consistent with activation of $P2X_7$. This was confirmed with studies using $P2X_7$-deficient mice where ATP-induced secretion of IL-1β was abolished (Qu et al., 2007, Solle et al., 2001).

Apart from $P2X_7$, there is generally no association with the activation of other P2X receptors and cytokine modulation. However, more recently, activation of $P2X_4$ has been shown to mediate prostaglandin E_2 (PGE_2) release by tissue-resident macrophages, initiating inflammatory pain (Ulmann et al., 2010). In addition to this, $P2X_4$ knockdown studies in mouse macrophages RAW264.7 showed that $P2X_4$ modulates $P2X_7$-dependent inflammatory functions such as release of high mobility group box 1 (HMGB1) and IL-1β production (Kawano et al., 2012a). Further study by Chen et al. (2013) illustrated that $P2X_4$ expression was co-localized with NLRP3 inflammasome, IL-1β and IL-18 expression and that ATP-$P2X_4$ signaling regulates IL-1 family cytokine secretion.

1.4.4.1.2   P2Y receptors

$P2Y_6$ is a P2YR subtype that has been well-studied in macrophages and has gained much interest. P2Y6 expression has been shown to be upregulated following macrophage activation (del Rey et al., 2006) and that knocking out $P2Y_6$ in mice impaired their ability to secrete cytokine IL-6 and macrophage inflammatory protein 2 (MIP-2) (Bar et al., 2008). Several reports have also linked $P2Y_6$ function to the expression of IL-8, which is important for the recruitment of neutrophils to sites of

infection (Luster, 1998, Mukaida, 2003). Although the mechanism by which $P2Y_6$ mediates cytokine production is still not clear, it is speculated that it may involve the activation of PLC and the involvement of intracellular Ca^{2+}. The rise in intracellular Ca^{2+} is thought to be coupled to an ERK-activated signaling pathway which ultimately leads to the expression of IL-8 (Warny et al., 2001). Another speculation is that a rise in intracellular Ca^{2+} concentrations is linked to NF-kβ transcription factor which has been associated with expression of cytokine genes (Korcok et al., 2005).

Amongst the P2Y receptors, $P2Y_{11}$ is another subtype that has been studied for their role in modulating cytokine secretion, especially in human dendritic cells. In dendritic cells, $P2Y_{11}$ has been associated with IL-12 and IL-23 production, both of which are key cytokines for the activation of Th_1 state (Trinchieri, 2003b, Trinchieri, 2003a, Langrish et al., 2004). $P2Y_{11}$ has also been reported as a functional receptor in macrophages with its activation speculated to induce polarization of macrophages towards M1 phenotype, characterized by an increase in the production of IL-12 cytokines (Sakaki et al., 2013b). Further to this, the regulation of IL-12 and IL-23 expression by $P2Y_{11}$ is thought to be achieved through the activation of $G_{\alpha s}$-type G protein which leads to the activation of adenylate cyclase and a rise in cAMP level (Wilkin et al., 2002, Gabel, 2007). Finally, $P2Y_2$ has also been shown to mediate potentiation of PGE_2 release which is involved in the induction of NOS resulting in the stimulation of chemokine CCL2 production (Stokes and Surprenant, 2007).

1.4.5 Therapeutic exploitation

In the past decade, P2XR and P2YR have gained significant interest as potential therapeutic targets as various studies have illustrated their link with diseases such as atherosclerosis, thrombosis, diabetes and neuropathic pain (Burnstock and Williams, 2000, Balasubramanian et al., 2010, Kaczmarek-Hajek et al., 2012). Many efforts have been invested in designing selective and potent agonists and antagonists, small molecules and antibodies to target these receptors. Despite continued efforts, few examples of therapeutically useful compounds exist. This is mainly because P2 receptors display a wide tissue distribution making it difficult to target them specifically. In addition to this, P2 receptors are tightly regulated by enzymes such as ectonucleotidases and may be co-activated with other receptors (purinergic and non-purinergic). For these reasons, developing novel drugs to target P2 receptors for the treatment of macrophage-associated pathologies remain a challenging area for the pharmaceutical industry.

Amongst the P2XRs, $P2X_3$ has been targeted for visceral pain due to its limited distribution on primary afferent fibers and more recently, it has also been targeted for treatment of chronic cough (Abdulqawi et al., 2015). $P2X_7$ have been studied extensively leading to the development of many potent small molecules and selective blockers by pharmaceutical companies. $P2X_7$ were initially identified as a potential target for the treatment of rheumatoid arthritis but trials only reached phase IIb before being terminated (Keystone et al., 2012, North and Jarvis, 2013). In addition to this, $P2X_4$ has gained significant interest as a target for the treatment of chronic pain. This was derived from several studies illustrating that following spinal cord injury or peripheral nerve injury, $P2X_4$ expression is upregulated in activated microglia and that $P2X_4$ knockout mice, tactile allodynia was significantly reduced compared with wild-type mice (Tsuda et al., 2003). Therapeutic exploitation of P2YR have been more successful with $P2Y_2$ agonist and antagonist being used as a treatment for dry eye disease and antimicrobial treatment, respectively (Jacobson et al., 2012, Lau et al., 2014), and $P2Y_{12}$ antagonists (i.e. clopidogrel and ticagrelor) being used clinically for the treatment of acute coronary syndrome (ACS) (Fuller and Chavez, 2012, Jacobson et al., 2012, Chua and Ignaszewski, 2009).

1.5   Key aims and outline of project

It is apparent from the current literature that human macrophages express various P2XRs and P2YRs. There is a clear understanding to what the role of $P2X_7$ is in human macrophages allowing it to be exploited therapeutically with several drugs being developed to target this receptor. However, even though $P2X_4$ is highly expressed in immune cells, the lack of selective antagonists and agonists for this receptor mean that our understanding of the functional role of $P2X_4$ in human macrophages is still lacking. Many recent studies have proposed potential roles of $P2X_4$ in the context of inflammatory responses within the immune system, which can be associated with inflammatory diseases. Therefore, this project hopes to study the contribution of $P2X_4$ towards ATP-evoked Ca^{2+} response in human macrophages using various pharmacological tools while also elucidating a functional role of $P2X_4$. To achieve this, three key aims were set during this project:

1) To identify key pharmacological tools which can be used to selectively isolate $P2X_4$-mediated Ca^{2+} influx in human cell lines. This will be discussed in chapter 3 of the thesis where I performed a side-by-side comparison of human THP-1 monocytic cell line *vs.* human THP-1 differentiated macrophages cell line.

2) To identify and characterize the contribution of $P2X_4$ activation towards intracellular Ca^{2+} level in human primary macrophages using the limited pharmacological tools available for $P2X_4$. As there are two main ways to generate human monocyte-derived macrophages (MDM); either through stimulation with recombinant human GM-CSF (GM-MDM) or M-CSF (M-MDM), chapter 4 will discuss a side-by-side comparison to identify which of the two, is a better model to study $P2X_4$-mediated Ca^{2+} response.

3) To elucidate a functional role of $P2X_4$ in human macrophages, mainly in the context of cytokine and chemokine secretion in response to ATP stimulation. This will be discussed in chapter 5 of the thesis focusing on the approaches used to select candidate genes that may be affected by $P2X_4$ activation.

Overall, this project hopes to increase the current understanding of the usefulness of some of the pharmacological tools commercially available for $P2X_4$ and expand our knowledge on the role of $P2X_4$ activation in human macrophages.

Chapter 2: Materials and Methods

2.1 Materials and reagents

A comprehensive list of all ligands, modulators and inhibitors used throughout the study are presented in tables 2.1 to 2.5.

Table 2.1: Extracellular nucleotides

Nucleotide	Supplier	Purity	Final conc.
ATP	Sigma	≥ 99%	$0.01 - 1000$ μM
α,β-meATP	Sigma	≥ 93%	$1 - 100$ μM
BzATP	Sigma	≥ 93%	$1 - 500$ μM

Table 2.2: Purinergic receptor modulator

Compound	Function	Supplier	Final conc.	Ref
Ivermectin	$P2X_4$ positive allosteric modulator	Tocris	3 μM	Li & Fountain, (2012)

Table 2.3: Purinergic receptor antagonists

Compound	Receptor target	Supplier	Final conc.	Ref
PSB-12062	$P2X_4$	Sigma	10 μM	Hernandez-Olmos et al. (2012)
5-BDBD	$P2X_4$	Tocris	10 μM	Fischer et al. (2004) Balazs et al. (2013)
A438079	$P2X_7$	Abcam	10 μM	Bhaskaracharya et al. (2014)
Ro0437626	$P2X_1$	Tocris	30 μM	Jaime-Figueroa et al. (2005)
MRS2211	$P2Y_{13}$	Tocris	10 μM	Kim et al. (2005)
NF340	$P2Y_{11}$	Tocris	10 μM	Kim et al. (2005)
AR-C118925xx	$P2Y_2$	Tocris	10 μM	Kemp et al. (2004)

Compound		Supplier	Final conc.	Ref
MRS2578	P2Y$_6$	Tocris	10 μM	Mamedova et al. (2004)
				Koizumi et al. (2007)
MRS2500	P2Y$_1$	Tocris	1 μM	Kim et al. (2003)
				Hechler et al. (2006)

Table 2.4: Inhibitors and modulators

Compound	Function	Supplier	Final conc.	Ref
Thapsigargin	SERCA pump inhibitor	Santa-Cruz	5 μM	Robinson et al. (1992)
				Shima et al. (1992)
U-73122	PLC inhibitor	Tocris	10 μM	Hollywood et al. (2010)
				McMillan & McCarron (2010)
Dynasore	Dynamin inhibitor	Sigma	80 μM	Macia et al. (2006)
				Kirchhausen et al. (2008)
Vacuolin-1	Ca^{2+}-dependent lysosomal fusion inhibitor	Santa-Cruz	1 μM	Cerny et al. (2004)
				Huynh et al. (2005)

Table 2.5: Differentiation and stimulating factors

Compound	Function	Supplier	Final conc.	Ref
PMA	PKC activator	Abcam	320 nM	Ke et al. (2015)
				Park et al. (2007)
				Zhang et al. (2014)
rhuGM-CSF	Differentiation factor	Peprotech	10 ng/ml	Dabritz et al. (2015)
				Buttari et al. (2014)
				Castiello et al. (2011)
rhuM-CSF	Differentiation factor	Peprotech	10 ng/ml	Buttari et al. (2014)

2.2 Cell culture

2.2.1 THP-1 cells

2.2.1.1 General maintenance

THP-1 cells are a human cell line originally derived from a patient with acute monocytic leukemia. They have become one of the most widely used cell lines to study function and regulation of monocytes and macrophages (Qin, 2012). Cells were obtained from European Collection of Cell Cultures (ECACC) and cultured in Roswell Park Memorial Institute (RPMI)-1640 media containing 0.3 g/L L-Glutamine (Lonza), supplemented with 10% (v/v) heat-inactivated foetal bovine serum (FBS; PAA Laboratories) and 1% (v/v) penicillin-streptomycin solution containing 50 units/ml penicillin and 50 μg/ml streptomycin (Life Technologies).

2.2.1.2 Cell passage

THP-1 cells were cultured in suspension, in vented T75 flasks (Nunc) at 37°C in a humidified 5% CO_2 incubator. Cells were routinely counted using a haemocytometer and passaged by diluting them to the required cell density. Cell density was maintained below 8×10^5 cells/ml to prevent spontaneous differentiation into macrophages.

2.2.1.3 Cryopreservation and Thawing

For cryopreservation, cells were stored at a density of 1×10^6/ml in THP-1 cell culture media supplemented with 10% (v/v) glycerol. Cells were added into cryovials (Nunc) and stored in a Mr Frosty™ freezing container (Thermo Scientific) for overnight storage at -80°C before being transferred into a liquid nitrogen tank (-196°C). To thaw, cells were removed from liquid nitrogen and gently warmed at 37°C in a water bath until 70% thawed. Cells were then diluted in 10 ml of THP-1 culture media in a gentle manner to dilute the cryopreservant. Cells were centrifuged at 805 x *g* for 7 minutes at room temperature and supernatant was removed. The resulting cell pellet was resuspended in 5 ml of THP-1 culture media and transferred to a vented T25 flask for incubation at 37°C in a humidified 5% CO_2 incubator.

2.2.1.4 P2X$_4$ Knockdown THP-1 cells

P2X$_4$ knockdown (P2X$_4$-KD) THP-1 cells were generated by infecting THP-1 cells with lentiviral pLKO.1-puro shRNA constructs that target the human P2X$_4$ receptor. Alongside this, THP-1 cells with non-target control vectors were also prepared.

These cells were cultured in THP-1 cell culture media and stable expression was maintained by puromycin supplementation at a final concentration of 1 μg/ml (InvivoGen).

2.2.1.5 THP-1-differentiated macrophages

THP-1-differentiated macrophages were generated by stimulating THP-1 cells with 320 nM of phorbol 12-myristate 13-acetate (PMA) (Sigma-Aldrich) for 48 hours at 37°C in a humidified 5% CO_2 incubator. To check for differentiation, a change in cell morphology with increasing granularity was observed through an inverted microscope.

2.2.2 1321N1 astrocytoma cells

2.2.2.1 General maintenance

1321N1 is a human astrocytoma cell line derived from the parent line U-118 MG that originates from malignant gliomas (Pontén and Macintyre, 1968). 1321N1 cells was a kind gift from Professor Jens George Leipziger (Aarhus University) and were cultured in Dulbecco's Modified Eagle Media containing L-Glutamine (0.6g/L) (DMEM) supplemented with 10% (v/v) heat-inactivated FBS and 1% (v/v) penicillin-streptomycin solution containing 50 units/ml penicillin and 50μg/ml of streptomycin.

2.2.2.2 Cell passage

Human 1321N1 cells are adherent and were cultured in vented T75 flasks (Nunc) at 37°C in a humidified 5% CO_2 incubator. Cells were passaged once they reached approximately 70% confluency. This was achieved by rinsing cells with 5 ml Dulbecco's phosphate buffered saline (dPBS) followed by treatment with 3 ml of Trypsin solution (Lonza) at 37°C for 2-3 minutes. To detach the adherent cells, gentle agitation was applied to the flask and the enzymatic reaction was terminated by diluting trypsin with 1321N1 cell culture media in a 1:1 ratio. Cells were centrifuged at 805 x g for 7 minutes at room temperature and the supernatant was discarded. The cell pellet was resuspended in 1321N1 culture media and used or re-seeded into fresh T75 flasks for culture.

2.2.2.3 Cryopreservation and Thawing

Cryopreservation of cells was performed as described for THP-1 cells (Section 2.2.1.3), substituting THP-1 cell culture media for 1321N1 culture media. In addition to this, cells were resuspended in 45% (v/v) 1321N1 culture media, 45% (v/v) FBS

and 10% (v/v) dimethyl sulfoxide (DMSO). DMSO was used in cryopreservation of 1321N1 cells in substitution of glycerol in THP-1 cells.

2.2.2.4 hP2X$_4$ pLVX-IRES-mCherry 1321N1 astrocytoma cells

hP2X$_4$ pLVX-IRES mCherry 1321N1 were cultured in 1321N1 culture media and stable expression of mCherry was maintained by regular confirmation using the fluorescence microscope and re-sorting for highly expressing mCherry cells. To limit heterogeneity of hP2X$_4$ mCherry 1321N1 cells within experiments, cells from the same passage were cryopreserved following sorting and were thawed out when necessary to perform an experiment.

2.2.3   HEK293T/17 cells

2.2.3.1 General maintenance

HEK293 is a cell line isolated from human embryonic kidney cells (Thomas and Smart, 2005). HEK293T/17 cells are derived from HEK293 cells that have been transfected with a gene encoding large T antigen, with clone 17 being selected specifically for its high transfectability. These cells were obtained from ECACC and were cultured in DMEM containing L-Glutamine (0.6 g/L) supplemented 10% (v/v) heat-inactivated FBS and 1% (v/v) penicillin-streptomycin solution containing 50 units/ml of penicillin and 50 μg/ml of streptomycin.

2.2.3.2 Cell passage

HEK293T/17 cells are adherent and were cultured in vented T75 flasks at 37°C in a humidified 5% CO_2 incubator. HEK293T cells were passaged in a similar manner to 1321N1 cells (Section 2.2.2.2), replacing 1321N1 cell culture media with HEK293T/17 culture media.

2.2.3.3 Cryopreservation and Thawing

HEK293T/17 cells were cryopreserved and thawed in a similar manner to 1321N1 cells (Section 2.2.2.3), replacing 1321N1 cells culture media with HEK293T/17 culture media.

2.2.3.4 Generation of lentiviral particles

For the generation of lentiviral particles, HEK293T/17 cells were plated in 150-mm^2 petri dishes (Nunc) at a density of 45x10^5 cells/ml. Cells were incubated overnight at 37°C in a humidified 5% CO_2 incubator (described in greater detail in section 2.6.3).

2.3   Primary Cell Isolation

Human whole blood was obtained from healthy volunteers through the NHS blood and transplant service.

2.3.1 Peripheral blood mononuclear cells (PBMC) isolation

Whole blood was centrifuged at 1000 x g for 10 minutes with no brake to isolate plasma. To inactivate complement, the collected plasma was heat-inactivated at 56°C for 30 minutes and centrifuged at 1000 x g for 20 minutes and supernatant was collected. Whole blood was diluted with RPMI in a 1:1 ratio and layered onto 15 ml of Histopaque-1077 density gradient media before centrifuging at 1000 x g for 25 minutes at room temperature with no brake. Following centrifugation, mononuclear cells were collected by gently transferring the opaque interface into a fresh centrifuge tube. Cells were washed with RPMI and sedimented at 300 x g for 10 minutes at room temperature. Once supernatant was discarded, cells were washed twice with dPBS. The resultant PBMC pellet was resuspended in RPMI before counting the number of PBMCs using trypan blue exclusion on a haemocytometer.

2.3.2 Monocyte adherence

PBMCs were seeded into vented T75 flasks (Nunc) in RPMI at a density of 1.5×10^6 cells for every cm^2 and incubated at 37°C in a humidified 5% CO_2 incubator for 2 hours. Following incubation, adhered monocytes were washed thoroughly 6 – 8 times with dPBS and cultured with tissue culture media (TCM). TCM were prepared by supplementing RPMI-1640 media containing 0.3 g/L L-Glutamine (Lonza) with 2.5% (v/v) heat-inactivated autologous serum and 1% (v/v) penicillin-streptomycin solution containing 50 units/ml penicillin and 50 μg/ml streptomycin (Lonza).

2.3.3 Generation of monocyte-derived macrophages

To allow complete differentiation of monocytes into macrophages, monocytes were cultured in TCM supplemented with a colony-stimulating factor (CSF): 10 ng/ml of recombinant human macrophage colony stimulating factor (rhuM-CSF) or recombinant human granulocyte-macrophage colony-stimulating factor (GM-CSF) (both from Peprotech). Cells were cultured with the desired CSF over a period of 6 days at 37°C in a humidified 5% CO_2 incubator. Cells were washed with dPBS and fresh CSF was added to the culture every 3 days.

Following 6 days culture, cells were detached from the flasks by treating each T75 flasks with 5 ml of TrypLE Express solution (Life Technologies) and incubating for 20 minutes at 37°C. Following gentle agitation to dislodge adherent cells, cells were centrifuged at 300 x g for 10 minutes at room temperature and the supernatant was discarded. The cell pellet was resuspended in TCM and used for experimentations.

2.4   Polymerase Chain Reaction (PCR)

2.4.1 Total RNA extraction

To obtain a cell lysate for RNA extraction, 1×10^6 cells were centrifuged at 805 x g for 7 minutes at room temperature to obtain a pellet. Supernatant was removed and cell pellet was resuspended in 1 ml of TRI Reagent® (Sigma) to allow complete cell lysis and vortexed for 1 minute. TRI Reagent® is a single-step total RNA isolation reagent that was adapted from Chomczynski and Sacchi (1987). For every 1 ml of TRI Reagent®, 100 μl of 1-bromo-3-chloropropane was added to allow complete separation of homogenate into aqueous and organic phases. Samples were thoroughly vortexed and allowed to stand at room temperature for 15 minutes before centrifuging at 14,800 x g for 15 minutes at 4°C. Centrifugation resulted in the formation of three phases, which included a lower red organic phase containing protein, a cloudy interphase containing denatured proteins and genomic DNA, and an upper aqueous clear phase which contain RNA. This upper phase containing RNA was transferred to a fresh 1.5 ml microcentrifuge tube and 0.5 ml of propan-2-ol (Fisher) was added to the RNA, vortexed and allowed to stand at room temperature for 15 minutes. Precipitation of the RNA was achieved by centrifuging the sample at 14,800 x g for 15 minutes at 4°C. Supernatant was discarded and the pellet was washed in 1 ml of ice-cold 75% (v/v) ethanol. The sample was centrifuged at 14,800 x g for 10 minutes at 4°C. Ethanol was gently removed from the tube, leaving the pellet to air-dry for up to 30 minutes. Rehydration of RNA was achieved through the addition of 20 μl of nuclease-free water followed by heating at 65°C for 5 minutes.

2.4.2 Elimination of genomic DNA using DNase I

To remove contaminating DNA from purified RNA and remove divalent cations to limit RNA degradation, Ambion® DNA-*free*™ Kit (Life Technologies) was used. To each RNA sample 0.1 volume of 10X DNase I Buffer and 1 μl of rDNase was added and mixed gently before incubation at 37°C for 30 minutes. DNase inactivation reagent was added to each RNA sample at 0.1 volume and was left to incubate at room temperature, for 2 minutes. Lastly, RNA samples were centrifuged at 10,000 x g for 90 seconds and supernatant was transferred to a fresh tube without agitating pellet. RNA samples were kept at -80°C for long-term storage.

2.4.3 Total RNA quantification

Total RNA (tRNA) concentration was quantified by adding 1 μl of the RNA sample to a NanoDrop 2000c UV-Vis spectrophotometer instrument (Thermo Scientific) and NanoDrop 2000c software. The absorbance was read at A260 (nm) and A280 (nm), with the ratio of the absorbance at 260 and 280 nm ($A_{260/280}$) being used to assess the purity of nucleic acids. Samples with the $A_{260/280}$ ratio value close to 2.00 were considered pure. RNA samples were kept at -80°C for long-term storage.

2.4.4 Complementary DNA synthesis

The isolated tRNA from section 2.4.1.2 was reverse transcribed into complementary DNA (cDNA). Reactions were prepared in duplicates where one reaction contained reverse transcriptase (RT) enzyme to allow the production of cDNA from target RNA sequence and a second sample contained no reverse transcriptase (RT') enzyme and was used as a negative control to confirm that any PCR amplicon was derived from synthesized cDNA rather than genomic DNA.

For each reaction, 1 μg of tRNA was randomly primed with 200 ng of random hexamers (Invitrogen) in a total volume of 11 μl and incubated at 70°C for 10 minutes. Following RNA priming, each reaction was added into a 1.5 ml centrifuge tubes containing 4 μl of 5x first strand buffer (Invitrogen), 2 μl (0.1 M) of DTT (Invitrogen), 1 μl (200 U) of Superscript II Reverse transcriptase (Invitrogen) enzyme (to RT samples only), 0.5 μl (5 μM) dNTPs (Bioline) and 0.75 μl (30 U) of RNasin® ribonuclease inhibitor (Promega) to limit RNA degradation. Each reaction was made up to a total volume of 20 μl with nuclease-free water. Reactions were incubated in a 42°C water bath for 1 hour followed by heat inactivation at 70°C for 10 minutes. cDNA samples were stored at -20°C until required.

2.4.5 Non-quantitative reverse transcription-PCR

Non-quantitative reverse transcription PCR (RT-PCR) technique was employed to detect gene expression of either functional or non-functional P2X$_5$ in THP-1 cells, THP-1 differentiated macrophages (TDM) or monocyte-derived macrophages (MDM).

2.4.5.1 Primers

All primers were supplied lypholised from Sigma-Aldrich and were reconstituted to 100 μM in nuclease-free water and stored at -20°C for long term storage. Working solutions of 10 μM concentration were prepared. ACTB primer pair serves as a positive control while P2X$_5$ primer pair was used to distinguish between functional and non-functional isoforms of the receptor. Amplification of functional (containing exon 10) P2X$_5$ will yield a band at 461 bp while amplification of non-functional (exon 10-less) P2X$_5$ will yield a band at 395 bp (Kotnis et al., 2010) (Table 2.6).

Table 2.6: Primer sequences for β-actin and P2X$_5$

Gene	Accession Number	Sequence	Direction	Size (bp)
ACTB	NM_001101.3	CACAGAGCCTCGCCTTTGCC	Sense	282
		CGATGCCGTGCTCGATGGGG	Antisense	
P2X$_5$	NM_001204520.1	CACTATTCTTTTAGCCGTCTGGAC	Sense	395 / 461
		TTCTGACTGCTGCTTCCACGCTTC	Antisense	

2.4.5.2 PCR

To investigate P2X receptor gene expression, prepared cDNA samples were used as a template for PCR amplification. Reactions for each primer were prepared in 0.2 ml thin-walled nuclease-free microcentrifuge tubes with β-actin serving as a housekeeping gene. To each reaction, 1 μl of cDNA (either RT or RT'), 1 μl (200 nM) of forward primer, 1 μl (200 nM) of reverse primer, and 25 μl of ReadyMix™ Taq PCR Reaction Mix (Sigma-Aldrich) were added. Reactions were made up to a final volume of 50 μl with nuclease-free water and mixed gently and briefly centrifuged. To allow selective amplification, each sample reaction was thermally cycled. The following cycle conditions were used: initial denaturation of DNA helix at 94^oC for 1 minute, followed by 35 cycles of denaturation at 94^oC for 30 seconds, annealing of primers to the DNA template at 55^oC for 30 seconds and finally, extension of the cDNA strand by dNTPs addition at 72^oC for 1 minute. The last step included extension at 72^oC for 5 minutes to allow any single-stranded DNA to be fully extended. Amplified samples were stored at -20^oC until further use.

2.4.5.3 Agarose gel electrophoresis

Agarose gel electrophoresis is one of the most common ways to separate DNA fragments by their size and allows visualization on a gel by the addition of ethidium bromide. DNA fragments are separated on the basis of charge with smaller fragments migrating faster than larger fragments. Agarose gel (Melford Laboratories) was prepared as a 1.5% (w/v) solution in 1x Tris-acetate-EDTA buffer (TAE, Thermo Scientific) and heated in a microwave until fully dissolved. To every 100 ml of agarose gel made, 4 μl of ethidium bromide solution was added. The gel was poured onto a cast and allowed to set at room temperature for 30 minutes, before being transferred to an electrophoresis chamber containing 1 x TAE buffer. Samples were prepared by mixing 40 μl of PCR reaction with 8 μl of 6x purple loading dye (New England Biolabs) and were loaded into the wells of the gel. Alongside the samples, a 100 base-pair (bp) DNA ladder (New England Biolabs) was used as a molecular weight marker reference. DNA electrophoresis was carried out at 90V (volts) for 75 minutes. Gel visualization was performed under ultra violet (UV) light using a ChemiDoc™ XRS visualizer (Bio-Rad).

2.4.6 Quantitative real time-PCR

Quantitative real-time PCR (qRT-PCR) combines PCR amplification and detection into a single step allowing quantification by labeling PCR products with fluorescent dyes during thermal cycling. qRT-PCR was performed using the TaqMan®-based detection using a fluorogenic probe specific to a target gene, which is detected as it accumulates during PCR.

2.4.6.1 Primers

All Taqman gene expression assays (primers and probes) were purchased from Applied Biosystems (Life Technologies) (Table 2.7 to 2.9) . All gene expression assays have FAM™ reporter dyes at the 5' end of the Taqman® MGB probe and a non-fluorescent quencher (NFQ) at the 3' end of the probe, with the MGB moiety attached to the quencher molecule. NFQ are advantageous in that it provides lower background signal giving more precise quantitation while the MGB moiety stabilizes the hybridized probe and effectively raises T_m. All TaqMan® MGB probes and primers were provided pre-mixed to a concentration of 18 μM for each primer and 5 μM for the probe at a 20X mix. The housekeeping genes used in the qRT-PCR reactions were either ACTB, RPLP0 or GAPDH, depending on the cell type being investigated.

2.4.6.2 Taqman RT-PCR assay

cDNA samples were diluted to 10 ng using nuclease-free water. Samples (5 μl) alongside Taqman probes (15 μl) were added, to duplicate wells for each gene tested, to wells of a 96-well MicroAmp® fast optical plate (Applied Biosystems). Negative control wells were prepared for each gene tested by substituting cDNA samples with nuclease-free water in separate wells. For each gene of interest, a reaction mix was prepared by adding 10 μl TaqMan® PCR master mix (Applied Biosystems), 1 μl TaqMan® Gene Expression assay mix (Applied Biosystems) and 4 μl nuclease-free water onto the diluted cDNA samples. The plate was then sealed with an optical adhesive cover (Applied Biosystems) and centrifuged briefly at 300 x *g*. Plates were loaded onto a 7500 fast real-time PCR machine (Applied Biosystems) and ran for 20 seconds at 50°C, 10 minutes at 95°C, followed by 40 cycles of 15 seconds at 95°C and 1 minute at 60°C and a lastly, a dissociation step to assess for primer dimers and target specificity. Data was analysed using 7500 software v.2.0.5 by recording the threshold cycle (Ct) value for each set of samples. Values were normalised against the geometric mean of housekeeping genes and

analysed using $\Delta\Delta$Ct method to calculate the relative quantification values ($2^{-\Delta\Delta Ct}$), which measures the fold-change in gene expression to control cells. Gene expression that appears above Ct value of 35 were considered to be absent.

Table 2.7: Endogenous control Taqman probes

Gene name	Assay ID	Reporter Dye	Reporter Quencher	Amplicon Length
ACTB	Hs01060665_g1	FAM	NFQ	63
RPLP0	Hs99999902_m1	FAM	NFQ	105
GAPDH	Hs02758991_g1	FAM	NFQ	93

Table 2.8: P2X and P2Y receptor Taqman probes

Gene name	Assay ID	Reporter Dye	Reporter Quencher	Amplicon Length
$P2X_1$	Hs00175686_m1	FAM	NFQ	73
$P2X_2$	Hs04176268_g1	FAM	NFQ	88
$P2X_3$	Hs01125554_m1	FAM	NFQ	84
$P2X_4$	Hs00602442_m1	FAM	NFQ	91
$P2X_5$	Hs01112471_m1	FAM	NFQ	83
$P2X_6$	Hs01003997_m1	FAM	NFQ	105
$P2X_7$	Hs00175721_m1	FAM	NFQ	89
$P2Y_1$	Hs00704965_s1	FAM	NFQ	73
$P2Y_2$	Hs04176264_s1	FAM	NFQ	82
$P2Y_4$	Hs00267404_s1	FAM	NFQ	91
$P2Y_6$	Hs00366312_m1	FAM	NFQ	70
$P2Y_{11}$	Hs01038858_m1	FAM	NFQ	72
$P2Y_{12}$	Hs01881698_s1	FAM	NFQ	136
$P2Y_{13}$	Hs03043902_s1	FAM	NFQ	63
$P2Y_{14}$	Hs01848195_s1	FAM	NFQ	155

Table 2.9: Cytokine and Chemokines Taqman probes

Gene name	Assay ID	Reporter Dye	Reporter Quencher	Amplicon Length
CXCL5	Hs01099660_g1	FAM	NFQ	93
TGFβ2	Hs00234244_m1	FAM	NFQ	92

2.5   Immunocytochemistry

Immunocytochemistry was employed to determine the presence of P2X receptor proteins in cells. Cells were seeded at a density of 2.5×10^4/ml in each well of a 6-well tissue culture plate (Nunc) lined with a sterile coverslip and were left to culture at 37°C in a humidified 5% CO_2 incubator. Media was aspirated from each well and cells were gently rinsed twice with PBS (pH 7.4) at room temperature. Cells were fixed with 4% (w/v) paraformaldehyde in PBS for 15 minutes at room temperature. Once fixed, cells were washed twice with PBS and permeabilized with 0.25% (v/v) Triton X-100 (in PBS) for 10 minutes at room temperature. Following permeabilization, cells were washed three times with PBS and blocked with 1% (w/v) bovine serum albumin (BSA) (in PBS) for 30 minutes at room temperature to prevent non-specific binding of the antibodies. Following the blocking step, cells were sufficiently washed with PBS to remove excess protein that may prevent detection of the target antigen. Cells were incubated overnight at 4°C with primary antibody diluted in 1% (w/v) BSA (in PBS) (Table 2.10).

Following overnight incubation with primary antibody, cells were washed thoroughly with PBS and incubated with secondary antibody in 1% (w/v) BSA (in PBS) for 1 hour at room temperature, away from light (Table 2.10). To confirm that the secondary antibodies do not bind non-specifically, negative controls were prepared in which cells were stained only with secondary antibody and no primary antibody. Finally, cells were washed thoroughly with PBS and were placed on to glass slides that contained 20 μl Vectashield Antifade mounting media with DAPI (Vectorlabs). This mounting media was used to prevent photobleaching while DAPI was used to detect nuclear staining. The coverslips containing cells were then sealed on to the glass slides using nail varnish and were dried completely at room temperature away from light. For long term storage, the slides were kept at 4°C in the dark.

2.5.1 Confocal microscopy

Laser-scanning confocal microscope Zeiss LSM510 META (Zeiss) at the Henry Welcome Laboratory for Cell Imaging was used to visualize fixed cells following immunocytochemistry described in section 2.5. Images for each sample were standardized to corresponding negative control, which was stained only with secondary antibody.

Table 2.10: Primary and Secondary Antibodies for immunocytochemistry and flow cytometry (FACS)

Target	1°/2° Ab	Reactivity	Host	Clonality	Dilution/ Conc.	Supplier
$P2X_1$	1°	Human	Goat	Polyclonal	1:200	Santa-Cruz
$P2X_4$	1°	Human	Rabbit	Polyclonal	1:200 (IC); 0.8mg/ml (FACS)	Alomone
$P2X_4$ (ext)	1°	Human	Rabbit	Polyclonal	0.8mg/ml (FACS)	Alomone
$P2X_5$	1°	Human	Goat	Polyclonal	1:200	Santa-Cruz
$P2X_7$	1°	Human	Goat	Polyclonal	1:200	Santa-Cruz
$P2Y_1$	1°	Human	Rabbit	Polyclonal	1:200	Santa-Cruz
$P2Y_2$	1°	Human	Goat	Polyclonal	1:200	Santa-Cruz
$P2Y_6$	1°	Human	Rabbit	Polyclonal	1:200	Alomone
$P2Y_{12}$	1°	Human	Goat	Polyclonal	1:200	Santa-Cruz
$P2Y_{13}$	1°	Human	Goat	Polyclonal	1:200	Santa-Cruz
Alexa Fluor 488 (AF488)	2°	Goat	Rabbit	Polyclonal	1:1000	Invitrogen
Alexa Fluor 488 (AF488)	2°	Rabbit	Goat	Polyclonal	1:1000	Invitrogen
IgG Isotype Control (IC)	1°	Human	Rabbit	Polyclonal	0.8mg/ml (FACS)	Cell Signaling Technology

2.6 Generation of P2X$_4$-knockdown THP-1 cells

To better understand the functional role of P2X$_4$ receptor, P2X$_4$-knockdown THP-1 cells were generated through a gene silencing strategy. The method selected was the delivery of short-hairpin ribonucleic acid (shRNA) sequences carried by lentiviral pLKO.1 puro (puromycin-resistant) vector (Moffat et al., 2006; Figure 2.1). This method was chosen as it enables the generation of long-term stable knockdown cell lines with the antibiotic used for selection maintenance. To generate the knockdown cell line, three components were required: a lentiviral vector (pLKO.1 puro vector) containing the shRNA or transgene, a packaging vector (psPAX2) and an envelope vector (pMD2.G). psPAX2 is a second-generation packaging plasmid containing a robust CAG promoter for efficient expression of packaging proteins. Meanwhile, pMD2.G envelope plasmid encodes for glycoproteins of vesicular stomatitis virus (VSV-G) that stabilise the viral particles.

2.6.1 Preparation of plasmid DNA for transfection

Bacterial glycerol stocks for pLKO.1 puro vectors carrying shRNA sequences targeting P2X$_4$ were selected from the RNA interference (RNAi) consortium (TRC) and purchased from MISSION™ shRNA library (Sigma-Aldrich, Table 2.11). Serving as a negative control, pLKO.1 puro non-target shRNA control plasmid DNA was also purchased (Sigma-Aldrich). Bacterial stocks of psPAX2 and pMD2.G were purchased from Addgene.

Bacterial glycerol stocks were streaked onto Luria Bertani agar plates (LB agar; 35 g of LB agar in 1 L distilled water and sterilized by autoclaving) supplemented with 100 μg/ml ampicillin. Plates were incubated facing down overnight at 37°C. A single colony from each plate was then transferred to 10 ml of LB broth (20 g of LB broth in 1 L of distilled water and sterilized by autoclaving), supplemented with 100 μg/ml ampicillin. Colonies were left shaking at 220 revolutions per minute (rpm) overnight at 37°C. Following growth of bacteria, colonies were centrifuged at 805 x g for 10 minutes and supernatant was discarded. Plasmid DNA was extracted using an E.Z.N.A Plasmid Mini Kit II (Omega Bio-Tek) following manufacturer's instructions. Quantification of DNA in the samples was carried out using the Nanodrop system as described in 2.4.1.2. A260/A280 ratio of 1.8 is usually regarded as pure for DNA samples.
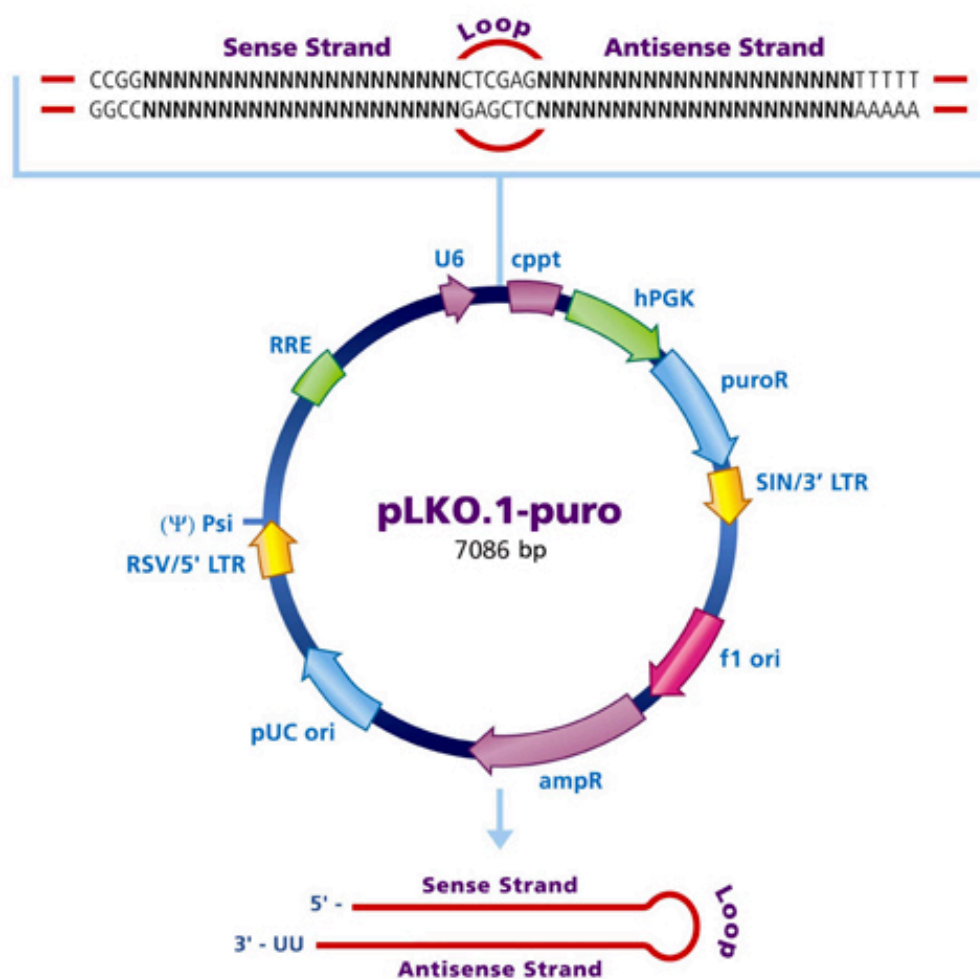
Figure 2.1 TRC1.5 vector map (pLKO.1-puro) with an shRNA insert. The length of the pLKO.1-puro plasmid including the shRNA insert is 7,086 bp. Image taken from sigma-aldrich website, accessed on 12th August 2015

Table 2.11: Sequence of shRNA P2X$_4$ plasmid DNA

TRC No.	Clone ID	Sequence
44962	NM_002560.2-563s1c1	CCGGGCGGATTATGTGATACCAGCTCTCG AGAGCTGGTATCACATAATCCGCTTTTTG

2.6.2 Puromycin kill curve

To determine the concentration of puromycin required to kill THP-1 cells, a puromycin kill curve was generated. A range of puromycin (InvivoGen) concentrations (0.1, 1 and 10 μg/ml) was tested over 5 days in triplicates. On day 0, in a 96-well black plate (Fisher Scientific), THP-1 cells were seeded at 200 μl per well with a density of 1×10^6 cells/ml in THP-1 culture media. Ranging concentrations of puromycin, or media alone as a blank, were added to the corresponding wells in the plate and cultured at 37^oC in a humidified 5% CO_2 incubator. Cell viability was tested every day for a total of 5-days period using CellTiter 96® AQueous One solution cell proliferation assay (Promega), a colorimetric assay that measures mitochondrial function through the ability of the cells to convert MTT into formazan. For each well 10 μl of CellTiter 96® AQueous One solution were added and incubated for 4 hours at 37^oC in a humidified 5% CO_2 incubator. Quantity of formazan product was then measured by performing absorbance reading using the Flex Station III plate reader (Molecular Devices) at 490 nm, which is directly proportional to the number of live cells in the culture. Cell viability was then measured by taking away the absorbance value of media alone from individual samples. Based on this data, the optimal puromycin concentration sufficient to kill THP-1 cells was 1 μg/ml over 5 days (Figure 2.2).
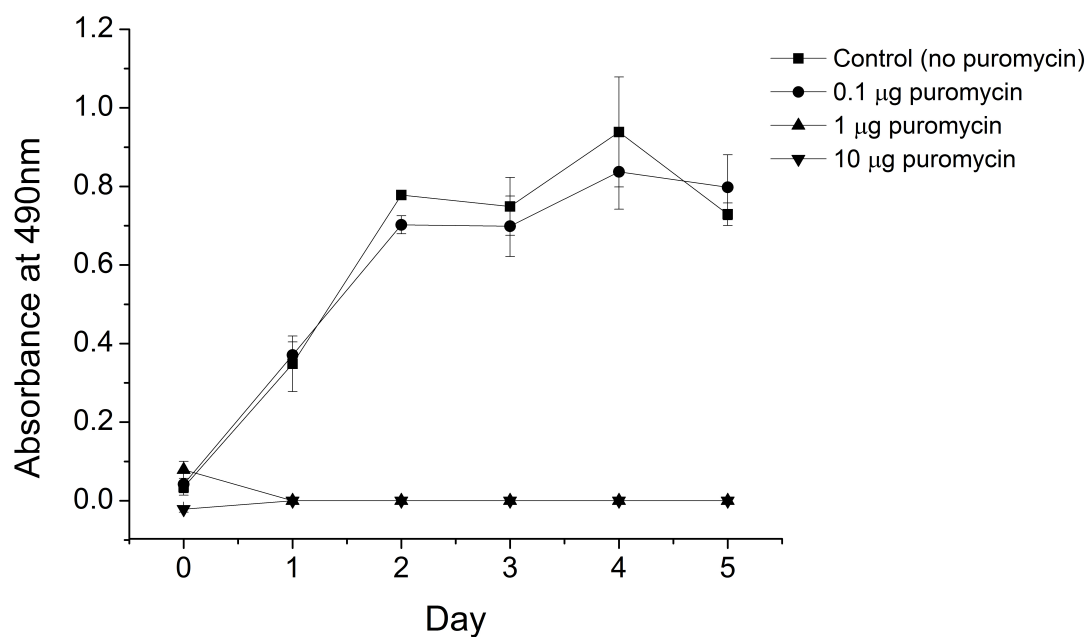
Figure 2.2 Puromycin kill curve on THP-1 cells. The effect of varying concentrations of puromycin (0.1, 1 and 10 μg/ml) to THP-1 cells was investigated over 5 days period (n=3). THP-1 cells were seeded at a density of 1 x 10^6 cells/ml and cell viability was tested upon exposure of varying concentrations of puromycin across different time points using CellTiter 96® AQueous One solution cell proliferation assay.

2.6.3 Lentivirus production in HEK293T/17

Lentivirus production was performed in HEK293T/17 cells (Section 2.2.3). For every pLKO.1 puro shRNA or non-target plasmid to be transfected, $9x10^6$ HEK293T/17 cells were seeded on a 150 mm petri dish (Thermo Scientific) in HEK293T/17 cell culture media without penicillin-streptomycin antibiotic. The cells were allowed to adhere overnight at 37^oC in a humidified 5% CO_2 incubator.

Following the overnight incubation, 1.2 ml of serum free OPTIMEM media (Life Technologies) was added to two sterile 1.5 ml centrifuge tubes designated as tube 1 and tube 2. To tube 1, 36 μl of lipofectamine 2000 transfection reagent (Life Technologies) was added. To tube 2, the following concentrations of plasmid DNA and lentivirus vectors were added: 9 μg lentiviral vector containing transgene (pLKO.1 puro *P2RX4* or pLKO.1 puro non-target shRNA DNA), 12 μg psPAX2 packaging vector and 3 μg pMD2.G envelope vector. Both reaction tubes were allowed to incubate for 5 minutes at room temperature followed by the addition of tube 1 contents to tube 2 and a further incubation for 20 minutes at room temperature. The reaction mix was added to the HEK293T/17 cells in a drop-wise manner and incubated at 37^oC in a humidified 5% CO_2 incubator for 6 hours. After 6 hours, the transfection reagent was removed, replaced with fresh 20 ml HEK293T cell culture media containing penicillin-streptomycin antibiotics and allowed to culture for a further 24 hours. For the next 3 days, 20 ml of media (virus) was collected from the cells and passed through a 0.45 μm polyethersulfone (PES) filter (GE Healthcare) to remove cells or debris followed by addition of 20 ml fresh HEK293T/17 cell culture media. At the end of third day, 10 ml of Lenti-X™ Concentrator (ClonTech Laboratory Inc.) to every 30 ml virus-containing media and mixed by gentle inversion. This reaction was left to incubate overnight at 4^oC. The following day, the virus was centrifuged at 1,000 x *g* for 45 minutes at 4^oC and pellet was gently resuspended in 0.5 ml DMEM media with no additives. Viral samples were immediately aliquoted and stored at -80^oC.

2.6.4 p24 ELISA and determining viral titre

To quantify lentivirus associated HIV-1 p24 core protein, QuickTiter™ Titer Kit (Lentivirus Associated HIV p24) was performed following the manufacturer's protocol (Cell Biolabs, Inc). In brief, after forming complexes with ViraBind™ lentivirus reagent (patented technology), while free p24 remains in supernatant, the amount of lentivirus associated p24 is measured by a HIV p24 ELISA. The kit has

detection sensitivity limit of 1 ng/ml HIV p24, or about 10,000 to 100,000 TU/ml VSVG-pseudotyped lentivirus samples (Li et al., 2015, Xu et al., 2015). Detection was performed using FITC-conjugated anti-HIV p24 monoclonal antibody and HRP-conjugated anti-FITC monoclonal antibody. Absorbance was read for each well using FlexStation III plate reader at 450 nm. The results are shown in Figure 2.3.

2.6.5 Transduction of lentiviral particles

Prior to transduction of lentiviral particles into THP-1 cells, it was necessary to optimize lentiviral particles titre based on survival of cells against puromycin antibiotic selection. Cells were transduced with varying titre of scrambled or shRNA P2X$_4$ lentiviral particles (0.5 – 50 μl) in the presence of 8 μg/ml hexadimethrine bromide for 24h at 37°C in a humidified 5% CO_2 incubator and media was changed the following day. At day 3, 1 μg/ml of puromycin was added to all cells and cell viability was assessed using MTT method (as described in Section 2.6.2) and absorbance recorded at 490nm. The lentiviral particle titre that offers the cells with the most resistance towards puromycin was selected for transduction. Figure 2.4A and B illustrated that for both scrambled and shRNA P2X$_4$ lentiviral particles, 5 μl served as the optimal titre for cell survival against antibiotic selection.

Following identification of optimal lentiviral particle titre for transduction, THP-1 cells were seeded into 24-well tissue culture plates at 2x10^4 cells per well in 2 ml THP-1 culture media. Several conditions were prepared: control well (cells alone with no treatment), scrambled shRNA well (5 μl of non-target shRNA transduction particles), P2X$_4$ shRNA well (5 μl of virus generated as described in section 2.6.3). To promote transduction, a final concentration of 8 μg/ml hexadimethrine bromide was added into each well. Plates were incubated at 37°C in a humidified 5% CO_2 incubator and media was changed the following day. At day 3, 1 μg/ml of puromycin was added to the non-control wells to select for cells stably incorporating the viral genome for a total of 5 days. Viability of cells was checked using the inverted microscope on a daily basis. Following 5 days, cells were removed from wells and centrifuged at 805 x *g* for 7 minutes at room temperature. Supernatant was discarded and cell pellet was resuspended in THP-1 culture media before transferring into a vented T25 flasks supplemented with 1 μg/ml puromycin.
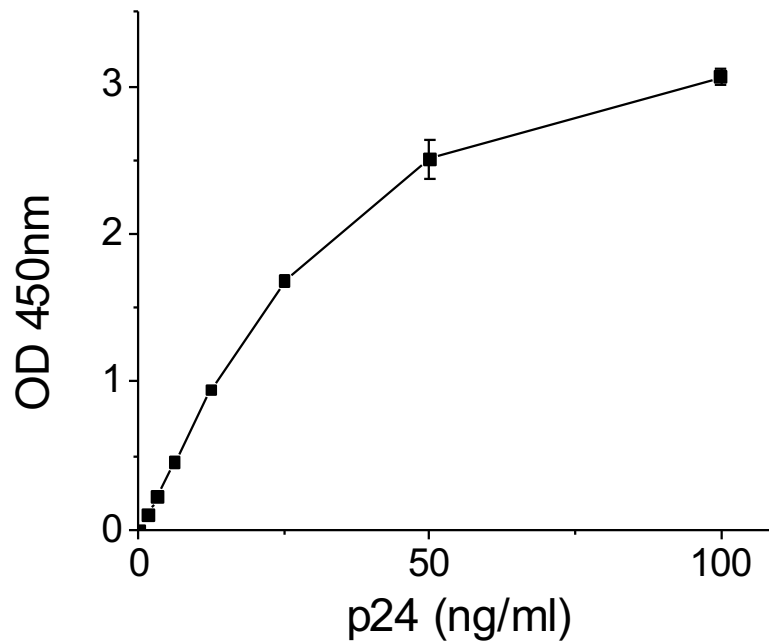
Figure 2.3 **HIV p24 ELISA standard curve of recombinant HIV-1 p24 antigen in the concentration range of 1 – 100 ng/ml**. Lentivirus associated p24 amount in the supernatant was calculated per manufacturer's guideline. The amount of virus-associated p24 titer (ng/ml) in each sample was calculated based on standard curve fitting. To calculate the amount of lentiviral particle (LP) in each sample, p24 titre was multiplied by a value of 1.25×10^7, with the assumption that 1ng p24 = 1.24×10^7 LPs.
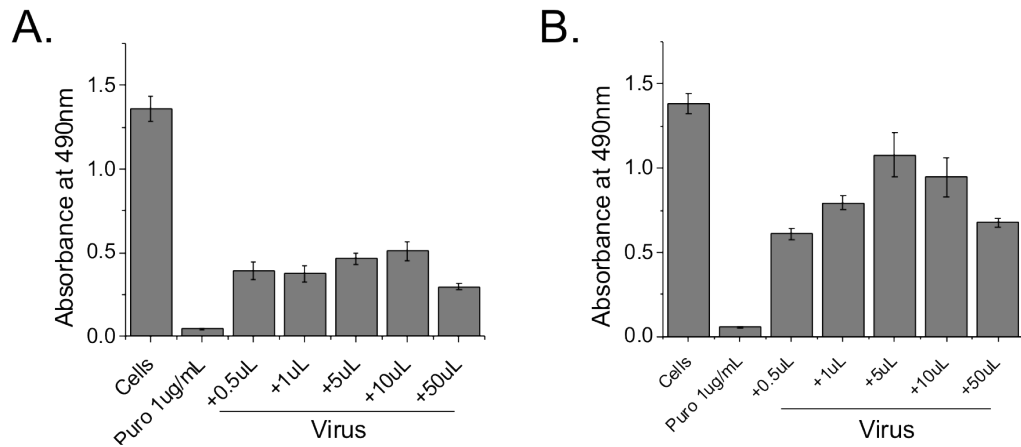
Figure 2.4 Identifying lentiviral particle titre for THP-1 transduction. THP-1 cells were seeded at a density of 1 x 10^6 cells/ml and transduced with varying amounts of lentiviral particles before exposure to 1 μM puromycin selection over 5 days. The optimal titre (0.5 – 50 μl) for lentiviral particle transduction was measured using CellTiter 96® AQueous One solution cell proliferation assay.

2.6.6 Flow cytometry

To determine surface expression of P2X$_4$ receptor in scrambled shRNA *vs.* P2X$_4$ shRNA cells, surface and total staining of P2X$_4$ receptor was performed on flow cytometry. 1×10^6 scrambled shRNA or P2X$_4$ shRNA TDM cells were prepared for surface staining. Cells were resuspended at a density of 1×10^6 cells/ml. For each staining, a negative control of 1) unstained cells, and 2) isotype control with secondary antibody were prepared. Cells were incubated with 1 μl Fc block for 10 minutes at room temperature prior to staining. Cells were then stained with primary antibody of either 1 μl of rabbit polyclonal αP2RX$_4$ (extracellular), 1 μl of rabbit polyclonal αP2RX$_4$ (intracellular) antibody or 1 μl of mouse IgG polyclonal antibody (isotype control) (Table 2.10) and left to incubate at room temperature for 60 minutes. Cells were washed with 3 ml of PBS once at 200 x *g* for 5 minutes and resuspended in 100 μl secondary antibody goat α-rabbit AF488, diluted in PBS (Table 2.9). Cells were incubated at room temperature for 60 minutes away from light. Finally, cells were washed with PBS at 200 x *g* for 5 minutes and transferred into 5 ml FACS tubes. Fluorescence intensity was read for AF488 using Cytoflex instrument (Beckman Coulter) and gates were set based on isotype control staining.

2.7 Generation of hP2X4 pLVX-IRES-mCherry over-expressing 1321N1 cells

pLVX-IRES-mCherry (Figure 2.5) is an HIV-1 based, lentiviral vector expressing two proteins from a bicistronic mRNA transcript, allowing mCherry to be expressed simultaneously with a protein of interest in any mammalian cell type. Additionally, the vector allows mCherry to be used as an indicator of transduction efficiency as well as a marker for selection by flow cytometry.

2.7.1 Preparation of plasmid DNA for transfection

$P2X_4$ pLVX-IRES-mCherry construct was previously made in-house and was used to generate $P2X_4$ overexpressing 1321N1 cell line. Briefly, BamHI restriction was performed on pLVX-IRES mCherry vector and $P2X_4$-pcDNA3.1 construct (Figure 2.6). Ligation of equal amounts of $P2X_4$ insert with pLVX-IRES-mCherry vector was performed overnight at $16^{o}C$ (T4 DNA ligase; New England Biolabs). Ligation product was transformed into Stbl3 chemically competent cells and plasmid DNA was isolated using E.Z.N.A Plasmid Mini Kit II (Omega Bio-Tek) following manufacturer's instructions.

2.7.2 Lentivirus production in HEK293T/17

Production of lentivirus was performed as described previously in section 2.6.2 with lentiviral vector containing transgene being either empty pLVX-IRES-mCherry or $hP2X_4$ pLVX-IRES-mCherry.
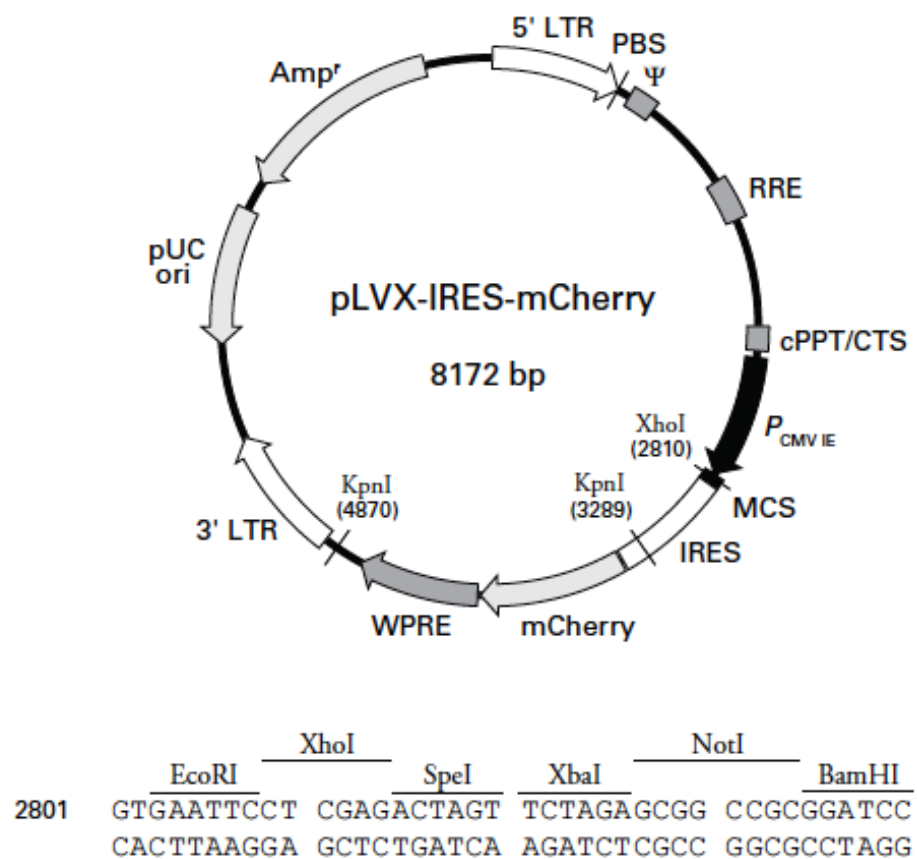
Figure 2.5 pLVX-IRES-mCherry vector map and multiple cloning site (MCS).
Total length of the vector is 8,172 bp. Image was taken from Clontech website, accessed on the 12th August 2015.
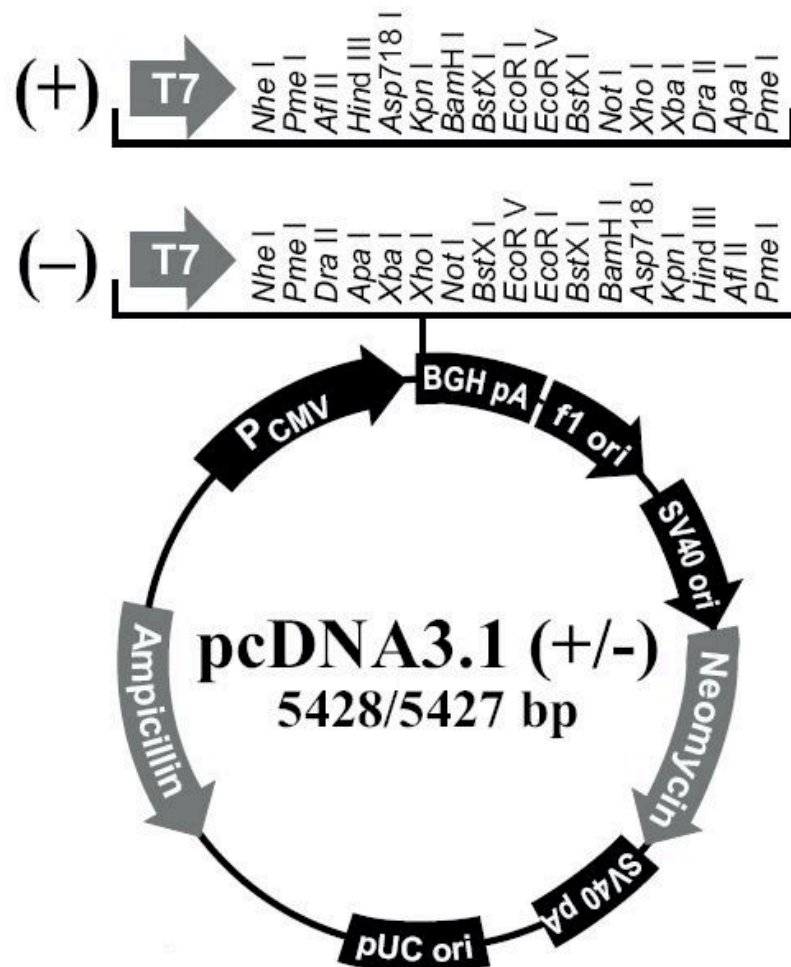
Figure 2.6 pcDNA™ 3.1(+) and pcDNA™ 3.1(-) vector map. The total length of the vector is 5428 bp and 5427 bp for pcDNA™ 3.1 (+) and pcDNA™ 3.1 (-), respectively. The vector consists of ampicillin and neomycin resistance genes. Image was taken from Invitrogen website, accessed on 12th August 2015.

2.7.3 Viral transduction through spinoculation

1321N1 cells are anecdotally known to not express any P2X receptors (Communi et al., 1996). $P2X_4$ over-expressing stable 1321N1 cell line was generated by spinoculating $hP2X_4$ pLVX-IRES-mCherry lentiviral particles into 1321N1 cells. A control of empty pLVX-IRES-mCherry 1321N1 cells was also generated. To perform spinoculation, 10 μl of lentiviral particles was added into every 1×10^5 1321N1 cells, supplemented with final concentration of 8 μg/ml of hexadimethrine bromide in a 15 ml falcon tube. The tube was centrifuged at 1,400 x g for 60 minutes at room temperature. Virus-containing media was gently aspirated and pellet was very gently resuspended in 1 ml 1321N1 cell culture media and transferred into a vented T25 flask incubated at 37°C in a humidified 5% CO_2 incubator.

2.7.4 Cell sorting

Highly expressing pLVX-IRES-mCherry 1321N1 cells (P4 population as shown in Figure 2.7A to C) were sorted using BD FACSAria™ III cell sorter (Becton Dickinson, BD) using standard FITC filter sets (Excitation: 587 nm; Emission: 610 nm) and put back into a vented T75 for culture. Successful transduction of $hP2X_4$ pLVX-IRES-mCherry into 1321N1 astrocytoma cells was also confirmed using fluorescence microscopy (Figure 2.7D).
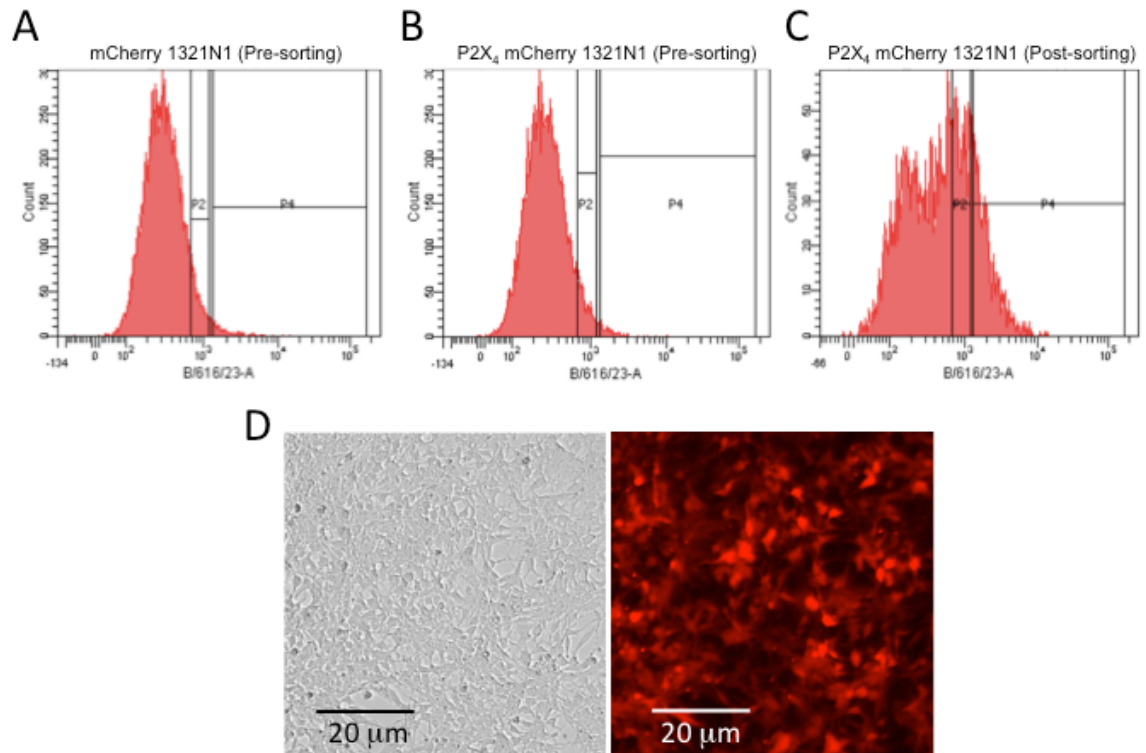
Figure 2.7 Sorting of mCherry-expressing 1321N1 astrocytoma cells. A) Histogram illustrating mCherry-expressing 1321N1 cells pre-sorting. P2 gating was set for low-expressing mCherry while P4 gating was set for highly-expressing mCherry. B) Histogram illustrating $P2X_4$-mCherry expressing 1321N1 cells pre-sorting. P2 and P4 gating was set as described above. C) Histogram illustrating $P2X_4$-mCherry expressing 1321N1 cells post-gating. As can be seen, a much higher proportion of the cells are found to be positive within the P4 gating. Cells were sorted using the BD FACS Aria instrument at a density of 1×10^6 cells/ml. D) $P2X_4$-mCherry 1321N1 cells as seen under the fluorescence microscope post-sorting (Left: brightfield image; Right: fluorescence image under FITC laser). Images are representative of n=3.

2.8   Calcium mobilization

Detection of intracellular calcium signals was performed using fluorescent Ca^{2+} indicator known as Fura-2 AM (Life Technologies), a ratiometric Ca^{2+} indicator. Fura-2 AM is a membrane-permeable indicator that can cross the cell membrane. Once inside the cell, their acetoxymethyl (AM) group is removed by cellular esterases resulting in the release of an ion-sensitive indicator that remains within the cell. Measurement of Ca^{2+}-induced fluorescence at both 340 nm and 380 nm allows for calcium quantification based on 340/380 ratios. The use of ratio minimizes effects of photobleaching and eliminates variables such as local differences in fura-2 concentration as well as cell thickness, resulting in more accurate and reproducible results. Fura-2 AM was used in all calcium mobilization assays in all cell types.

A.
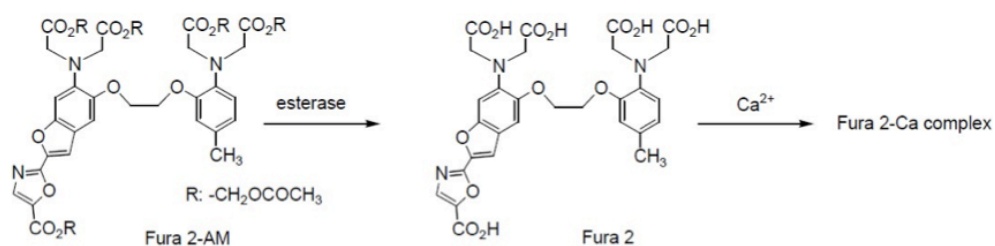
B.
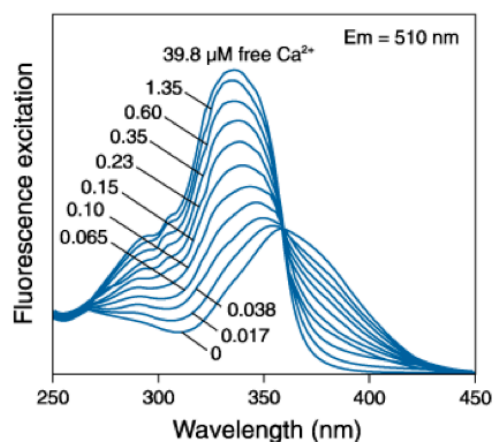
Figure 2.8 Fura-2AM calcium indicator dye. (A) Hydrolysis of AM ester to allow the formation of Fura-2 and Ca^{2+} complex and fluorescence detection. Image was adapted from Dojindo Europe website, accessed on 12th August 2015. (B) Fluorescence excitation spectra of Fura-2 AM in solutions containing 0-39.8 μM free Ca^{2+}. Image was taken from Life Technologies website, accessed on 12th August 2015.

2.8.1 Calcium mobilization buffers

Buffers required for the Ca^{2+} mobilization assay are shown in tables 2.12 and 2.13. Ca^{2+} loading buffer was prepared as described above in Table 2.12 with the addition of 0.01% (w/v) pluronic acid.

Table 2.12: Ca^{2+} **Salt-Buffered Solution (SBS) – pH 7.4**

Reagents	Concentration (mM)
Sodium chloride	130
Potassium chloride	5
Magnesium chloride	1.2
Calcium chloride	1.5
D-Glucose	8
HEPES	10

Table 2.13: Ca^{2+}**-free SBS – pH 7.4**

Reagents	Concentration (mM)
Sodium chloride	130
Potassium chloride	5
Magnesium chloride	1.2
EGTA	2
D-Glucose	8
HEPES	10

2.8.2 Intracellular Ca^{2+} measurements on cells in suspension

THP-1 cells were counted and harvested as triplicates at a density of 1×10^6 cells/ml. The required number of cells was centrifuged at 805 x g for 7 minutes at room temperature and supernatant was discarded. The resultant cell pellet was resuspended and loaded with a final concentration of 2 μM of Fura-2 AM in Ca^{2+} loading buffer (section 2.8.1) to a final cell density of 1×10^6 cells/ml. Cells were incubated in the dark for 1 hour at 37°C with gentle inversion every 15 minutes to prevent cells pelleting. Cells were washed twice with either Ca^{2+}-SBS or Ca^{2+}-free SBS at 805 x g for 7 minutes at room temperature. Cells were resuspended in SBS to a final concentration of 1×10^6 cells/ml and were plated into sterile black 96-well, clear-bottomed plate (Corning) at a final volume of 200 μl per well and allowed to settle for 1 hour at 37°C. Halfway through the incubation, if the effect of antagonists or modulators need to be investigated, the relevant compounds were added into the corresponding wells and were left to incubate for the rest of the 30 minutes at 37°C. Nucleotides were added by a FlexStation III microplate reader (Molecular Devices) set to deliver 50 μl from 96-well U-bottomed plates (Thermo Scientific). Fluorescence measurements were taken at λ_{em} = 510 nm, λ_{ex} = 340 nm and λ_{ex} = 380 nm. Fluorescence at 340 nm and 380 nm were used to quantify the change in intracellular calcium levels, represented as F-ratio, following subtraction of baseline response.

2.8.3 Intracellular Ca^{2+} measurements on adherent cell lines

Adherent cells (human astrocytoma 1321N1 or HEK293T/17 cells) were diluted with their designated cell culture media to 1.25×10^5 cells/ml and added to wells (200 μl) of a sterile black 96-well, clear-bottomed plate (Corning) such that each well contained 2.5×10^4 cells. For primary cells (human MDM), cells were diluted in TCM to 1×10^6 cells/ml and each well consisted of 2×10^5 cells. Plates were incubated at 37°C in a humidified 5% CO$_2$ incubator overnight to allow cells to adhere and form a monolayer. The following day, media was carefully aspirated and replaced with 200 μl of 2 μM Fura-2 AM diluted in Ca^{2+} loading buffer (section 2.8.1) followed by incubation for 1 hour at 37°C. After cells were loaded, the wells were washed twice in either Ca^{2+} containing or Ca^{2+} free SBS buffer. It is important to note, however, that leaving the cells with Ca^{2+} free SBS buffer is likely to affect intracellular store size by depleting them of intracellular Ca^{2+}. To test the effect of various antagonists or modulators, compounds were added to the corresponding wells and left to incubate for another 30 minutes at 37°C in the dark. For all experiments, agonist

ATP was added by a FlexStation III microplate reader (Molecular Devices) set to deliver 50 μl from 96-well U-bottomed plates (Thermo Scientific). As described in section 2.8.2, fluorescence measurements were taken at λ_{em} = 510 nm, λ_{ex} = 340 nm and λ_{ex} = 380 nm. Fluorescence at 340 nm and 380 nm were used to quantify the change in intracellular calcium levels, represented as F-ratio, following subtraction of baseline response.

2.9 Quantification of mRNA expression, secretion and synthesis of cytokines and chemokines

2.9.1 human MDM stimulation

GM-MDM cells were differentiated from monocytes following 6 days stimulation with rhuGM-CSF as described in section 2.3.3. Cells were seeded into sterile 24 well plates (Nunc) at a final amount of $0.5x10^6$ cells per condition and allowed to settle for 24 hours at 37^oC in a humidified 5% CO_2 incubator. Following settling period, cells were washed once with sterile PBS and fresh TCM was added into each well. For the purpose of initial study to identify candidate genes using the profiler array, cells were stimulated for 6 hours with 100 μM ATP, with or without 30 minutes pre-treatment of 10 μM PSB-12062. Unstimulated cells treated with vehicle (0.5% final DMSO concentration) served as negative control while 100 ng/ml lipopolysaccharide was used as positive control. For qRT-PCR time point studies, stimulation was performed at 6h, 9h, 18h and 24h. Following each stimulation time points, cells were lysed with TriReagent® and stored at -80^oC until further use.

2.9.2 RT^2 profiler PCR Array

To investigate if P2X$_4$ receptor could mediate cytokine and chemokine expression, human Cytokines & Chemokines RT^2 Profiler PCR Array (Qiagen) was done as a screening tool for potential candidate genes. This PCR array profiles the expression of 84 key secreted proteins (common cytokines as well as growth factors and hormones) that is central to the immune response (Figure 2.9 and Table 2.14).

To each well of a 96-well human cytokines & chemokines RT^2 profiler PCR Array (Qiagen), 5 μl cDNA samples (0.5 ng) were added alongside 20 μl of PCR master mix (2xRT^2 SYBR Green ROX Mastermix diluted in RNase-free water) were added using multi-channel pipette, to reduce variability. Plate was then sealed with an optical adhesive cover and centrifuged briefly at 300 x *g*. Plates were loaded onto a 7500 fast real-time PCR machine (Applied Biosystems) and ran for 20 seconds at 50^oC, 10 minutes at 95^oC, followed by 40 cycles of 15 seconds at 95^oC and 1 minute at 60^oC. This was followed by a continuous melt curve stage run for 15 seconds at 95^oC, 1 minute at 60^oC, 30 seconds at 95^oC and a final step for 15 seconds at 60^oC.

Data was analysed using 7500 software v.2.0.5 by recording down the threshold cycle (Ct) value for each samples. Values were corrected against the geometric mean of 5 housekeeping genes (ACTB, B2M, GAPDH, RPLP0 and HPRT1) and analysed using $\Delta\Delta C_t$ method to calculate the relative quantification values.

2.9.3 Identifying the most stable housekeeping genes

The RT[2] Profiler PCR array included 5 internal housekeeping genes: ACTB, B2M, GAPDH, RPLP0 and HPRT1. It was important to identify which of the housekeeping genes served as the most stable reference genes for normalization of gene expression in human primary GM-MDM cells. Using RefFinder online database tool, the stability of the five reference genes were evaluated and compared using four different computational programs (geNorm, Normfinder, BestKeeper and the comparative $\Delta\Delta Ct$ method). Data shown in Figure A1 (Appendix section) illustrated that GAPDH serves as the most stable housekeeping genes in GM-MDM cells (N=5).

2.9.4 Generating Heat Map for RT[2] profiler analysis

Heat Map was generated using Matrix2png tool (http://www.chibi.ubc.ca/matrix2png/) and data was represented as $\log_2$ fold change whereby the value 0 denotes no change in fold expression. Positive value denotes up-regulation in gene expression and negative value denotes down-regulation in gene expression.

	1	2	3	4	5	6	7	8	9	10	11	12
A	ADIPOQ	BMP2	BMP4	BMP6	BMP7	C5	CCL1	CCL11	CCL13	CCL17	CCL18	CCL19
B	CCL2	CCL20	CCL21	CCL22	CCL24	CCL3	CCL5	CCL7	CCL8	CD40LG	CNTF	CSF1
C	CSF2	CSF3	CX3CL1	CXCL1	CXCL10	CXCL11	CXCL12	CXCL13	CXCL17	CXCL2	CXCL5	CXCL9
D	FASLG	GPI	IFNA2	IFNG	IL10	IL11	IL12A	IL12B	IL13	IL15	IL16	IL17A
E	IL17F	IL18	IL1A	IL1B	IL1RN	IL2	IL21	IL22	IL23A	IL24	IL27	IL3
F	IL4	IL5	IL6	IL7	CXCL8	IL9	LIF	LTA	LTB	MIF	MSTN	NODAL
G	OSM	PPBP	SPP1	TGFB2	THPO	TNF	TNFRSF11B	TNFSF10	TNFSF11	TNFSF13B	VEGFA	XCL1
H	ACTB	B2M	GAPDH	HPRT1	RPLP0	HGDC	RTC	RTC	RTC	PPC	PPC	PPC

Figure 2.9 Genes investigated in the human cytokine and chemokine RT[2] Profiler PCR Array. Each of the 96-wells plate consisted of 84 different human cytokine and chemokine genes (blue; listed on Table 2.14), 5 internal reference genes (red; ACTB – Actin B, B2M – Beta-2-microglobulin, GAPDH – Glyceraldehyde-3-phosphate dehydrogenase, HPRT1 – Hypoxanthine phosphoribosyltransferase 1, RPLP0 – ribosomal protein, large P0), 2 internal negative controls (green; HGDC – human genomic DNA contamination; RTC – reverse transcription control) and internal positive control (orange; PPC – positive PCR control).

Table 2.14 Gene Table: RT^2 Profiler PCR Array

Symbol	Description
ADIPOQ	Adiponectin, C1Q and collagen domain containing
BMP2	Bone morphogenetic protein 2
BMP4	Bone morphogenetic protein 4
BMP6	Bone morphogenetic protein 6
BMP7	Bone morphogenetic protein 7
C5	Complement component 5
CCL1	Chemokine (C-C motif) ligand 1
CCL11	Chemokine (C-C motif) ligand 11
CCL13	Chemokine (C-C motif) ligand 13
CCL17	Chemokine (C-C motif) ligand 14
CCL18	Chemokine (C-C motif) ligand 18
CCL19	Chemokine (C-C motif) ligand 19
CCL2	Chemokine (C-C motif) ligand 2
CCL20	Chemokine (C-C motif) ligand 20
CCL21	Chemokine (C-C motif) ligand 21
CCL22	Chemokine (C-C motif) ligand 22
CCL24	Chemokine (C-C motif) ligand 24
CCL3	Chemokine (C-C motif) ligand 3
CCL5	Chemokine (C-C motif) ligand 5
CCL7	Chemokine (C-C motif) ligand 7
CCL8	Chemokine (C-C motif) ligand 8
CD40LG	CD40 ligand
CNTF	Ciliary neurotrophic factor
CSF1	Colony stimulating factor 1 (macrophage)
CSF2	Colony stimulating factor 2 (granulocyte-macrophage)
CSF3	Colony stimulating factor 3 (granulocyte)
CX3CL1	Chemokine (C-X3-C motif) ligand 1
CXCL1	Chemokine (C-X-C motif) ligand 1
CXCL10	Chemokine (C-X-C motif) ligand 10
CXCL11	Chemokine (C-X-C motif) ligand 11
CXCL12	Chemokine (C-X-C motif) ligand 12
CXCL13	Chemokine (C-X-C motif) ligand 13
CXCL16	Chemokine (C-X-C motif) ligand 16
CXCL2	Chemokine (C-X-C motif) ligand 2
CXCL5	Chemokine (C-X-C motif) ligand 5
CXCL9	Chemokine (C-X-C motif) ligand 9
FASLG	Fas ligand (TNF superfamily, member 6)
GPI	Glucose-6-phosphate isomerase
IFNA2	Interferon, alpha 2
IFNG	Interferon, gamma
IL10	Interleukin 10
IL11	Interleukin 11

Symbol	Description
IL12A	Interleukin 12A (natural killer cell stimulatory factor 1, p35)
IL12B	Interleukin 12B (natural killer cell stimulatory factor 2, p40)
IL13	Interleukin 13
IL15	Interleukin 15
IL16	Interleukin 16
IL17A	Interleukin 17A
IL17F	Interleukin 17F
IL18	Interleukin 18 (Interferon-gamma-inducing factor)
IL1A	Interleukin 1, alpha
IL1B	Interleukin 1, beta
IL1RN	Interleukin 1 receptor antagonist
IL2	Interleukin 2
IL21	Interleukin 21
IL22	Interleukin 22
IL23A	Interleukin 23, alpha subunit p19
IL24	Interlukin 24
IL27	Interleukin 27
IL3	Interleukin 3 (colony-stimulating factor, multiple)
IL4	Interleukin 4
IL5	Interleukin 5 (colony-stimulating factor, eosinophil)
IL6	Interleukin 6 (interferon, beta 2)
IL7	Interleukin 7
CXCL8	Interleukin 8
IL9	Interleukin 9
LIF	Leukemia inhibitory factor (cholinergic differentiation factor)
LTA	Lymphotoxin alpha (TNF superfamily, member 1)
LTB	Lymphotoxin beta (TNF superfamily, member 3)
MIF	Macrophage migration inhibitory factor
MSTN	Myostatin
NODAL	Nodal homolog (mouse)
OSM	Oncostatin M
PPBP	Pro-platelet basic protein (chemokine (C-X-C motif) ligand 7)
SPP1	Secreted phosphoprotein 1
TGFB2	Transforming growth factor, beta 2
THPO	Thrombopoietin
TNF	Tumor necrosis factor
TNFRSF11B	Tumor necrosis factor receptor superfamily, member 11b
TNFSF10	Tumor necrosis factor (ligand) superfamily, member 10
TNFSF11	Tumor necrosis factor (ligand) superfamily, member 11
TNFSF13B	Tumor necrosis factor (ligand) superfamily, member 13b
VEGFA	Vascular endothelial growth factor A
XCL1	Chemokine (C motif) ligand 1

2.10 Sandwich Enzyme-Linked Immunosorbent Assay (Sandwich ELISA)

ELISA is a technique used commonly for detecting and quantifying substances like proteins, peptides, antibodies and hormones. First developed in early 1970s, ELISAs rely on specific interaction between an epitope on an antigen and a matching antibody binding site. Sandwich ELISA requires the use of two antibodies: the capture and detection antibody. Detection is achieved through the assessment of conjugated enzyme activity by incubation with a substrate that gives a measurable product.

2.10.1 Collection of supernatant samples and protein lysates for ELISA quantification

To quantify secreted CXCL5 and TGFβ2 protein, supernatants were collected at various time points following different agonist or antagonist treatments. Supernatants were stored at $-80^{o}C$ and freeze-thawing was avoided. To quantify the amount of synthesized CXCL5, protein was extracted from MDM cells using RIPA lysis and extraction buffer (ThermoFisher, UK) using the manufacturer's instructions. In brief, $0.5x10^{6}$ MDM cells in a 24-well plate format were lysed using 100 μl of RIPA buffer containing protease inhibitor (1:200 dilution) for 10 minutes at $4^{o}C$. Lysed cells were centrifuged at 10,000 x g for 10 minutes at $4^{o}C$, supernatants containing extracted protein were collected and stored at $-80^{o}C$. The amount of protein in each sample was quantified using a colorimetric-based bicinchoninic acid (BCA) Protein Assay (ThermoFisher, UK) as per manufacturer's instruction. BCA Protein Assay relies is a two-step protein detection assay that includes an initial step of biuret reaction which involve the chelation of copper with protein in an alkaline environment followed by a second step that involves a color development reaction. This color development is formed when BCA encounters reduced cation generated in the initial first step.

2.10.2 Human CXCL5 ELISA

The amount of secreted CXCL5 protein in conditioned supernatants or synthesized CXCL5 in protein lysates were quantified using the human CXCL5 ELISA Max™ Deluxe Set (Biolegend) as described per manufacturer's protocol. In brief, 96-well Nunc™ Maxisorp™ ELISA plate was coated with Capture Antibody overnight at $4^{o}C$. Plate was blocked with assay diluent A for 1h at RT followed by the addition of standards (1.9 – 125 pg/ml human CXCL5), supernatant samples (diluted 1:1), or

protein lysate samples (diluted 1:10) and left to incubate at RT for 2h. Detection antibody was added for 1h at RT followed by addition of avidin-HRP solution for a further 30 minutes. Finally, substrate solution was added to each well and left for 10 minutes before stop solution was added to stop the reaction. Absorbance was recorded at 450 nm and 570 nm within 15 minutes of reaction. In between each step described above, plate was washed 4 times with wash buffer (PBS + 0.05% Tween) and complete removal of wash buffer was achieved by firmly tapping plate on clean absorbent paper.

2.10.3 Human TGF-β2 ELISA

The amount of secreted TGF-β2 protein in conditioned supernatants of MDM stimulation studies were performed using the human TGF-β2 DuoSet ELISA (R&D Systems) as described in the manufacturer's protocol. In brief, 96-well microplate was coated with Capture Antibody overnight at RT. Plate was blocked with assay diluent for 1h at RT followed by the addition of standards (31.3 – 2000 pg/ml human TGF-β2) or supernatant samples (diluted 1:1) and left to incubate at RT for 2h. Prior to addition of supernatant samples to the plate, activation of latent TGF-β2 was performed using sample activation kit 1 (R&D systems), as per manufacturer's protocol. Detection antibody was added for 2h at RT followed by addition of Streptavidin-HRP solution for a further 20 minutes. Finally, substrate solution was added to each well and left for 20 minutes before stop solution was added to stop the reaction. Absorbance was recorded at 450 nm and 570 nm. In between each step described above, plate was washed 3 times with wash buffer and complete removal of wash buffer was achieved by firmly tapping plate on clean absorbent paper.

2.11 Lactate Dehydrogenase (LDH) Cytotoxicity Assay

LDH cytotoxicity assay (CaymanChem, UK) quantitates cell death in response to either chemical compounds or environmental factors. LDH is a soluble enzyme that is found within the cytosol of cells and it is released upon cell damage or lysis into the surrounding culture medium. The kit relies on measuring LDH activity in the culture medium as an indicator of cell membrane integrity, and therefore cytotoxicity. This assay was performed to identify if incubation with the P2X$_4$ antagonist, PSB-12062, over various time points were able to induce cytotoxicity to cells. Experiments were performed according to manufacturer's protocol. In brief, conditioned supernatants collected from primary MDM stimulation experiments were centrifuged at 400 x *g* for 5 minutes to eliminate debris. Into a 96-well tissue culture plate, 100 μl of LDH standard or 100 μl of conditioned supernatants was incubated with 100 μl of LDH reaction solution with gentle shaking on an orbital shaker for 30 minutes, at room temperature. Absorbance was read at 490 nm with a plate reader.

2.12 Data and Statistical Analysis

All data were analyzed using Origin Pro 9.1 software (Origin Lab Corporation, USA) or Excel (Microsoft Corporation, USA). Data are represented as mean ± SEM (standard error of the mean), with n representing the number of experiments or replicates. For all experiments involving cell lines, 'n' number represents technical replicates while all experiments involving primary macrophages, 'N' number represents biological replicates as obtained from human donors. Statistical analysis between paired data was performed by means of Student's paired t-tests while unpaired data was performed by means of Student's unpaired t-tests statistical analysis. Statistical significance at the 5% ($p<0.05$), 1% levels ($p<0.01$) and 0.1% levels ($p<0.001$) has been indicated by the asterisks *, ** and *** respectively.

2.12.1 Analysis of intracellular Ca^{2+} measurements

Concentration response curves were fitted with Hill1 equation as described below, where start and end refers to lowest and highest point of the y-axis peak, respectively. If the value of (end – start) is greater than 0, n can be defined as 5 and k can be defined as 1.

$$y = start + (end - start)\frac{x^n}{k^n + x^n}$$

Analysis of peak magnitude was performed on SoftmaxPro software by deducting baseline Ca^{2+} level (lowest point of y-axis) from highest point of y-axis denoting the peak in F ratio unit (Figure 2.10). Analysis of decay kinetics (τ) and area under the curve was performed using ExpDecay1 function and Integrate function in OriginPro 9.1 software (Figure 2.10), respectively. ExpDecay1 function quantifies decay kinetics using the formula shown below, whereby y_0, A1, and t_1 represents Y offset, amplitude, and 'time' constant, respectively.

$$y = y0 + A1 \times \exp\left(-\frac{x - xo}{t_1}\right)$$
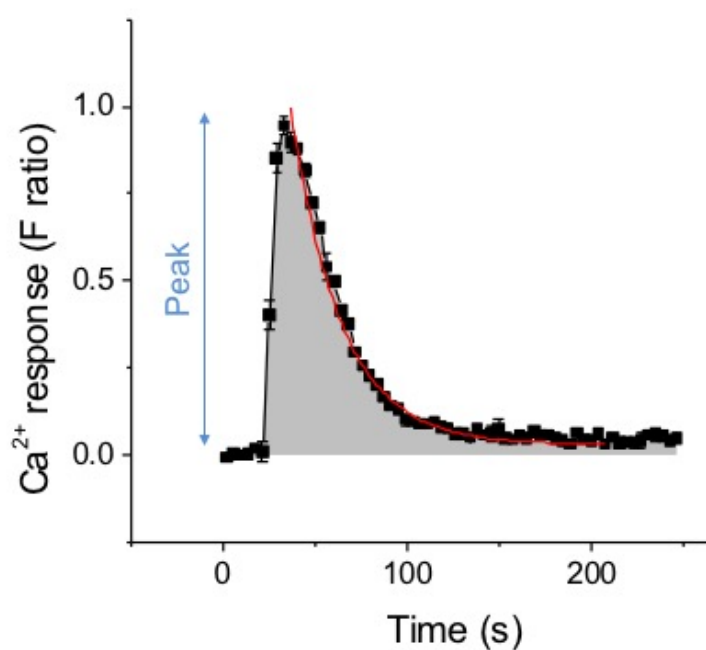
Figure 2.10 Representative time-trace response to illustrate analysis of Ca^{2+} response data. Peak magnitude response of Ca^{2+} response was quantified as the difference between the highest y-axis value minus the lowest y-axis value (represented as blue arrow). Decay kinetics (τ) of Ca^{2+} response is quantified using the exponential decay function in OriginPro 9.1 software (represented as fitted red line). Net calcium movement within cell is quantified as area under the curve using integration function in OriginPro 9.1 (represented as grey shaded area).

Chapter 3: Investigating contribution of P2X$_4$-mediated Ca^{2+} response in THP-1 monocyte/macrophage system

3.1. Introduction

P2X receptor family (P2X$_{1-7}$) is widely distributed in both neuronal and non-neuronal tissues (Knight and Burnstock, 2004). Two receptors belonging to this family, P2X$_4$ and P2X$_7$, are highly expressed in immune cells such as monocytes and macrophages and have generated increasing interest as potential anti-inflammatory drug targets (Bowler et al., 2003, Tsuda et al., 2003, Raouf et al., 2007, Li et al., 2008, Ulmann et al., 2010). Due to the early identification of highly selective and potent P2X$_7$ receptor antagonists, research development focusing on mechanism to which P2X$_7$ could be targeted therapeutically have grown rapidly (Donnelly-Roberts and Jarvis, 2007). However, the case for P2X$_4$ receptor remains tentative. This is mainly due to two reasons: the lack of selective P2X$_4$ receptor antagonists and the complicating presence of P2X$_7$, which is generally co-expressed with P2X$_4$ in macrophages and microglia (Knight and Burnstock, 2004, Surprenant and North, 2009).

More recently, two selective P2X$_4$ receptor antagonists have been made commercially available: 5-BDBD and PSB-12062. 5-BDBD, a derivative of benzodiazepine, was the first P2X$_4$ antagonist to be described in a patent (Fisher et al., 2005) and has been shown to have a competitive nature (Balazs et al., 2013a). Therefore, most current studies involving P2X$_4$ receptor have utilized 5-BDBD as a tool to block the receptor. The second and less known P2X$_4$ antagonist is a derivative of N-substituted phenoxazine known as PSB-12062 (Hernandez-Olmos et al., 2012). It has been described to possess an allosteric nature with equal potency in three species: human, mouse and rat (IC$_{50}$: 0.928 – 1.76 μM) (Hernandez-Olmos et al., 2012). With the development of selective P2X$_4$ antagonists, research on the P2X$_4$ receptor has slowly progressed.

The lack of available selective pharmacological tools to manipulate $P2X_4$ has hampered research to identify its functional roles in immune cells. Despite reports that $P2X_4$ is highly expressed in monocytes and macrophages, very little evidence has shown its relevance in these cells (Boumechache et al., 2009). So far, $P2X_4$ has only been shown to play a secondary role in facilitating $P2X_7$ in mouse macrophages with their co-expression illustrating enhanced $P2X_7$-mediated cell death via Ca^{2+} influx (Kawano et al., 2012b). Further evidence showed that mice lacking $P2X_4$ had reduced IL-1β production and M1 monocyte-derived macrophages (de Rivero Vaccari et al., 2012, Kawano et al., 2012b, Kawano et al., 2012a). These preliminary studies demonstrate the urgent need to explore $P2X_4$ function in monocytes and macrophages and the prospect of identifying this receptor as therapeutic target for treatments of inflammatory conditions.

One of the main sources of cells to study the monocyte/macrophage system comes from freshly isolated human monocytes. However, this remains technically challenging due to low availability of human samples, low cell yields and a high degree of variability due to their heterogeneous nature. The human monocytic THP-1 cell line is a well-established *in vitro* model for studying monocyte function (Qin, 2012). THP-1 cells have been shown to share a similar cell morphology and molecular marker expression as human monocytes (Auwerx, 1991). In addition to this, they can differentiate into cells that highly resemble macrophages following stimulation with low concentrations of phorbol 12-myristate 13-acetate (PMA) to allow *in vitro* study of macrophage function (Daigneault et al., 2010, Park et al., 2007).

3.2. Aims

THP-1 cells and THP-1-differentiated macrophages (TDM) were employed as *in vitro* models to investigate the $P2X_4$-mediated Ca^{2+} response. To address this aim, several pharmacological tools were employed to help characterize $P2X_4$ through quantification of intracellular Ca^{2+} release. In addition to this, this chapter also aims to discuss which of the two is a better model to study the contribution of $P2X_4$ towards ATP-evoked Ca^{2+} responses.

3.3. Results

3.3.1. Expression of P2X receptors in THP-1 monocytes *vs.* TDM

Although THP-1 cells and TDM cells have been used widely to study P2X receptor functions, the expression of P2XR in these cells is not well documented. Therefore, mRNA and protein expression studies using qRT-PCR and confocal microscopy, respectively, was initially performed.

mRNA expression of P2XR in THP-1 cells and TDM cells are described in Figure 3.1. Quantitative comparison of the expression of each receptor was observed through the cycle threshold (Ct) values. Genes with Ct values greater than 35 were considered absent. As can be seen (Figure 3.1A), mRNA of $P2X_1$, $P2X_4$, $P2X_5$, $P2X_6$ and $P2X_7$ was found to be expressed in both THP-1 cells and TDM cells. $P2X_2$ mRNA expression was only observed in THP-1 cells while $P2X_3$ mRNA expression was absent in both cell types. With these Ct values, it was possible to quantitatively measure the fold change of each receptor in TDM cells *vs*. THP-1 cells. Figure 3.1B illustrated a significant down regulation of $P2X_1$ and $P2X_2$ mRNA expression ($P2X_1$: 0.38 ± 0.058 fold and $P2X_2$: 0.13 ± 0.074 fold; n=5; P<0.001) in TDM cells compared to THP-1 cells. Interestingly, mRNA expression of $P2X_4$ in TDM was significantly up regulated when compared to THP-1 cells (2.61 ± 0.52 fold; n=5; P<0.0.5; Figure 3.1B). No significant changes in mRNA expression of $P2X_5$, $P2X_6$ and $P2X_7$ were observed in the two cell types. In addition to this, non-quantitative reverse transcription (RT)-PCR was also performed to investigate if THP-1 and TDM cells express the functional or non-functional isoform of $P2X_5$. Studies showed that a single-nucleotide polymorphism (SNP) at the 3' splice end of exon 10 of human $P2X_5$ gene can result in an exon 10-deleted isoform of $P2X_5$ yielding a non-functional and cytoplasmic distributed $P2X_5$. A study investigated by Kotnis et al. (2010) showed that genotyping of human samples revealed predominance of the non-functional $P2X_5$. Figure 3.1C and D illustrated that representative of n=3 replicates, both THP-1 cells and TDM cells, respectively, express the non-functional (exon 10-less) $P2X_5$ as observed with a band size of 395 bp.

A

	Average Ct Values (N=3)	
	THP-1 cells	TDM cells
P2X1	29.2 ± 0.43	28.3 ± 0.38
P2X2	33.7 ± 0.75	37.8 ± 0.45
P2X3	N/A	N/A
P2X4	26.4 ± 0.12	25.2 ± 0.61
P2X5	31.2 ± 0.98	32.1 ± 0.48
P2X6	32.8 ± 0.16	32.3 ± 0.34
P2X7	34.8 ± 0.68	31.0 ± 0.21
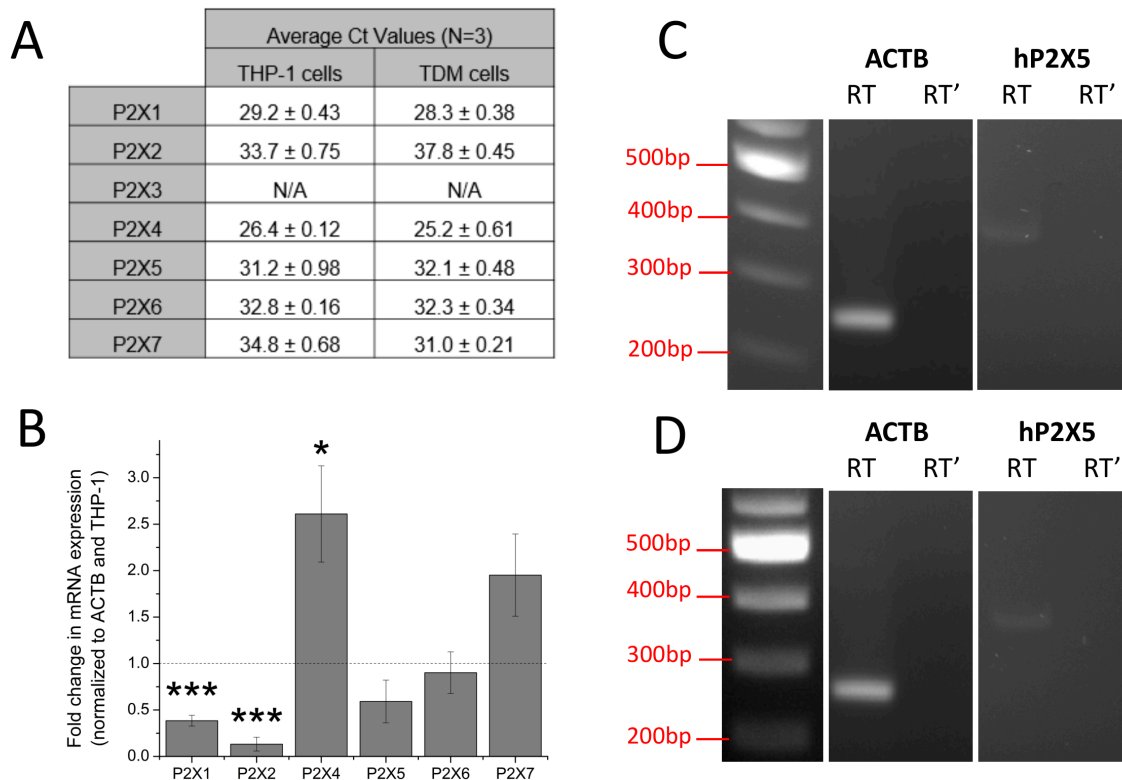
Figure 3.1. Expression of P2X receptor genes in THP-1 differentiated macrophages. A) Table showing qRT-PCR Ct values to identify which P2X genes are expressed in THP-1 cells and TDM cells. Ct values that appear >35 were considered absent (n=3). Undetected genes are represented as N/A. B) Fold change in mRNA expression of P2X receptor genes in TDM cells, normalised to housekeeping gene and THP-1 cells (n=3). Asterisks include significant changes towards control (*** $p < 0.001$, * $p < 0.05$, Student's t-test). C and D) Non-quantitative RT-PCR analysis of $P2X_5$ mRNA expression to distinguish non-functional (395 bp) and functional isoform (461 bp) of the receptor in THP-1 and TDM, respectively. β-Actin was used as a positive control. Images are representative of n=3 donors.

Expression of P2XR in the two cell types was also studied at protein level using confocal microscopy. All P2XR antibodies employed in this study detect the intracellular epitope of each receptor, which required the cells to be fixed and permeabilized prior to staining with the antibodies. Staining with secondary antibody (goat AF488 and rabbit AF488) alone was performed as a negative control to ensure no false positive staining was detected. As shown in Figure 3.2, protein expression of $P2X_1$, $P2X_4$, $P2X_5$ and $P2X_7$ was found present in both THP-1 cells and TDM cells and appear to have a punctate distribution throughout the cell. However, it was not possible to differentiate whether the expression is found predominantly within the surface of the cell, in the cytoplasm, perinuclear or within the nucleus of the cells. Despite the inability to describe receptor localization within the two types of cells, these data collectively illustrate that $P2X_1$, $P2X_4$, $P2X_5$ and $P2X_7$ receptors are expressed at the mRNA and protein level in both cell types.
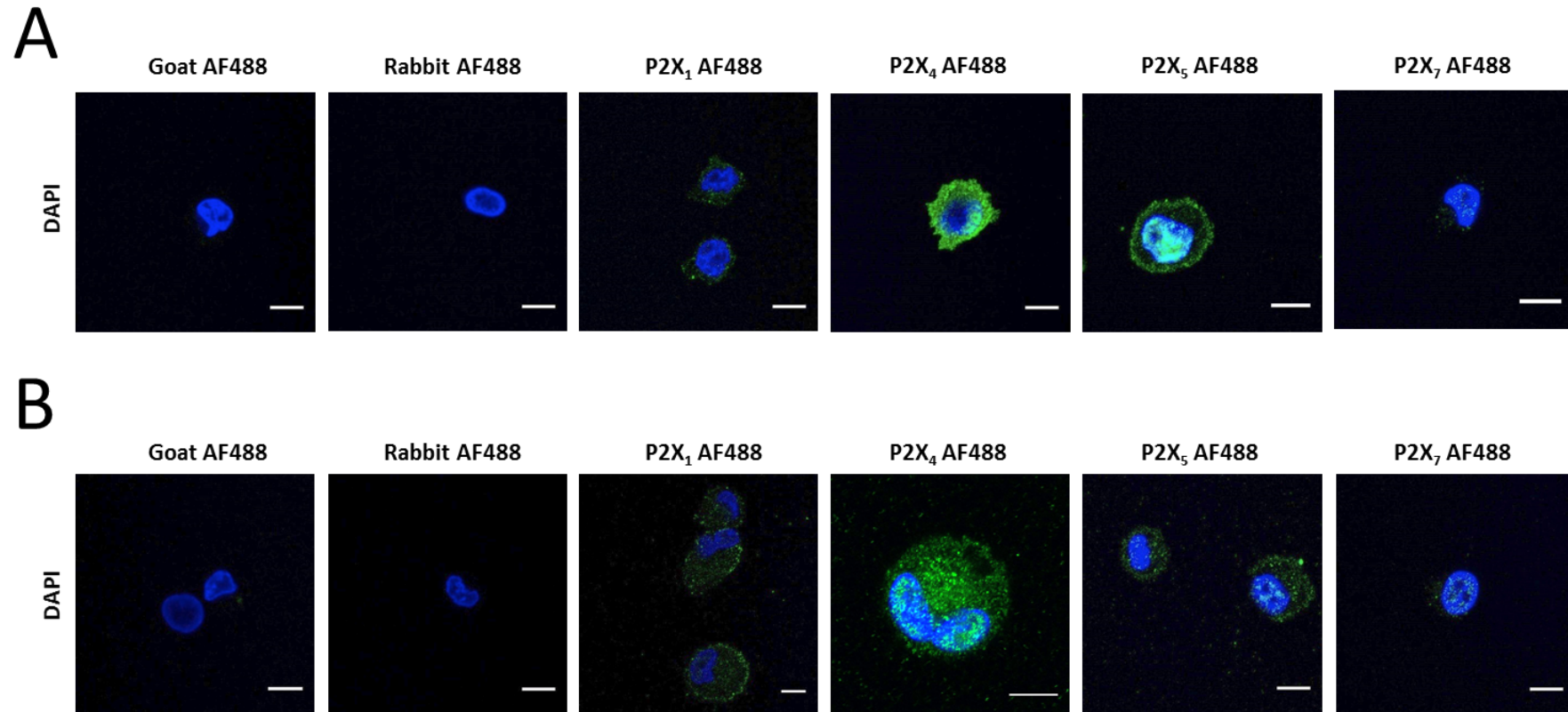
Figure 3.2. **Expression of P2X receptor in THP-1 and TDM.** Immunocytochemistry of P2X receptor expression in: A) THP-1 cells and B) TDM cells, as seen under confocal microscopy. Blue represents DAPI nuclear stain while green represents human P2X receptor conjugated with AF488. Scale bar represents 10 μm. Images represent n=3 replicates.

3.3.2. Investigating the selectivity of P2XR antagonists on over expressing cell lines

As the main aim of this chapter is to identify the contribution of $P2X_4$ to ATP-evoked Ca^{2+} response, various pharmacological tools such as receptor antagonists were utilized. To confirm the selectivity of each of the antagonists, each compound was initially tested on either $hP2X_1$, $hP2X_4$ or $hP2X_7$ recombinant over expressing cell lines. $P2X_4$ antagonists were tested on both $hP2X_4$ (for identification of IC_{50}) and $hP2X_7$ (for selectivity study) recombinant over-expressing cell line, while $P2X_1$ and $P2X_7$ antagonists were tested for inhibitory effects on $hP2X_1$, $hP2X_4$ and $hP2X_7$ recombinant over-expressing cell line. In addition to this, the compound IVM was also tested in both $hP2X_1$ and $hP2X_7$ over expressing cell lines to test for selectivity.

3.3.2.1. Selectivity of IVM and $P2X_1$ antagonist on $hP2X_1$ over expressing cell line

Ivermectin (IVM) has been accepted widely as a selective positive allosteric modulator for $P2X_4$. However, studies by Norenberg et al. (2012) illustrated that IVM can potentiate currents of human monocyte-derived macrophages that endogenously express $hP2X_7$ without influencing the decay kinetics. These findings indicated that effect of IVM is not selective for $hP2X_4$. There has been no further evidence that IVM can act on any other hP2XR. As $hP2X_1$ recombinant over expressing cell lines is available in-house, the effect of 3 μM IVM was tested.

A dose response curve for α,β me-ATP was initially performed to identify the maximal concentration required for activation of $P2X_1$. As shown (Figure 3.3A), α,β me-ATP elicited a concentration-dependent increase in intracellular Ca^{2+} level in $hP2X_1$ over expressing cell line (EC_{50}= 0.21 ± 0.022 μM, n=3). Maximal Ca^{2+} response was obtained from application of 1 μM of α,β me-ATP with representative time-response traces being shown in Figure 3.3B. 1 μM α,βme-ATP was used to investigate the effect of IVM and $P2X_1$ antagonist, Ro0437626. Pre-treatment of $hP2X_1$ over expressing cells with 3 μM IVM resulted in a significant inhibition of the magnitude of α,β me-ATP-evoked Ca^{2+} response (0.31 ± 0.04 F ratio *vs.* 0.15 ± 0.03 F ratio, n=3, P<0.05) (Figure 3.3C). This finding indicated that while IVM has been reported to have a positive modulatory effect on $hP2X_4$ and $hP2X_7$, it does not affect $hP2X_1$ in a similar manner. Pre-treatment of cells with 30 μM Ro0437626 resulted in

a significant reduction of the magnitude of α,β me-ATP-evoked Ca^{2+} response (0.33 ± 0.045 F ratio *vs.* 0.13 ± 0.011 F ratio) (Figure 3.3D). Unfortunately, a dose response of the effect of Ro0437626 as well as the effect of $P2X_4$ antagonists was not performed due to difficulty in getting a stable and consistent α,β me-ATP-evoked Ca^{2+} response in these over expressing cell line.
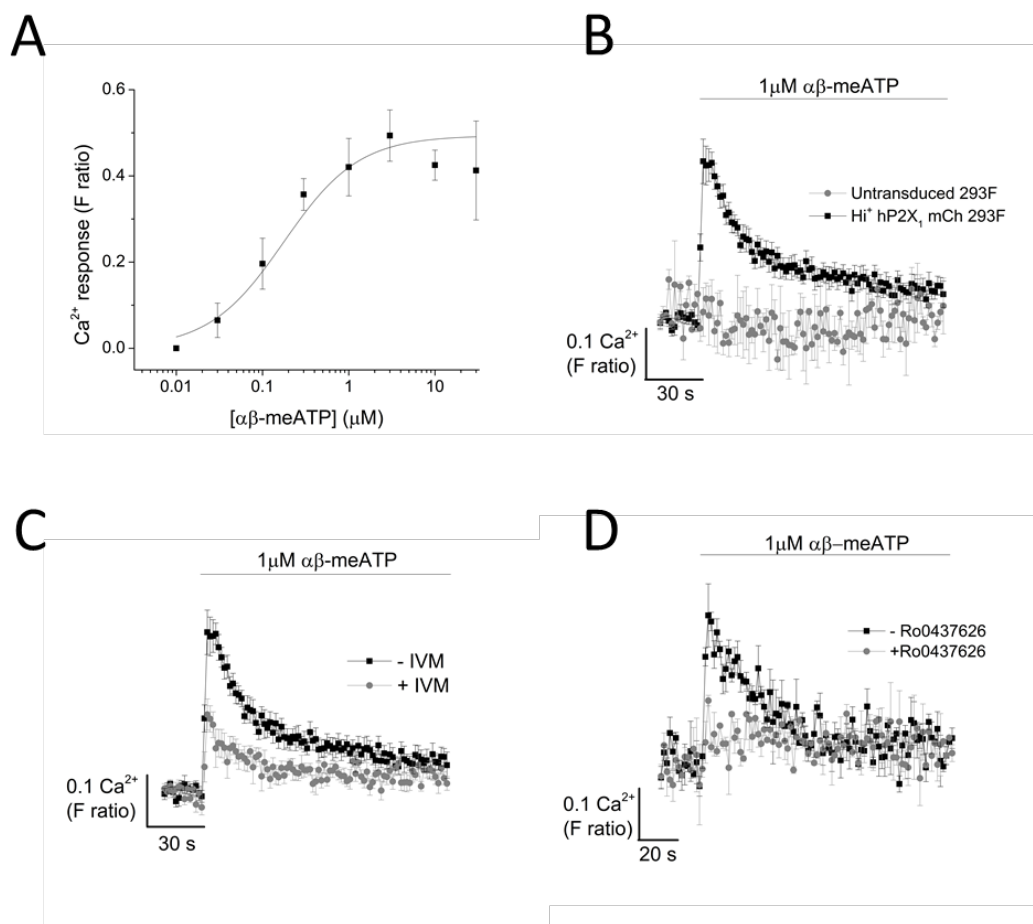
Figure 3.3. hP2X$_1$ mCherry HEK 293F cells as a tool to test selectivity of compounds. A) α, β me-ATP dose-response curve on hP2X$_1$ mCherry HEK 293F cells (n=3). B) Representative time-response curve at 1 μM α,β me-ATP on the hP2X$_1$ mCh HEKF 293F cells (n=3). Representative time-response curve on the effect of compounds on α, β me-ATP-mediated Ca^{2+} response: C) 3 μM IVM (n=3) and D) 30 μM Ro0437626 (n=3).

3.3.2.2. Testing the selectivity of P2XR antagonists on hP2X$_4$ over expressing cell line

As various P2XR antagonists were used throughout this study, it is important to ensure that the P2X$_1$ and P2X$_7$ antagonist were selective towards their reported receptor target and not act on P2X$_4$. In addition to this, it is also important to identify the IC$_{50}$ values for P2X$_4$ antagonists (5-BDBD and PSB-12062) that were used throughout this study. To achieve this, the effect of each compounds was tested on ATP-evoked Ca^{2+} response in hP2X$_4$ over expressing cell line.

As shown (Figure 3.4A), ATP elicited a dose-dependent increase in intracellular Ca^{2+} level in hP2X$_4$ over expressing cells (EC$_{50}$ = 0.12 ± 0.0031 μM; n=3), with maximal response observed at 1 μM ATP. Application of higher concentrations of ATP (300 μM and 1 mM) resulted in the reduction of intracellular Ca^{2+} response which may suggests receptor desensitization. Representative time response traces (Figure 3.4B) illustrated a rise in intracellular Ca^{2+} level following application of 100 μM ATP, which is then followed by a sustained elevated phase. Here, a dose response of P2X$_4$ antagonists: 5-BDBD and PSB-12062 was performed to identify the IC$_{50}$ values. IC$_{50}$ values of 5-BDBD and PSB-12062 were quantified to be 9.42 ± 1.09 μM (n=3) and 3.06 ± 0.57 μM (n=3), respectively (Figure 3.4C and D, respectively). At the highest concentration of 30 μM, 5-BDBD was only able to induce a 52.37 ± 6.40 % (n=3, P<0.001) inhibition on the hP2X4 over expressing cell line, while PSB-12062 was able to induce a 78.92 ± 4.99 % (n=3, P<0.001) inhibition. The IC$_{50}$ values obtained in this study, however, differ from those reported previously with 5-BDBD having IC$_{50}$ of 1.6 μM (Balazs et al., 2013a) and PSB-12062 having IC$_{50}$ of 1.38 μM (Hernandez-Olmos et al., 2012). Having quantified the IC$_{50}$ of the P2X$_4$ antagonists, it is possible to claim that PSB-12062 is a much more potent antagonist than 5-BDBD. Despite its high potency, PSB-12062 was unable to completely wipe out ATP-evoked Ca^{2+} response in hP2X$_4$ over expressing cells.

The effect of other P2XR antagonists, P2X$_7$ (A438079) and P2X$_1$ (Ro0437626), were also tested. At all concentrations, A438079 was unable to cause any significant inhibition to ATP-evoked Ca^{2+} response (100 μM) in hP2X$_4$ over expressing cells (Figure 3.4E). Meanwhile, pre-treatment of cells with Ro0437626 caused a slight inhibition to ATP-evoked Ca^{2+} response at concentrations above 1

μM. At 30 μM, Ro0437626 caused a significant inhibition to ATP-evoked Ca^{2+} response by 22.89 ± 4.41 % (n=3, P<0.001; Figure 3.4F).
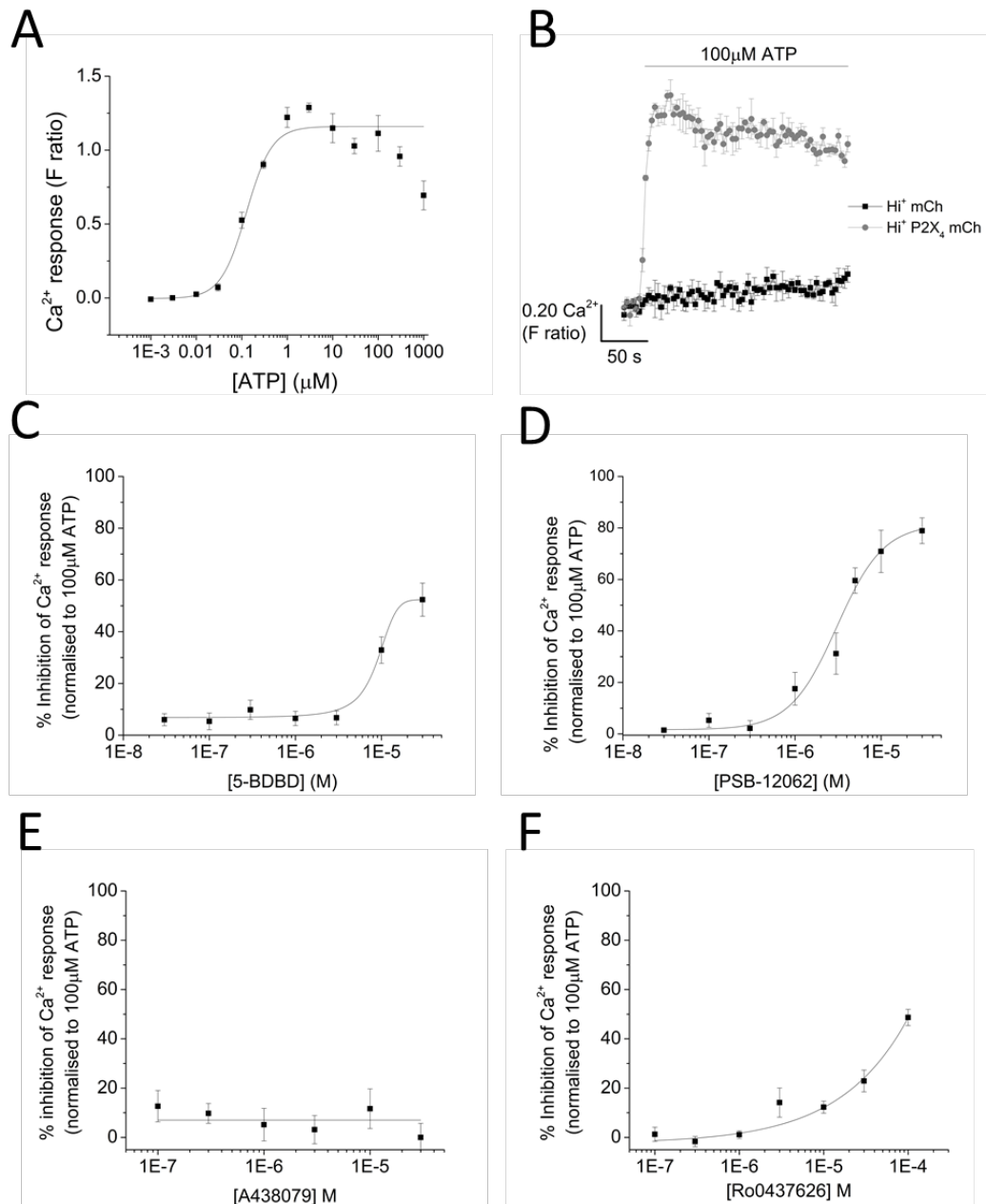
Figure 3.4. hP2X$_4$ mCherry over expressing 1321N1 cells as a tool to test selectivity of antagonists. A) ATP dose-response curve on hP2X$_4$ mCherry 1321N1 cells (n=3). B) Representative time-response curve at 100 μM ATP on the Hi$^+$ mCherry 1321N1 cells vs. Hi$^+$ P2X$_4$ mCherry over expressing cells (n=3). Inhibition curves of antagonists on ATP-mediated Ca^{2+} responses: C) 5-BDBD (n=3), D) PSB-12062 (n=3), E) A438079 (n=3) and F) Ro0437626 (n=3).

3.3.2.3. Testing the selectivity of P2XR antagonists on hP2X$_7$ over expressing cell line

P2X$_4$ and P2X$_7$ have been described to be the most abundantly expressed subtypes of P2XR in immune cells. While much effort has been invested to study the role of P2X$_7$ in immune cells, the same cannot be said for P2X$_4$, mainly due to the lack of selective antagonists. The main pharmacological tools for P2X$_4$ that are used throughout the course of this study are selective antagonists, 5-BDBD and PSB-12062, and positive allosteric modulator IVM. To test the selectivity of these compounds, their effects on BzATP-evoked Ca^{2+} response in hP2X$_7$ over expressing cell were studied.

Prior to testing the effect of each of the compounds, a BzATP dose response was performed on the hP2X$_7$ over expressing cell line with concentrations ranging from 1 μM to 500 μM (EC$_{50}$ = 43.4 ± 7.23 μM; n=3; Figure 3.5A), with maximal responses observed at approximately 100 μM. All compounds of interest were tested against 100 μM BzATP. To ensure that the BzATP-mediated Ca^{2+} response is elicited by activation of P2X$_7$ receptor alone, a selective P2X$_7$ antagonist (A438079) was employed. Pre-treatment of cells with 5 μM A438079 resulted in a significant inhibition of the BzATP-evoked intracellular Ca^{2+} response (88.85 ± 9.08 %; n=3, P<0.001; Figure 3.5C and D). ATP dose response on hP2X$_7$ over expressing cell line was also performed at concentrations ranging from 3 μM to 3 mM. Intracellular Ca^{2+} response was only detected at the highest agonist concentration of 3 mM (Figure 3.5B).
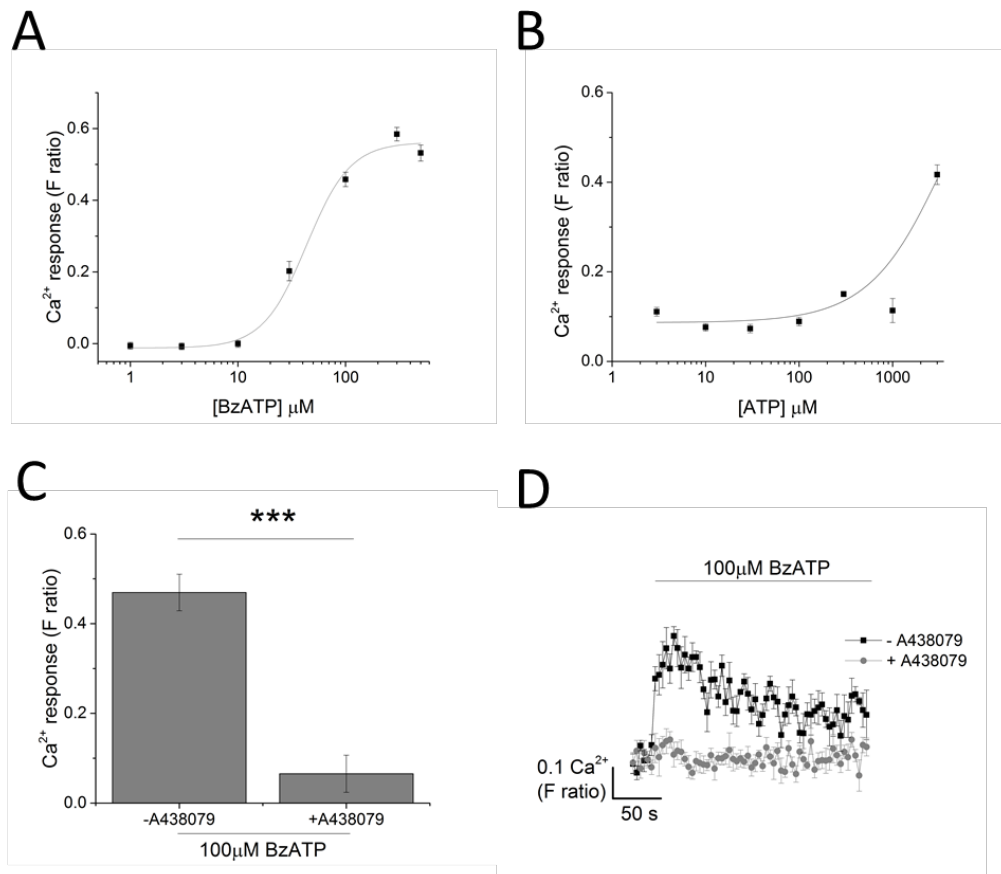
Figure 3.5. hP2X$_7$ mCherry over expressing 1321N1 cells as a tool to test selectivity of compounds. A) BzATP dose-response curve on hP2X$_7$ mCherry over expressing 1321N1 cells. B) ATP dose-response curve on hP2X$_7$ mCherry over expressing 1321N1 cells. C and D) Effect of 5 μM A438079 on 100 μM BzATP-evoked Ca^{2+} response represented as bar chart (n=3) and representative time-response curve (n=3), respectively. Asterisks include significant changes towards control (*** $p < 0.001$, Student's t-test).

Due to high variability of BzATP-evoked Ca^{2+} response in the $hP2X_7$ over expressing cell line, only selected concentrations of compounds were tested. As shown on Figure 3.6A and B, 3 μM IVM caused a significant potentiation in the magnitude of the Ca^{2+} response evoked by 100 μM BzATP (0.47 ± 0.041 *vs.* 0.67 ± 0.040, n=3; P<0.01) but showing limited effect on the decay response, which is in line with previous studies by Norenberg et al. (2012).

The effect of $P2X_4$ receptor antagonists, 5-BDBD and PSB-12062 was next studied. As shown on Figure 3.6C and D, 10 μM 5-BDBD had no significant effect on both the magnitude of the Ca^{2+} response evoked by 100 μM BzATP (0.47 ± 0.041 *vs.* 0.54 ± 0.053 n=3, P>0.05). Therefore, although the effect of 5-BDBD has not been tested on other P2XR and P2YR, it is safe to assume that 10 μM 5-BDBD does not have the capacity to inhibit responses mediated by $P2X_7$ activation. A dose response of PSB-12062 (0.3 μM to 30 μM) was tested on the BzATP-evoked Ca^{2+} response in $hP2X_7$ over expressing cells (Figure 3.6E). All concentrations, except 10 μM did not have a significant effect on the BzATP-evoked Ca^{2+} response. As shown on Figure 3.6E and F, 10 μM PSB-12062 caused a significant inhibition of 27.32 ± 7.88 % to the magnitude of the Ca^{2+} response (0.47 ± 0.041 *vs.* 0.33 ± 0.025, n=3, P<0.05). This is contradictory to what was described in a study by Hernandez-Olmos et al. (2012), whereby PSB-12062 was reported to be 35-fold selective towards $P2X_4$ versus all other human P2XR subtypes.

Together, these data illustrate that while A438079 and Ro0437626 can be used to selectively target $P2X_7$ and $P2X_1$ respectively, $P2X_4$ antagonists (5-BDBD and PSB-12062) must be employed with caution, avoiding use at high concentrations. In addition to this, the use of ATP concentration below 1 mM as an agonist is recommended to avoid the activation of $P2X_7$. It is therefore important that to isolate $P2X_4$-mediated Ca^{2+} responses in monocytes/macrophage, the use of a single antagonist for $P2X_4$ must not be relied upon and that a combination of these tools is used.
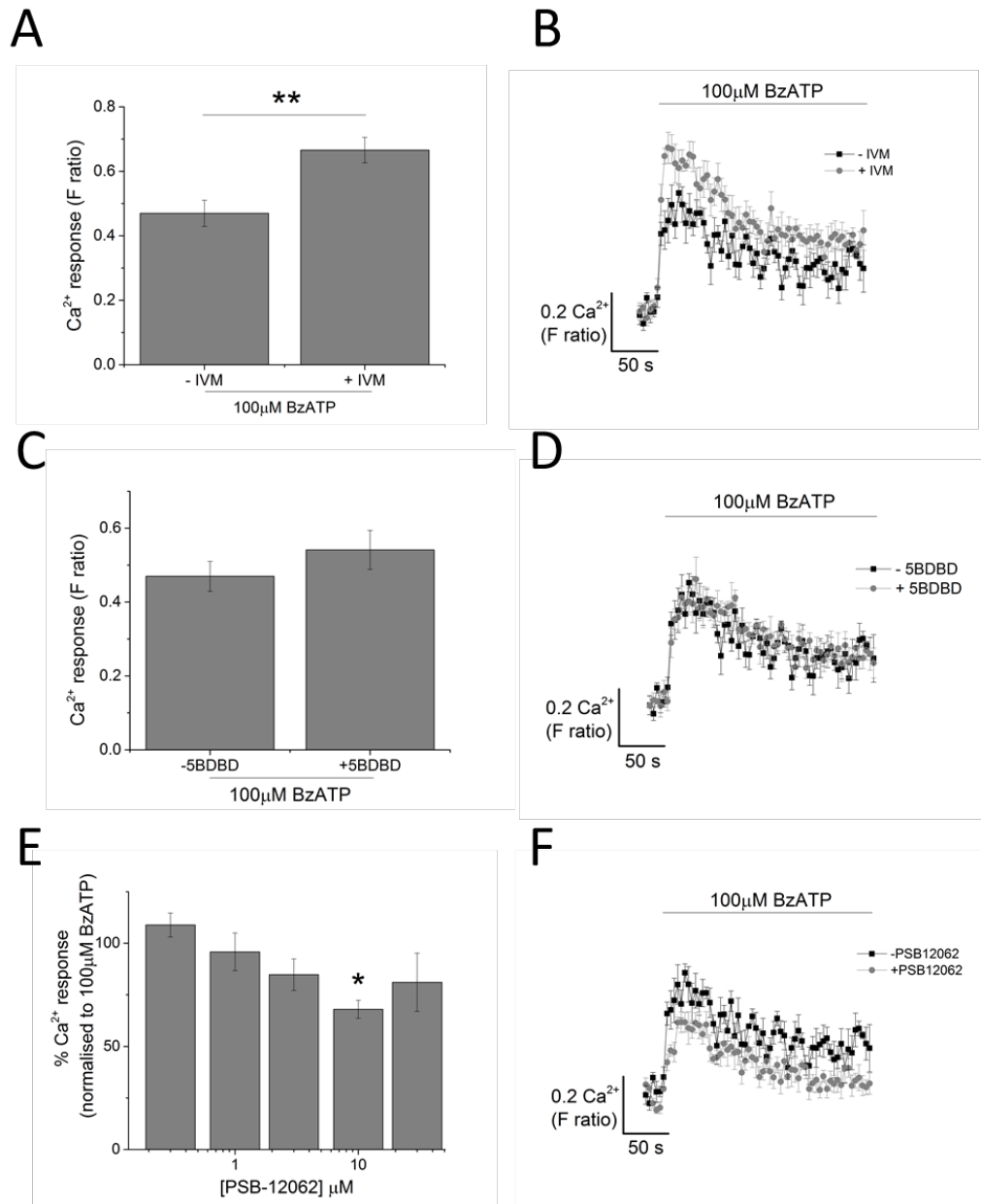
Figure 3.6. **Effect of IVM, 5BDBD and PSB-12062 on hP2X$_7$ mCherry over expressing 1321N1 cells.** Effect of: A and B) 3 μM IVM, C and D) 10 μM 5-BDBD and E and F) dose response of PSB-12062, on 100 μM BzATP-evoked Ca^{2+} response represented as bar chart (n=3) and representative time-response curve (n=3) for 10 μM PSB-12062, respectively. Asterisks include significant changes towards control (** $p < 0.01$, * $p < 0.05$, Student's t-test).

3.3.3. Pharmacological characterization of $P2X_4$-mediated Ca^{2+} response in THP-1 monocytes versus TDM

Nucleotides such as ATP can be released in high concentrations following necrotic cell death to mediate physiological responses in cells by activating two major cell surface receptors: P2X and P2Y receptors. While ATP act as the main ligand for P2X receptors, it is known to only activate some P2Y receptors (Jacobson et al., 2009). Unlike GPCRs, the wild-type P2XRs do not show constitutive activity in the absence of agonist (North, 2002). To investigate the contribution of $P2X_4$-mediated Ca^{2+} response in THP-1 cells and TDM, the initial aim of this chapter was to determine a dose response curve to ATP and the maximal concentration to activate $P2X_4$ in both cell lines.

ATP elicited a concentration-dependent increase in intracellular Ca^{2+} level in both cell types. Figure 3.7A illustrated a rightward shift in the concentration response curve of ATP in TDM (EC_{50}= 6.25 ± 1.92 μM, n=6) versus THP-1 cells (EC_{50}= 0.174 ± 0.01 μM, n=12). Maximal Ca^{2+} response was observed at 10 μM in THP-1 cells while in TDM cells, maximal Ca^{2+} response was observed at higher ATP concentration of 100 μM. To ensure maximal activation of $P2X_4$, a supra-maximal ATP concentration of 100 μM was used throughout this study. In both cell types, high ATP concentrations (above 300 μM) appear to cause receptor desensitization as illustrated from the reduction in intracellular Ca^{2+} level. The representative Ca^{2+} time-response trace in THP-1 cells and TDM upon stimulation with 100 μM ATP is represented in Figure 3.7B. Here, ATP caused a significant increase in intracellular Ca^{2+} response, which then decayed to a sustained elevated phase in THP-1 cells or back to the baseline level in TDM. However, two striking phenotype differences of the ATP response were observed from these two cell types: 1) magnitude of Ca^{2+} response – THP-1 cells being significantly higher than TDM (F ratio 3.24 ± 0.127 THP-1 *vs.* 1.09 ± 0.077 TDM; n=12 and 6, respectively; P<0.001; Figure 3.7B) and, 2) decay kinetics – Ca^{2+} response in TDM decay at a rate approximately four-fold faster than THP-1 cells (18.64 ± 2.18 s TDM *vs.* 84.0 ± 5.28 s THP-1 cells) (Figure 3.7C). These differences may be a result of several factors which include varying cell numbers, different receptors expressed on the cell membranes, or the varying calcium buffering capacity of the two cell types.

To identify if varying cell numbers may be responsible for the difference in ATP-evoked intracellular Ca^{2+} responses in THP-1 monocytes and TDM cells, cells were stained with nuclear dye Hoechst-33342. The fluorescence read-out illustrated no significant differences in number of cells being assayed, indicating that the phenotype differences is likely due to other factors, such as lower expression of other ATP receptors in TDM such as P2YR (Figure 3.7D). However, this was not further explored during the study.
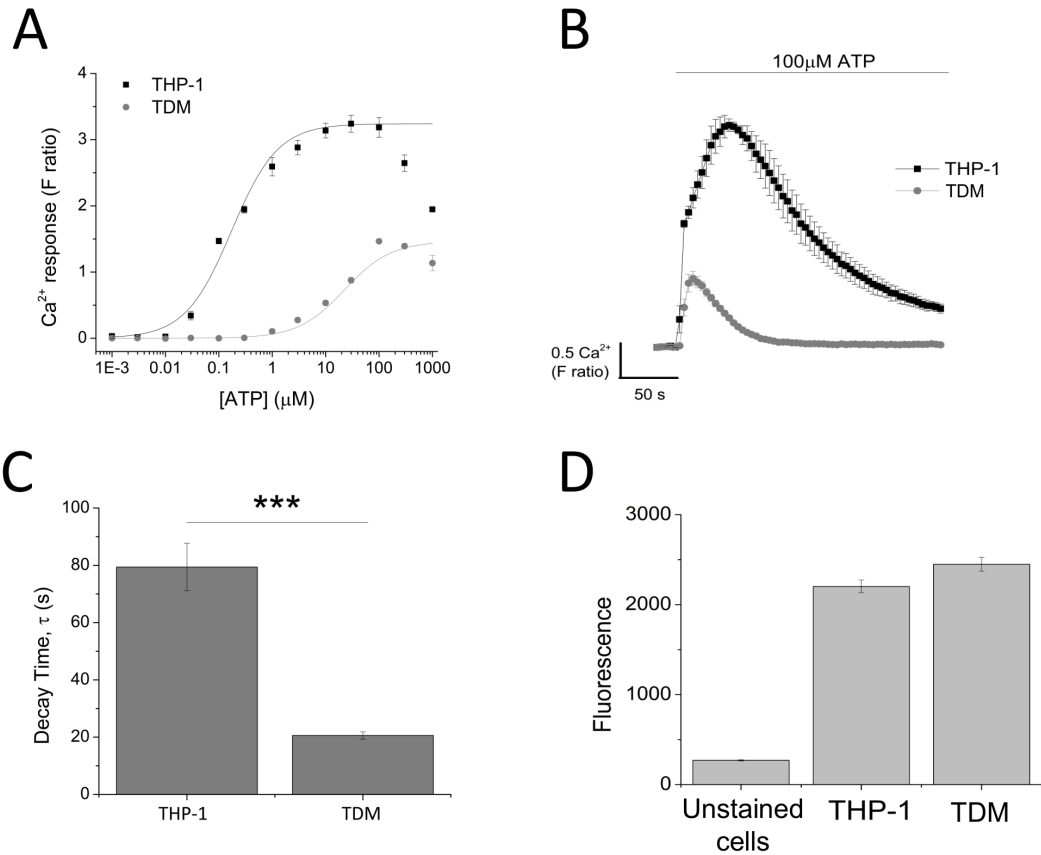
Figure 3.7. **ATP-elicited Ca^{2+} response in both THP-1 cells and TDM**. A) Dose-response curve of ATP (0.01 – 1000 μM) in THP-1 monocytes (n=12) and TDM cells (n=6). Ca^{2+} response is represented as F ratio. B) Representative time-response curve of THP-1 cells and TDM upon the application of 100 μM ATP recorded over 250 s. C) Bar chart representing decay kinetics of THP-1 cells (n=12) and TDM (n=6). D) Cell quantification assay using nuclear stain H-33342. Asterisks include significant changes towards control (***p<0.001, Student's t-test).

3.3.3.1. Dependency of ATP-evoked Ca^{2+} response on extracellular Ca^{2+}

Within cells, both P2XR and P2YR are involved in extracellular ATP-dependent signalling. P2XR are Ca^{2+} permeable ligand-gated ion channels which, upon activation, results in an increase in intracellular Ca^{2+} level that is dependent on extracellular Ca^{2+} (Ryu et al., 2010). Unlike P2XR, P2YR are GPCR-coupled which involve a more complex downstream signalling pathway (Bhatt and Topol, 2003). To investigate the contribution of ionotropic receptors to ATP-evoked Ca^{2+} response in THP-1 cells and TDM cells, ATP concentration response curves were performed in the presence and absence of extracellular Ca^{2+}.

The effect of extracellular Ca^{2+} removal on ATP-evoked Ca^{2+} response in THP-1 cells can be seen in Figure 3.8A and 3.8B. In the presence of 1.5 mM extracellular Ca^{2+}, 100 μM ATP evoked an expected intracellular Ca^{2+} response generating a response of 3.18 ± 0.15 F ratio (n=3). In contrast, in the absence of extracellular Ca^{2+}, ATP response was significantly reduced to 0.25 ± 0.01 F ratio (n=3), indicating a 92.0 ± 0.46% reduction (n=3, P<0.001). In TDM cells, in the presence of 1.5 mM extracellular Ca^{2+}, 100 μM ATP evoked an expected intracellular Ca^{2+} response of 1.47 ± 0.03 F ratio (n=3) while in the absence of extracellular Ca^{2+}, F ratio value for ATP was significantly reduced to 0.43 ± 0.046 F ratio (n=3), indicating a 71.2 ± 4.0 % (n=3, P<0.01) reduction (Figure 3.8C and 3.8D). As the majority of ATP-evoked Ca^{2+} response in both cell types was significantly inhibited by the absence of extracellular Ca^{2+}, this may indicate that P2X receptors are key players that drive the ATP-evoked Ca^{2+} response in both THP-1 and TDM cells.
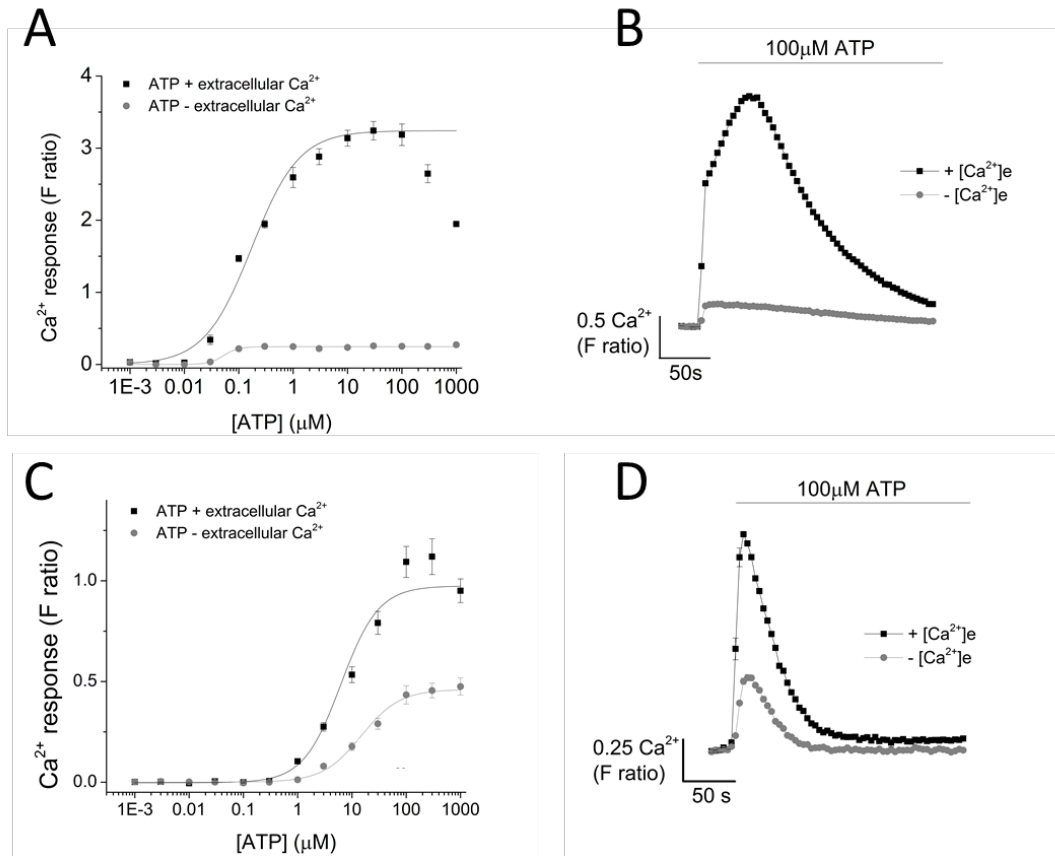
Figure 3.8. **Extracellular Ca^{2+}-dependent ATP-mediated response in THP-1 cells and TDM**. Dose response curve of ATP (0.01 – 1000 μM) in the presence and absence of extracellular Ca^{2+} and its representative time traces at 100 μM ATP in: A and B) THP-1 cells (n=3) or C and D) TDM (n=3).

3.3.3.2. Blocking metabotropic receptor-mediated Ca^{2+} responses using pharmacological tools

As mentioned previously, ATP evoked a global Ca^{2+} response mediated by various receptors, which includes both P2XR and P2YR. In the previous section (3.3.3.1), it was not possible to investigate the contribution of P2XR activation by simply eliminating extracellular Ca^{2+} due to possible involvement of SOC channels. Therefore, to pharmacologically isolate P2X$_4$ contribution to ATP-mediated Ca^{2+} response in THP-1 cells and TDM, pharmacological tools specifically targeting Ca^{2+} response mediated by metabotropic receptors were utilized. Here, two different compounds, PLC inhibitor U-73122 and non-competitive SERCA inhibitor Thapsigargin (Tg), were employed to reveal Ca^{2+} responses dependent of ionotropic receptors. Following this, additional pharmacological tools to confirm the contribution of P2X$_4$ on Ca^{2+} response were utilized.

3.3.3.2.1. Effect of PLC inhibition on ATP-mediated Ca^{2+} response

The activation of G$_{\alpha q}$-coupled P2YRs by ATP and its metabolite lead to downstream signalling pathway involving phospholipase C (PLC), which in turn results in the rise of intracellular Ca^{2+} signalling. To block this downstream signalling, PLC inhibitor, U-73122 was employed in this study. Pre-treatment of cells with a dose-response of U-73122 produced a dose-dependent inhibition of Ca^{2+} response in both THP-1 cells and TDM cells, with maximal inhibition observed at 10 μM (Figure 3.9A and 3.9B, respectively). However, a residual Ca^{2+} response that appear to be insensitive to U-73122 was seen in both cell types. This was quantified to be 20 ± 1.2% (n=6; p<0.01) and 20 ± 0.8% (n=6; p<0.01) in THP-1 and TDM cells, respectively. To confirm that this residual U-73122-resistant Ca^{2+} response is mediated by ionotropic receptors, the experiments were performed in the absence of extracellular Ca^{2+}. In the absence of extracellular Ca^{2+}, U-73122-resistant Ca^{2+} response was completely abolished in THP-1 cells while 65.3 ± 1.8% was inhibited in TDM cells (Figure 3.9C and Figure 3.9D, respectively). This indicates that U-73122-resistant Ca^{2+} response is dependent on extracellular Ca^{2+} and is likely to be mediated by P2XR. However, as previously mentioned in the methodology section, leaving the cells in Ca^{2+}-free SBS buffer is likely to deplete the intracellular stores of Ca^{2+}, hence over-estimating the contribution of Ca^{2+} influx in ATP-evoked Ca^{2+} response.
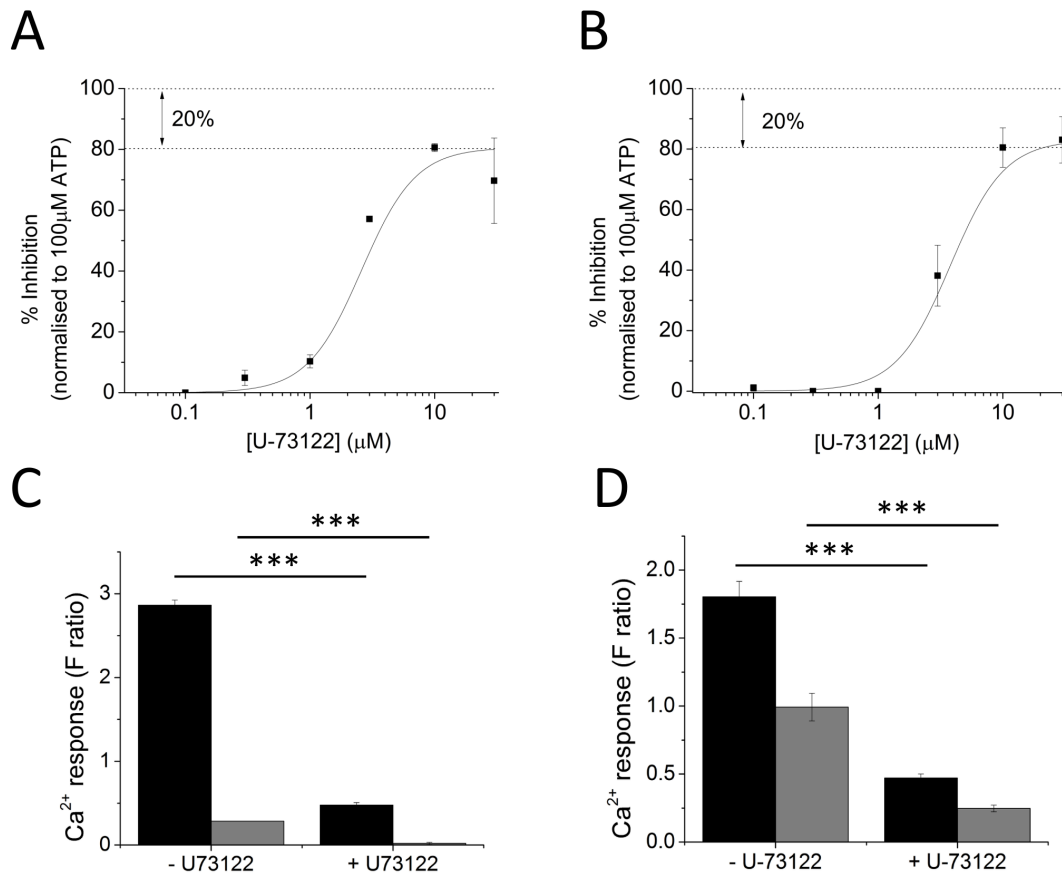
Figure 3.9. U-73122-resistant Ca^{2+} response is mediated by Ca^{2+} influx. Dose-response inhibition curve of U-73122 in: A) THP-1 cells (n=6) and B) TDM (n=6). Data is normalized to calcium response (F ratio) at 100 μM alone. C) Effect of U-73122, represented in F ratio, in the presence (black bars) and absence (grey bars) of extracellular calcium in THP-1 cells (n=6). D) Effect of U-73122, represented in F ratio, in the presence (black bars) and absence (grey bars) of extracellular calcium in TDM (n=3). Asterisks include significant changes towards control (*** p<0.001, Student's t-test).

3.3.3.2.2. Effect of IVM on U-73122-resistant Ca^{2+} response

To identify the contribution of $P2X_4$ to the U-73122-resistant Ca^{2+} response, a $P2X_4$ positive allosteric modulator, IVM, was utilized. IVM has been shown to be a selective $P2X_4$ allosteric modulator used routinely as a pharmacological tool to identify the contribution of $P2X_4$ in ATP-mediated processes (Asatryan et al., 2010, Khakh et al., 1999). IVM has also been described to potentiate $P2X_4$ responses by reducing endocytosis resulting in increased pool of functional $P2X_4$ in the plasma membrane (Toulme et al., 2006).

Pre-treatment of cells with IVM caused a dose-dependent potentiation of magnitude of ATP-evoked intracellular Ca^{2+} response in both THP-1 cells and TDM cells (Figure 3.10A and 3.10B, respectively), with maximal potentiation of U-73122-resistant Ca^{2+} response seen following pre-treatment with $3\mu M$ IVM. Pre-treatment of cells with $3\mu M$ IVM potentiated Ca^{2+} response in THP-1 cells by 2.2-fold (0.25 F ratio to 0.53 F ratio, n=6, p<0.001) and in TDM cells by 3.3-fold (0.20 F ratio to 0.654 F ratio, n=6, p<0.001). To accompany the potentiation of the magnitude of Ca^{2+} response, IVM also appeared to cause a delay in the decay kinetics of the Ca^{2+} response as observed through the time-response traces for THP-1 cells (Figure 3.10C) and TDM cells (Figure 3.10D). These are typical characteristics of IVM effect on $P2X_4$-mediated Ca^{2+} responses (Norenberg et al., 2012). Lastly, IVM also increased the net calcium movement (as measured by area under the curve) in both THP-1 cells (40.6 ± 6.85 AUC without IVM versus 69.0 ± 5.87 AUC with IVM; n=6; P<0.01) and TDM cells (8.80 ± 1.80 AUC without IVM *vs*. 86.3 ± 11.08 with IVM; n=6; P<0.001) (Figure 3.10E and 3.10F, respectively).
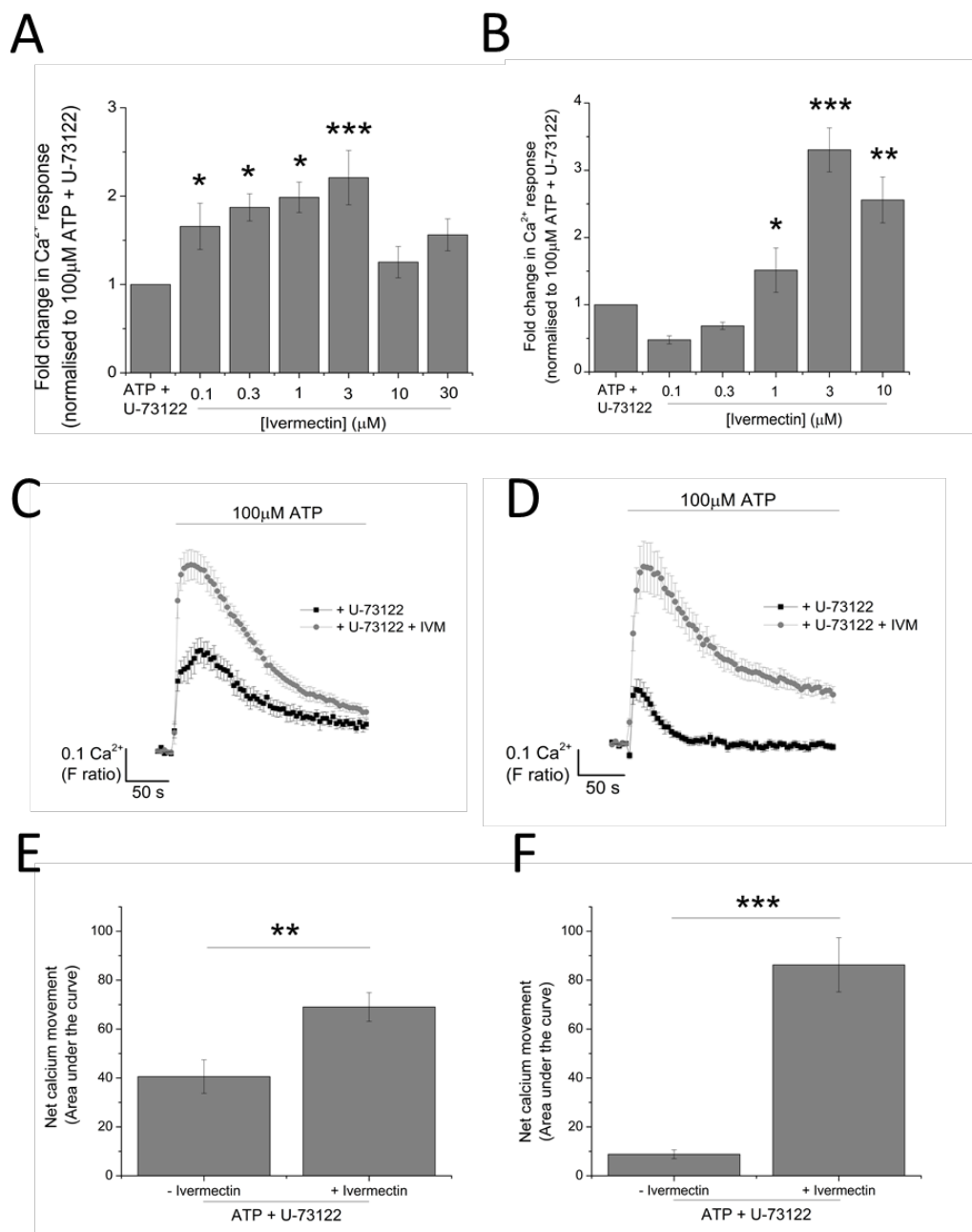
Figure 3.10. **Effect of P2X$_4$ allosteric modulator, ivermectin, on U-73122 resistant component of THP-1 cells and TDM.** Plot of dose-response effect of IVM, represented as fold change normalized to 100 μM ATP in the presence of 10 μM U-73122 on: A) THP-1 cells (n=6) and B) TDM (n=3). Representative time-response curve at 100 μM ATP in the presence or absence of 3 μM IVM in: C) THP-1 cells (n=6) and D) TDM (n=3). Net calcium movement is quantified as area under the curve in: E) THP-1 cells (n=6) and F) TDM (n=6). Asterisks include significant changes towards control (*** $p<0.001$, ** $p<0.01$, * $p<0.05$, Student's t-test).

3.3.3.2.3. Effect of P2XR antagonists on U-73122-resistant ATP-evoked Ca^{2+} response

To further identify the contribution of P2XR on the U-73122-resistant Ca^{2+} response in the two cell lines, various P2XR ($P2X_1$, $P2X_4$ and $P2X_7$) antagonists were tested. Unfortunately, to date, no selective $P2X_5$ and $P2X_6$ antagonists are available commercially to be tested in this study. In THP-1 cells, none of the P2XR antagonists appear to have any significant effect on the U-73122-resistant Ca^{2+} response. However, in TDM cells, $P2X_1$ antagonist (30 μM Ro0437626) significantly potentiated the U-73122-resistant Ca^{2+} response by 2.84 $\pm$ 0.56-fold while $P2X_7$ antagonist A438079 had no significant effect (Figure 3.11A and 3.11B, respectively). Both $P2X_4$ antagonists, 5-BDBD and PSB-12062, caused a significant inhibition at 10 μM in TDM cells, but not in THP-1 cells (Figure 3.11C and 3.11D, respectively). 5-BDBD caused a 44.4 $\pm$ 9.8% (n=6, p<0.01) while PSB-12062 caused a 31.0 $\pm$ 5.9% (n=3, p<0.01) inhibition to the magnitude of the Ca^{2+} response.
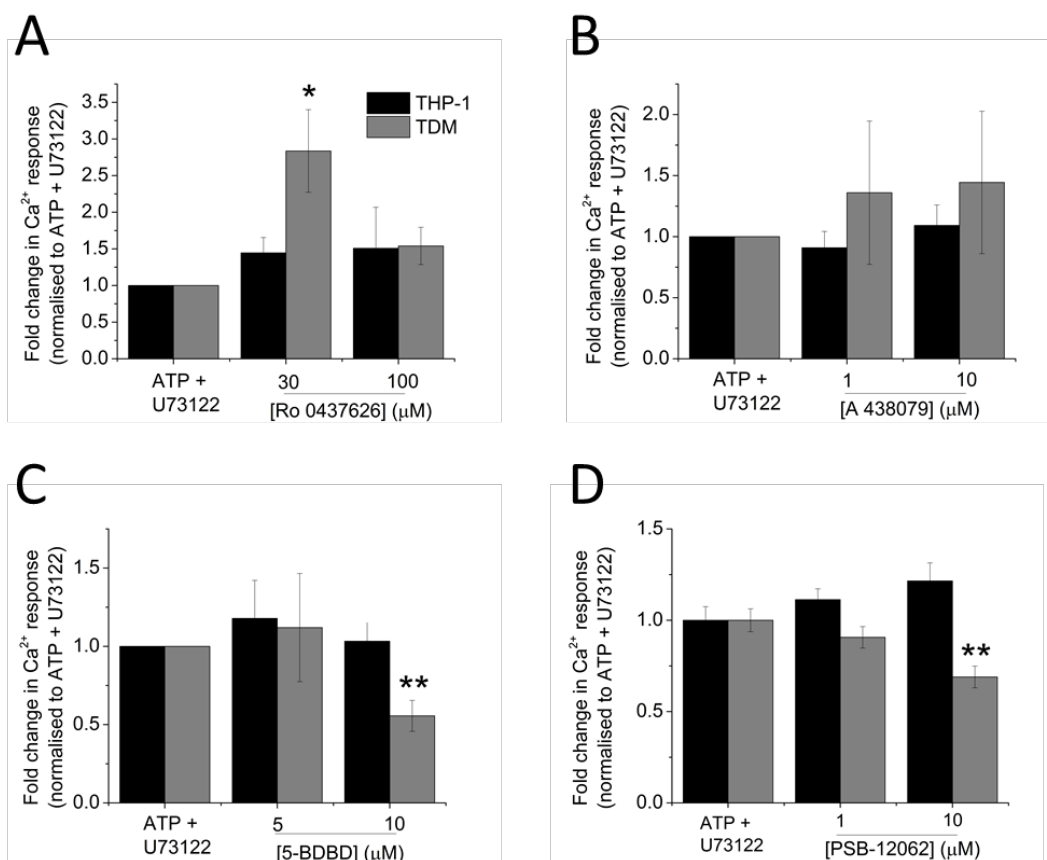
Figure 3.11. **Effect of P2X receptor antagonists on U-73122-resistant component of THP-1 cells and TDM.** The effect of: A) 30 µM and 100 µM $P2X_1$ receptor antagonist (Ro0437626) (n=3), B) 1 µM and 10 µM $P2X_7$ receptor antagonist (A438079) (n=3), C) 5 µM and 10 µM $P2X_4$ receptor antagonist (5-BDBD) (n=6) and D) 1 µM and 10 µM $P2X_4$ receptor antagonist (PSB-12062) (n=3), were studied on THP-1 cells and TDM. Asterisks include significant changes towards control (** $p < 0.01$, * $p < 0.05$, Student's t-test).

3.3.3.3. Blocking metabotropic receptor-mediated Ca^{2+} responses using Thapsigargin

Another pharmacological tool used to eliminate metabotropic responses to ATP is Thapsigargin (Tg). Tg is a SERCA inhibitor, which acts by depleting intracellular Ca^{2+} stores. The depletion of intracellular Ca^{2+} store means that upon activation of metabotropic P2YR, no mobilization of Ca^{2+} from the stores can be achieved resulting in no Ca^{2+} responses. Depletion of intracellular Ca^{2+} stores is evident from higher cytosolic Ca^{2+} level (F ratio 1.35 ± 0.0082 without Tg *vs.* 2.24 ± 0.065 with Tg; n=6; P<0.001, TDM cells, Figure 3.12F).

Pre-treatment of THP-1 cells with 5 μM Tg resulted in a complete inhibition of ATP-evoked Ca^{2+} response (Figure 3.12A and 3.12B). However, pre-treatment of TDM cells with 5 μM Tg resulted in 88.7 ± 3.29 % inhibition (n=6; P<0.001) of Ca^{2+} response, as shown on Figure 3.12C. Despite a significant inhibition, 11.3 ± 3.29 % of the Ca^{2+} response appeared to be insensitive to Tg. This Tg-insensitive Ca^{2+} response in TDM cells was accompanied by a second slower response above the baseline (Figure 3.12D). To test if this Tg-insensitive response is dependent on Ca^{2+} influx, the experiment was performed in the absence of extracellular Ca^{2+}. Removal of extracellular Ca^{2+} resulted in Tg-insensitive Ca^{2+} response to be completely abolished (Figure 3.12E) implying that it is sensitive to extracellular Ca^{2+} and is likely to be mediated by ionotropic receptors such as P2XR. As pre-treatment with Tg completely abolished the ATP-evoked Ca^{2+} response in THP-1 cells, the rest of the chapter will focus only in the use of TDM cells to characterize $P2X_4$-mediated Ca^{2+} entry.
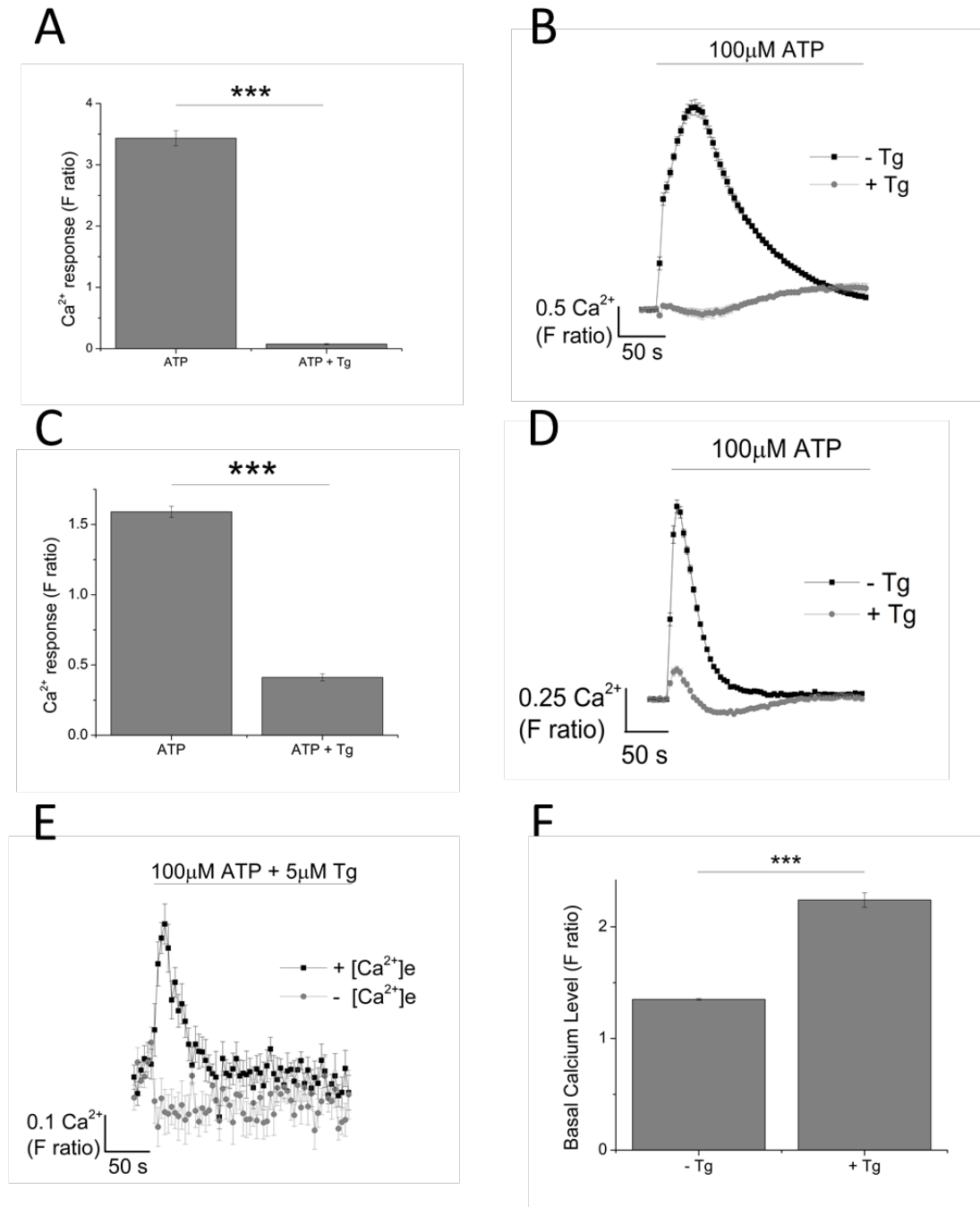
Figure 3.12. Dependency of ATP-evoked Ca²⁺ response on ER Ca²⁺ store.
Effect of 100 μM ATP in the presence and absence of 5 μM Tg in: A and B) THP-1 cells (n=3) and C and D) TDM (n=6). E) Time-response curve of the effect of Tg on 100 μM ATP in the presence and absence of extracellular Ca²⁺ (n=6). F) Effect of 5 μM Tg on basal calcium level in TDM (n=6). Asterisks include significant changes towards control (*** p<0.001, Student's t-test).

3.3.3.3.1. Effect of IVM on Tg-resistant Ca^{2+} response

To identify if P2X$_4$ contribute to the Tg-insensitive Ca^{2+} response, the effect of 3 μM IVM was tested in TDM cells. As can be seen, pre-treatment of TDM cells with IVM potentiated Tg-resistant ATP-evoked intracellular Ca^{2+} response by 2.1 fold (F ratio 0.42 ± 0.025 without IVM to 0.90 ± 0.042 with IVM; n=6; P<0.001) (Figure 3.13A), delayed decay kinetics by 3.67 ± 0.37 fold (14.4 ± 0.78 s without IVM to 49.9 ± 3.8s with IVM; n=6; p<0.005) (Figure 3.13B and C) and significantly increased net calcium movement in TDM cells as quantified by area under the curve (AUC 19.48 ± 2.45 without IVM *vs.* 80.01 ± 5.44 with IVM; n=6; p<0.001) (Figure 3.13D). The data so far illustrated a possible contribution of P2X$_4$ towards Tg-resistant ATP-evoked intracellular Ca^{2+} response in TDM cells.
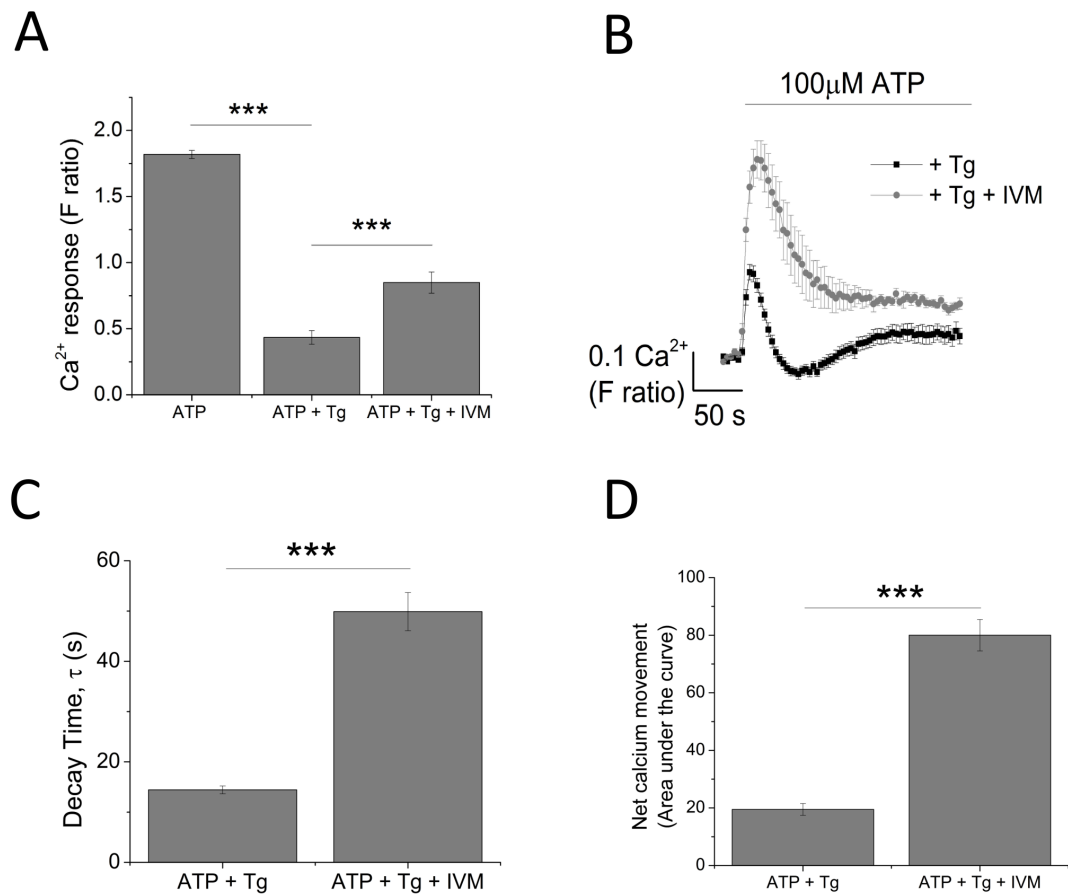
Figure 3.13. Investigating Thapsigargin (Tg) as an alternative pharmacological tool to isolate P2X$_4$-mediated Ca^{2+} influx. A and B) Effect of 3 μM IVM in Tg-resistant component represented as bar chart and time-response curve, respectively (n=6). C) Effect of 3 μM IVM on decay kinetics (τ) of TDM (n=6). D) Effect of 3 μM IVM on net calcium movement as quantified by area under the curve of TDM (n=6). Asterisks include significant changes towards control (*** $p<0.001$, Student's t-test).

3.3.3.3.2. Effect of P2X$_4$ antagonists on Tg-resistant Ca^{2+} response

To further confirm that P2X$_4$ contribute to the Tg-resistant Ca^{2+} response in TDM cells, selective P2X$_4$ antagonists, 5-BDBD and PSB-12062, were used. In the presence of Tg, both 5-BDBD and PSB-12062 (10 μM) significantly inhibited ATP-elicited Ca^{2+} response by 52.9 ± 1.99 % (n=3; p<0.01; Figure 3.14A) and 78.5 ± 3.23 % (n=3; p<0.001; Figure 3.14D), respectively. In addition to inhibiting the magnitude of the Ca^{2+} response, both antagonists also appear to abolish the second slower response observed in the presence of Tg (Figure 3.14B and 3.14E). Although it is still unclear what the second slower response underlies, it appeared to be dependent on P2X$_4$ activation. Finally, when quantifying area under the curve, 5-BDBD and PSB-12062 appeared to significantly reduce net calcium movement in TDM cells. 5-BDBD caused AUC to be reduced from 17.45 ± 2.24 to 4.43 ± 7.69 (Figure 3.14C) while PSB-12062 caused AUC to be reduced from 17.45 ± 2.24 to 7.21 ± 10.3 (Figure 3.14F). Together with the effect of IVM on Tg-resistant Ca^{2+} response, the data suggests contributions of P2X$_4$ towards the magnitude and the decay phase of ATP-evoked Ca^{2+} response TDM cells.
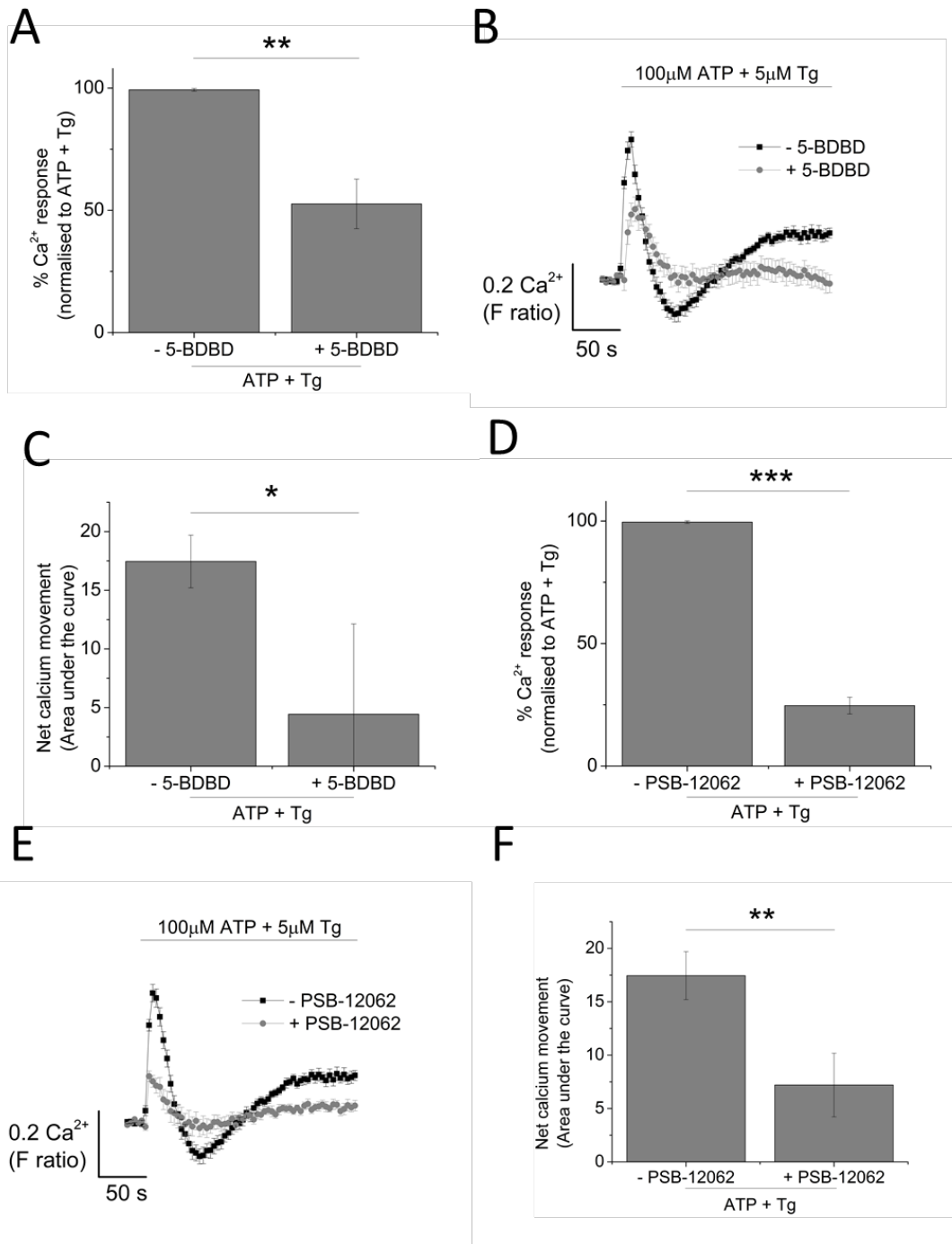
Figure 3.14. Effect of P2X$_4$ receptor antagonists on Tg-resistant ATP-evoked Ca^{2+} response in TDM cells. A-C) Effect of 10 μM 5-BDBD on magnitude of calcium response and net calcium movement on Tg-resistant Ca^{2+} response of TDM (n=3). D-F) Effect of 10 μM PSB-12062 on magnitude of Ca^{2+} response and net calcium movement on Tg-resistant Ca^{2+} response of TDM (n=3). Asterisks include significant changes towards control (*** $p<0.001$, ** $p<0.01$, * $p<0.05$, Student's t-test).

3.3.3.3.3. Effect of P2XR antagonists on Tg-resistant Ca^{2+} response

As can be seen on the data discussed above on section 3.3.3.3.2, the use of selective $P2X_4$ antagonists was insufficient to abolish the Tg-resistant Ca^{2+} response in TDM cells. This implies that although $P2X_4$ may contribute to this Ca^{2+} influx, other ionotropic receptors may play a role too. Two P2XR antagonists were used to test for this: A438079 ($P2X_7$ antagonist; 5 μM) and Ro0437626 ($P2X_1$ antagonist; 30 μM). A438079 is reported to be a selective $P2X_7$ antagonist with IC_{50} value of 0.13 μM (Donnelly-Roberts and Jarvis, 2007, Carroll et al., 2009) while Ro0437626 is reported to be a selective $P2X_1$ antagonist with IC_{50} value of 3 μM (Jaime-Figueroa et al., 2005). For antagonist experiments, concentrations of at least 10 times the IC_{50} value was chosen to ensure maximal inhibition.

In the presence of 5 μM Tg, both A438079 and Ro0437626 had no effect on the magnitude of ATP-evoked Ca^{2+} response (Figure 3.15A and 3.15D, respectively). However, as can be seen (Figure 3.15B), pre-treatment of TDM cells with Tg and A438079 appeared to cause a significant increase in the second slower Ca^{2+} response compared to Tg pre-treatment alone. When area under the curve was quantified, A438079 appeared to cause a significant increase in net calcium movement (AUC 17.45 ± 2.24 without A438079 versus 35.63 ± 2.84 with A438079 AUC; n=3; P<0.001) (Figure 3.15C). On the other hand, Ro0437626 had no significant effect on the second slower Ca^{2+} response (Figure 3.15E) as well as on the net calcium movement (Figure 3.15F). Altogether, these data suggest that Tg-resistant Ca^{2+} response is dependent on Ca^{2+} influx and while $P2X_4$ contributes to the Ca^{2+} response, $P2X_1$ and $P2X_7$ do not appear to have any contribution.
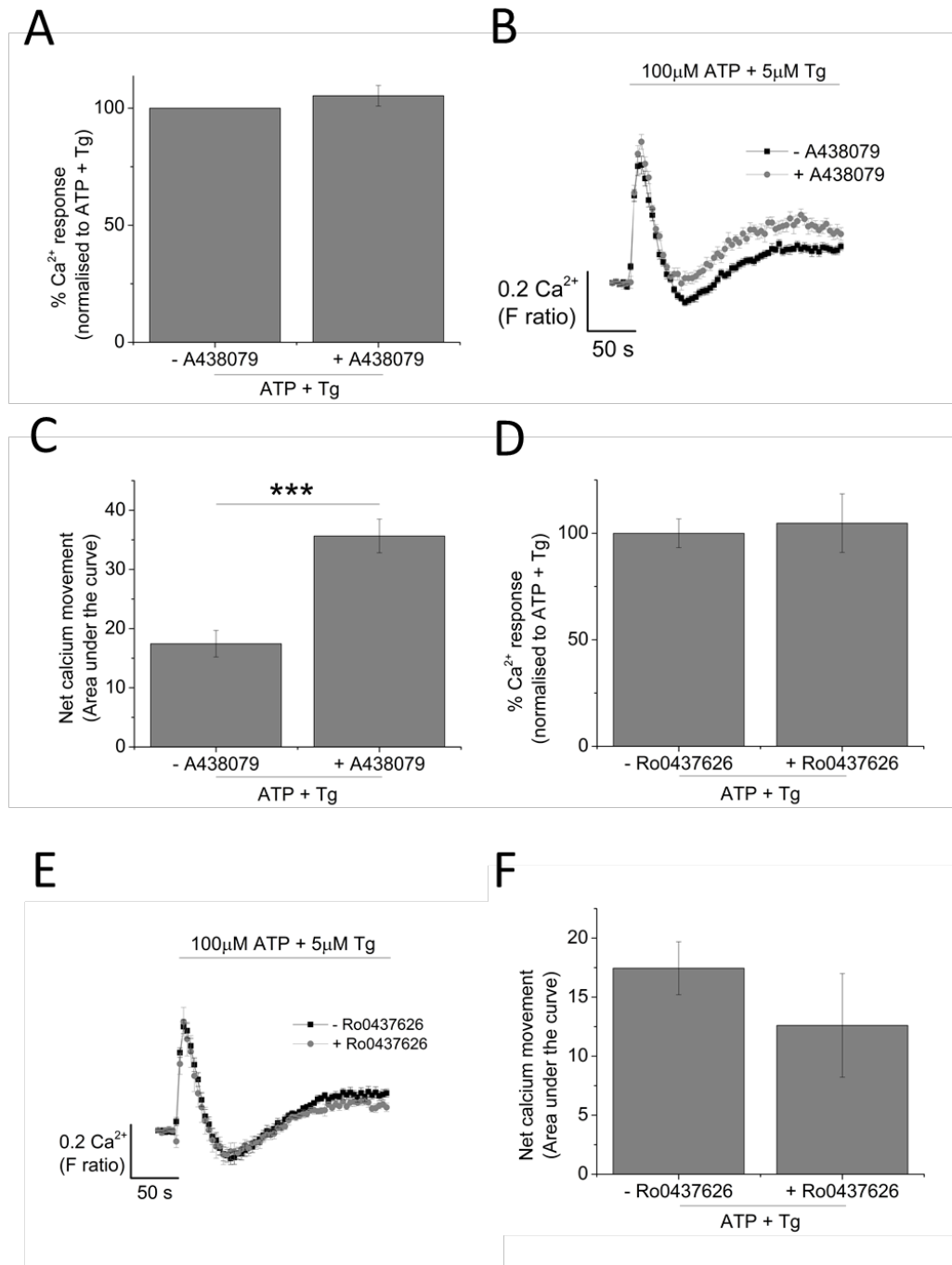
Figure 3.15. Effect of P2X$_1$ and P2X$_7$ receptor antagonist on Tg-resistant Ca^{2+} response. A-C) Effect of 5 μM P2X$_7$ receptor antagonist (A438079) on magnitude of Ca^{2+} response and net calcium movement on Tg-resistant Ca^{2+} response of TDM (n=3). D-F) Effect of 30 μM P2X$_1$ receptor antagonist (Ro0437626) on magnitude of Ca^{2+} response and net calcium movement on Tg-resistant Ca^{2+} response of TDM (n=3). Asterisks include significant changes towards control (*** p<0.001, Student's t-test).

3.3.4. Generation and evaluation of P2X$_4$ KD THP-1 monocytes

To provide further evidence for the contribution of P2X$_4$ in ATP-evoked Ca^{2+} responses in TDM cells, it was necessary to employ a molecular-based approach to silence the P2X$_4$ gene. The approach taken to perform this study involved the use of a lentiviral vector to deliver an shRNA sequence that is targeted for *P2X$_4$* gene into THP-1 cells. This enabled the generation of a stable and long-term gene knockdown THP-1 cell line which can then be differentiated into TDM cells. As a negative control, non-target-shRNA lentiviral particle (scrambled shRNA) was used.

3.3.4.1. qRT-PCR and FACS analysis

Following the generation of stable P2X$_4$ shRNA cell line, two methods were utilized to confirm the rate of knockdown of P2X$_4$: 1) quantification of P2X$_4$ mRNA expression using qRT-PCR approach and 2) flow cytometry staining to quantify the amount of extracellular and total P2X$_4$ protein expression.

As shown (Figure 3.16A), a 48.8 ± 9.64 % (n=4; P<0.01) reduction in P2X$_4$ mRNA expression was observed in the P2X$_4$ shRNA TDM cells in comparison to scrambled shRNA TDM cells using qRT-PCR. Having identified that mRNA expression of P2X$_4$ was successfully knocked down, extracellular and total protein expression of P2X$_4$ was quantified using flow cytometry for further confirmation. Cells were stained with rabbit polyclonal anti-human P2X$_4$ that recognizes either the extracellular or C-terminal epitope (cell surface or internal/total), followed by secondary staining with goat anti-rabbit AF488 antibody. As shown (Figure 3.16B), there was a significant reduction in the amount of P2X$_4$(ext)$^+$ cells in the P2X$_4$ shRNA system compared to the scrambled shRNA control (57.7 ± 4.37 % reduction, n=4, P<0.01). Despite this reduction, it was an interesting observation that constitutive expression of P2X$_4$(ext)$^+$ cells in the control scrambled shRNA system was relatively low (18.61 ± 4.01%, n=3). The low constitutive expression of cell surface P2X$_4$ in TDM cells may be a result of the predominant intracellular lysosomal localization of the receptor (Qureshi et al., 2007). Interestingly, despite a significant reduction in the expression of cell surface P2X$_4$ in the P2X$_4$ shRNA TDM cells, no significant differences in the amount of total P2X$_4$ expression was observed (Figure 3.16C).
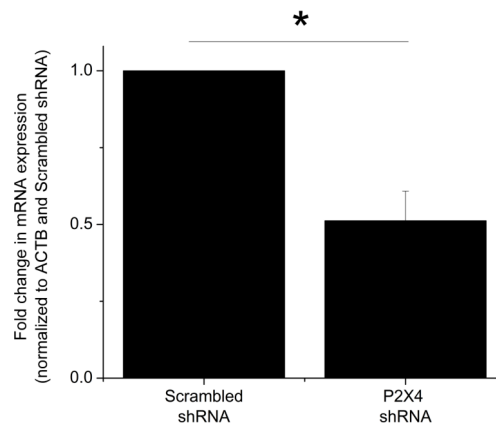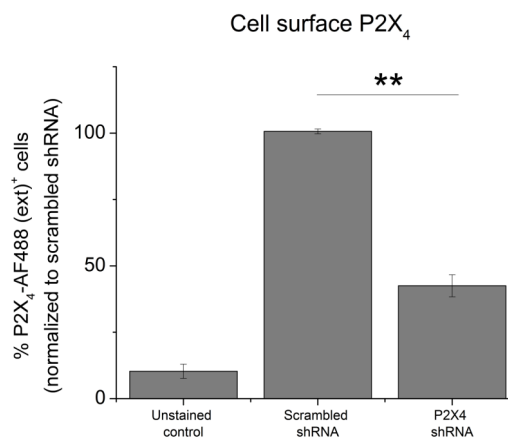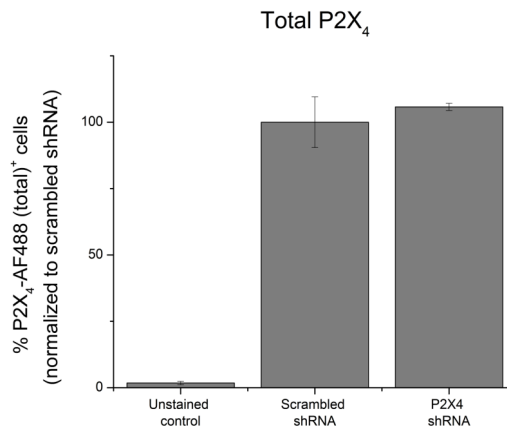
Figure 3.16. Generation of P2X$_4$ knockdown TDM cells. Success of knockdown approach was quantified using two methods: A) quantitative RT-PCR (n=4), B) FACS analysis to quantify cells expressing surface P2X$_4$ receptor (n=4) and C) FACS analysis to quantify cells expressing total (cell surface and internal) P2X$_4$ receptor (n=4). Asterisks include significant changes towards control (** $p<0.01$, * $p<0.05$, Student's t-test).

3.3.4.2. Effect of P2X$_4$ knockdown on ATP-evoked Ca^{2+} responses in TDM cells

Having confirmed the success of P2X$_4$ knockdown approach in the TDM cells, intracellular Ca^{2+} measurements were performed in both scrambled shRNA TDM versus P2X$_4$ shRNA TDM cells. Here, several pharmacological tools that have been assessed earlier in the chapter were used to identify changes in Ca^{2+} responses following knockdown approach and the potential contribution P2X$_4$ in TDM cells.

Despite FACS analysis data illustrating reduction of cell surface expression of P2X$_4$ in the P2X$_4$ shRNA system (Figure 3.16B), no significant changes in 100 μM ATP-evoked intracellular Ca^{2+} responses were observed in P2X$_4$-KD TDM cells when compared to scrambled shRNA TDM cells (Figure 3.17A). It was difficult to explain this lack of effect of P2X$_4$ knock down on the magnitude of 100 μM ATP-evoked Ca^{2+} response, however, it may be due to compensatory mechanism within the cell upon silencing of P2X$_4$. When P2X$_4$ shRNA TDM cells were pre-treated with pharmacological tools selective for P2X$_4$ antagonist, significant differences were observed in the ATP-evoked Ca^{2+} response compared to scrambled shRNA TDM cells. When cells were pre-treated with IVM, P2X$_4$ shRNA TDM cells were found to be significantly less sensitive towards the allosteric positive modulator, which was visible from the time-response traces (Figure 3.17C and D for scrambled shRNA versus P2X$_4$ shRNA TDM cells, respectively). As shown (Figure 3.17B), IVM potentiated the AUC of scrambled shRNA by 2.06 ± 0.23-fold (43.09 ± 3.89 without IVM *vs.* 135.55 ± 2.29 with IVM; n=4; P<0.01) but was only able to potentiate AUC of P2X$_4$ shRNA TDM cells by 1.53 ± 0.055 fold (45.8 ± 4.23 without IVM *vs.* 93.3 ± 7.18 with IVM; n=4, P<0.01). In addition to this, when compared to scrambled shRNA cells, ATP-evoked Ca^{2+} response in P2X$_4$ shRNA TDM cells appeared to be insensitive to pre-treatment of 10 μM PSB-12062 (Figure 3.17E and F for scrambled shRNA *vs.* P2X$_4$ shRNA cells, respectively). Finally, in the presence of IVM, ATP-evoked Ca^{2+} response in the P2X$_4$ shRNA cells appeared to be insensitive towards PSB-12062 (AUC 117.23 ± 4.22 without PSB-12062 *vs.* 91.02 ± 20.38 with PSB-12062; n=4; P>0.05; Figure 3.17F), when compared to scrambled shRNA (AUC 166.73 ± 18.66 without PSB-12062 *vs.* 72.17 ± 26.49 with PSB-12062; n=4; P<0.05; Figure 3.17E). These data suggest that P2X$_4$ shRNA TDM cells are less sensitive to IVM and PSB-12062, indicating a reduction in functional P2X$_4$ within the cell, as assessed through intracellular Ca^{2+} measurements.
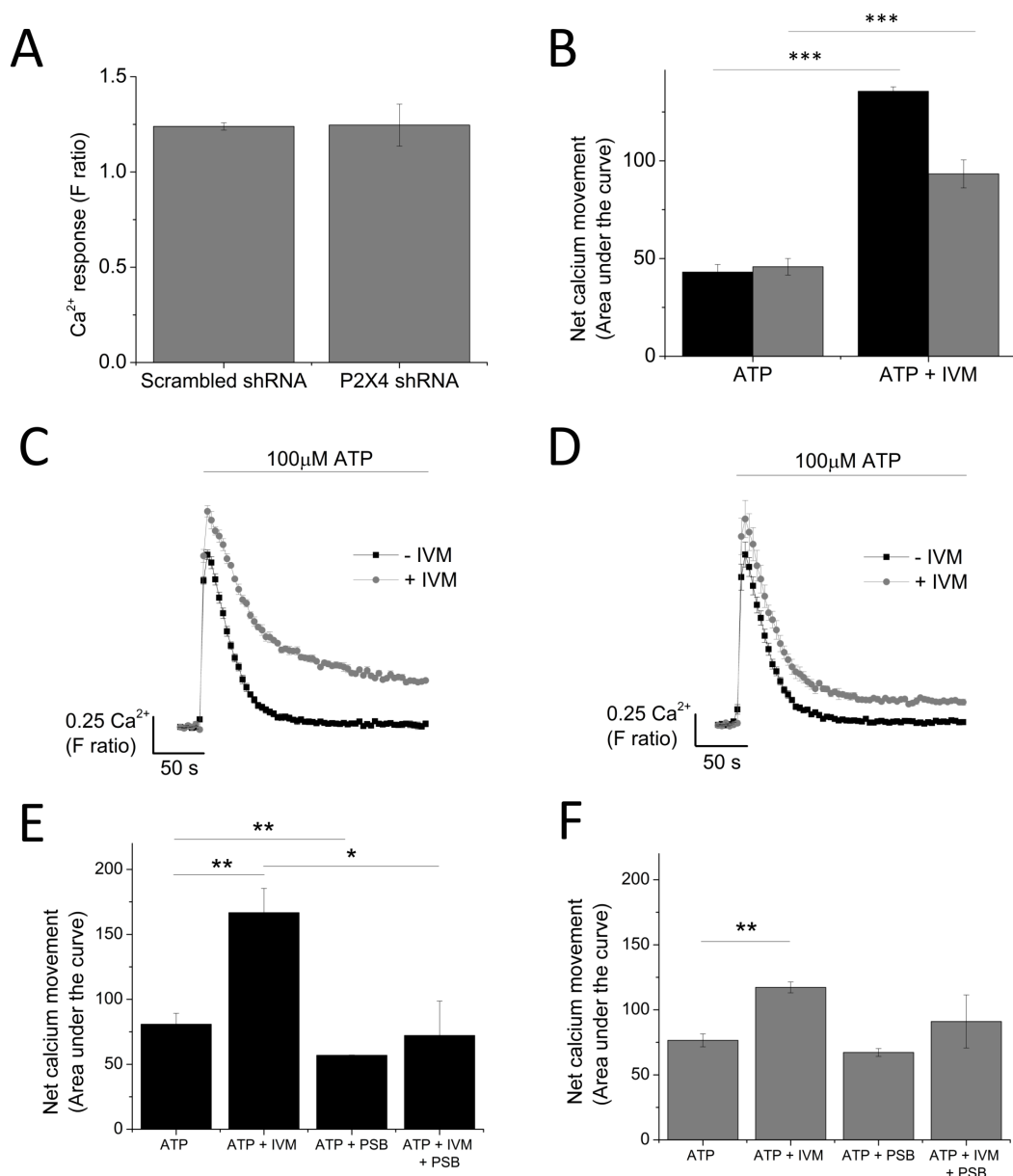
Figure 3.17. Knocking down of P2X$_4$ receptor reduced the effect of IVM on ATP-mediated calcium response in TDM. A) ATP-mediated calcium response at 100 μM on scrambled shRNA and P2X$_4$ shRNA TDM cells (n=4). B) Bar chart illustrating the effect of IVM on 100 μM ATP response in scrambled (black bars) versus P2X$_4$ shRNA (grey bars) TDM (n=6). Representative time-response curves of the effect of IVM on ATP response in: C) scrambled shRNA TDM (n=4) versus D) P2X$_4$ shRNA TDM (n=4). Effect of 10 μM PSB-12062 on ATP response in the presence and absence of IVM in: E) scrambled shRNA TDM (n=4) *vs.* F) P2X$_4$ shRNA TDM (n=4). Asterisks include significant changes towards control (*** $p<0.001$, ** $p<0.01$, * $p<0.05$, Student's t-test).

3.3.4.3. Effect of P2X$_4$ knockdown on Tg-resistant Ca^{2+} response

Earlier in the chapter, some evidence was provided suggesting the use of Tg to remove metabotropic responses in TDM cells (Section 3.3.3.3). Here, the effect of Tg on ATP-evoked Ca^{2+} responses of the P2X$_4$ shRNA TDM cells was investigated. As shown on Figure 3.18A, silencing of P2X$_4$ resulted in a significant reduction in magnitude of Tg-resistant Ca^{2+} response, when compared to scrambled shRNA control cells (0.14 ± 0.02 scrambled shRNA *vs.* 0.025 ± 0.014 P2X$_4$ shRNA; both n=3; P<0.001). This can also be observed in the representative time-response traces for scrambled shRNA and P2X$_4$ shRNA TDM cells (Figure 3.18C and D, respectively). In addition to this, the ability of IVM to potentiate Tg-resistant ATP-evoked Ca^{2+} response was tested in the P2X$_4$ shRNA cells. As shown on Figure 3.14B, Tg-resistant ATP-evoked Ca^{2+} response was significantly less sensitive towards IVM in the P2X$_4$ shRNA TDM when compared to scrambled shRNA control TDM (0.55 ± 0.053 scrambled *vs.* 0.095 ± 0.022 P2X$_4$ shRNA; n=3; P<0.001). With these observations, it was possible to confirm the contribution of P2X$_4$ towards the Tg-resistant response of ATP-evoked Ca^{2+} response in TDM cells.
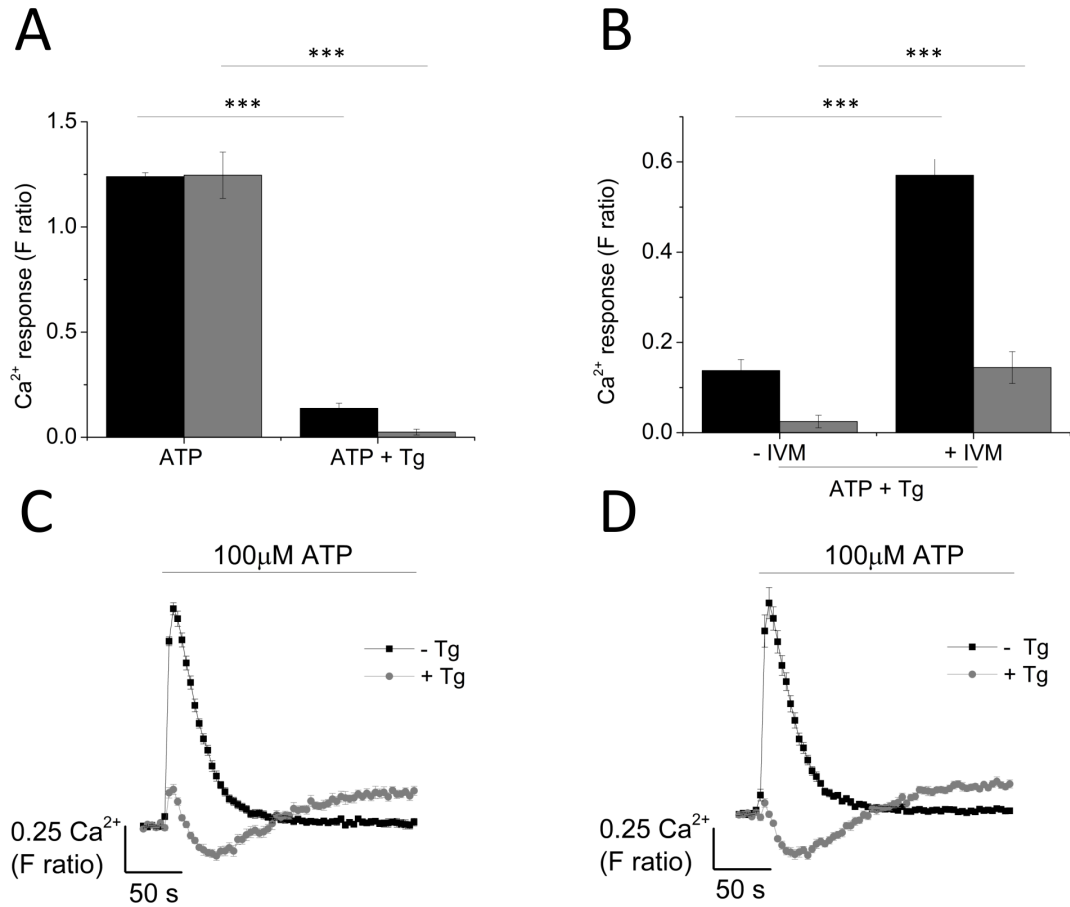
Figure 3.18. Knocking down of P2X$_4$ receptor resulted in reduction of Tg-resistant ATP-evoked Ca^{2+} response in TDM. A) Effect of Tg on 100 μM ATP response in scrambled versus P2X$_4$ shRNA TDM (n=3). B) Effect of IVM on Tg-resistant response in scrambled versus P2X$_4$ shRNA TDM (n=3). Representative time response curve on the effect of Tg on 100 μM ATP response in: C) Scrambled (n=3) and D) P2X$_4$ shRNA TDM (n=3). Asterisks include significant changes towards control (*** p<0.001, Student's t-test).

3.3.5. Investigating contribution of P2X$_4$ towards ATP-evoked Ca^{2+} response by targeting mechanism of receptor trafficking

The results described within this chapter, so far, elaborated that P2X$_4$ can contribute to ATP-evoked Ca^{2+} responses. Since P2X$_4$ have been described to be predominantly localized within lysosomal compartments (Qureshi et al., 2007) and are constantly recycled from the cell surface to intracellular compartments, targeting mechanism of receptor trafficking will allow the further confirmation of P2X$_4$ contribution towards ATP-evoked Ca^{2+} responses in TDM cells.

3.3.5.1. Effect of dynasore on Tg-resistant ATP-evoked Ca^{2+} response

Previous studies have revealed that plasma membrane expression of P2X$_4$ receptor is regulated by dynamin-dependent endocytosis (Stokes et al., 2013), therefore it is important to identify if the Tg-resistant Ca^{2+} response in TDM cells can be blocked by a dynamin inhibitor, dynasore. Dynasore is a GTPase inhibitor, which target dynamin-1, dynamin-2 and Drp2 resulting in the blocking of dynamin-dependent endocytosis (Boumechache et al., 2009). As shown (Figure 3.19A), in the presence of Tg, pre-treatment of TDM cells with 80 μM dynasore caused a significant reduction in the magnitude of ATP-evoked Ca^{2+} response in TDM cells (0.42 ± 0.17 *vs.* 0.17 ± 0.25; n=3; P<0.001). However, dynasore appeared to cause a significant delay in the decay kinetics of the ATP-evoked Ca^{2+} response (16.2 ± 1.20 s *vs.* 81.5 ± 7.03 s; n=3; P<0.001; Figure 3.19B) as well as a significant increase in the net calcium movement within the cell as quantified using area under the curve (AUC 19.9 ± 2.02 without dynasore *vs.* 33.36 ± 5.56 with dynasore; n=3; P<0.05; Figure 3.19C).
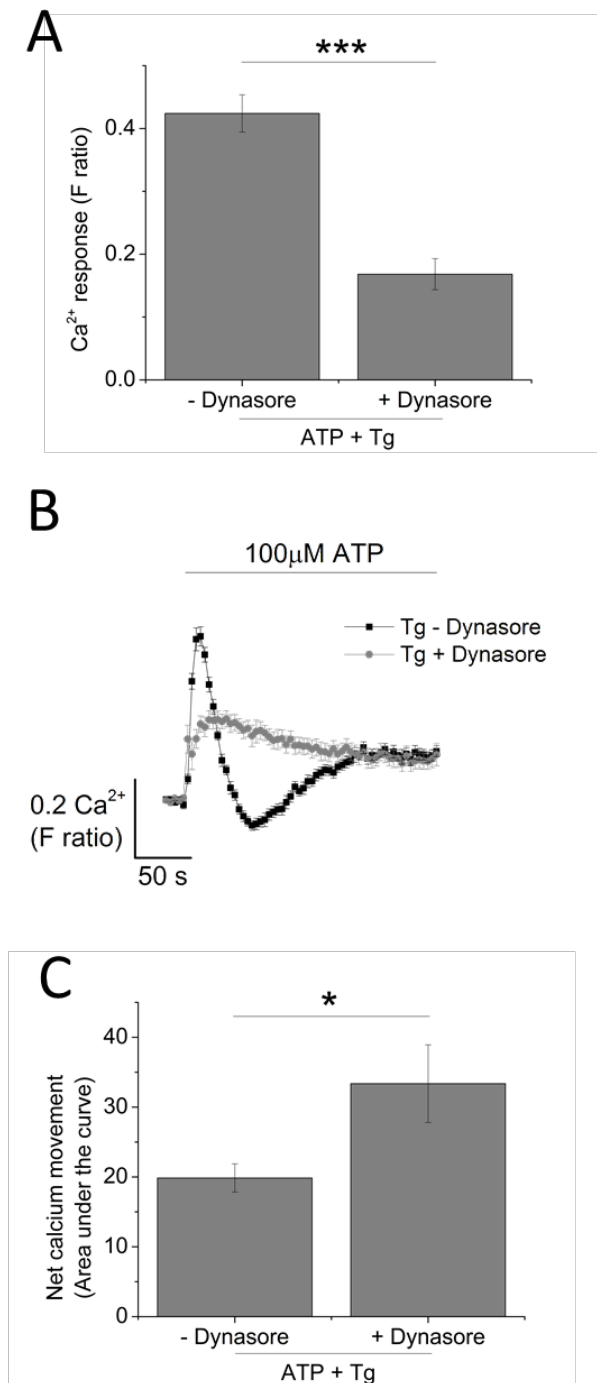
Figure 3.19. Dynasore significantly reduced magnitude of Tg-resistant ATP-evoked Ca^{2+} response and delayed decay kinetics. A-C) Effect of 80 μM dynasore on magnitude of Tg-resistant ATP-evoked Ca^{2+} response and net calcium movement in TDM (n=3). Asterisks include significant changes towards control (*** $p<0.001$, * $p<0.05$, Student's t-test).

3.3.5.2. Effect of vacuolin-1 on Tg-resistant ATP-evoked Ca^{2+} response

Lysosomal exocytosis induced by factors such as Ca^{2+} ionophores resulted in the trafficking of P2X$_4$ to the plasma membrane of cells (Qureshi et al., 2007). To investigate if P2X$_4$ contribution to Tg-resistant Ca^{2+} response in TDM cells is dependent on lysosomal exocytosis, vacuolin-1 was used. Vacuolin-1 is a lipid-soluble polycyclic triazine that can selectively increase the size of intracellular endosomes and lysosomes as well as causing a block to Ca^{2+}-dependent exocytosis of lysosomes (Huynh & Andrews, 2005).

As shown (Figure 3.20A and B), 1 μM of vacuolin-1 had no significant effect on the magnitude of ATP-evoked Ca^{2+} response in TDM cells. However, net calcium movement in TDM cells was significantly reduced when cells were pre-treated with vacuolin-1 (Figure 3.20C) (AUC 57.45 ± 2.10 *vs*. 47.75 ± 3.04, n=3, P<0.05). The effect of vacuolin-1 on Tg-insenstive Ca^{2+} response in TDM cells was also investigated and data is shown in Figure 3.20D-F. As shown (Figure 3.20D and E), vacuolin-1 had no significant effect on the magnitude of Tg-insensitive Ca^{2+} response. In addition to this, vacuolin-1 also caused no significant effect on net calcium movement of Tg-resistant Ca^{2+} response in TDM cells (Figure 3.20F). These findings illustrated that inhibition of lysosomal exocytosis in TDM cells had little or no significant effect on magnitude of Ca^{2+} response. Although vacuolin-1 appeared to significantly reduce net calcium movement in ATP-evoked Ca^{2+} response, it was unable to cause any inhibition in the presence of Tg, indicating that these Ca^{2+} responses are likely to be independent on the receptor trafficking from lysosomes to plasma membrane.
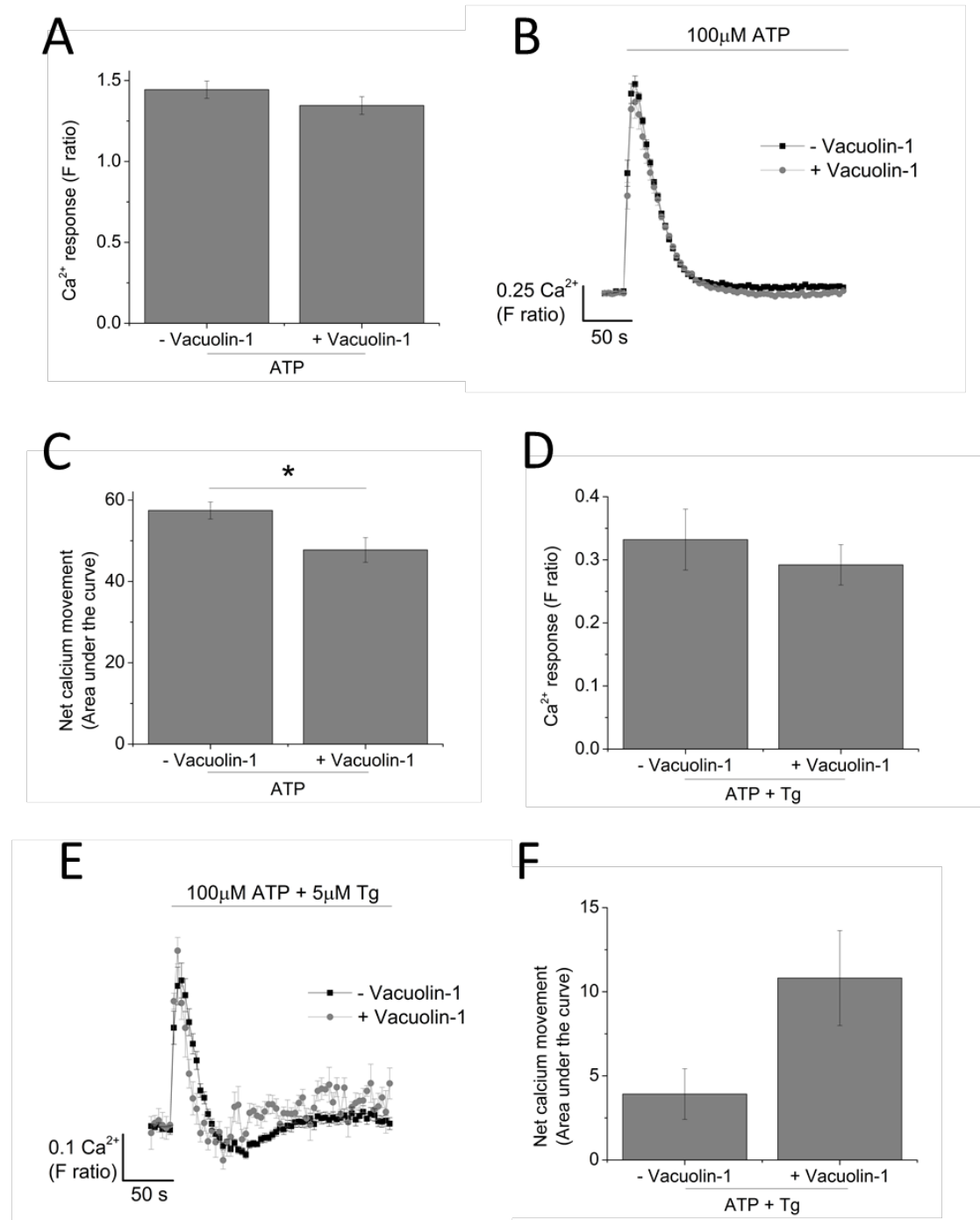
Figure 3.20. **Effect of vacuolin-1 on ATP response and Tg-resistant Ca^{2+} response.** Effect of 1 μM vacuolin-1 on: A-C) ATP-elicited Ca^{2+} response in TDM (n=3) or D-F) Tg-resistant component in TDM (n=3). Asterisks include significant changes towards control (* $p<0.05$, Student's t-test).

3.4. Summary

This chapter utilized THP-1 cells and TDM cells as *in vitro* models to pharmacologically characterize contribution of $P2X_4$ towards ATP-evoked Ca^{2+} responses. As working with human primary cells can proof challenging due to low cell number yield, this chapter also serves to identify which of the two cells – monocytes or macrophages – is a better model to study $P2X_4$. Through qRT-PCR and confocal microscopy, $P2X_4$ was shown to be expressed at both the transcriptional and translational level in both THP-1 cells and TDM cells. In addition to this, at the mRNA level, $P2X_4$ expression was shown to be up-regulated in TDM compared to THP-1 cells.

To study functional $P2X_4$ in THP-1 and TDM cells, intracellular Ca^{2+} measurement was employed. Agonist (ATP) concentration of 100 μM was used throughout the study to maximally activate $P2X_4$ receptor. To reveal the contribution of $P2X_4$ in these cells, two pharmacological tools were employed to block metabotropic-mediated Ca^{2+} responses in the two cell lines: U-73122 and Tg. In the presence of U-73122 or Tg, ATP-evoked Ca^{2+} responses in THP-1 cells lack sensitivity towards P2XR antagonists, suggestive of their limited contribution. On the other hand, in the presence of U-73122 or Tg, ATP-evoked Ca^{2+} responses in TDM cells were sensitive towards IVM, 5-BDBD and PSB-12062. The $P2X_4$ shRNA knockdown approach also confirmed the contribution of $P2X_4$ towards ATP-evoked Ca^{2+} responses in TDM cells, whereby $P2X_4$ shRNA cells were found to have reduced sensitivity towards IVM and PSB-12062. The knockdown approach also allowed the verification of IVM and PSB-12062 as a good pharmacological tool to study $P2X_4$. However, it was important to note that although PSB-12062 has been reported as a selective non-competitive antagonist for $P2X_4$, it must be used with caution as selectivity studies on $hP2X_7$ over expressing cell line illustrated that at 10 μM, it was not selective for $P2X_4$. Taken together, these findings suggested that TDM cells act as a better model to study functional $P2X_4$ when compared to THP-1 cells and when used in conjunction, IVM, PSB-12062 and 5-BDBD are reliable pharmacological tools for the study of $P2X_4$. In the next chapter, contribution of $P2X_4$ towards ATP-evoked Ca^{2+} responses in primary macrophages will be investigated, although the use of U-73122 or Tg will be minimized to mimic physiological condition as much as possible.

Chapter 4: Investigating contribution of P2X$_4$-mediated Ca^{2+} response in primary human monocyte-derived macrophages differentiated using GM-CSF versus M-CSF

4.1. Introduction

The generation of *in vitro* monocyte-derived macrophages (MDMs) can be achieved through the use of colony-stimulating factors (CSFs). CSFs are secreted glycoproteins, which can recognize and bind to receptor proteins found on the surface of haemopoietic stem cells that induces cells to proliferate and differentiate into a specific type of blood cell. There are currently three types of CSFs: CSF1 or also known as macrophage colony-stimulating factor (M-CSF), CSF2 or granulocyte macrophage colony-stimulating factor (GM-CSF) and finally, CSF3 or granulocyte colony-stimulating factors (G-CSF). The CSFs classically used for the generation of *in vitro* monocyte-derived macrophages are M-CSF and GM-CSF. While M-CSF is ubiquitously produced by various tissues and plays a key role in controlling macrophage numbers (Stanley et al., 1997, Wiktor-Jedrzejczak et al., 1990), GM-CSF is found at low basal circulating levels and is often only elevated in response to inflammatory reactions (Lacey et al., 2012). Each of the two CSFs is able to activate different receptors leading to different downstream signalling pathways. Their receptors have different distribution on myeloid cell populations with one common example being macrophages (Hamilton, 2008). Despite acting on different receptors, both CSFs are capable of promoting cell survival and proliferation, differentiation as well as activation in macrophages (Chitu and Stanley, 2006, Fleetwood et al., 2005).

Monocytes have been reported to respond differently to M-CSF and GM-CSF but there is limited understanding to the nature and mechanism underlying this difference. M-CSF-treated human blood monocytes are widely used to generate MDMs as a model for tissue macrophages. Differentiated macrophages resulting from the treatment with M-CSF are often referred to as M2-macrophages with 'anti-inflammatory' cytokine profile (Verreck et al., 2004). They were first described by Akagawa et al. (1988) as cells resembling peritoneal macrophages. Meanwhile, differentiated macrophages resulting from the treatment with GM-CSF are often referred to as M1 macrophages with 'pro-inflammatory' cytokine profile and resembling tissue macrophages in lung alveoli (Akagawa et al., 1988). GM-CSF-treated human blood monocytes are also often used to generate cells with dendritic cell antigen-presenting properties. However, bioinformatics analysis of the GM-CSF-treated monocytes transcriptome revealed that they are in fact closer to macrophages than to DCs (Lacey et al., 2012). To further polarize these MDMs towards M1- or M2- macrophages, the supplementation of cytokines are often used. This includes the use of IFN-γ and LPS in combination with GM-CSF to generate M1- polarized macrophages and IL-4 and IL-13 in combination with M-CSF to generate M2- polarized macrophages (Mantovani et al., 2002, Mosser and Edwards, 2008). Throughout this thesis, M-CSF-differentiated MDMs will be referred to as M-MDM while GM-CSF-differentiated MDMs will be referred to as GM-MDM.

4.2. Aims

GM-MDM and M-MDM were employed in a side-by-side comparison study as *in vitro* primary monocyte-derived macrophage (MDM) models to investigate the contribution of functional P2X$_4$ receptor towards ATP-evoked Ca^{2+} responses. To address this aim, several pharmacological tools that were investigated in chapter 3 were employed to help characterize P2X$_4$ through quantification of intracellular Ca^{2+} measurements. In addition to this, this chapter also aimed to characterize the contribution of other functional purinergic receptors (P2X and P2Y receptors) within the two macrophage models.

4.3. Results

4.3.1. Morphological differences between GM-MDM *vs.* M-MDM cells

It has been well defined in the literature that MDMs possess different morphological features depending on their cytokine microenvironments (Waldo et al., 2008). Human monocytes differentiated in the presence of GM-CSF have been described to possess a classic rounded shape of the original monocyte precursor resembling the 'fried egg' phenotype (Babu and Brown, 2013, Baj-Krzyworzeka et al., 2016, Eligini et al., 2013, Waldo et al., 2008). On the other hand, human monocytes that are differentiated in the presence of M-CSF resulted in macrophages with numerous vacuoles and elongated shape (Eligini et al., 2013). In order to better characterize the two types of macrophage lineages used throughout the study, a comparative study of the morphological differences between the two cells were performed. This was performed using a combination of observations under high-magnification microscopy and flow cytometry scatter analysis. Staining of cells with CD14 surface markers was also performed on the two types of macrophages.

As shown in Figure 4.1A and 4.1B, following 6d treatment with colony stimulating factors (GM-CSF or M-CSF, respectively), morphological characteristics of both GM-MDM and M-MDM cells resemble structure described in the literature. GM-MDM cells possess a classical granular and rounded 'fried-egg' morphology while M-MDM cells possess an elongated structure that appear to be less granular. To further confirm this, the size and granularity of each of the two macrophage lineages were analysed using forward (FSC) and side scatter (SSC) plot through the use of flow cytometer. FSC analysis is proportional to cell surface area or size while SSC analysis is proportional to cell granularity or internal complexity. Two sets of gating were established, P2 that cover cells of smaller surface area and lower granularity and P3 that cover cells of larger surface area and higher granularity. As can be seen in Figure 4.1C and 4.1D, an excess of approximately 15% of the M-MDM cells were found within P2 gate compared to GM-MDM cells. Meanwhile, a higher proportion of GM-MDM cells were found within P3 gate when compared with M-MDM cells. This is in line with the general observation that GM-MDM cells possess a more rounded and granular structure in comparison to M-MDM cells, which tend to be less granular and more elongated in shape.

To further characterize each of the two macrophage lineages in culture, expression of CD14 on the cell surface were studied using flow cytometry. CD14 is a classical cell surface marker that is found in monocytes, macrophages, neutrophils as well as some dendritic cells (Ziegler-Heitbrock and Ulevitch, 1993). Following 6d treatment with colony stimulating factors, 70.5 ± 4.6 **%** of GM-MDM cells and 99.6 ± 2.8 **%** of M-MDM cells were found to be CD14^{+} (Figure 4.1E and F, respectively). This is in line with immunocytochemistry studies performed by Waldo et al. (2008), which confirmed enhanced expression of cell surface marker CD14 in M-MDM when compared to GM-MDM cells. Studies by Kruger et al. (1996) also revealed that GM-CSF treatment down-regulates CD14 expression in *in vitro* cultured monocytes in a dose-dependent manner.
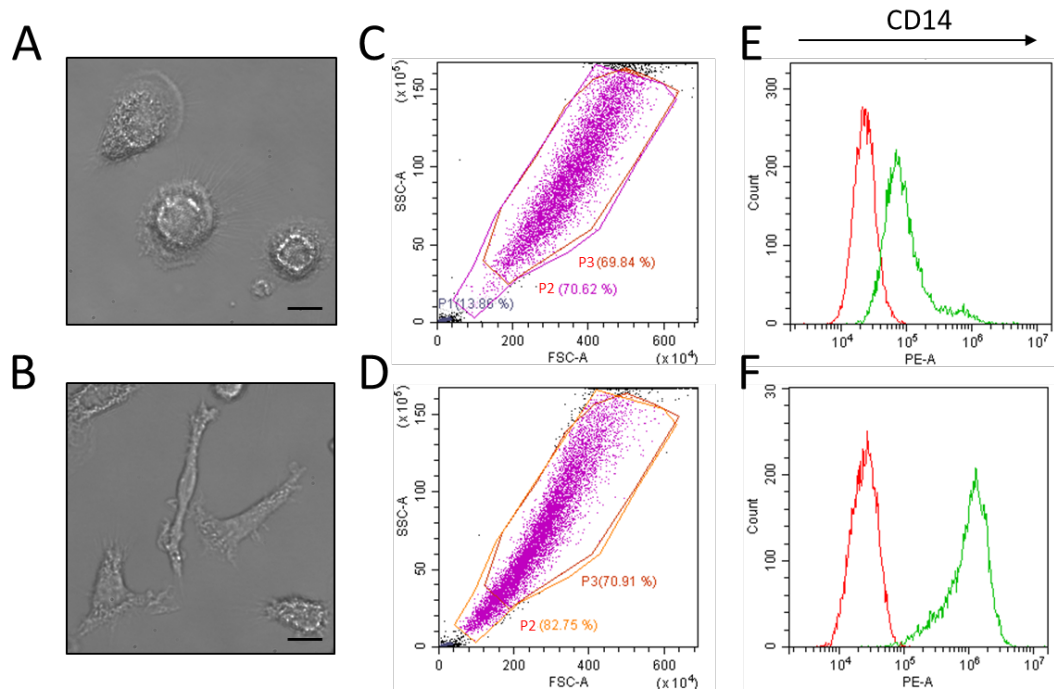
Figure 4.1. **Morphological characteristics of monocyte-derived macrophages following 6d treatment with colony stimulating factor.** Morphological differences as seen under inverted microscope of: A) GM-MDM and B) M-MDM following 6d treatment with colony stimulating factor (representative of N=6 donors). Scale bar on each images is representative of 20 μm. Flow cytometry forward (FSC) and side (SSC) scatter analysis for: C) GM-MDM and D) M-MDM cells. Flow cytometry analysis of CD14 surface marker on: E) GM-MDM and F) M-MDM cells. Red: cells stained with isotype control IgGκ PE, Green: cells stained with CD14 PE. All flow cytometry analysis is representative of N=3 donors.

4.3.2. Investigating the mRNA and protein expression of P2XR and P2YR in GM-MDM and M-MDM

4.3.2.1. Quantification of mRNA transcript using qRT-PCR

Monocyte-derived macrophages generated by colony stimulating factor stimulation has become a well-established model for studying human macrophages (Daigneault et al., 2010, Erbel et al., 2013, Gantner et al., 1997). However, expression of purinergic receptors (P2X and P2Y receptors) in these cells has not been documented. Here, through the use of qRT-PCR, mRNA expression of P2XR and P2YR in both macrophage models was investigated. Initially, the presence or absence of P2XR and P2YR genes were assessed in GM-MDM and M-MDM cells, following 6d treatment with the respective colony stimulating factors, based on their Ct values (Figure 4.2A). Genes amplified at Ct values higher than 35.0 were considered absent. Across five independent donors, mRNA transcript of $P2X_1$, $P2X_4$, $P2X_5$ and $P2X_7$ were all expressed in both GM-MDM and M-MDM cells while mRNA transcript of $P2X_2$, $P2X_3$ and $P2X_6$ were found to be absent in both cell systems. As for the mRNA transcript of P2YR, all but $P2Y_{12}$ and $P2Y_{14}$, were expressed in both GM-MDM and M-MDM. In addition to this, non-quantitative RT-PCR was also performed to investigate if MDM cells express the functional or non-functional isoform of $P2X_5$. As previously mentioned in chapter 3, SNP at the 3' splice end of exon 10 of human $P2X_5$ gene can result in an exon 10-deleted isoform of $P2X_5$ yielding a non-functional receptor. Figure 4.2B and C illustrated that both GM-MDM and M-MDM express the non-functional (exon 10-less) $P2X_5$ as observed with a band size of 395 bp, respectively.

Having identified which receptors are present at the transcriptional level in the GM-MDM and M-MDM cells, differences in the fold change of mRNA expression level of each receptor were quantified (Figure 4.3 and 4.4), respectively. Figure 4.3 illustrated no significant differences in mRNA expression of $P2X_1$, $P2X_4$, $P2X_5$ and $P2X_7$ in M-MDM *vs.* GM-MDM cells. Unlike P2XR genes, Figure 4.4 illustrated significant differences in several of the P2YR genes. As can be seen, mRNA expression of $P2Y_1$ is significantly down regulated in M-MDM cells by 2.05 ± 0.078 fold (N=5; P<0.01) when compared to GM-MDM cells (normalized value of 1.0 indicated no change). On the other hand, mRNA expression of $P2Y_6$ and $P2Y_{11}$ was found to be significantly up-regulated in M-MDM cells by 18.64 ± 4.54 fold (N=5;

P<0.05) and 5.58 ± 1.60 fold (N=5; P<0.05), respectively, when compared to GM-MDM cells. No significant differences in mRNA expression were observed for $P2Y_2$, $P2Y_4$ and $P2Y_{13}$ genes in both macrophage systems.

A

	Average Ct Values (N=5)	
	GM-MDM cells	M-MDM cells
P2RX		
P2X1	28.8 ± 0.46	29.1 ± 0.82
P2X2	N/A	N/A
P2X3	36.2 ± 0.22	37.6 ± 0.22
P2X4	25.1 ± 0.60	25.3 ± 0.35
P2X5	30.2 ± 0.51	30.1 ± 0.13
P2X6	35.1 ± 0.35	36.0 ± 0.51
P2X7	28.1 ± 0.30	28.2 ± 0.42
P2RY		
P2Y1	28.2 ± 1.39	28.6 ± 0.63
P2Y2	33.6 ± 0.67	29.8 ± 0.35
P2Y4	29.9 ± 0.49	34.4 ± 0.71
P2Y6	33.7 ± 0.38	30.0 ± 0.91
P2Y11	30.2 ± 0.33	28.3 ± 0.48
P2Y12	36.0 ± 0.55	37.5 ± 0.62
P2Y13	31.1 ± 0.26	31.5 ± 0.73
P2Y14	38.1 ± 0.07	37.8 ± 0.88
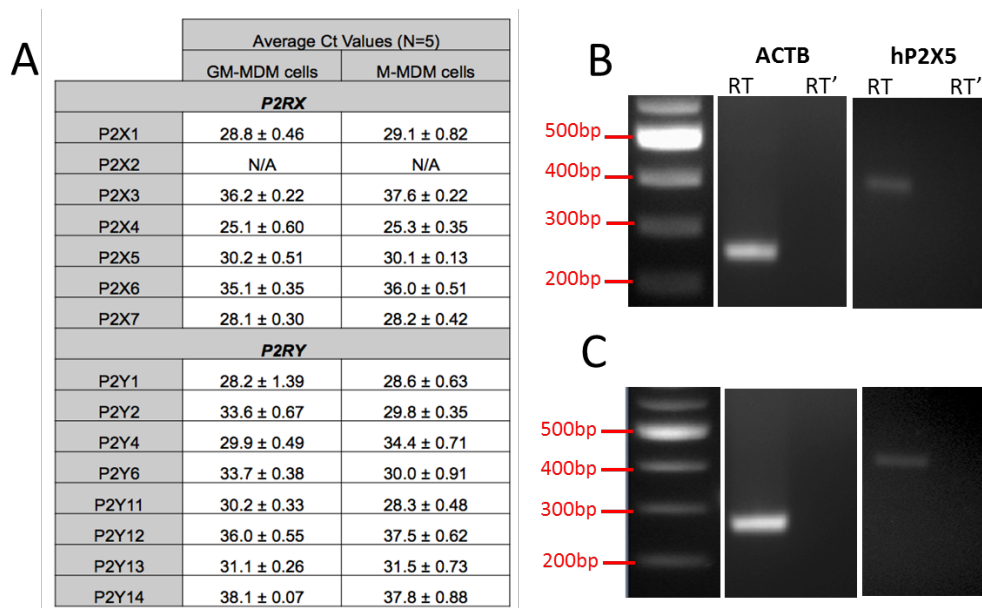
Figure 4.2. mRNA expression of P2XR and P2YR genes in GM-MDM and M-MDM cells. A) Average Ct values for P2XR and P2YR genes. Ct values were obtained from qRT-PCR for both GM-MDM (N=5 donors) and M-MDM (N=5 donors) cells. Ct values that appear >35 were considered absent. N/A denotes genes that were found undetected during 40 cycles of amplification. Reaction containing no reverse transcriptase (No RT') enzyme serve as negative control in these experiments and Ct values for these samples were ensured to be >39.0 (N=5 donors). B and C) Non-quantitative RT-PCR analysis of $P2X_5$ mRNA expression to distinguish non-functional and functional isoform of the receptor in GM-MDM and M-MDM, respectively. Bands corresponding to functional $hP2X_5$ is found at 461 bp while bands corresponding to non-functional $hP2X_5$ is found at 395 bp. β-Actin was used as a positive control. Images are representative of N=3 donors.
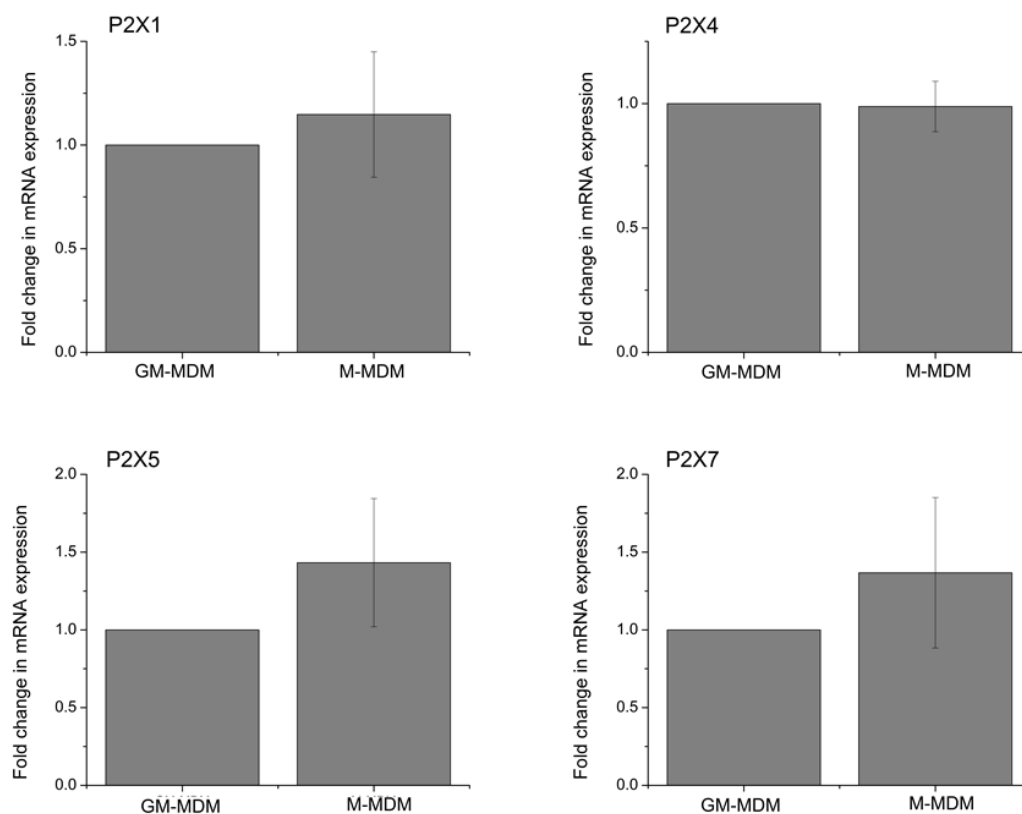
Figure 4.3. **Quantitative real-time PCR to identify fold change of mRNA expression of P2X receptor genes in M-MDM cells *vs.* GM-MDM cells.** For each donor, Ct values were normalized to housekeeping gene RPLP0 and to GM-MDM cells to obtain $\Delta\Delta$Ct (N=5 donors). No change in fold change of mRNA expression is represented by a value of 1.0. Values greater than 1.0 illustrated an up-regulation while values lower than 1.0 illustrated a down-regulation in mRNA expression.
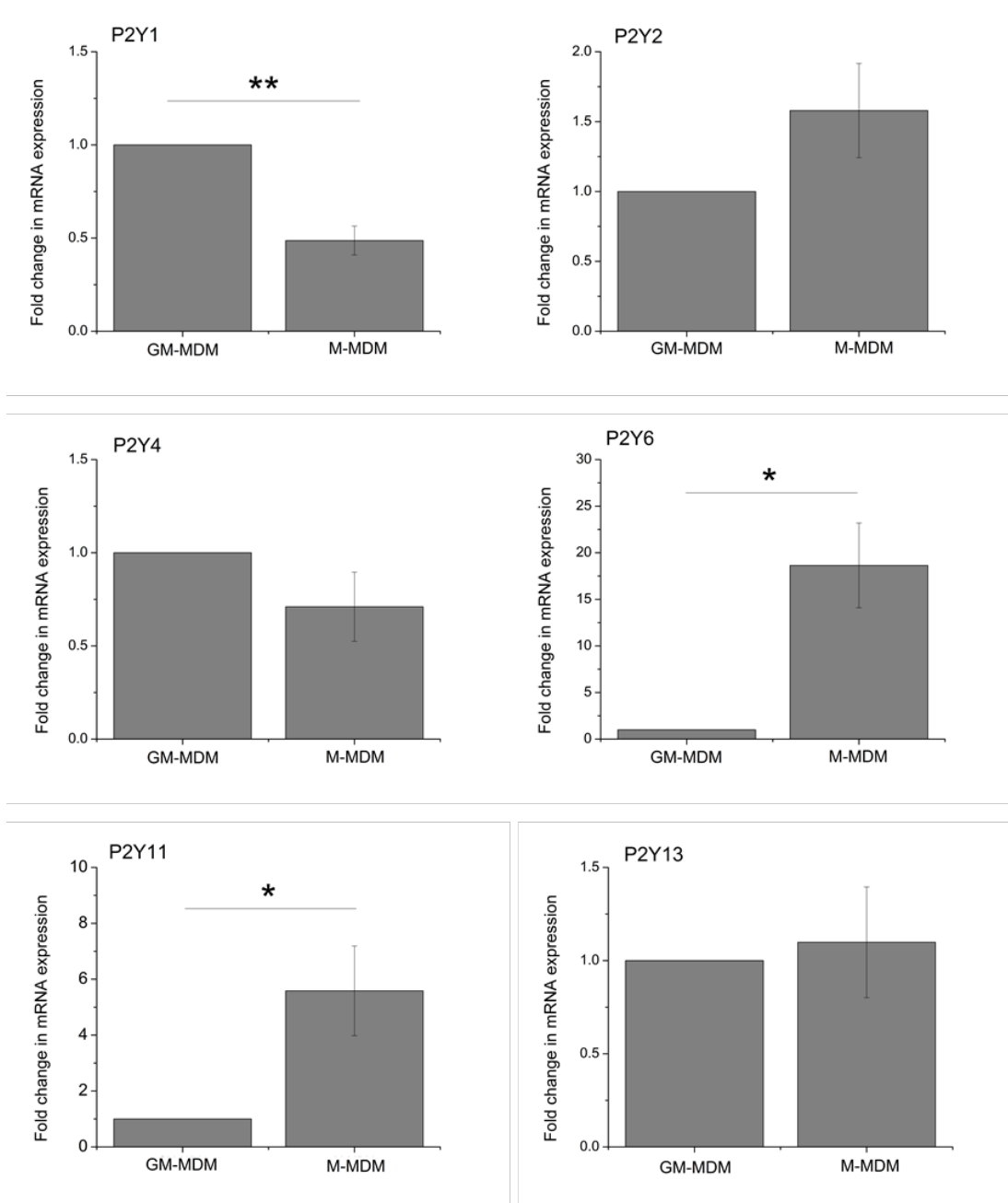
Figure 4.4. Quantitative real-time PCR to identify fold change of mRNA expression of P2Y receptor genes in M-MDM cells *vs.* GM-MDM cells. For each donor, Ct values were normalized to housekeeping gene RPLP0 and to GM-MDM cells to obtain $\Delta\Delta$Ct (N=5 donors). No change in fold change of mRNA expression is represented by a value of 1.0. Values greater than 1.0 illustrated an up-regulation while values lower than 1.0 illustrated a down-regulation in mRNA expression. Asterisks include significant changes towards control (** $p<0.01$, * $p<0.05$, Student's t-test).

4.3.2.2. Assessing protein expression of P2XR and P2YR using confocal microscopy

Expression of P2X and P2Y receptors in the GM-MDM and M-MDM was also studied at the protein level using confocal microscopy (Figure 4.5 and 4.6, respectively). All P2X and P2Y receptor antibodies detected intracellular epitope, which required the cells to be fixed and permeabilized prior to staining.

Figure 4.5A and B illustrated similar expression of P2X receptors in GM-MDM and M-MDM, respectively. Corresponding with the mRNA expression of P2X receptors, protein expression was detected for $P2X_1$, $P2X_4$, $P2X_5$ and $P2X_7$ in both cell types, with each receptors showing punctate distribution. Similarly, Figure 4.6A and 4.6B illustrated protein expression of P2Y receptors in GM-MDM and M-MDM, respectively. In both cell types, the expression of $P2Y_1$, $P2Y_2$, $P2Y_6$ and $P2Y_{13}$ was all detected at the protein level and illustrated a punctate distribution. No positive staining was observed for $P2Y_{12}$, which corroborates with the absence of $P2Y_{12}$ mRNA expression in these cells (Figure 4.2A). Altogether, the data illustrated that GM-MDM and M-MDM cells express similar profile of P2X and P2Y receptors at both the mRNA and protein level.
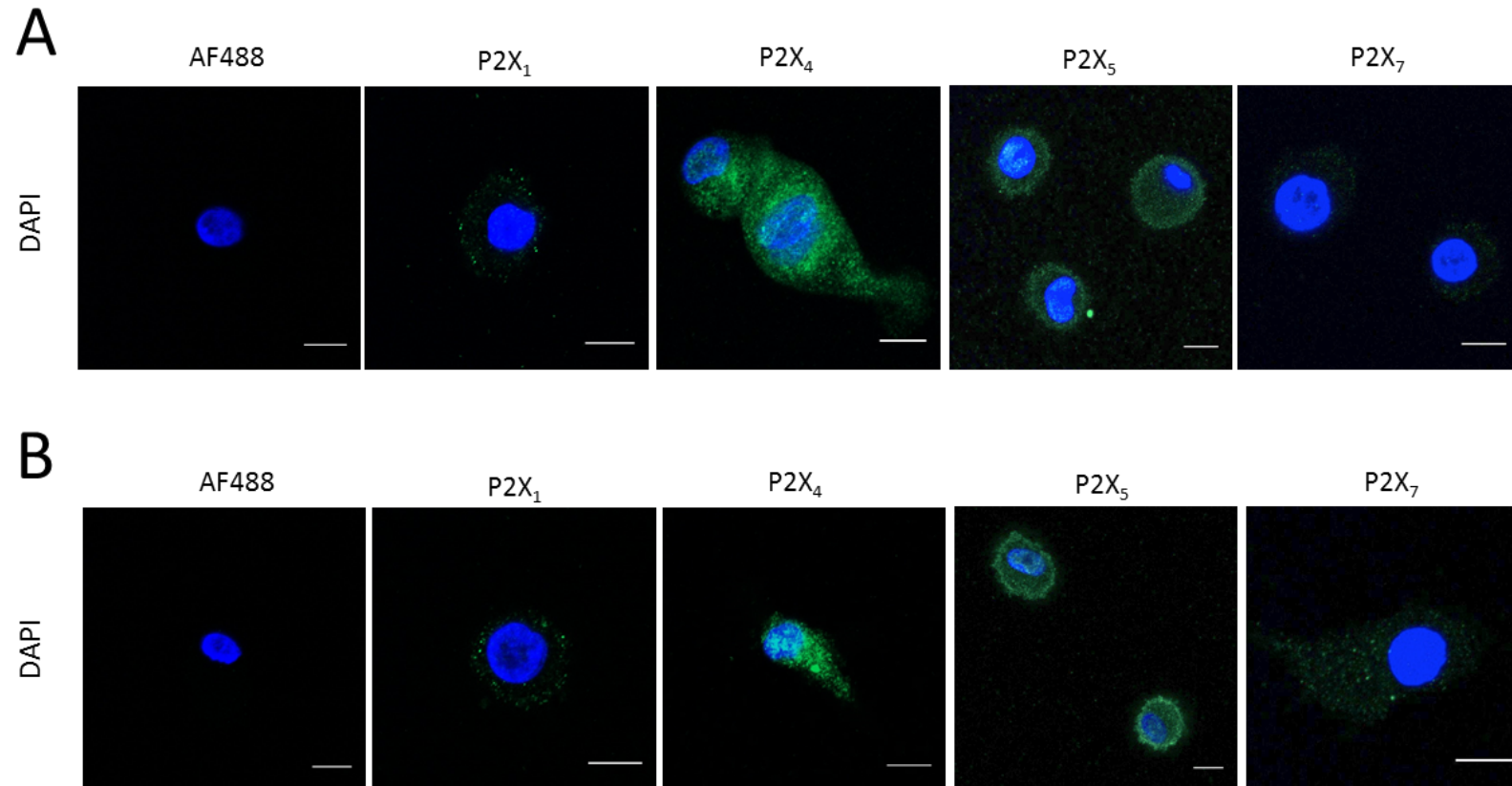
Figure 4.5. **Expression of P2X receptors in human MDM cells**. Expression of $P2X_1$, $P2X_4$, $P2X_5$ and $P2X_7$ conjugated to Alexa Fluor 488 (AF488) fluorochrome on A) GM-MDM cells and B) M-MDM cell. AF488 alone represented a secondary antibody negative control and scale bar on each image is representative of 10 μm. Images are representative of N=3 donors.
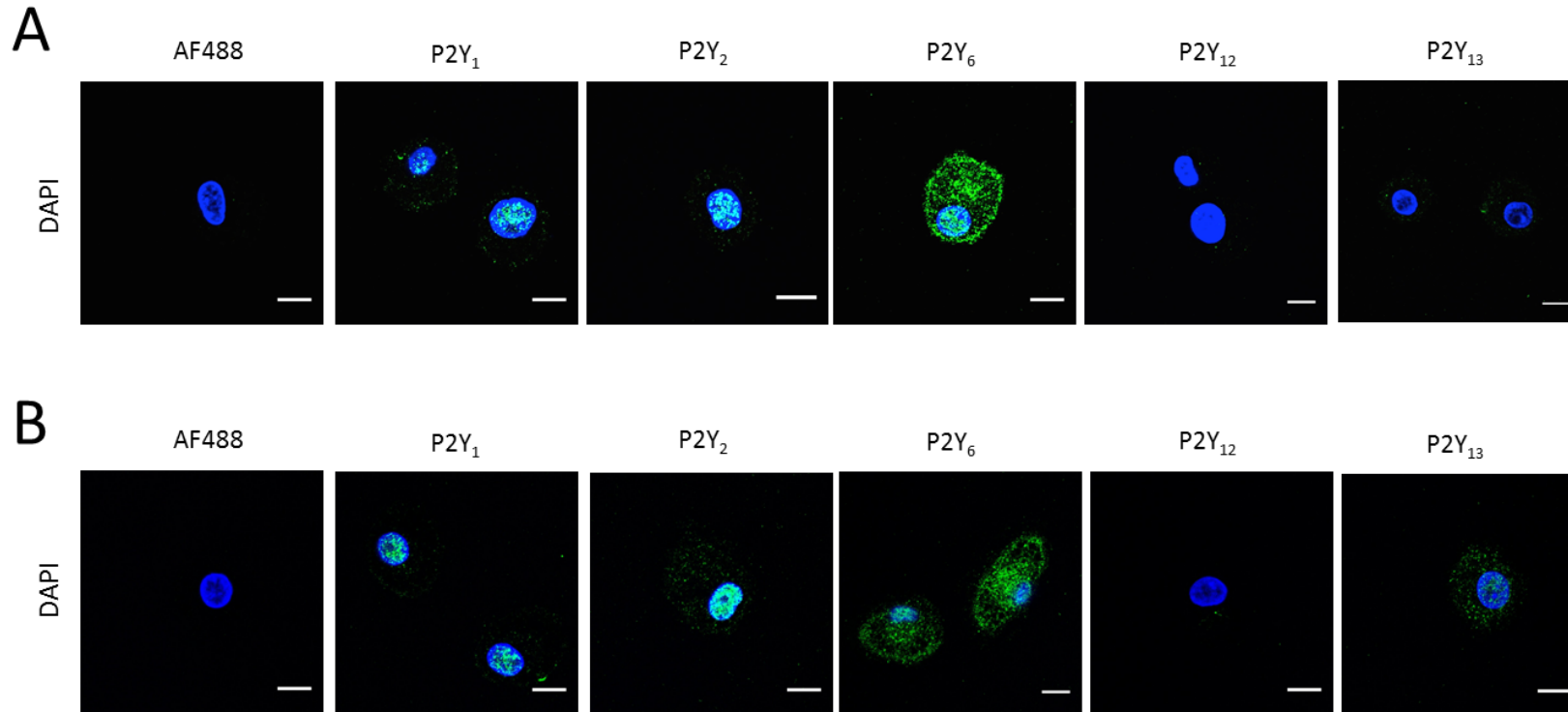
Figure 4.6. **Expression of P2Y receptors in human MDM cells**. Expression of $P2Y_1$, $P2Y_2$, $P2Y_6$, $P2Y_{12}$ and $P2Y_{13}$ conjugated to Alexa Fluor 488 (AF488) fluorochrome on A) GM-MDM cells and B) M-MDM cell. AF488 alone represented a secondary antibody negative control and scale bar on each image is representative of 10 μm. Images are representative of N=3 donors.

4.3.3. ATP-evoked intracellular Ca^{2+} response in primary human MDMs

In the previous chapter, the contribution of $P2X_4$-mediated Ca^{2+} response in macrophage cell line model, TDM, was investigated using various pharmacological tools. Here, the contribution of $P2X_4$-mediated Ca^{2+} response in human primary macrophages – GM-MDM and M-MDM – was investigated thoroughly. The initial aim of this chapter was to determine a dose response curve of ATP and the maximal concentration to activate $P2X_4$ in both macrophage systems.

ATP elicited a concentration-dependent increase in intracellular Ca^{2+} level in both GM-MDM and M-MDM cells. Figure 4.7A and 4.7B illustrated concentration-response curve in presence and absence of extracellular Ca^{2+} for GM-MDM and M-MDM, respectively. In both macrophage systems, maximal Ca^{2+} responses were observed at a similar ATP concentration, which is at 100 μM, similar to that observed in macrophage cell line. For this reason, ATP concentration of 100 μM was used for the rest of the study involving human primary MDM. In the presence of extracellular Ca^{2+}, similar EC_{50} values were observed in both macrophage systems, with GM-MDM having EC_{50} of 11.4 ± 2.9 μM (N=3 donors; Figure 4.7A) and M-MDM having EC_{50} of 13.3 ± 1.4 μM (N=3 donors; Figure 4.7B). However, in the absence of extracellular Ca^{2+}, GM-MDM illustrated an EC_{50} value of 9.77 ± 2.4 μM (N=3 donors; Figure 4.7A) while M-MDM illustrated an EC_{50} value of 7.8 ± 2.9 μM (N=3 donors; Figure 4.7B). The representative Ca^{2+} time-response trace in GM-MDM and M-MDM cells upon stimulation with 1, 10 and 100 μM ATP is represented in Figure 4.7C and 4.7D, respectively. As shown in Figure 4.7C, 100 μM ATP caused a significant increase in intracellular Ca^{2+} response, which was followed by a decay back to baseline level in GM-MDM cells. However, as shown in Figure 4.7D, ATP elicited a different Ca^{2+} response profile in M-MDM cells. Following challenge with lower ATP concentration (1 and 10 μM), ATP elicited a significant increase in intracellular Ca^{2+} response, which decayed back to baseline level. Despite having a similar profile to GM-MDM cells at lower agonist concentrations, higher ATP concentration (100 μM) application in M-MDM cells caused a significant increase in intracellular Ca^{2+} response followed by a second slower response before decaying back to a sustained elevated phase. The difference in Ca^{2+} profile evoked by 100 μM ATP in GM-MDM and M-MDM cells was confirmed through quantification of area under the curve (AUC 41.93 ± 6.41 GM-MDM *vs.* 147.36 ± 9.94 M-MDM; N=3

donors; P<0.01; Figure 4.7E). Factors underlying this difference will be discussed further in section 4.3.4.
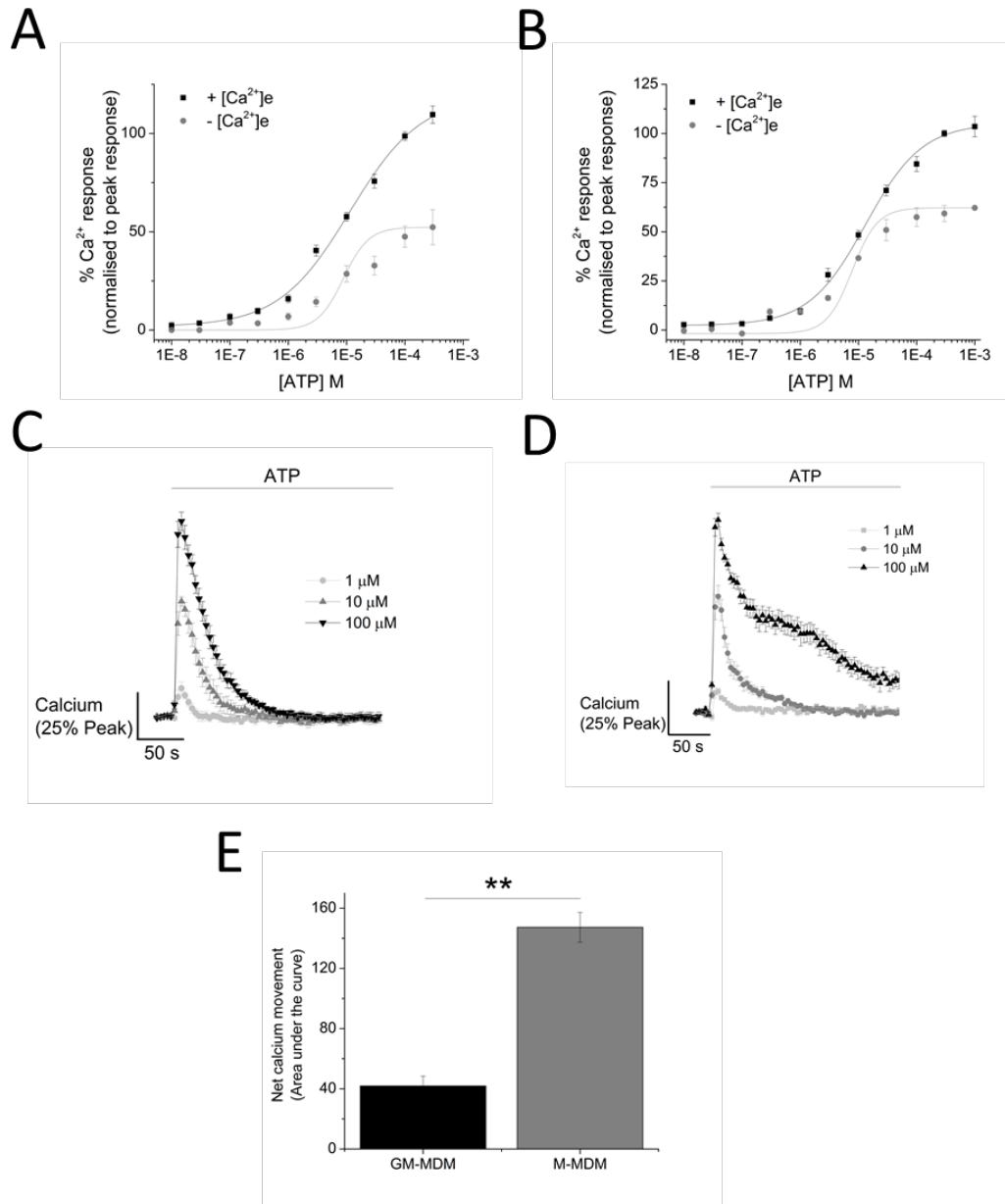
Figure 4.7. **ATP elicited a dose-dependent intracellular Ca^{2+} response in both GM-MDM and M-MDM cells.** Dose-response curve of ATP (0.01 – 1000 μM) in the presence and absence of extracellular Ca^{2+} in: A) GM-MDM cells (N=3 donors) and B) M-MDM cells (N=3 donors). C) Representative time-response curve of GM-MDM cells in response to 1 – 100 μM ATP recorded over 250 s. D) Representative time-response curve of M-MDM cells in response to 1 – 100 μM ATP recorded over 250 s. E) Area under the curve quantified following 100 μM ATP challenge in GM-MDM and M-MDM cells. Asterisks include significant changes towards control (** p<0.01, Student's t-test).

4.3.4. Contribution of metabotropic receptor to ATP-evoked Ca^{2+} responses in GM-MDM *vs*. M-MDM cells

As discussed in section 4.3.3, 100 μM ATP elicited a Ca^{2+} response profile that was significantly different in macrophage systems GM-MDM and M-MDM. As discussed previously in section 4.3.2.1, there are key differences in mRNA expression of various P2YR genes in GM-MDM and M-MDM, which may be one of the key factors underlying the difference in ATP-evoked Ca^{2+} response found in both macrophage systems. Hence, to better understand the nature and phenotype of the two cells, it was important to investigate the contribution of metabotropic P2Y receptors through the use of pharmacological tools such as U73122 and selective P2YR antagonists.

4.3.4.1. Effect of PLC inhibitor, U73122, on ATP-mediated Ca^{2+} response in GM-MDM versus M-MDM

To identify the contribution of G$_q$-coupled P2YR on ATP-evoked Ca^{2+} responses in human GM-MDM and M-MDM, U73122 was utilized. Pre-treatment of cells with 10 μM U-73122 significantly inhibited the magnitude of ATP-evoked Ca^{2+} response in both macrophage systems (GM-MDM: 90.0 ± 0.96 %; N=3; P<0.001; Figure 4.8A and B, and M-MDM: 65.0 ± 3.08 %; N=3; P<0.001; Figure 4.8C and D). These data illustrated that the magnitude of ATP-evoked Ca^{2+} response in both macrophage systems is highly dependent upon the activation of metabotropic P2YR coupled to G$_{\alpha q}$ subunit. For this reason, the effect of several P2YR antagonists were tested to assess their contribution towards ATP-evoked Ca^{2+} response. However, due to the lack of commercially available selective antagonists for P2Y$_4$ and P2Y$_{14}$, these receptors were not investigated.
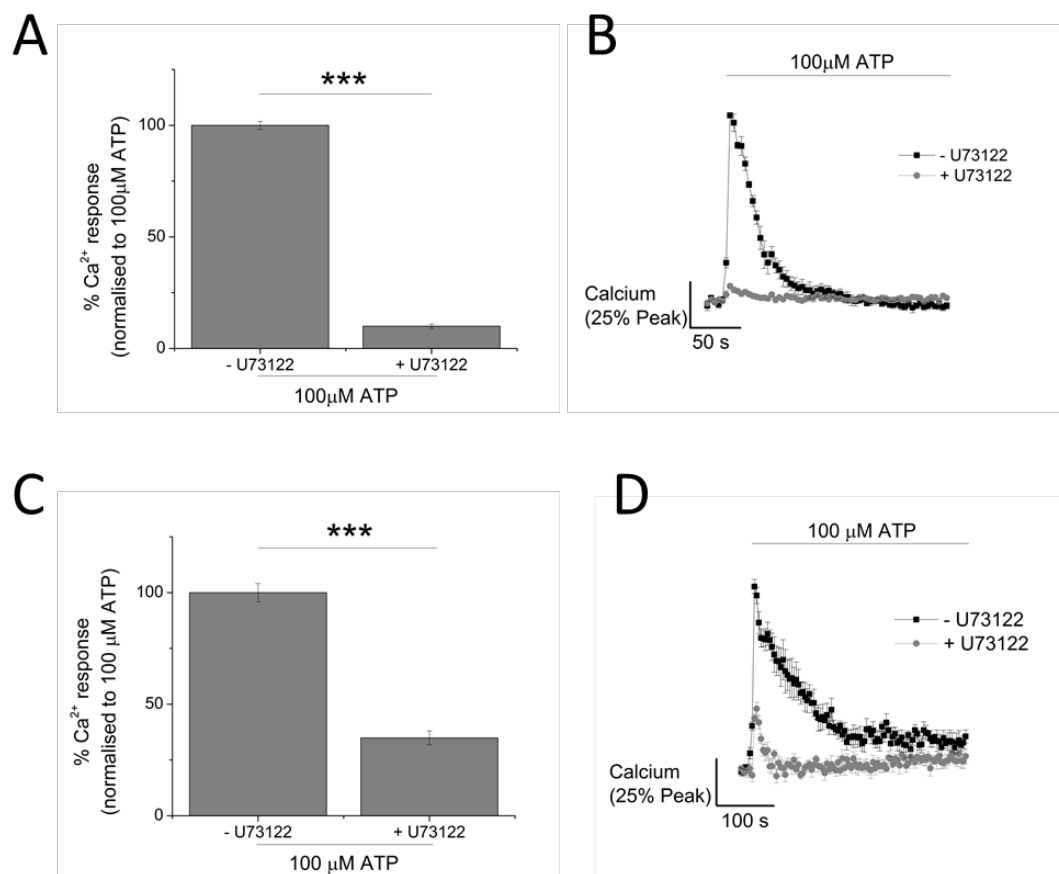
Figure 4.8. **Effect of PLC inhibitor, 10 μM U73122, on ATP-mediated calcium response in GM-MDM.** Data is represented as: A and C) percentage increase in Ca^{2+} response and B and D) representative time-response curve at 100 μM ATP in the presence or absence of 10 μM U73122 in GM-MDM (N=3 donors) and M-MDM cells (N=3 donors), respectively. Asterisks include significant changes towards control (** $p<0.01$, * $p<0.05$, Student's t-test).

4.3.4.2. Using P2Y receptor selective antagonist

To identify which metabotropic P2Y receptors may be responsible for the magnitude of the Ca^{2+} response in GM-MDM and M-MDM cells, various selective antagonist of P2Y receptors were employed. Two groups of P2Y receptors will be investigated: ADP-activated P2Y receptors ($P2Y_2$, $P2Y_6$ and $P2Y_{11}$) and ATP-activated P2Y receptors ($P2Y_1$, $P2Y_{12}$ and $P2Y_{13}$). The agonist that was employed throughout this study is 100 μM ATP.

4.3.4.2.1. Targeting ADP-activated P2Y receptors

Although ATP was used as the main agonist in these studies, it was important to investigate the contribution of ADP-activated P2YR since extracellular ATP can be hydrolysed into ADP and AMP. Local increase in nucleotides is controlled by ectonucleotidases such as CD39/E-NTPDase family and CD73/ecto-5'-nucleotidase. CD39 hydrolyzes extracellular nucleotides (ATP) to their respective nucleosides (AMP) with the transient production of free ADP, which can subsequently activate P2Y receptors (Robson et al., 2006).

P2Y receptors that can be activated by ADP include $P2Y_1$, $P2Y_{12}$ and $P2Y_{13}$. Although not the main agonist, ADP has been speculated to be able to activate $P2Y_6$ (Communi et al., 1996). While $P2Y_1$ and $P2Y_6$ are coupled to $G_{\alpha q}$ subunit leading to activation of PLCβ, $P2Y_{12}$ and $P2Y_{13}$ are coupled to $G_{\alpha i}$ subunit leading to adenylyl cyclase (AC) inhibition (Jacobson et al., 2009). Although activation of $G_{\alpha i}$-coupled P2Y receptors, such as $P2Y_{13}$, in theory do not lead to a raise in intracellular Ca^{2+} response, there is a possibility that it can form heterodimers with other P2YR such as $P2Y_1$ to activate PLC resulting in increase in intracellular Ca^{2+} level (Perez-Sen et al., 2015) or even possibly interacting with P2X receptors leading to intracellular Ca^{2+} increase. However, no evidence has ever been made on this account. Here, only the contribution of $P2Y_1$, $P2Y_6$ and $P2Y_{13}$ were investigated as $P2Y_{12}$ mRNA and protein expression was undetected in both macrophage systems (Table 4.2).

4.3.4.2.1.1. P2Y$_1$ Receptor

A selective and competitive antagonist for P2Y$_1$, MRS2500, was utilized in this study. MRS2500 is reported to be a highly potent antagonist with K$_i$ of 0.78 nM (Kim et al., 2003). Pre-treatment of GM-MDM and M-MDM cells with 1 μM MRS2500 had a small but insignificant effect on the magnitude of the Ca^{2+} response in both macrophage systems (Figure 4.9). Moreover, the antagonist had no effect on the decay kinetics and net calcium movement of the Ca^{2+} response. This indicates minimal contribution of P2Y$_1$ towards ATP-evoked Ca^{2+} response in both GM-MDM and M-MDM cells.
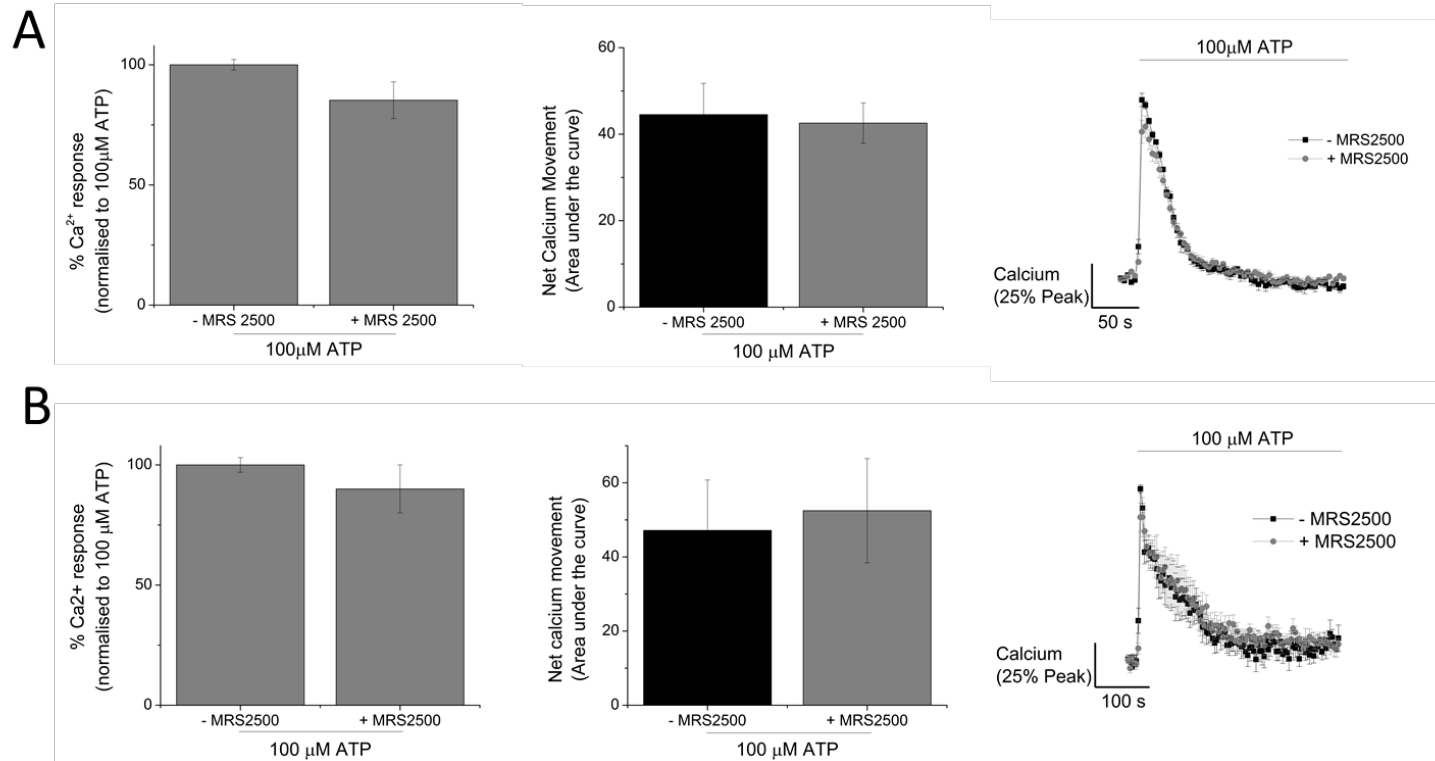
Figure 4.9. Effect of P2Y$_1$ receptor antagonist, 1 μM MRS2500, on ATP-evoked Ca^{2+} response in GM-MDMs versus M-MDMs. Data is represented as percentage increase in Ca^{2+} response, representative time-response curve and bar chart representing net calcium movement (AUC) at 100 μM ATP in the presence or absence of 1 μM P2Y$_1$ antagonist, MRS2500, for: A) GM-MDM cells (N=3 donors) or B) M-MDM cells (N=3 donors). Asterisks include significant changes towards control (** $p<0.01$, * $p<0.05$, Student's t-test).

4.3.4.2.1.2. P2Y$_6$ Receptor

A selective and non-competitive antagonist for P2Y$_6$, MRS2578, was utilized to assess the contribution of P2Y$_6$ towards ATP-evoked Ca^{2+} response in human macrophages. MRS2578 has a reported IC$_{50}$ value of 37 ± 16 nM when tested for inhibition of UDP response in over expressing astrocytoma cell line (Mamedova et al., 2004). Although it is well established that the main agonist for P2Y$_6$ is UDP, it is thought that ADP can also act as a weak agonist (Communi et al., 1996). Pre-treatment of GM-MDM cells with 10 μM of MRS2578 had no significant effect on the magnitude of ATP-evoked Ca^{2+} response but appeared to cause a slight increase towards the decay phase of the response (Figure 4.10A). Despite subtly increasing the decay phase of the Ca^{2+} response, no significant change was observed in the net Ca^{2+} movement as quantified by area under the curve. Similarly, pre-treatment of M-MDM cells with MRS2578 antagonist had no significant effect towards magnitude of the ATP-evoked Ca^{2+} response as well as area under the curve (Figure 4.10B).
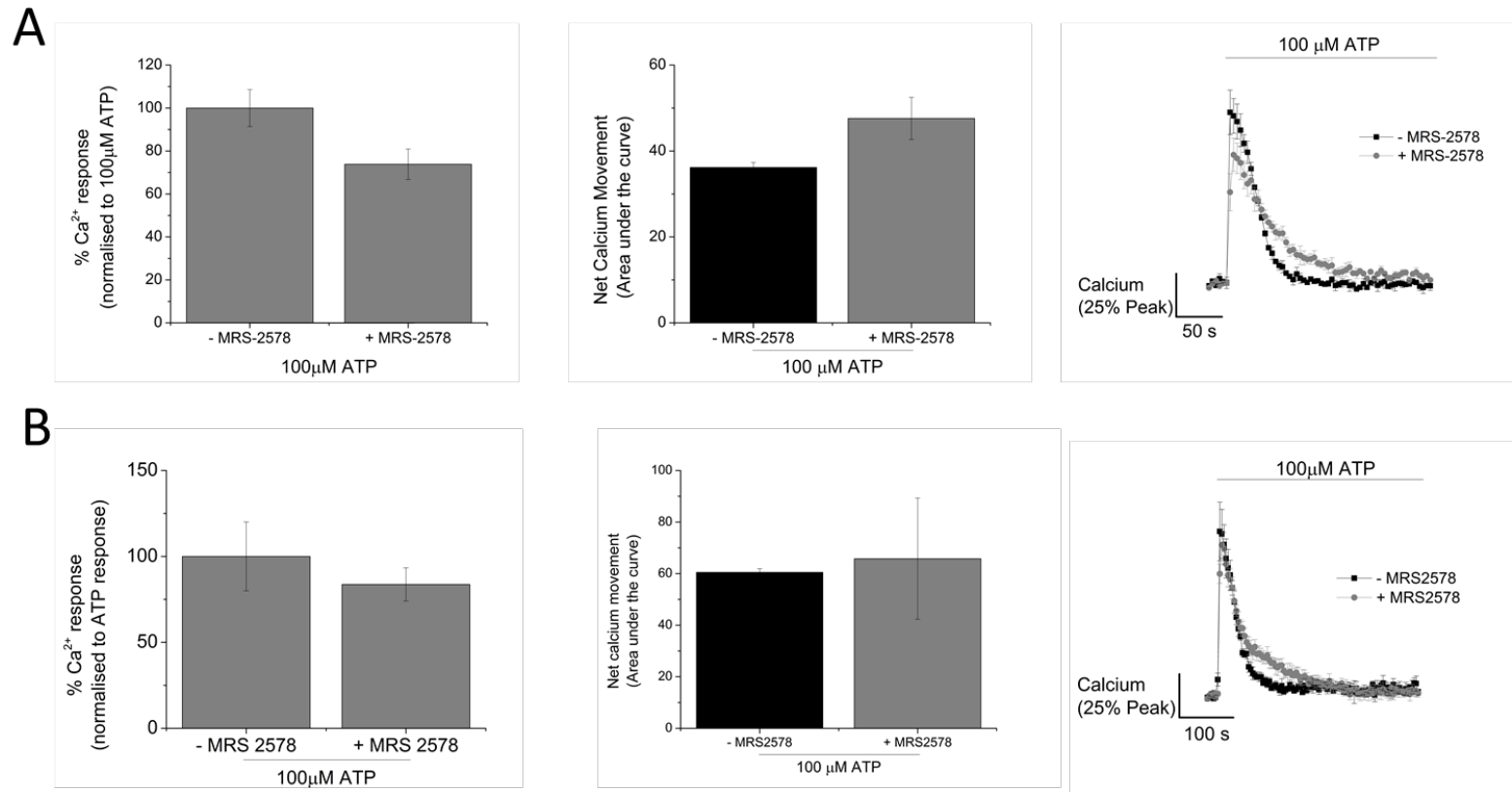
Figure 4.10. Effect of P2Y$_6$ antagonist, 10 μM MRS2578, on ATP-evoked Ca^{2+} response of human GM-MDMs versus M-MDMs. Data is represented as percentage increase in Ca^{2+} response, representative time-response curve and bar chart representing net calcium movement (AUC) at 100 μM ATP in the presence or absence of 10 μM P2Y$_6$ antagonist, MRS2578, for: A) GM-MDM cells (N=3 donors) or B) M-MDM cells (N=3 donors).

4.3.4.2.1.3. P2Y$_{13}$ Receptor

The contribution of P2Y$_{13}$ on ATP-evoked Ca^{2+} response in primary macrophages was studied using a competitive P2Y$_{13}$ antagonist, MRS2211. MRS2211 is reported to be a selective antagonist for P2Y$_{13}$ with pIC$_{50}$ of 5.97 with over 20-fold selectivity against other P2YR such as P2Y$_1$ (Kim et al., 2005). Pre-treatment of GM-MDM with 10 μM of MRS2211 significantly inhibited magnitude of Ca^{2+} response in GM-MDM cells (48.6 ± 4.56 % inhibition; N=3 donors; P<0.001; Figure 4.11A) as well as area under the curve (AUC 44.52 ± 7.23 without MRS2211 *vs.* 25.52 ± 4.37 with MRS2211; N=3 donors; P<0.01; Figure 4.11A). It can also be seen that although MRS2211 significantly inhibited peak of the Ca^{2+} response, it appeared to have little effect on the decay phase of the response. On the contrary, in M-MDM cells, MRS2211 did not have any significant effect towards the magnitude of Ca^{2+} response as well as the area under the curve (Figure 4.11B).
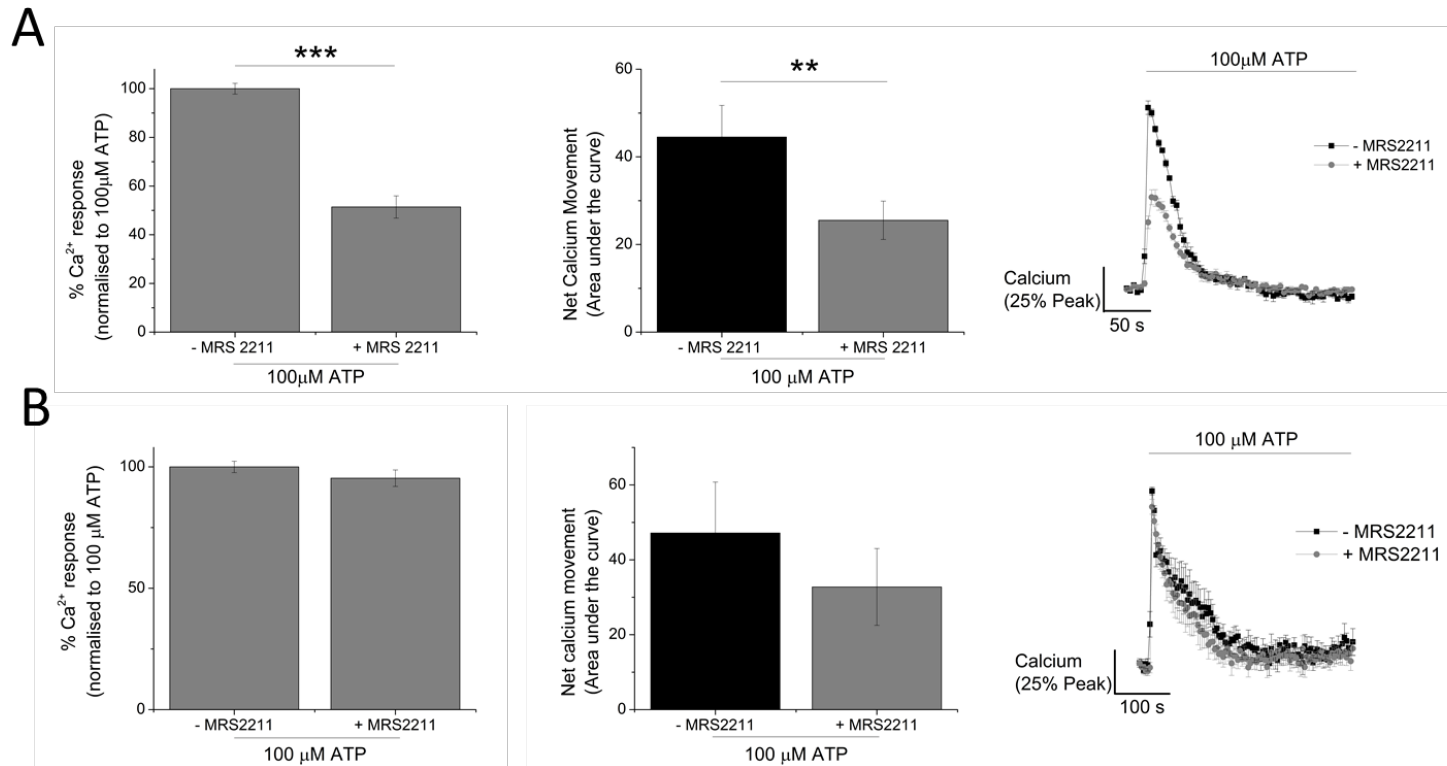
Figure 4.11. Effect of P2Y$_{13}$ antagonist, 10 μM MRS2211, on ATP-evoked Ca^{2+} response in GM-MDMs vs. M-MDMs. Data is represented as percentage increase in Ca^{2+} response, representative time-response curve and bar chart representing net calcium movement (AUC) at 100 μM ATP in the presence or absence of 10 μM P2Y$_{13}$ antagonist, MRS2211, for: A) GM-MDM cells (N=3 donors) or B) M-MDM cells (N=3 donors). Asterisks include significant changes towards control (*** p<0.001, ** p<0.01, Student's t-test).

4.3.4.2.2. Targeting ATP-activated P2Y receptors

The main P2Y receptors activated by ATP are $P2Y_2$ (coupled to $G_{\alpha q}$ subunit) and $P2Y_{11}$ (coupled to $G_{\alpha q}$ subunit or $G_{\alpha s}$ subunit). Activation of $P2Y_2$ leads to $PLC\beta$ activation while activation of $P2Y_{11}$ leads to $PLC\beta$ and AC activation (Erb and Weisman, 2012, Jacobson et al., 2009). The activation of $PLC\beta$ results in mobilization of intracellular Ca^{2+}.

4.3.4.2.2.1. $P2Y_2$ Receptor

A selective and competitive antagonist of $P2Y_2$, ARC-118925XX, was utilized in this study to identify contribution of $P2Y_2$ in ATP-evoked Ca^{2+} response of GM-MDM and M-MDM. It has a reported IC_{50} of 1 μM in bronchial epithelial cells and has been shown to be inactive against 37 other receptors when used at concentration of 10 μM (Kemp et al., 2004). Pre-treatment of macrophages with 10 μM ARC-118925XX had no significant inhibitory effect on the magnitude of ATP-evoked Ca^{2+} response in both GM-MDM and M-MDM cells (Figure 4.12A and 4.12B, respectively). Instead, ARC-118925XX significantly increase the magnitude of Ca^{2+} response (23.74 ± 7.54 % potentiation; N=3 donors; P<0.05; Figure 4.12B) in M-MDM cells but not GM-MDM cells.
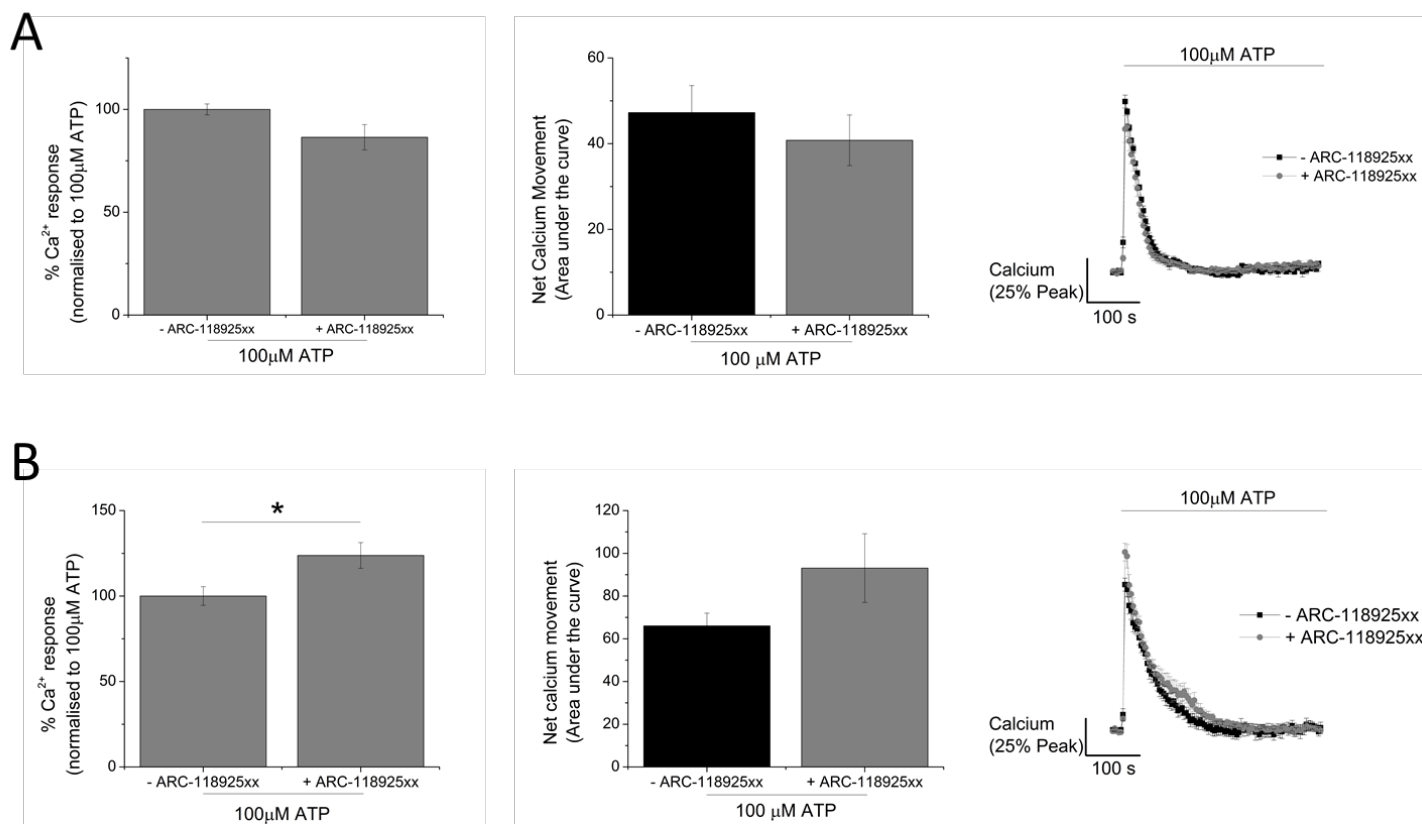
Figure 4.12. **Effect of P2Y$_2$ antagonist, 10 μM ARC-118925xx, on ATP-evoked Ca^{2+} response in GM-MDMs versus M-MDMs.** Data is represented as percentage increase in Ca^{2+} response, representative time-response curve and bar chart representing net calcium movement (AUC) at 100 μM ATP in the presence or absence of 10 μM P2Y$_2$ antagonist, ARC-118925xx for: A) GM-MDM cells (N=3 donors) or B) M-MDM cells (N=3 donors). Asterisks include significant changes towards control (* p<0.05, Student's t-test).

4.3.4.2.2.2. $P2Y_{11}$ Receptor

Lastly, a $P2Y_{11}$ receptor antagonist, NF340, was utilized to identify its role in ATP-evoked Ca^{2+} response of human primary macrophages. NF340 is reported have a pIC_{50} value of 6.43 through Ca^{2+} measurements and to be highly selective for $P2Y_{11}$ receptor with 520-fold selectivity over $P2Y_1$, $P2Y_2$, $P2Y_4$, $P2Y_6$ and $P2Y_{12}$ (Meis et al., 2010). Pre-treatment of GM-MDM cells with 10 μM NF340 significantly reduced the magnitude of the ATP-evoked Ca^{2+} response by 20.52 ± 3.20 % (N=3 donors; P<0.05; Figure 4.12A). Moreover, blocking $P2Y_{11}$ had no effect on the decay kinetics of the ATP-evoked Ca^{2+} response in GM-MDM cells as reflected by no significant change in area under the curve (AUC 56.06 ± 4.20 without NF340 versus 57.46 ± 5.86 with NF340; N=3 donors; P>0.05; Figure 4.13B). Interestingly, pre-treatment of M-MDM cells with 10 μM NF340 significantly reduced not only the magnitude of the ATP-evoked Ca^{2+} response (35.54 ± 2.60 % inhibition; N=3 donors; P<0.001; Figure 4.12B), but also abolished the second slower decay phase that was induced by 100 μM ATP (AUC 78.69 ± 20.26 without NF340 *vs.* 32.52 ± 12.73 with NF340; N=3 donors; P<0.05; Figure 4.12B). Based on this observation, $P2Y_{11}$ is a major contributor for the decay phase observed in M-MDM cells following stimulation with high ATP concentration (100 μM). This observation is in accordance with findings shown in Figure 4.4 illustrating that $P2Y_{11}$ mRNA expression is up-regulated (5.58 ± 1.60 fold; N=5 donors; P<0.05) in M-MDM cells, when compared to GM-MDM cells.

The data so far illustrated that the activation of $P2Y_{11}$ and $P2Y_{13}$ are responsible for the magnitude of the ATP-evoked Ca^{2+} response in both GM-MDM and M-MDM cells. In addition to this, $P2Y_{11}$ appeared to also be responsible for the decay response in M-MDM cells, but not GM-MDM cells. Surprisingly, $P2Y_1$, $P2Y_2$ and $P2Y_6$ lack contribution towards the ATP-evoked Ca^{2+} response in these cells although this may be explained by the competitive nature of the antagonists being used in this study.
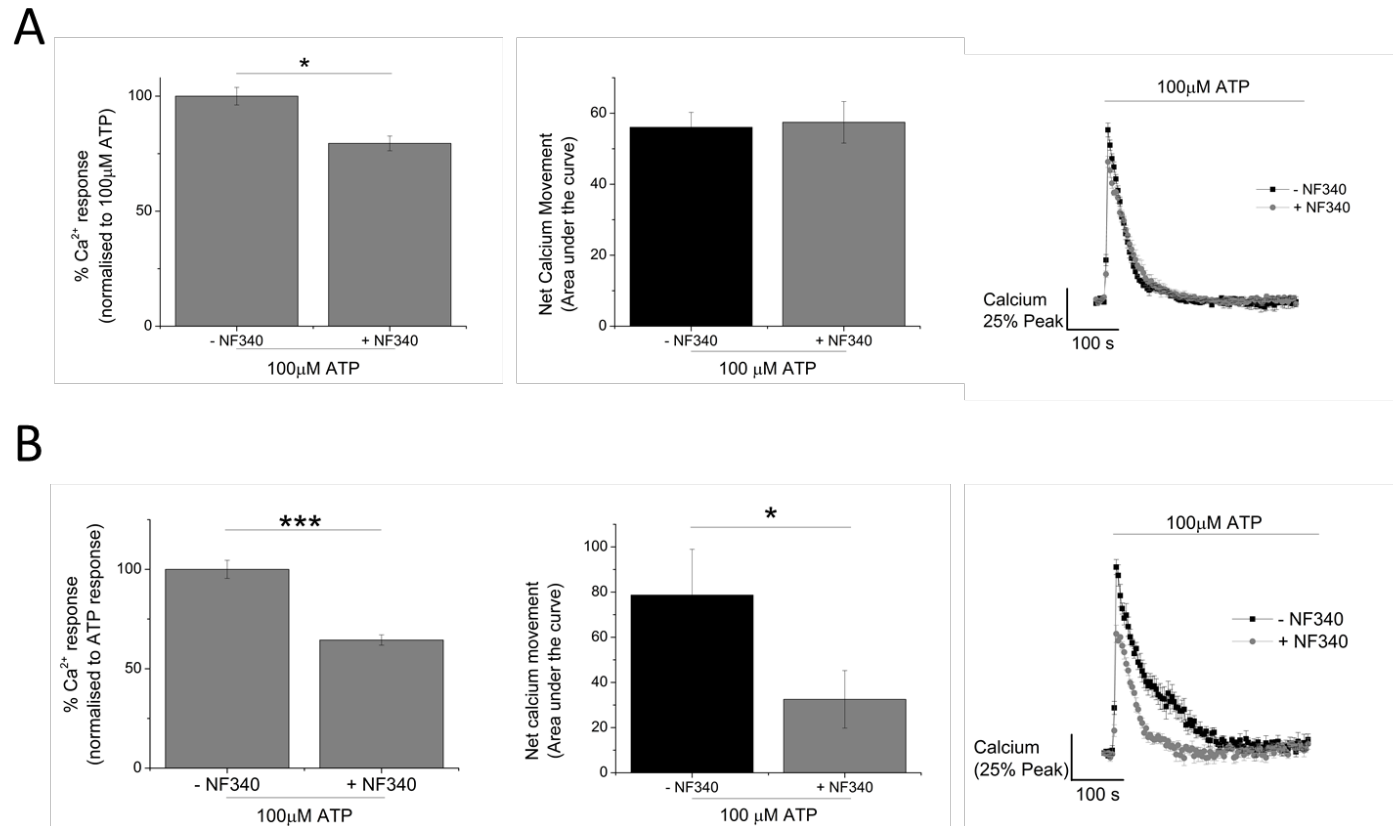
Figure 4.13. **Effect of P2Y$_{11}$ antagonist, 10 μM NF340, on ATP-evoked Ca^{2+} response in GM-MDMs versus M-MDMs.** Data is represented as percentage increase in Ca^{2+} response, representative time-response curve and bar chart representing net calcium movement (AUC) at 100 μM ATP in the presence or absence of 10 μM P2Y$_{11}$ antagonist, NF340, for: A) GM-MDM cells (N=3 donors) or B) M-MDM cells (N=3 donors). Asterisks include changes towards control (*** $p<0.001$, ** $p<0.01$, * $p<0.05$, Student's t-test).

4.3.5. Pharmacological characterization of P2X$_4$-evoked Ca^{2+} response in human MDMs

One of the key aims of this chapter was to identify the contribution of P2X$_4$ receptor towards ATP-evoked Ca^{2+} responses in human primary macrophages. In the previous chapter, P2X$_4$ appeared to contribute to the magnitude of ATP-evoked Ca^{2+} response in TDM cells. It was therefore important to identify if P2X$_4$ can contribute in a similar manner in primary macrophages. A side-by-side comparison of P2X$_4$ contribution in GM-MDM and M-MDM cells was studied using pharmacological tools. These pharmacological tools include previously used P2X$_4$ positive allosteric modulator (IVM), selective P2X$_4$ antagonists (5-BDBD and PSB-12062) and other P2X antagonists (P2X$_1$ antagonist, Ro0437626, and P2X$_7$ antagonist, A438079). Although there were no significant differences in the level of P2X$_4$ mRNA expression in GM-MDM and M-MDM cells (Figure 4.3), flow cytometry analysis was also performed to allow the quantitation of P2X$_4$ protein on the surface of the cells as well as P2X$_4$ protein localized within intracellular compartments.

4.3.5.1. Effect of Ivermectin (IVM) on ATP-evoked Ca^{2+} response in human GM-MDM versus M-MDM

IVM has been reported to act on both hP2X$_4$ and hP2X$_7$ receptor (Norenberg et al., 2012). Despite the lack of selectivity, it is still one of the most commonly used pharmacological tools to characterize activation of P2X$_4$. Here, 3 μM IVM was used to isolate contribution of P2X$_4$-mediated Ca^{2+} responses in human GM-MDM and M-MDM cells. Pre-treatment of GM-MDM cells with IVM resulted in significant potentiation in magnitude of Ca^{2+} response (18.2 ± 4.58 %, N=12 donors, P<0.01; Figure 4.14A) and significantly delayed decay kinetics. This can be observed from the time-response trace as well as bar chart representing a significant increase in net calcium movement as measured by area under the curve (AUC 45.3 ± 8.1 without IVM versus 90.1 ± 11.0 with IVM; N=12 donors; P<0.01; Figure 4.14A). These observations are consistent to the effect of IVM that was observed in TDM cells (Chapter 3), and to the literature, whereby IVM not only potentiated P2X$_4$-mediated current but also delayed decay kinetics (Norenberg et al., 2012).

Unlike the effect it has on GM-MDM cells, IVM affected M-MDM cells differently. As shown on Figure 4.14B, IVM caused a significant potentiation in the magnitude of ATP-evoked Ca^{2+} response in M-MDM cells (127.14 ± 4.97 %; N=7; P<0.001).

However, IVM did not appear to have any effect on the decay kinetic of the Ca^{2+} response in M-MDM cells, therefore no significant effect on net calcium movement as quantified by area under the curve (AUC 91.89 ± 35.07 without IVM versus 162.5 ± 48.1 with IVM; N=7 donors; P>0.05; Figure 4.14B). The different effect IVM has on the GM-MDM and M-MDM cells may be due to several factors such as different amount of functional $P2X_4$ receptor in the two macrophage systems studied as well as different mechanism of $P2X_4$ recruitment from intracellular stores. Although the latter will not be investigated within this study, the amount of surface and intracellular $P2X_4$ was quantified using flow cytometry (section 4.3.5.5).
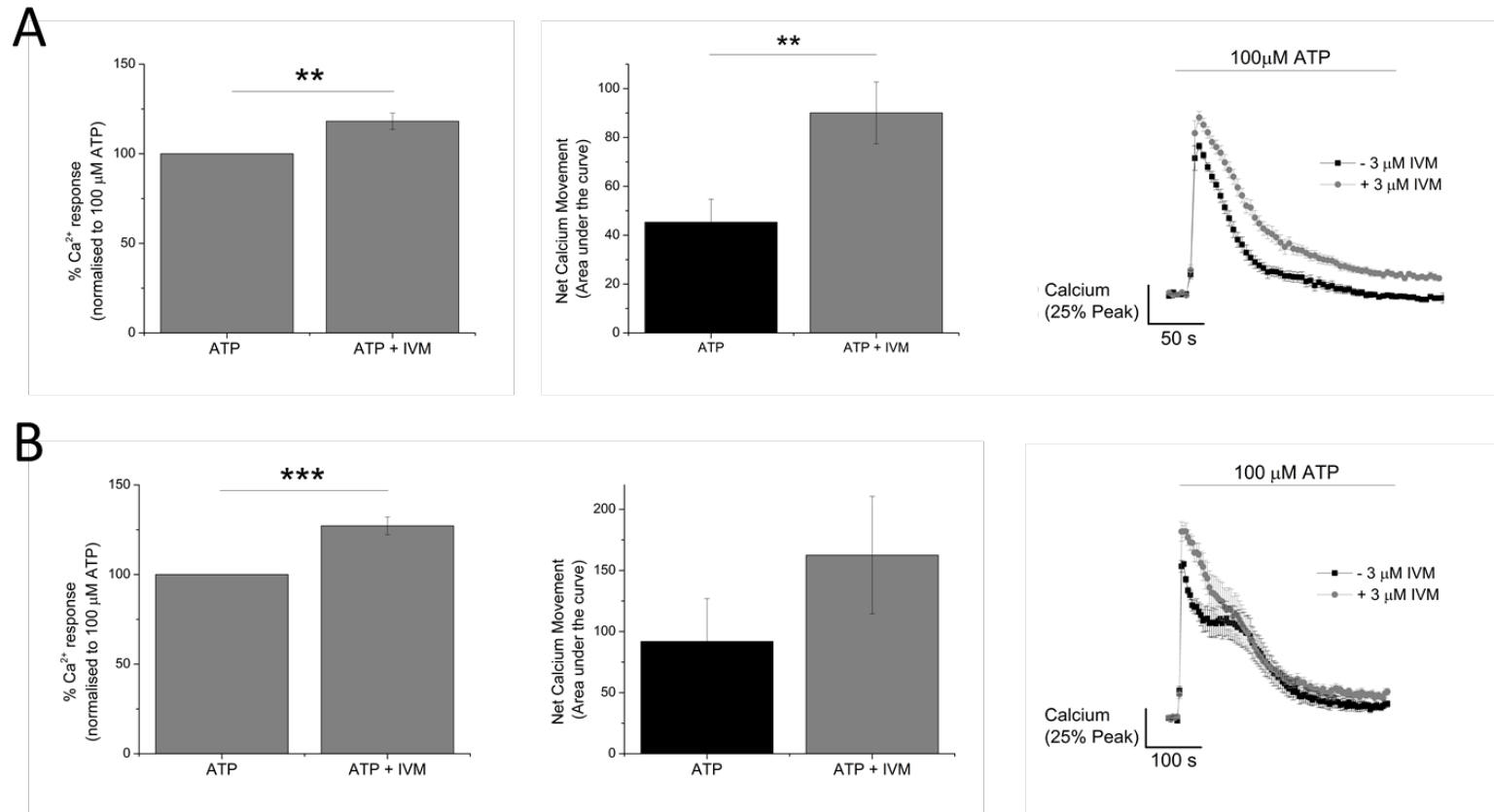
Figure 4.14. **Effect of P2X$_4$ positive allosteric modulator, 3 μM Ivermectin, on ATP-evoked Ca^{2+} response in GM-MDMs versus M-MDMs.** Data is represented as percentage increase in Ca^{2+} response, net calcium movement and representative time-response curve at 100 μM in the presence or absence of 3 μM IVM in: A) GM-MDM cells (N=12 donors) and B) M-MDM cells (N=7 donors). Asterisks include significant changes towards control (*** $p<0.001$, ** $p<0.01$, Student's t-test).

4.3.5.2. Effect of selective P2X$_4$ antagonists on ATP-evoked Ca^{2+} response in GM-MDM versus M-MDM cells

Two selective antagonists for P2X$_4$ receptor, PSB-12062 and 5-BDBD, were utilized in this chapter to characterize the contribution of P2X$_4$ in ATP-evoked Ca^{2+} responses in human primary macrophages. Both antagonists were used at 10 μM concentration to ensure maximal inhibition of P2X$_4$, as determined through an IC$_{50}$ curve described previously (Figure 3.18C and D).

4.3.5.2.1. PSB-12062

Treatment of GM-MDM cells with 10 μM PSB-12062 had a significant effect on both magnitude of ATP-evoked Ca^{2+} response as well as net calcium movement (Figure 4.14A). Blocking P2X$_4$ receptor resulted in a small but significant reduction in magnitude of ATP-evoked Ca^{2+} response (7.7 $\pm$ 2.7 %; N=12 donors; P<0.05) and a significant reduction in net calcium movement as quantified by area under the curve (AUC 44.8 $\pm$ 7.9 without PSB-12062 versus 27.5 $\pm$ 6.3 with PSB-12062; N=12 donors; P<0.01). As shown on the time-response curve (Figure 4.14A), blocking P2X$_4$ shifted the decay phase of the ATP-evoked Ca^{2+} response towards the left. Similarly, pre-treatment of M-MDM cells with 10 μM PSB-12062 resulted in a small but significant reduction in magnitude of ATP-evoked Ca^{2+} response (10.52 $\pm$ 3.16 %; N=7 donors; P<0.05; Figure 4.15B). As shown on the time-response curve (Figure 4.14B), blocking P2X$_4$ shifted the decay phase of the Ca^{2+} response towards the left, just as observed in GM-MDM cells. However, due to large donor-to-donor variability in M-MDM cells, this shift did not equate to significant reduction in net calcium movement (AUC 162.98 $\pm$ 31.68 without PSB-12062 versus 134.50 $\pm$ 24.22 with PSB-12062; N=7 donors; P>0.05).
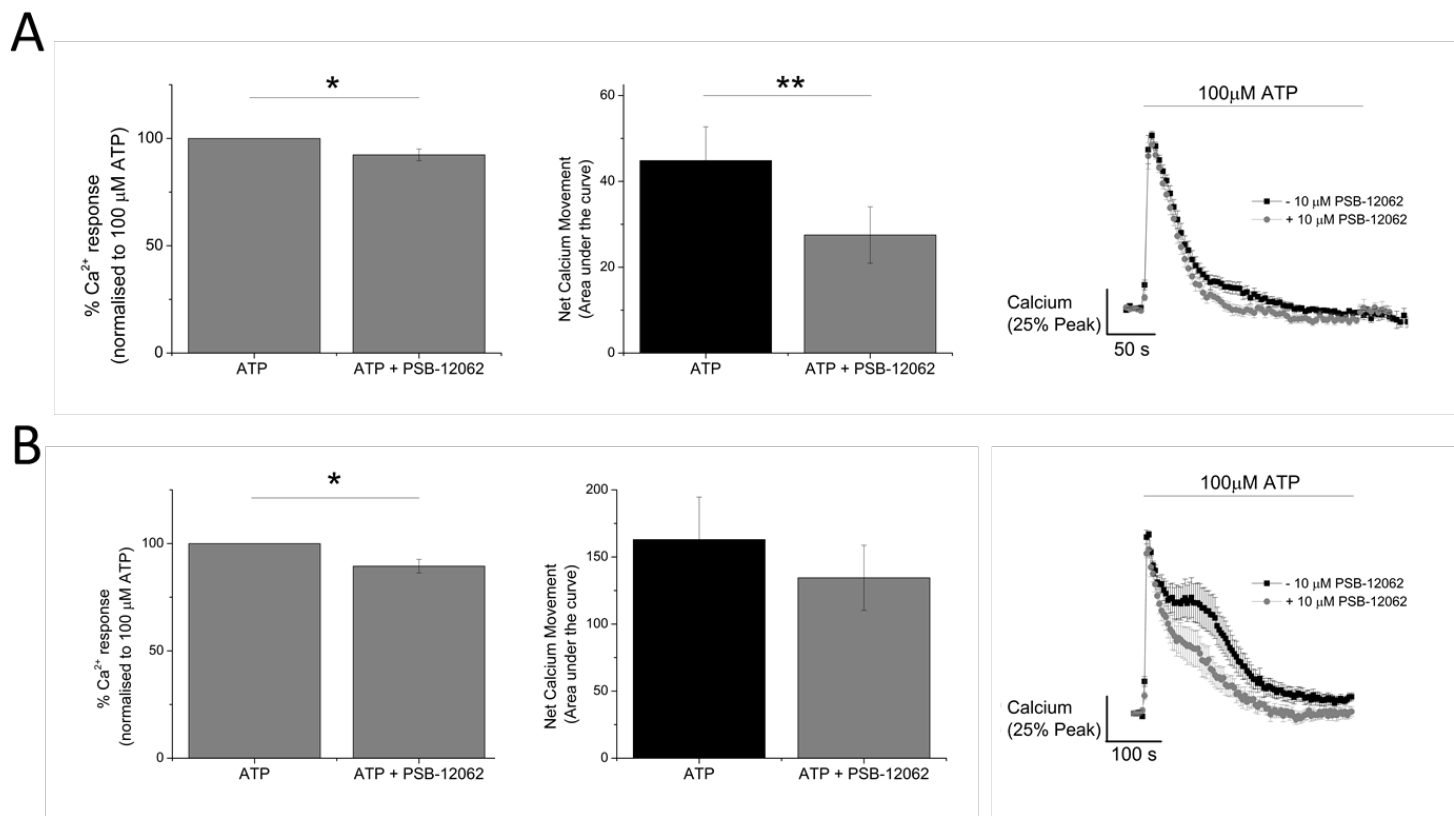
Figure 4.15. **Effect of P2X$_4$ receptor antagonist, 10 μM PSB-12062 on ATP-evoked Ca^{2+} response in GM-MDMs versus M-MDMs.** Data is represented as percentage increase in Ca^{2+} response, net calcium movement and representative time-response curve at 100 μM in the presence or absence of 10 μM PSB-12062 in: A) GM-MDM cells (N=12 donors) and B) M-MDM cells (N=7 donors). Asterisks include significant changes towards control (** $p<0.01$, * $p<0.05$, Student's t-test).

4.3.5.2.2. 5-BDBD

Treatment of GM-MDM cells with 10 μM 5-BDBD had a significant effect on magnitude of ATP-evoked Ca^{2+} response (17.47 ± 6.74 %; N=4 donors; P<0.05; Figure 4.16A) but no effect on the decay kinetics and net calcium movement (AUC 37.07 ± 7.61 without 5-BDBD versus 37.50 ± 14.26 with 5-BDBD; N=4 donors; P>0.05; Figure 4.16A). Similar to the effect 5-BDBD had on GM-MDM, blocking $P2X_4$ in M-MDM cells using 5-BDBD significantly reduced magnitude of Ca^{2+} response (31.75 ± 9.11 %; N=4 donors; P<0.05; Figure 4.16B) but had no significant effect on the decay kinetics as well as net calcium movement (AUC 70.70 ± 28.03 without 5-BDBD versus 46.81 ± 3.395 with 5-BDBD).

The difference in effect observed with these two selective $P2X_4$ receptor antagonists, PSB-12062 and 5-BDBD, may be due to the difference in their nature of mechanism. While PSB-12062 has been described to act as an allosteric antagonist of $P2X_4$, 5-BDBD has been reported to act as a competitive antagonist of $P2X_4$. When effect of IVM or PSB-12062 was observed, it was apparent that although $P2X_4$ activation appeared to play a minor role in the magnitude of ATP-evoked Ca^{2+} response, it had a bigger contribution towards the decay phase of the ATP-evoked Ca^{2+} response instead. However, the effect of 5-BDBD on ATP-evoked Ca^{2+} response did not mimic the effect observed by pre-treatment of PSB-12062. This may be due to the fact that as a competitive antagonist, the agonist concentration (100 μM ATP) utilized in these experiments was too high, shielding the inhibitory effect of 5-BDBD.
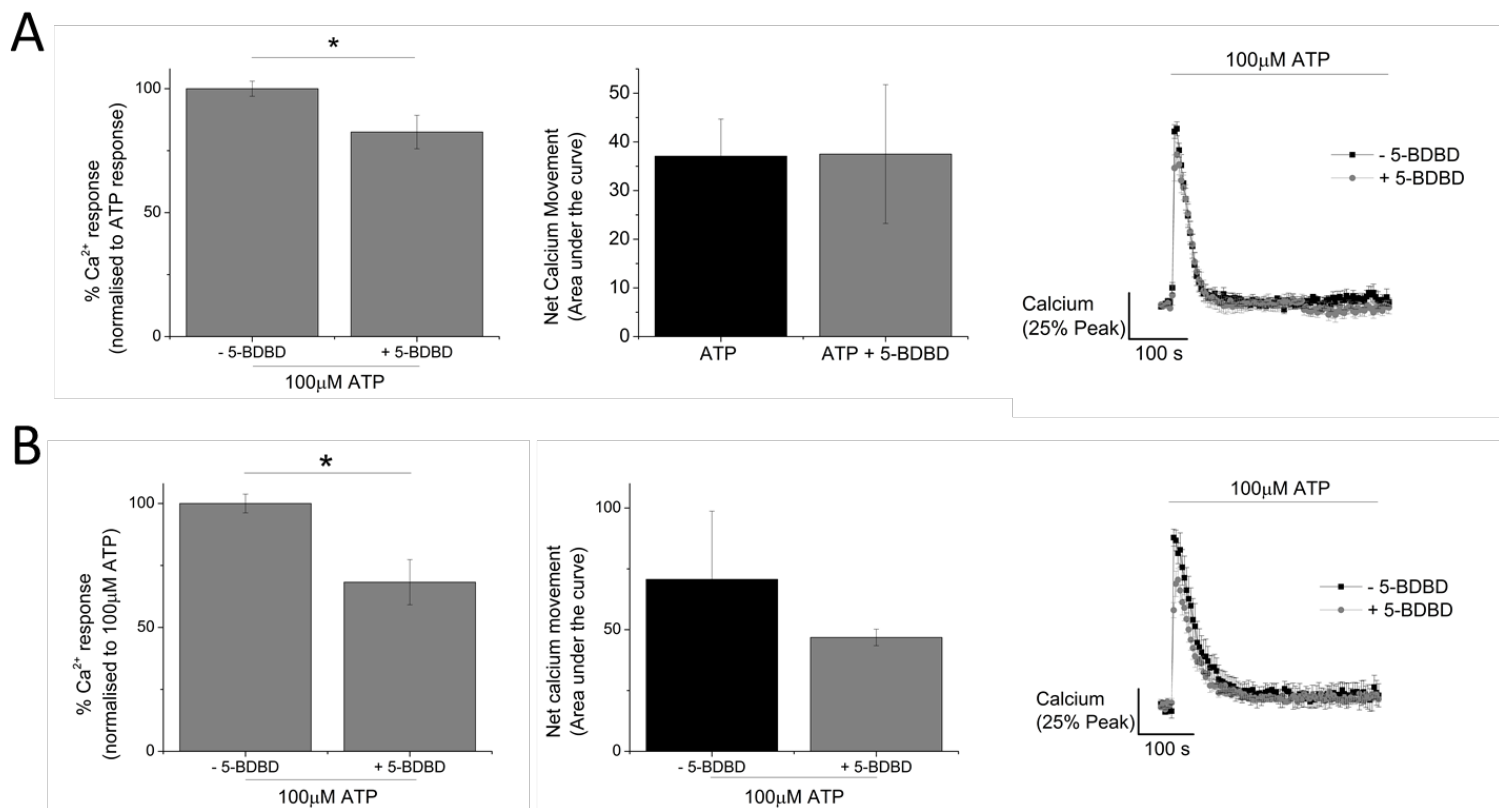
Figure 4.16. Effect of P2X$_4$ receptor antagonist, 10 μM 5-BDBD, on ATP-evoked Ca^{2+} response in GM-MDMs versus M-MDMs. Data is represented as percentage increase in Ca^{2+} response, net calcium movement and representative time-response curve at 100 μM ATP in the presence or absence of 10 μM 5-BDBD in: A) GM-MDM cells (N=4 donors) and B) M-MDM cells (N=4 donors). Asterisks include significant changes towards control (* p<0.05, Student's t-test).

4.3.5.3. Effect of selective P2X$_4$ antagonists on IVM-potentiated ATP-evoked Ca^{2+} response in GM-MDM versus M-MDM cells

To further confirm the contribution of P2X$_4$ towards ATP-evoked Ca^{2+} response in human primary macrophages, the effect of PSB-12062 and 5-BDBD were tested in the presence of IVM.

4.3.5.3.1. PSB-12062

Blocking P2X$_4$ with PSB-12062 caused no significant effect towards the magnitude of the IVM-potentiated ATP-evoked Ca^{2+} response but significantly reduced decay response in GM-MDM cells. This can be observed in the time-response curve as well as area under the curve (AUC 98.83 ± 15.41 without PSB-12062 versus 63.42 ± 13.92 with PSB-12062; N=12 donors; Figure 4.17A). On the other hand, blocking P2X$_4$ activation in M-MDM cells appeared to have a different effect. As shown in Figure 4.17B, PSB-12062 caused a significant reduction in the magnitude of IVM-potentiated Ca^{2+} response (11.53 ± 4.47 %; N=6 donors; P<0.05) but had no significant effect towards the net calcium movement in M-MDM cells (AUC 162.5 ± 48.11 without PSB-12062 versus 108.35 ± 15.11 with PSB-12062; N=6 donors; P>0.05). Although the time-response curve illustrated a slight shift towards the left of the decay response, the error bars were large and no significant changes were observed. However, it was noticeable that blocking P2X$_4$ in M-MDM cells did not return the decay response back to the baseline, rather it remained on a sustained elevated phase. This difference in effect of PSB-12062 on the two macrophage system may be due to the fact that the amount of functional P2X$_4$ within the two systems is different.
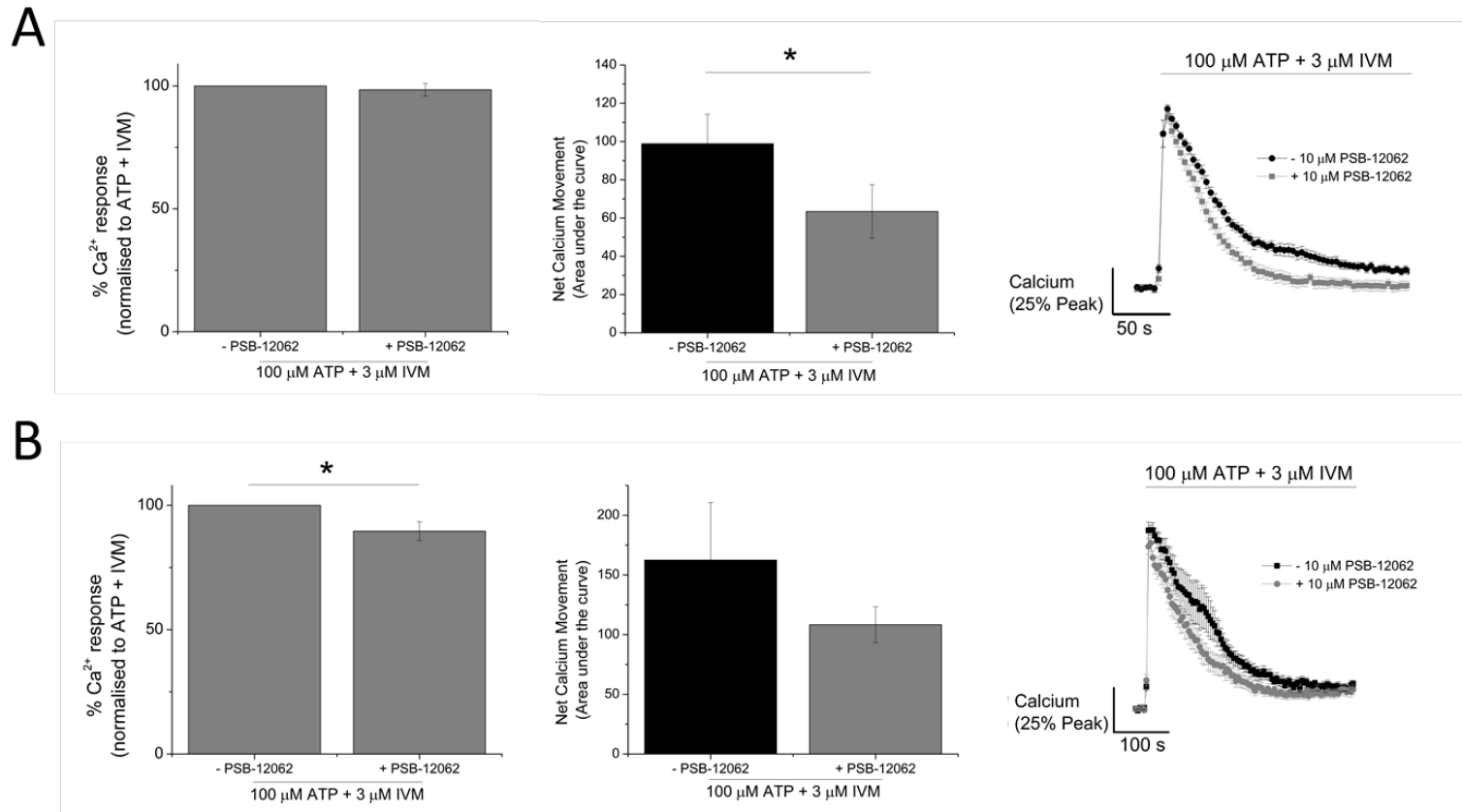
Figure 4.17. Effect of P2X$_4$ receptor antagonist, 10 μM PSB-12062, on IVM-potentiated ATP-evoked Ca^{2+} response in GM-MDMs versus M-MDMs. Data is represented as percentage increase in Ca^{2+} response, net calcium movement and representative time-response curve upon stimulation with 100 μM ATP and 3 μM IVM in the presence or absence of 10 μM PSB-12062 in: A) GM-MDM cells (N=12 donors) and B) M-MDM cells (N=6 donors). Asterisks include significant changes towards control (* $p < 0.05$, Student's t-test).

4.3.5.3.2. 5-BDBD

To study the effect of selective antagonist, 5-BDBD, on IVM-potentiated ATP-evoked Ca^{2+} response in human primary macrophages, IVM treatment was performed in the presence of vehicle (1% DMSO). In Figure 4.18A and B, the presence of 1% DMSO vehicle (illustrated as '– 5-BDBD') altered the IVM-potentiated ATP-evoked Ca^{2+} response in these cells. Pre-treatment of GM-MDM cells with 5-BDBD caused a significant reduction in the magnitude of IVM-potentiated ATP-evoked Ca^{2+} response (16.31 ± 3.47 %; N=3 donors; P<0.05; Figure 4.18A) and decay kinetics as represented by time-response curves and net calcium movement (64.08 ± 12.08 without 5-BDBD *vs.* 27.49 ± 7.47 with 5-BDBD; N=3 donors; P<0.01; Figure 4.18A). Pre-treatment of M-MDM cells with 5-BDBD also had a similar effect in which 5-BDBD caused a significant reduction in the magnitude of IVM-potentiated Ca^{2+} response (22.06 ± 3.60 %; N=3 donors; P<0.01; Figure 4.18B) and net calcium movement (AUC 75.38 ± 17.37 without 5-BDBD versus 33.92 ± 0.84 with 5-BDBD; N=3 donors; P>0.05; Figure 4.18B). Unlike the effect of PSB-12062 on IVM-potentiated ATP-evoked Ca^{2+} response in M-MDM cells, 5-BDBD caused the decay response to return to its baseline level.

Taken together, the effects observed by the use of IVM, PSB-12062 or 5-BDBD allowed the conclusion that P2X$_4$ receptor found in GM-MDM and M-MDM cells are functional and contribute mainly towards the decay phase of the ATP-evoked Ca^{2+} response.
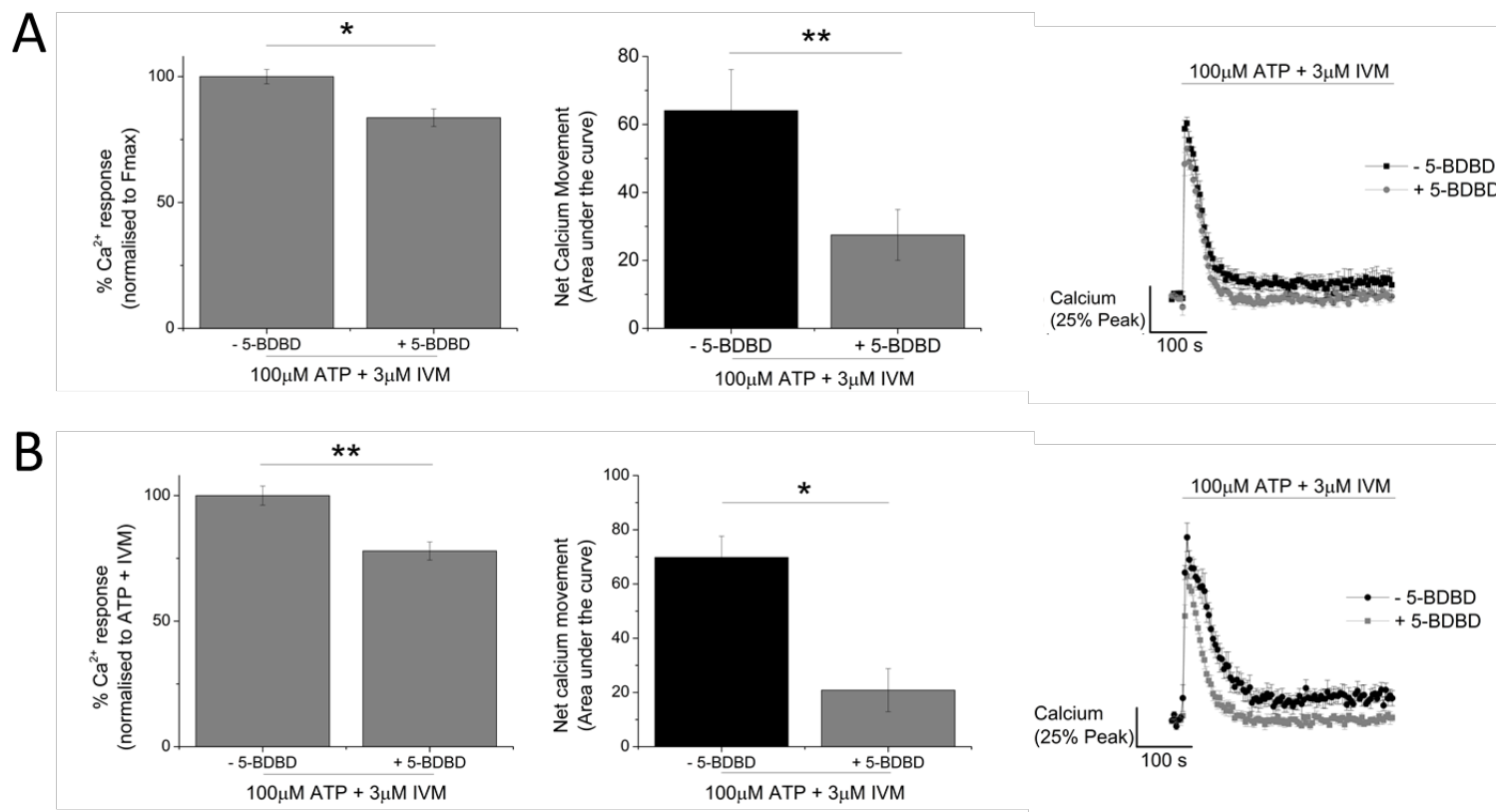
Figure 4.18. Effect of P2X$_4$ receptor antagonist, 10 μM 5-BDBD, on IVM-sensitive ATP-evoked Ca^{2+} response in GM-MDMs versus M-MDMs. Data is represented as percentage increase in Ca^{2+} response, net calcium movement and representative time-response curve upon stimulation with 100 μM ATP and 3 μM IVM in the presence or absence of 10 μM 5-BDBD in: A) GM-MDM cells (N=3 donors) and B) M-MDM cells (N=3 donors). Asterisks include changes towards control (** $p<0.01$, * $p<0.05$, Student's t-test).

4.3.5.4. Assessing P2X$_4$ protein expression in GM-MDM versus M-MDM cells using flow cytometry analysis

Distribution of P2X$_4$ has been described as predominantly localized within intracellular lysosomal compartments of human macrophages (Stokes and Surprenant, 2009). This observation has also been shown in both rodent macrophages and microglial cells (Boumechache et al., 2009). Study by Stokes and Surprenant (2009) also revealed that unstimulated macrophages showed high total protein expression of P2X$_4$ but very low functional expression. It is unknown if the expression of P2X$_4$ receptor protein in human primary macrophage models, GM-MDM and M-MDM, are different. Results obtained from functional Ca^{2+} response in these cells using P2X$_4$-specific pharmacological tools (section 4.3.5), so far, revealed that GM-MDM cells are more sensitive to IVM and P2X$_4$ antagonists (PSB-12062 and 5-BDBD) when compared to M-MDM cells. One of the main factors that may underlie the difference in sensitivities of the macrophage systems could be the different expression of surface and total P2X$_4$ protein. Therefore, it was important to quantify the expression of P2X$_4$ in both macrophage systems using flow cytometry.

Flow cytometry was performed on GM-MDM and M-MDM cells following 6 days treatment with the corresponding colony stimulating factors. As shown in Figure 4.19A, surface staining of P2X$_4$ on the two macrophage systems revealed that in fact, both macrophage models express very low amount of the receptor on the cell surface membrane. Across three independent donors, GM-MDM cells averaged to 3.34 ± 0.071 % P2X$_4$(ext)$^+$ positive cells while M-MDM cells averaged to 1.53 ± 0.11 % P2X$_4$(ext)$^+$ positive cells. Despite very low expression of P2X$_4$ on the surface of the cells, there was significantly less P2X$_4$(ext)$^+$ M-MDM cells compared to GM-MDM cells (54.08 ± 4.14 % reduction; N=3 donors; P<0.01; Figure 4.19A). Total P2X$_4$ protein expression was also quantified in GM-MDM and M-MDM cells. Across three independent donors, GM-MDM cells averaged to 73.9 ± 6.93 % total P2X$_4$(total)$^+$ cells while M-MDM cells averaged to 54.96 ± 9.21 % total P2X$_4$(total)$^+$ cells (Figure 4.19B). Comparing the data obtained from both macrophage systems, M-MDM cells had significantly lower proportion of cells expressing total P2X$_4$ (23.01 ± 0.64 %; N=4 donors; P<0.01; Figure 4.19B) when compared to GM-MDM. As there is currently no reported knowledge about the expression of P2X$_4$ in GM-MDM and M-MDM cells, these observations are important in identifying if P2X$_4$ receptor activation has a bigger contribution in either one of the macrophage model.
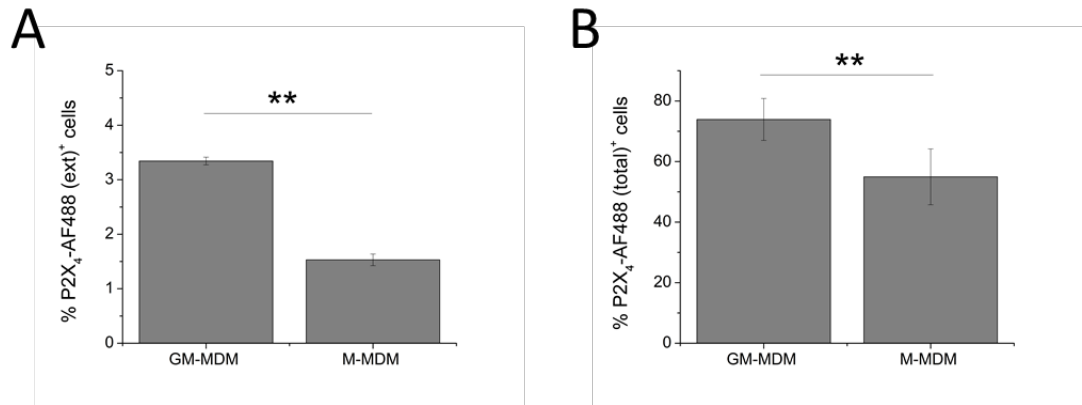
Figure 4.19. **Flow cytometry analysis to quantify P2X$_4$-positive cells in GM-MDM and M-MDM cells.** Quantification of macrophages expressing: A) P2X$_4$ receptor on the cell surface membrane (N=3 donors) and B) total (cell surface and internal) P2X$_4$ receptor (N=3 donors). Data is represented as percentage of positive cells gated against negative isotype control. Asterisks include significant changes towards control (** $p < 0.01$, Student's t-test).

4.3.5.5. Effect of selective P2XR antagonists on ATP-evoked Ca^{2+} response in GM-MDM versus M-MDM cells

The main P2X receptors expressed in immune cells are P2X$_4$ and P2X$_7$. As the main interest in this research is to study the contribution of P2X$_4$ receptor towards ATP-evoked Ca^{2+} response in human primary macrophages as well as identifying its functional role, it was important to investigate the contribution of other P2X receptors, in particular P2X$_7$, towards ATP-evoked Ca^{2+} responses. In addition to P2X$_7$, P2X$_1$ was also investigated. Other P2X receptors were not investigated, as they are either not expressed in these primary macrophages (P2X$_2$, P2X$_3$ and P2X$_6$, Table 4.2) or are known to be expressed as non-functional isoform (P2X$_5$) (Kotnis et al., 2011). Here, two pharmacological tools were used to study possible contributions of P2X$_1$ and P2X$_7$ to ATP-evoked Ca^{2+} response in human GM-MDM and M-MDM cells.

4.3.5.5.1. P2X$_1$ antagonist

Selective P2X$_1$ antagonist, Ro0437626, was used to study the possible contribution of P2X$_1$ in human primary macrophages. This antagonist has been reported to be a competitive antagonist with IC$_{50}$ value of 3 μM and over 30-fold selectivity against other P2XR (Jaime-Figueroa et al., 2005). Since the agonist concentration used in this study was 100 μM ATP, maximal concentration of the antagonist (30 μM) was tested to ensure maximal activity. Pre-treatment of GM-MDM and M-MDM cells with Ro0437626 did not cause any inhibition towards the magnitude of ATP-evoked Ca^{2+} response. Instead, it significantly potentiated magnitude of ATP-evoked Ca^{2+} response in both cells (GM-MDM 31.29 ± 10.26 %; N=4 donors; P<0.01; Figure 4.20A versus M-MDM 17.31 ± 7.21 %; N=4 donors; P<0.01; Figure 4.20B). In both macrophage systems, pre-treatment of cells with Ro0437626 had no significant effect towards the net calcium movement as measured through area under the curve (AUC GM-MDM 40.76 ± 12.67 without Ro0437626 versus 49.56 ± 10.07 with Ro0437626; N=4 donors; P>0.05; Figure 4.20A and AUC M-MDM 99.27 ± 37.21 without Ro0437626 versus 107.88 ± 29.89 with Ro0437626; N=4 donors; P>0.05; Figure 4.20B). This observation correlated with findings in the macrophage cell line whereby treatment with P2X$_1$ antagonist resulted in significant potentiation of the ATP-evoked Ca^{2+} response, instead of inhibition (Figure 3.7A).
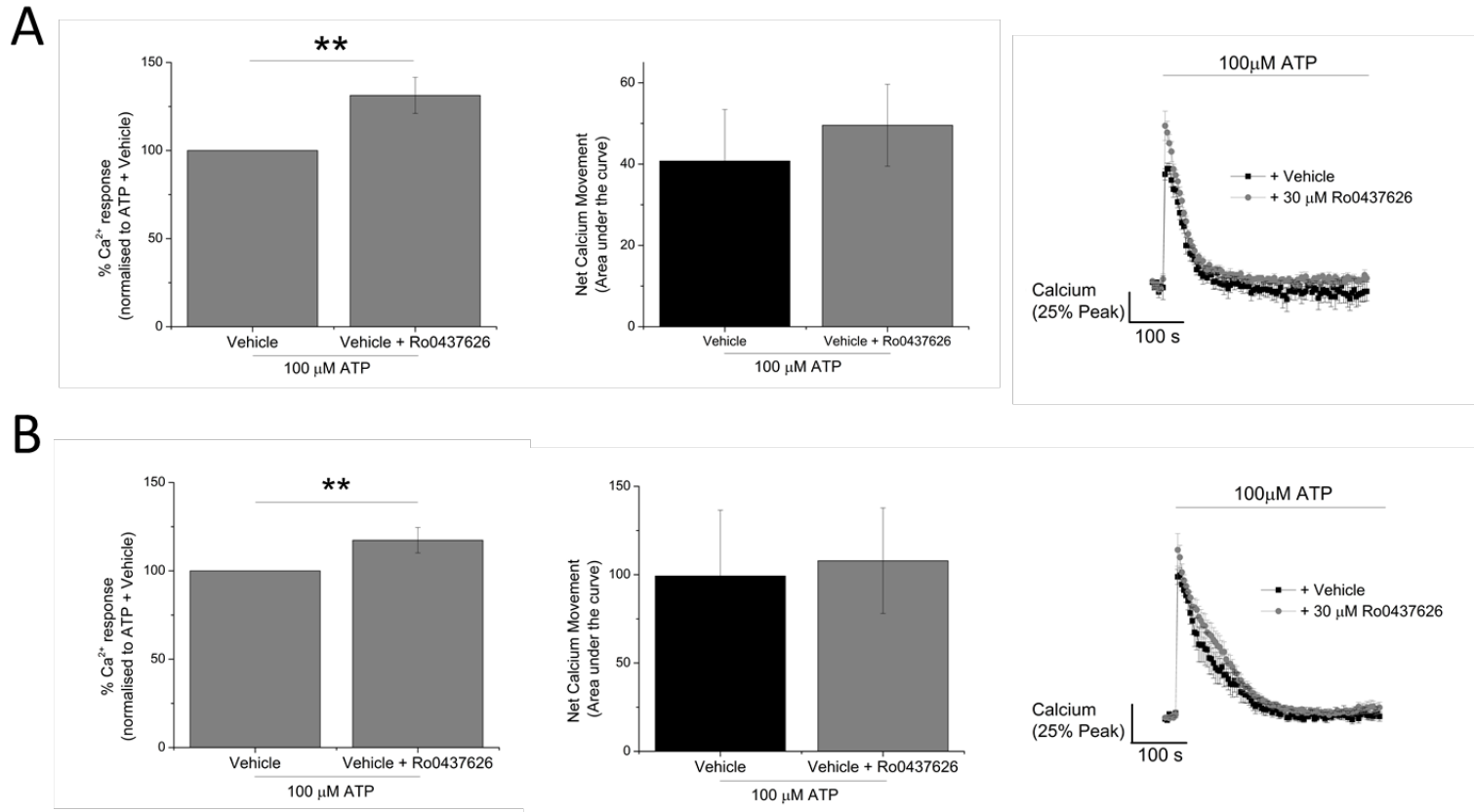
Figure 4.20. **Effect of P2X$_1$ receptor antagonist, 30 μM Ro0437626, on ATP-evoked Ca^{2+} response in MDMs.** Data is represented as percentage increase in Ca^{2+} response, net calcium movement and representative time-response curve at 100 μM in the presence or absence of 30 μM Ro0437626 in: A) GM-MDM cells (N=4 donors) and B) M-MDM cells (N=4 donors). Asterisks include significant changes towards control (** $p<0.01$, Student's t-test).

4.3.5.5.2. P2X$_7$ antagonist

Selective P2X$_7$ antagonist, A438079, was used to study the contribution of P2X$_7$ in ATP-evoked Ca^{2+} response of human primary macrophages. A438079 is a competitive P2X$_7$ antagonist with reported pIC$_{50}$ of 6.9 for the inhibition of Ca^{2+} influx in human recombinant P2X$_7$ cell line (Donnelly-Roberts and Jarvis, 2007, Nelson et al., 2006). To ensure maximal antagonism of the compound, 5 μM A438079 was used in this study. Pre-treatment of GM-MDM and M-MDM cells with A438079 had no significant inhibitory effect on the magnitude of ATP-evoked Ca^{2+} response (Figure 4.21A and 4.21B, respectively). In addition to this, A438079 also had no significant effect on the net calcium movement in both macrophage systems. P2X$_7$ receptor is highly expressed on immune cells which include glial cells and macrophages (Surprenant, 1996). Compared to other P2XR, the activation of P2X$_7$ requires higher concentrations of ATP (EC$_{50}$ > 100 μM). The lack of effect by A438079 on GM-MDM and M-MDM cells (Figure 4.21A and 4.21B) indicated that P2X$_7$ do not contribute to ATP-evoked Ca^{2+} response at 100 μM concentration and this may be due to the lack of activation of P2X$_7$ at the agonist concentration used, in these human primary macrophages. Hence, it is likely that the agonist concentration used throughout the study (100 μM) is not sufficient to activate P2X$_7$ in human primary MDM.
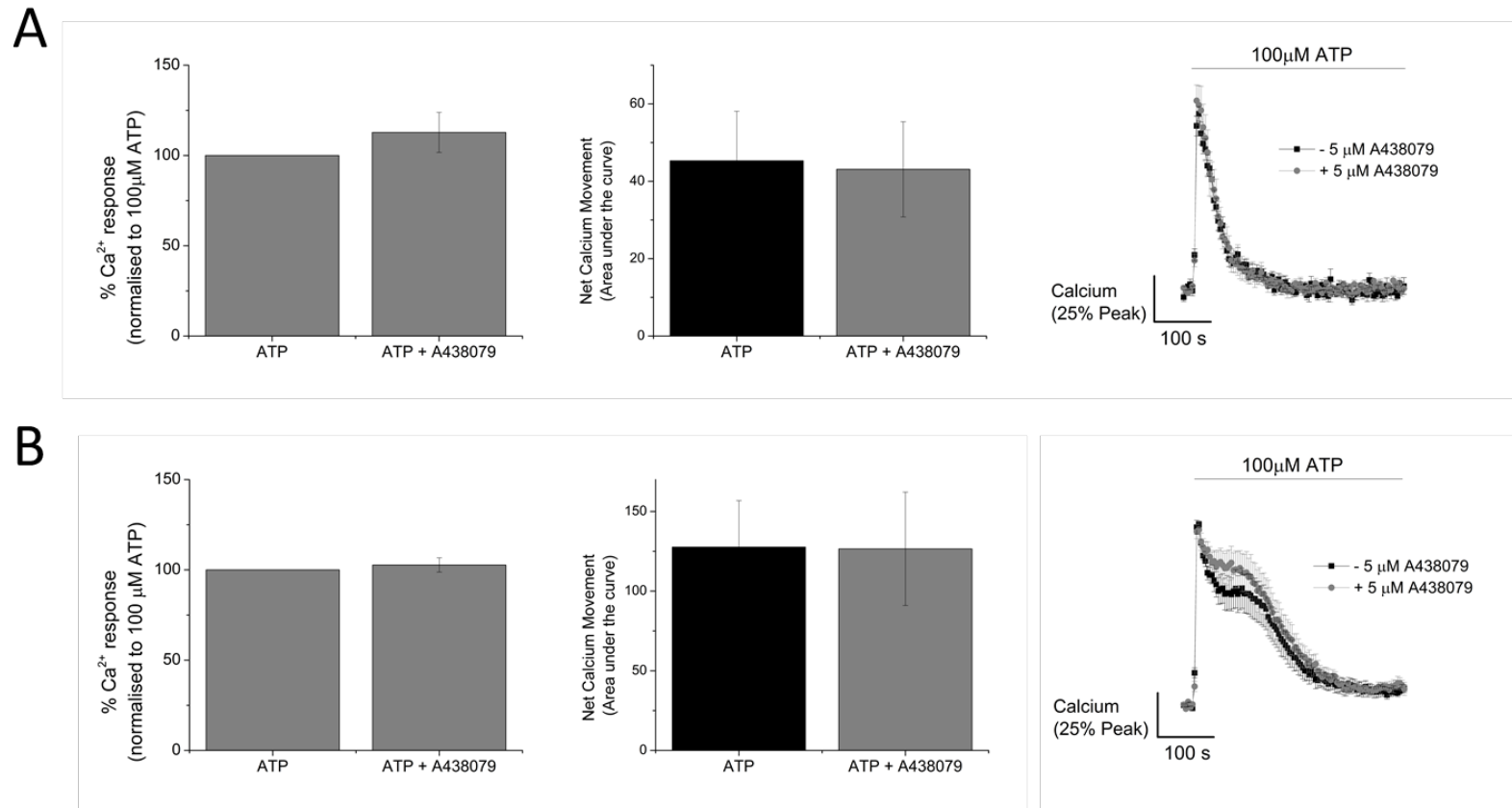
Figure 4.21. Effect of P2X$_7$ receptor antagonist, 5 μM A438079, on ATP-evoked Ca^{2+} response in GM-MDMs versus M-MDMs. Data is represented as percentage increase in Ca^{2+} response, net calcium movement and representative time-response curve at 100 μM in the presence or absence of 5 μM A438079 in: A) GM-MDM cells (N=6 donors) and B) M-MDM cells (N=6 donors).

4.4. Summary

Monocyte-derived macrophages differentiated using GM-CSF or M-CSF serve as a well-established tool to study primary tissue-specific macrophages (van Wilgenburg et al., 2013). This chapter utilized both GM-MDMs and M-MDMs in a side-by-side comparison to study ATP-evoked Ca^{2+} responses with the goal of identifying $P2X_4$ contribution. To accompany this, the involvement of other purinergic receptors in ATP-evoked Ca^{2+} response was also studied.

All P2XR (with the exception of $P2X_2$, $P2X_3$ and $P2X_6$) were found to be expressed at the transcriptional and translational level in both GM-MDM and M-MDM cells. In both cell types, all P2YR (with the exception of $P2Y_{12}$ and $P2Y_{14}$) were also found to be expressed at the transcriptional level but only the expression of $P2Y_1$, $P2Y_2$, $P2Y_6$ and $P2Y_{13}$ were confirmed at the translational level. While no significant differences were observed in mRNA expression of P2XR in the two MDMs, $P2Y_1$ were found to be significantly down-regulated while $P2Y_6$ and $P2Y_{11}$ were significantly up-regulated in M-MDM, compared to GM-MDM.

In both GM-MDM and M-MDM cells, ATP elicited a biphasic Ca^{2+} response involving an increase in intracellular Ca^{2+} reflected by peak magnitude and a second response which corresponds to decay phase. Unlike observations made in TDM cells (Chapter 3), pre-treatment of both GM-MDM and M-MDM with U73122 almost completely abolished the magnitude of the ATP-evoked Ca^{2+} response suggesting $G_{\alpha q}$-coupled P2YR activation to be the sole contributor to the peak response. Using selective P2YR antagonists, it was revealed that the activation of both $P2Y_{11}$ and $P2Y_{13}$ contribute towards the peak of the response in GM-MDM and M-MDM cells, with $P2Y_{11}$ also playing a substantial role in the decay phase of the ATP-evoked Ca^{2+} response in M-MDM cells. This observation corroborated findings from qRT-PCR illustrating a significant up-regulation of $P2Y_{11}$ mRNA expression in M-MDM cells, when compared to GM-MDM cells. In the interest of studying contribution of P2XR towards the ATP-evoked Ca^{2+} response in GM-MDM and M-MDM cells, the effect of positive allosteric modulator IVM and P2XR selective antagonists were assessed. While $P2X_1$ and $P2X_7$ did not appear to contribute towards the ATP-

evoked Ca^{2+} response of both macrophages, P2X$_4$ appeared to significantly contribute towards the second decay phase of the ATP-evoked Ca^{2+} response, although a more significant role of P2X$_4$ was observed in GM-MDM vs. M-MDM. This was evident from the effect observed using IVM, PSB-12062 or 5-BDBD. The fact that P2X$_4$ appear to contribute only towards the second decay response of the ATP-evoked Ca^{2+} response in these cells illustrate a possibility that they may work in close relationship with P2YR. The lack of effect of P2X$_4$ antagonist on the peak of the Ca^{2+} response may also be explained by the low surface P2X$_4$ expression in both macrophage systems. In addition to this, the difference in sensitivity of GM-MDM and M-MDM cells towards IVM and P2X$_4$ antagonist may be explained by the difference in level of surface and intracellular expression of P2X$_4$ as quantified via flow cytometry. FACS analysis illustrated that across three independent donors, GM-MDM cells expressed a higher amount of both surface and total P2X$_4$, in comparison to M-MDM cells. Altogether, this chapter has illustrated that to elucidate a functional role of P2X$_4$ in human primary MDM, GM-MDM cells may act as a better system due to higher expression of surface and total P2X$_4$ receptor.

Chapter 5: Involvement of P2X$_4$ in ATP-induced cytokine and chemokine levels in human monocyte-derived macrophages

5.1. Introduction

Cytokines and chemokines are potent signalling molecules produced by many cell types, especially those of the immune system. These molecules regulate inflammation and play a vital role in regulating the immune response in health and disease. This includes regulation of cellular proliferation, chemotaxis, tissue repair as well as metabolism (Arango Duque and Descoteaux, 2014). While their function within the immune system has been explored greatly in the literature, little is known about how they are packaged and secreted from various immune cells. The common assumption for the mechanism of cytokine and chemokine trafficking and secretion is through endoplasmic reticulum (ER) and Golgi pathway before being transported to cell surface through a simple, unidirectional secretory vesicle (Lacy, 2015). However, the pathway is much more complex involving a combination of secretory granules and vesicles for trafficking and various endocytic pathways for secretion. The release of cytokines and chemokines by activated macrophages are a major component of the innate immune response (Hume, 2006). Macrophages, being one of the most abundant sources of inflammatory cytokines, can secrete these proteins inappropriately leading to chronic conditions such as diabetes and obesity to vascular and neurodegenerative diseases (Chawla et al., 2011, Neurath, 2014, Tabas and Glass, 2013). Therefore, many of the newer therapeutics aim to target cytokines directly, either through their modes of release or receptor engagement.

One of the most studied endogenous insults that can activate the immune system is ATP. Extracellular ATP is elevated following inflammation and injury and can act on

purinergic receptors such as $P2X_4$ and $P2X_7$, which are the predominant purinergic P2X receptor subtypes expressed on immune cells (de Rivero Vaccari et al., 2012). Extensive research has been invested in studying the role of $P2X_7$ in inflammation and pain (Chessell et al., 2005, McGaraughty et al., 2007), where it has been identified to provide physiological stimulus for activation of caspase-1 and release of pro-inflammatory cytokine, IL-1β (Pelegrin and Surprenant, 2006). However, due to the lack of selective pharmacological tools, efforts to elucidate the function of $P2X_4$ in human macrophages have been hampered significantly. More recently, $P2X_4$ has been associated with roles such as mediating PGE_2 release, initiating inflammatory pain (Ulmann et al., 2010) and regulating inflammasome signalling that involves caspase-1 activation and IL-1β processing (de Rivero Vaccari et al., 2012). Despite this, there has been no direct report correlating the role of $P2X_4$ and cytokine secretion. Increasing understanding of $P2X_4$ functional role in macrophages may offer a potential target for treatment of inflammatory conditions.

5.2. Aims

The aim of this chapter is to elucidate a functional role of $P2X_4$ within the macrophage system. Although abundantly expressed in immune cells, it is unknown if $P2X_4$ can regulate ATP-induced cytokine and chemokine production in human monocyte-derived macrophages. To address this aim, an mRNA profiler screen was performed to identify candidate genes that are induced following ATP stimulation in the presence and absence of $P2X_4$ antagonist. This was then further studied at the protein level using ELISA technique.

5.3. Results

5.3.1. RT^2 Profiler mRNA Array

To identify a functional role of $P2X_4$ in human macrophages, RT^2 profiler mRNA array was employed to screen for 84 different genes of various cytokines and chemokines that has been associated with inflammation of the immune system. Throughout the study, 100 μM ATP was used as the main stimulus for activation of $P2X_4$ in human GM-MDM cells. Transcriptional screening for candidate genes were performed at one time point (6h) following pre-treatment of either vehicle or $P2X_4$ selective antagonist (10 μM PSB-12062).

5.3.1.1. Identifying genes constitutively expressed in human monocyte-derived macrophages

By screening for 84 different genes that are expressed in human GM-MDM cells, it was possible to identify which genes are constitutively expressed in the absence of any agonist stimulation. As shown on Table 5.1, under no agonist stimulation, GM-MDM constitutively expressed various genes, as quantified across 6 independent donors. Genes that were amplified at cycle threshold 35 or above were considered absent and these genes included BMP4, CCL19, CXCL11, CXCL12, IFNγ, IL12α, IL17A, IL2, TNFRSF11B and XCL1 (highlighted in Table 5.1 as grey). A few genes were found to be highly abundant (amplified <Ct 20) and this included CCL22, CSF1, CXCL16, GPI and SPP1. These were important observations as to date, there has been no detailed report elaborating what genes are constitutively expressed in GM-MDM cells. In addition to this, identification of constitutively expressed genes may allow the phenotype of these macrophage system to be studied in greater detail.

	Average Ct values (N=6)			Average Ct values (N=6)
ADIPOQ	33.5 ± 0.31		IL12A	35.7 ± 0.82
BMP2	28.9 ± 0.54		IL12B	32.2 ± 0.66
BMP4	N/A		IL13	30.0 ± 0.60
BMP6	26.9 ± 0.58		IL15	28.0 ± 0.21
BMP7	29.4 ± 0.47		IL16	22.2 ± 0.36
C5	27.9 ± 0.28		IL17A	36.7 ± 0.51
CCL1	26.4 ± 0.70		IL17F	29.2 ± 0.47
CCL11	35.1 ± 0.49		IL18	22.5 ± 0.24
CCL13	28.1 ± 0.61		IL1A	26.5 ± 0.20
CCL17	29.0 ± 0.37		IL1B	24.1 ± 0.25
CCL18	26.9 ± 0.51		IL1RN	20.6 ± 0.35
CCL19	35.1 ± 0.43		IL2	37.2 ± 0.42
CCL2	23.0 ± 0.19		IL21	31.0 ± 0.53
CCL20	27.0 ± 0.77		IL22	31.2 ± 0.35
CCL21	32.6 ± 0.42		IL23A	27.6 ± 0.26
CCL22	16.7 ± 0.30		IL24	24.0 ± 0.33
CCL24	26.4 ± 0.51		IL27	28.9 ± 0.33
CCL3	20.2 ± 0.35		IL3	31.7 ± 0.41
CCL5	27.1 ± 0.84		IL4	35.1 ± 0.41
CCL7	21.3 ± 0.33		IL5	29.4 ± 0.42
CCL8	33.1 ± 0.49		IL6	31.9 ± 0.54
CD40LG	29.3 ± 0.52		IL7	27.4 ± 0.65
CNTF	26.2 ± 0.21		CXCL8	22.5 ± 0.48
CSF1	17.5 ± 0.48		IL9	32.4 ± 0.50
CSF2	31.7 ± 0.68		LIF	23.6 ± 0.49
CSF3	30.6 ± 0.48		LTA	31.4 ± 0.46
CX3CL1	27.0 ± 0.36		LTB	29.2 ± 0.29
CXCL1	29.6 ± 0.51		MIF	20.1 ± 0.28
CXCL10	34.7 ± 1.24		MSTN	30.8 ± 0.20
CXCL11	36.2 ± 1.38		NODAL	29.8 ± 0.30
CXCL12	38.2 ± 0.61		OSM	28.7 ± 0.36
CXCL13	31.9 ± 0.21		PPBP	29.9 ± 0.66
CXCL16	19.0 ± 0.18		SPP1	15.4 ± 0.45
CXCL2	25.9 ± 0.40		TGFB2	28.3 ± 0.60
CXCL5	29.4 ± 0.44		THPO	26.6 ± 0.48
CXCL9	32.1 ± 0.39		TNF	24.9 ± 0.32
FASLG	32.0 ± 0.49		TNFRSF11B	N/A
GPI	19.2 ± 0.31		TNFSF10	26.9 ± 0.30
IFNA2	33.8 ± 0.83		TNFSF11	31.9 ± 0.28
IFNG	35.0 ± 0.40		TNFSF13B	25.2 ± 0.30
IL10	25.3 ± 0.58		VEGFA	24.5 ± 0.19
IL11	32.7 ± 0.53		XCL1	37.4 ± 0.86

Table 5.1. RT^2 Profiler mRNA Array to identify constitutively expressed genes in human GM-MDM. Average Ct values were taken from 6 independent donors and represented ± SEM values. Genes amplified at or above Ct 35.0 were considered absent and are highlighted in grey. Genes that were undetected during the amplification run are represented as N/A.

5.3.1.2. Identifying genes induced by ATP stimulation

Extracellular ATP is regarded as a danger signal which can activate the immune system by acting on purinergic receptors (P2X and P2Y) found in immune cells. The activation of purinergic receptors by extracellular ATP in macrophages can trigger the secretion of various cytokines and chemokines (Zhang and Mosser, 2008). Although macrophages have been described to be capable of secreting various cytokines and chemokines (Fujiwara and Kobayashi, 2005), a thorough transcriptional screening has not been performed to investigate what genes may be expressed in GM-MDMs following 100 μM ATP stimulation. Log$_2$ fold change in expression of all the genes screened are shown as a heat map in Figure 5.1, with blue and negative value representing down-regulation while red and positive value representing up-regulation of mRNA expression. Genes that were unaffected following ATP stimulation are represented as white. Expression levels were normalized to the geometric mean of five housekeeping genes (ACTB, GAPDH, B2M, RPLP0 and HPRT1) and to unstimulated control with no change in expression denoted as a value of 0. As a positive control, GM-MDM cells were also treated with 100 ng/ml of LPS for 6h.

As discussed in section 5.3.1.1, ten genes (BMP4, CCL19, CXCL11, CXCL12, IFNγ, IL12α, IL2, IL17A, TNFRSF11B and XCL1) were found at undetectable levels in all conditions and have therefore been excluded from the heat map. As can be seen, LPS stimulation caused the up-regulation of no less than 35 genes and the down-regulation of no less than 15 genes. In comparison to LPS treatment, stimulation of GM-MDM cells with 100 μM ATP resulted in a more subtle effect with only 6 genes that were up regulated. These genes include CXCL2, CXCL5, IL12β, OSM, PPBP and TGF-β2 (Table 5.2).

GENE	LOG$_2$ FOLD CHANGE	$\Delta\Delta$CT FOLD CHANGE
CXCL2	1.64	3.12
CXCL5	1.40	2.44
IL12b	1.31	2.49
OSM	1.98	3.95
PPBP	1.84	3.59
TGF-β2	1.25	2.37

Table 5.2. **Genes up-regulated following 6h stimulation with 100 μM ATP.** Averaged across 4 independent donors, fold change is represented as Log$_2$ values and $\Delta\Delta$Ct values in which positive values indicate up-regulation, normalized to unstimulated control indicated by a value of 0 for log$_2$ fold change or 1 for $\Delta\Delta$CT fold change.
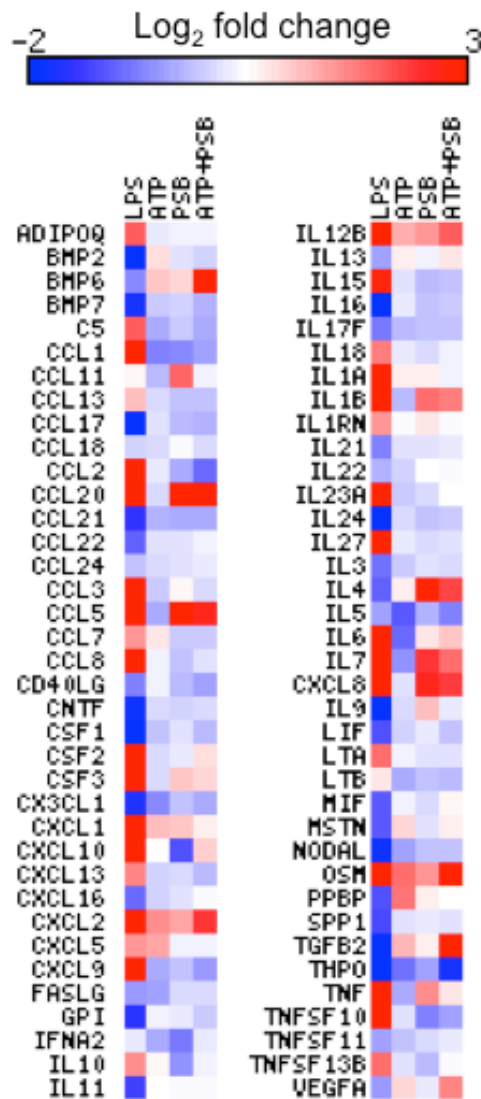
Figure 5.1. **ATP induced the expression of various genes in human GM-MDM cells.** Heat map summarizing expression data for 76 genes exhibiting differential expression across various stimulation conditions at 6h (LPS (N=1 donor), ATP (N=5 donors), PSB-12062 (N=5 donors) and ATP + PSB-12062 (N=3 donors)). Expression of genes presented by intensity of colour as $\log_2$ fold change.

5.3.1.3. Identification of CXCL5 and TGF-β2 as potential candidate genes

To screen for potential candidate genes using the RT^2 profiler PCR array, selective antagonist for $P2X_4$ (PSB 12062) was utilized. The effect on cytokines and chemokines expression in GM-MDM following 30 min pre-treatment with 10 μM PSB-12062 in the presence and absence of agonist ATP was assessed. Several criteria were set to filter out potential genes for further study whereby the genes: 1) were induced following agonist stimulation, 2) were unaffected by pre-treatment of antagonist alone in the absence of agonist and, 3) had their mRNA expression levels altered in the presence of both agonist and antagonist. Taking these criteria together allowed the selection of two candidate genes for further study in GM-MDMs: CXCL5 and TGF-β2 (Figure 5.1).

Stimulation of GM-MDM cells with 100 μM ATP positively induced mRNA expression of CXCL5 by 2.44 ± 0.47 fold (N=4 donors, P<0.05; Figure 5.2A). Pre-treatment of antagonist PSB-12062 alone had no significant effect on the mRNA expression of CXCL5 in these cells, but in the presence of the agonist (100 μM ATP), PSB-12062 inhibited ATP-induced CXCL5 mRNA expression by 45.4 ± 1.32 % (N=3 donors; P>0.05; Figure 5.2A). Similarly, pre-treatment of GM-MDM cells with 100 μM ATP positively induced mRNA expression of TGF-β2 by 2.37 ± 0.54 fold (N=4 donors; P>0.05; Figure 5.2B) while PSB-12062 alone had no significant effect on TGFβ2 mRNA expression. However, in the presence of agonist (100 μM ATP), PSB-12062 caused a significant up-regulation of the ATP-induced TGF-β2 mRNA expression by 495.91 ± 375.03 % (N=3 donors; P>0.05; Figure 5.2B). Although the data did not yield a significant result due to large donor-to-donor variability and small sample size, the pattern of the PSB-12062 effect on ATP-induced genes were consistent across the three independent samples. For this reason, these two genes were chosen to be studied in greater detail.
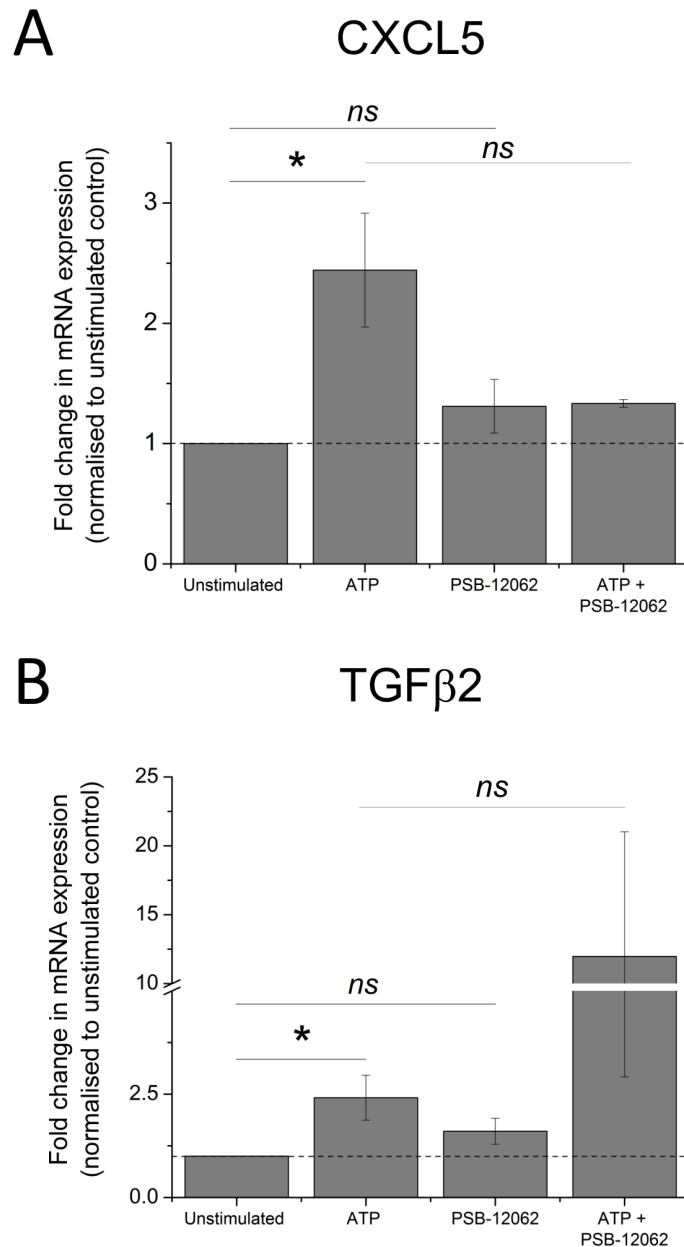
Figure 5.2. **Effect of P2X$_4$ antagonist, 10 μM PSB-12062, on mRNA transcript levels of two candidate genes arising from the RT^2 profiler PCR array: A) CXCL5 (N = 3-5 donors) and B) TGF-β2 (N = 3-5 donors).** Primary GM-MDM cells were treated with 10 μM PSB-12062 for 30 minutes followed by stimulation with 100 μM ATP for 6 h. Fold change in mRNA expression is represented as normalized value to reference genes and vehicle control. Asterisks include significant changes towards control (* p<0.05, Student's t-test).

5.3.1.4. Identifying genes induced by PSB-12062

As a negative control, the effect of PSB-12062 (10 μM) in the absence of an agonist, was included in all experiments. As P2X$_4$ activation requires ATP as an agonist to be present, the purpose of PSB-12062 stimulation alone was to eliminate any effect that may not be a true result of P2X$_4$ inhibition. Supernatants from PSB-12062 treatment alone were collected across various time points and various donors to test for toxicity using LDH assay. LDH quantification illustrated little or no toxicity induced by PSB-12062, up to 10 μM and 48 h, on GM-MDM cells (Table A1; Appendix). However, during this study, several things were not controlled for: 1) GM-MDM cells were cultured in the presence of 10% heat-inactivated autologous serum which may contain low levels of ATP (Gorman et al., 2007) and 2) GM-MDM cells may constitutively secrete ATP during the 6 h stimulation period and levels of ATP in supernatant was not quantified. Therefore, in the PSB-12062 stimulation alone samples, it is not possible to rule out the presence of low levels of ATP which can then activate purinergic receptors.

Out of the 84 different genes screened, pre-treatment with PSB-12062 up-regulated the mRNA expression of 8 genes: CCL5, CXCL1, CXCL2, IL1α, IL1β, CXCL8, OSM and TNF (Figure 5.3A). Only 6 of the genes were significantly up-regulated: CCL5 2.20 ± 0.57 fold (N=4; p<0.05), CXCL2 2.62 ± 0.44 fold (N=4; p<0.05), IL-1α 1.73 ± 0.26 fold (N=4; p<0.05), IL-1β 4.30 ± 0.93 fold (N=4; p<0.05), CXCL8 7.00 ± 2.58 (N=4; p<0.05) and OSM 2.90 ± 0.35 fold (N=4; p<0.05). Using STRING v9.1 software, the protein-protein interaction network was also predicted for these genes to identify if they were closely related (Figure 5.3B). Based on the predicted protein network interaction, these 8 genes work very closely together in biological setting with all of them being produced by activated macrophages in response to inflammation (Beuscher et al., 1990, Owen and Mohamadzadeh, 2013).
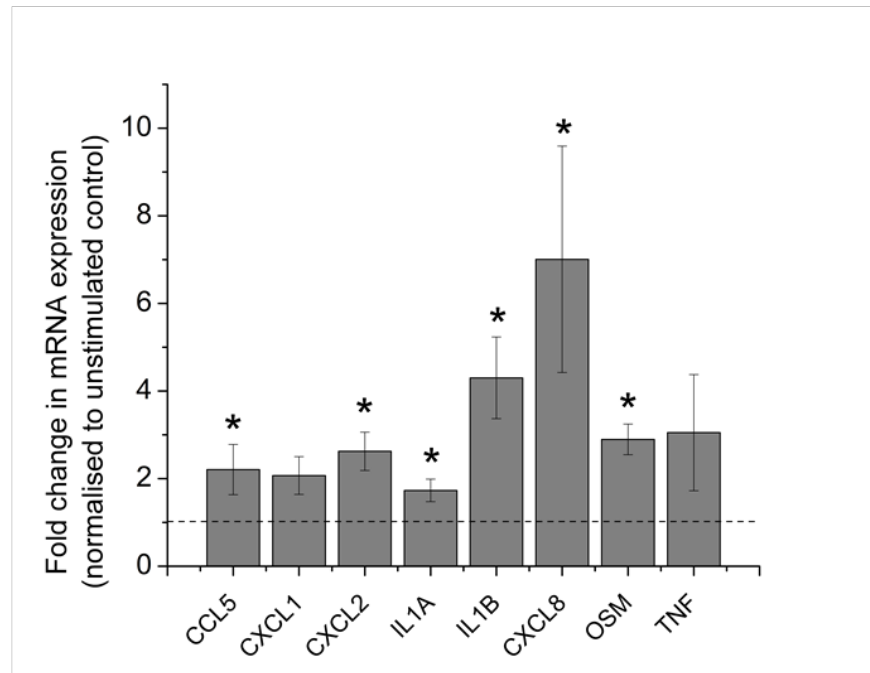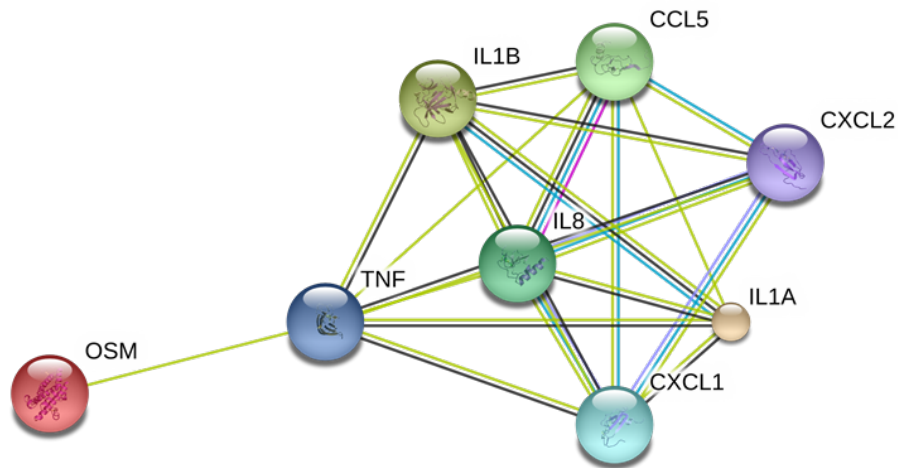
Figure 5.3. Effect of P2X$_4$ antagonist, 10 μM PSB-12062, on mRNA expression of various cytokines and chemokines. A) Fold change in mRNA transcript level was quantified using RT^2 profiler mRNA array following treatment with 10 μM PSB-12062 (N=4 donors). Data is normalized to housekeeping genes and vehicle control. B) Network of protein-protein interactions generated from genes in (A) using the software STRING v9.1. Asterisks include significant changes towards control (* $p<0.05$, Student's t-test).

5.3.2. Role of $P2X_4$ activation in ATP-induced TGF-β2 mRNA expression and protein secretion

TGF-β proteins are distributed throughout the body and play a key role in almost every biological process such as regulating cell function, proliferation, differentiation and modulating the immune system (Taylor, 2009). To date, it is known that almost every cell in a human body can produce TGF-β and respond to it. In mammals, there are three TGF$-\beta$ genes, each encoding for individual isoforms but functioning through the same signalling systems: TGF-β1, TGF-β2 and TGF-β3 (Derynck et al., 1985, Derynck and Rhee, 1987, Massague, 2000). TGF-β signalling is initiated by the binding of the protein to two receptors known as type I and type II and is mediated by a family of effector proteins also known as Smads (Massague and Chen, 2000). Despite its huge importance within the immune system, there has been limited studies performed to explore the possibility that $P2X_4$ may play a role in modulating the production of TGF-β. As TGF-β2 was identified as one of the candidate genes through the profiler PCR screen, this section of the thesis chapter will focus on the contribution of $P2X_4$ activation in modulating level of TGF-β2 in human macrophages.

5.3.2.1. Determining kinetics of ATP-induced TGF-β2 mRNA expression and protein secretion

As the RT^2 Profiler PCR screening was performed only at one-time point (6 h), it was important to identify the kinetics of ATP-induced TGF-β2 mRNA expression and secretion in GM-MDM cells. The effect of 100 μM ATP stimulation on GM-MDM cells were investigated at different time points: 6, 9, 18 and 24 h for mRNA quantification and 24, 32 and 48 h for protein quantification. As shown on Figure 5.4, ATP significantly induced the mRNA expression of TGF-β2 at 6h (2.69 $\pm$ 0.16 fold, N=4, P<0.05) and 18h (1.66 $\pm$ 0.19, N=4, P<0.05) but not at 9h (2.40 $\pm$ 0.79 fold, N=4, P>0.05) and 24h (1.07 $\pm$ 0.26, N=4, P>0.05). The amount of TGF-β2 protein secreted was also quantified using ELISA technique at various time points. Surprisingly, no TGF-β2 protein was detected at any of the time points studied. This was repeated on three independent donor samples with FBS being used as a positive control to ensure that the assay is working. Since no protein was detected, the effect of $P2X_4$ on ATP-induced TGF-β2 level was only studied at the transcriptional level.
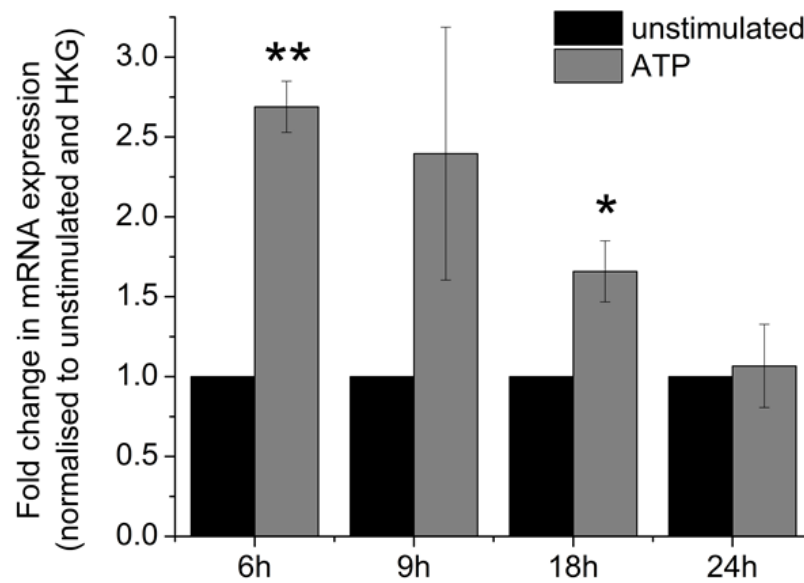
Figure 5.4. **Time course study to investigate the kinetics of 100 μM ATP-induced TGF-β2 mRNA expression.** Kinetics of ATP-induced TGF-β2 mRNA expression was assessed across 4 time points (6, 9, 18 and 24h) across 4 independent donors. Asterisks include significant changes towards control (** $p<0.01$, * $p<0.05$, Student's t-test).

5.3.2.2. Effect of blocking P2X$_4$ on ATP-induced TGF-β2 mRNA expression

To study the importance of P2X$_4$ activation on ATP-induced TGF-β2 mRNA expression, the effect of PSB-12062 was studied at various time points across 4 independent donors. Figure 5.5A-D illustrated $\Delta\Delta$CT analysis from individual donors while Figure 5.5E illustrated an average data represented as ratio of fold change ($\Delta\Delta$Ct ATP+PSB normalised to $\Delta\Delta$Ct ATP) across the 4 independent donors. The average data is represented as a ratio of fold change due to the large donor-to-donor variation readout. As can be seen from Figure 5.5, pre-treatment of GM-MDM cells resulted in a significant up regulation of ATP-induced mRNA expression of TGF-β2 at all time points. In three out of the four donors (Figure 5.5A, 5.5B and 5.5D), the maximal effect of PSB-12062 on ATP-induced TGF-β2 mRNA expression was observed following 9 h stimulation with ATP while at higher time points (24 h), the effect was significantly reduced. Across 4 independent donors (Figure 5.5E), a significant up regulation in mRNA expression of TGF-β2 was observed at 6h (2.69 ± 0.16 fold without PSB-12062 versus 9.45 ± 1.83 fold with PSB-12062, N=4 donors, P<0.05), 9h (2.40 ± 0.79 fold without PSB-12062 versus 12.84 ± 5.88 fold with PSB-12062, N=4 donors, P<0.01) and 18h (1.66 ± 0.19 fold without PSB-12062 versus *5.91* ± 0.60 fold with PSB-12062, N=4 donors, P<0.05). No significant effect was observed at 24h (1.07 ± 0.26 fold without PSB-12062 versus 6.48 ± 2.38 fold with PSB-12062, N=4 donors, P>0.05). These observations illustrated a possible role of P2X$_4$ activation in negatively regulating TGF-β2 mRNA expression.
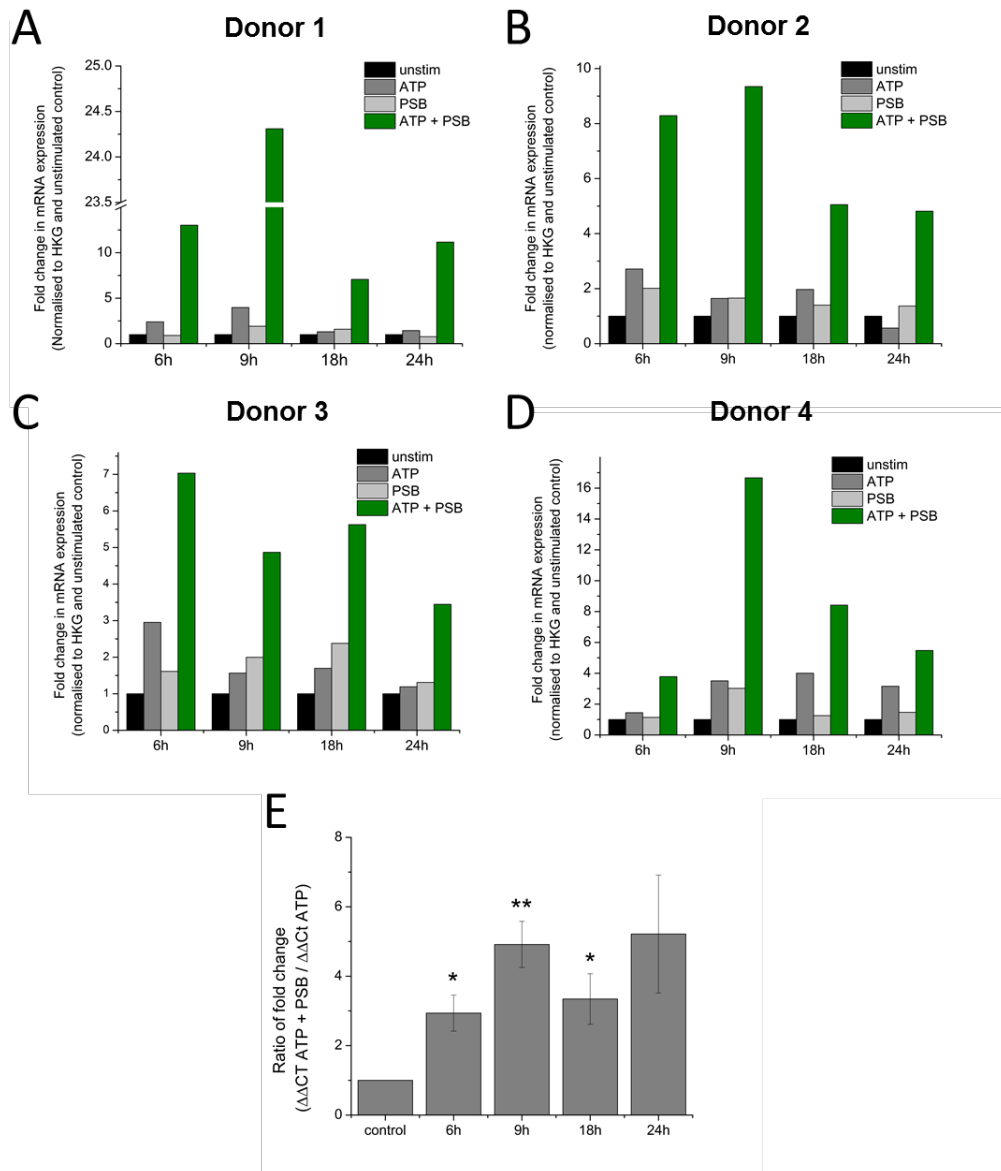
Figure 5.5. **Time course study to investigate the effect P2X$_4$ antagonist, 10 μM PSB-12062, on 100 μM ATP-induced TGF-β2 mRNA expression.** A-D) Time course study was performed at four different time points: 6 h, 9 h, 18 h and 24 h in human primary GM-MDM cells obtained from four independent donors. Fold change in mRNA expression is represented as normalized value to reference genes and vehicle control. E) Average data to represent the effect of P2X$_4$ antagonist, 10 μM PSB-12062 on various time points of ATP-induced CXCL5 mRNA expression, across 4 donors represented as ratio of fold change. Asterisks include significant changes towards control (** $p < 0.01$, * $p < 0.05$, Student's t-test).

5.3.3. Role of P2X$_4$ in ATP-induced CXCL5 mRNA expression and protein secretion

CXCL5 is a pro-inflammatory chemokine playing a key role in regulating CXCR2-dependent neutrophil trafficking. Although it has been reported that CXCL5 can be produced by various cells such as platelets, lung epithelial cells following severe infection and macrophage fraction of adipose tissue, it has not been reported if human monocyte-derived macrophages can secrete CXCL5 upon exposure to a DAMP signal such as ATP and if purinergic receptors may play a role in this. Like TGF-β2, CXCL5 was identified as one of the candidate genes for further study and this section of the chapter will focus on studying the importance of P2X$_4$ and other purinergic receptors in the level of expression and secretion of ATP-induced CXCL5 in human macrophages.

5.3.3.1. Determining kinetics of ATP-induced CXCL5 mRNA expression and protein secretion

Following the PCR screening, kinetics of ATP-induced CXCL5 mRNA and protein secretion was studied across various time points. For quantification of mRNA expression, 4 time points (6 h, 9 h, 18 h and 24 h) were assessed while for protein secretion quantification, 3 later time points (24 h, 32 h and 48 h) were assessed. Stimulation with ATP caused a time-dependent increase in mRNA expression of CXCL5 with maximal induction observed at 24 h (6 h: 6.57 ± 2.78 fold, N=4 donors, $P>0.05$; 9 h: 9.66 ± 2.16 fold, N=4 donors, $P<0.05$; 18 h: 18.75 ± 2.78 fold, N=4 donors, $P<0.01$, and 24 h: 23.52 ± 5.00 fold, N=4 donors, $P<0.05$; Figure 5.6A). Similarly, stimulation of GM-MDM cells with ATP also resulted in a time-dependent increase in CXCL5 protein secretion with maximal secretion being observed at 48 h time point (24 h: 388.9 ± 125.4 pg/ml, N=9 donors; 32 h: 618.6 ± 139.0 pg/ml, N=7 donors; 48 h: 686.9 ± 148.3 pg/ml; N=7 donors; Figure 5.6B).
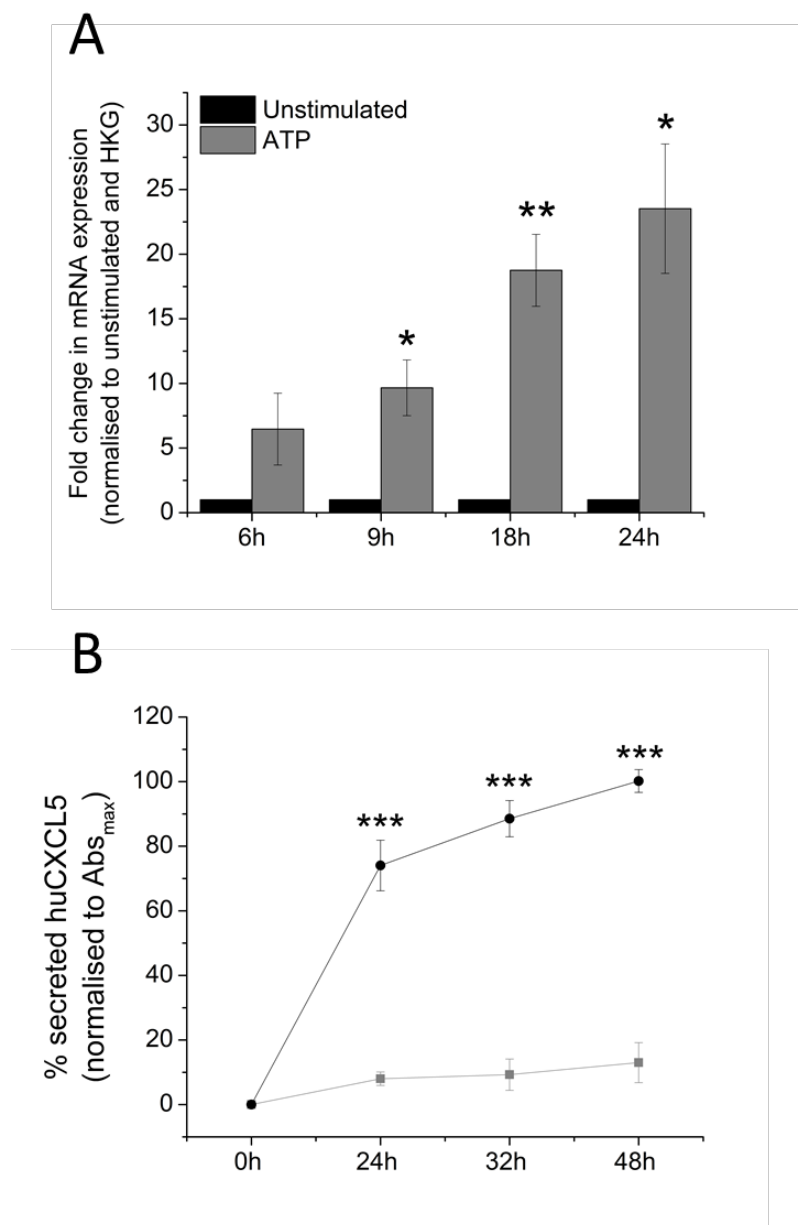
Figure 5.6. **Time course study to investigate the kinetics of 100 μM ATP-induced CXCL5 level.** A) 100 μM ATP-induced CXCL5 mRNA expression assessed across 4 time points (6 h, 9 h, 18 h and 24 h) across 4 independent donors. Data is represented as fold change of $\Delta\Delta$CT normalised to HKG and unstimulated control. B) 100 μM ATP-induced CXCL5 protein secretion across 4 time points (24 h, 32 h and 48 h) across 7-9 independent donors. Data is represented as % secreted CXCL5 due to high variability between donors. Asterisks include significant changes towards control (*** $p<0.001$, ** $p<0.01$, * $p<0.05$, Student's t-test).

5.3.3.2. Effect of blocking P2X$_4$ on ATP-induced CXCL5 mRNA expression

To study the importance of P2X$_4$ activation on ATP-induced CXCL5 mRNA expression, the effect of PSB-12062 was tested across the different time points. Pre-treatment of GM-MDM cells with 10 μM PSB-12062 inhibited ATP-induced CXCL5 mRNA expression at lower time points (6 h and 9 h) across 4 independent donors (Figure 5.7A-D). However, at higher time points (18 h and 24 h), PSB-12062 pre-treatment resulted in an increase of ATP-induced CXCL5 mRNA expression in 3 out of the 4 donors (Figure 5.7A, B and D). The effect of PSB-12062 on ATP-induced CXCL5 mRNA expression was quantified as average across the 4 donors and the data is represented as ratio of fold change between ATP + PSB-12062 treatment versus ATP alone due to high donor-to-donor variability (Figure 5.7E). On average, pre-treatment of GM-MDM cells with PSB-12062 resulted in a significant inhibition of ATP-induced CXCL5 mRNA expression at 6 h (40.36 ± 4.86 %, N=4 donors, P<0.01) and 9 h (34.77 ± 8.05 %, N=4 donors, P<0.05; Figure 5.7E) but not at 18 h and 24 h. This data illustrated that activation of P2X$_4$ may play a modulatory role towards ATP-induced CXCL5 mRNA expression.
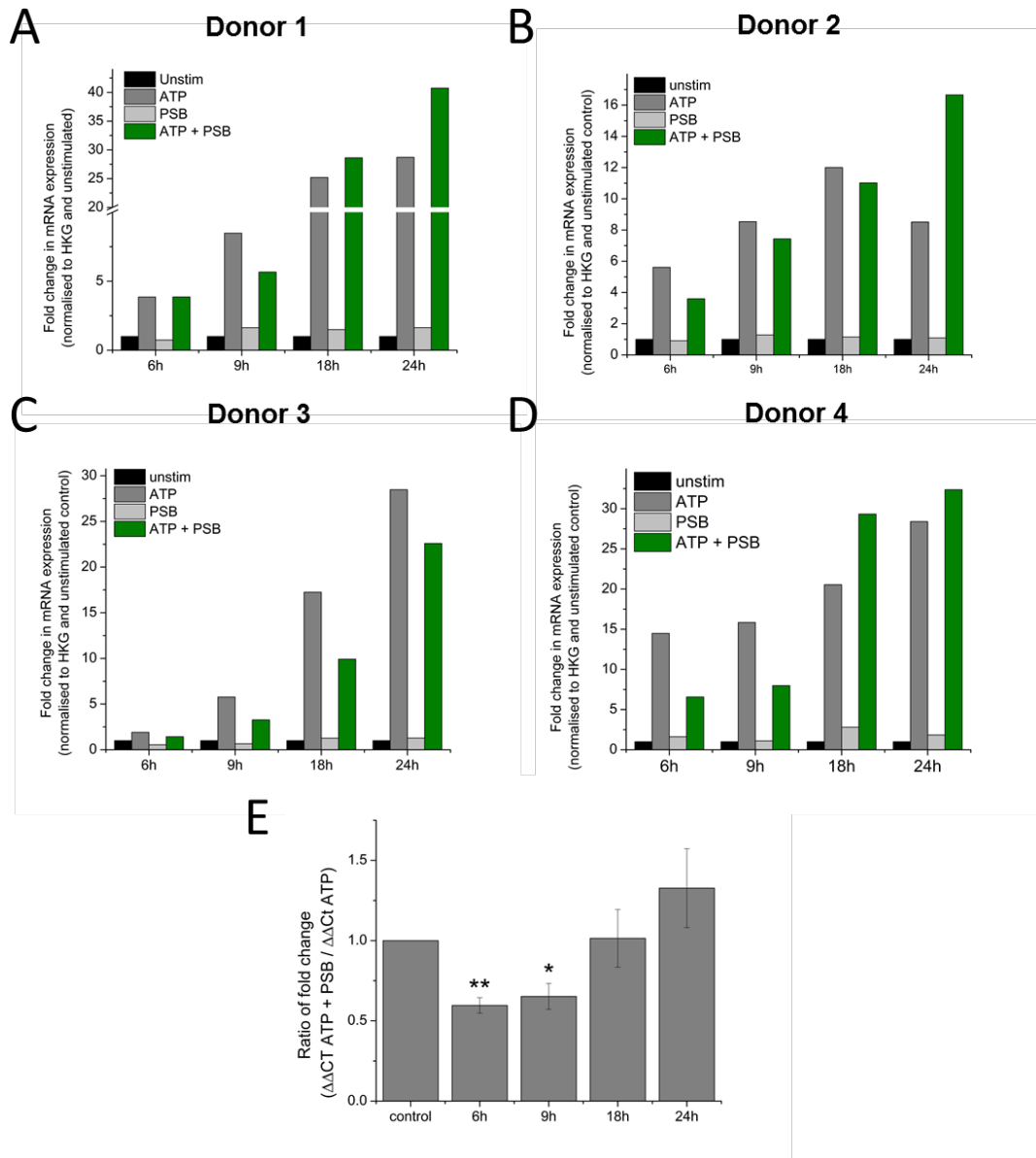
Figure 5.7. **Time course study to investigate the effect P2X$_4$ antagonist, 10 μM PSB-12062, on 100 μM ATP-induced CXCL5 mRNA expression.** A-D) Time course study was performed at four different time points: 6 h, 9 h, 18 h and 24 h in human primary GM-MDM cells obtained from four independent donors. Fold change in mRNA expression is represented as normalized value to HKG and vehicle control. E) Average data across 4 donors represented as ratio of fold change. Asterisks include significant changes towards control (** $p<0.01$, * $p<0.05$, Student's t-test).

5.3.3.3. Role of P2X$_4$ activation on ATP-induced CXCL5 protein secretion

To confirm if the effect of blocking P2X$_4$ on ATP-induced CXCL5 mRNA expression can be mirrored at the protein level, ELISA technique was utilized to measure the amount of secreted CXCL5 protein in the supernatants collected at various time points. In the absence of agonist, pre-treatment of GM-MDM cells with PSB-12062 alone had no significant effect towards the level of secreted CXCL5 when compared to unstimulated control (Figure 5.8B). However, in the presence of agonist (100 μM ATP), pre-treatment of GM-MDM cells with PSB-12062 resulted in significant inhibition of ATP-induced CXCL5 secretion at 32 h (22.91 ± 8.47 %, N=6 donors, P<0.05; Figure 5.8A and B) and 48 h (30.7 ± 6.3 %, N=9 donors, P<0.05; Figure 5.8A and B) but not at 24 h. The effect of varying concentrations of PSB-12062 (1, 5 and 10 μM) was also tested on 100 μM ATP-mediated CXCL5 secretion at one single time point of 48 h. Across three independent donors, PSB-12062 caused a significant reduction in ATP-mediated CXCL5 secretion in a dose dependent manner (1 μM PSB-12062: 12.0 ± 4.6 %, N=3 donors, P<0.05; 5 μM PSB-12062: 27.4 ±7.2 %, N=3 donors, P<0.05; and 10 μM PSB-12062: 30.7 ± 6.3 %, N=9 donors, P<0.001, Figure 5.9C).

To further confirm the possible involvement of P2X$_4$ towards the level of ATP-induced CXCL5 secretion in human macrophages, the effect of selective P2X$_4$ positive allosteric modulator IVM was also studied at 48 h. In the absence of the agonist, IVM pre-treatment had no significant effect on CXCL5 secretion level when compared to unstimulated control. In the presence of agonist (100 μM ATP), pre-treatment of GM-MDM cells with 3 μM IVM significantly augmented ATP-induced CXCL5 secretion (26.48 ± 10.70 % increase, N=6 donors, P<0.05; Figure 5.9D). Across the six donors investigated, all but one resulted in an increase in ATP-induced CXCL5 secretion following IVM stimulation (Figure A5). Together, the effect of PSB-12062 and IVM suggests a possible role of P2X$_4$R activation in the modulation of ATP-induced CXCL5 mRNA expression and secretion.
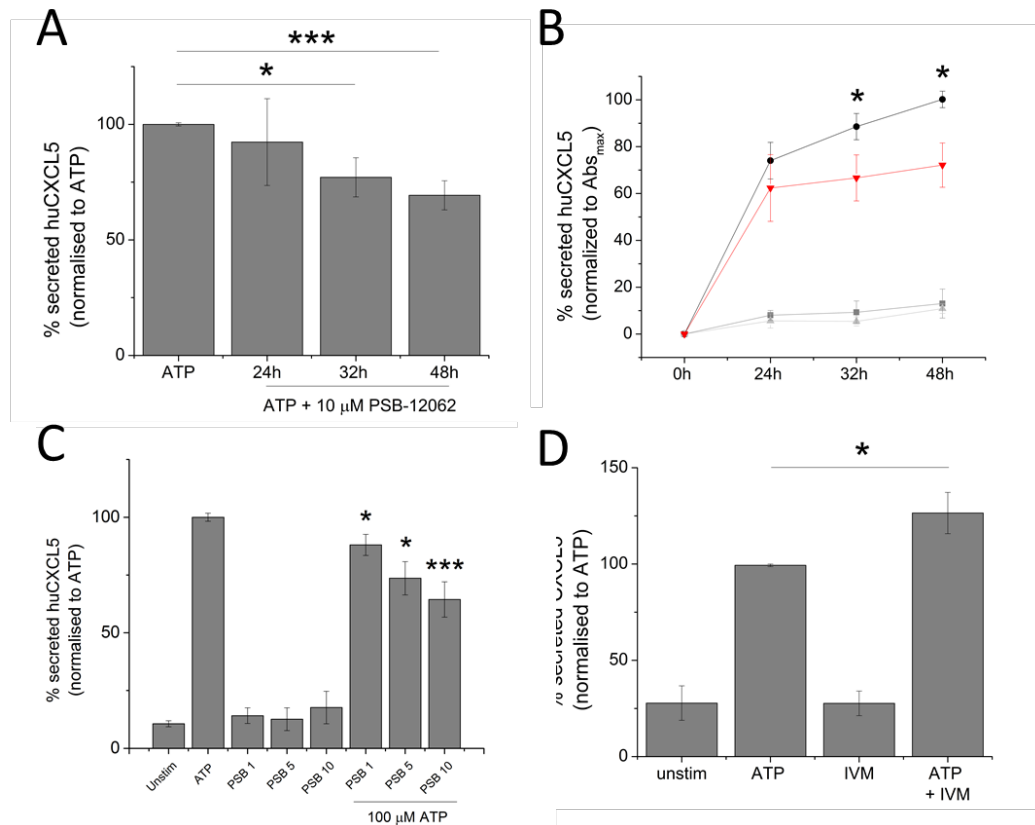
Figure 5.8. Role of P2X$_4$ activation on 100 μM ATP-induced CXCL5 secretion.
The importance of P2X$_4$ activation on ATP-induced CXCL5 secretion in GM-MDM
cells was studied using two pharmacological tools: A and B) selective antagonist 10
μM PSB-12062 at 24 h (N=6 donors), 32 h (N=6 donors) and 48 h (N=9 donors), C)
dose response of PSB-12062 (1 μM, 5 μM and 10 μM) at 48 h (N=3-9 donors), and
D) positive allosteric modulator 3 μM IVM at 48 h (N=6 donors). In Figure B, light
grey: unstimulated control, dark grey: PSB-12062 control, black: 100 μM ATP and
red: 100 μM ATP + 10 μM PSB-12062. Asterisks include significant changes
towards control (*** $p < 0.001$, * $p < 0.05$, Student's t-test).

5.3.3.4. Effect of blocking P2X$_4$ on ATP-induced CXCL5 protein synthesis

Having established that P2X$_4$ activation play a modulatory role towards ATP-induced CXCL5 mRNA expression and secretion, it was important to identify if P2X$_4$ can potentially have an affect towards CXCL5 synthesis. This was studied across 3 different time points (24 h, 32 h and 48 h) and the amount of synthesized CXCL5 within the protein lysates were quantified by ELISA technique. As shown on Figure 5.9, the amount of synthesized CXCL5 upon stimulation with ATP is maximal at 24 h (495.98 ± 94.03 pg/ml, N=3 donors, P<0.05; Figure 5.9A) followed by a time-dependent reduction, which seemed to plateau at 48 h (215.03 ± 18.97 pg/ml, N=5 donors; P<0.01; Figure 5.9A). This observation could potentially be explained by the fact that at 48 h, the majority of the synthesized CXCL5 have been secreted (Figure 5.6). Blocking of P2X$_4$ activation had no significant effect on the level of ATP-induced CXCL5 synthesis at 24 h and 32 h (Figure 5.9B and C, respectively) but caused a significant reduction at 48 h time point (41.78 ± 13.04 %, N=5 donors, P<0.05; Figure 5.9D).
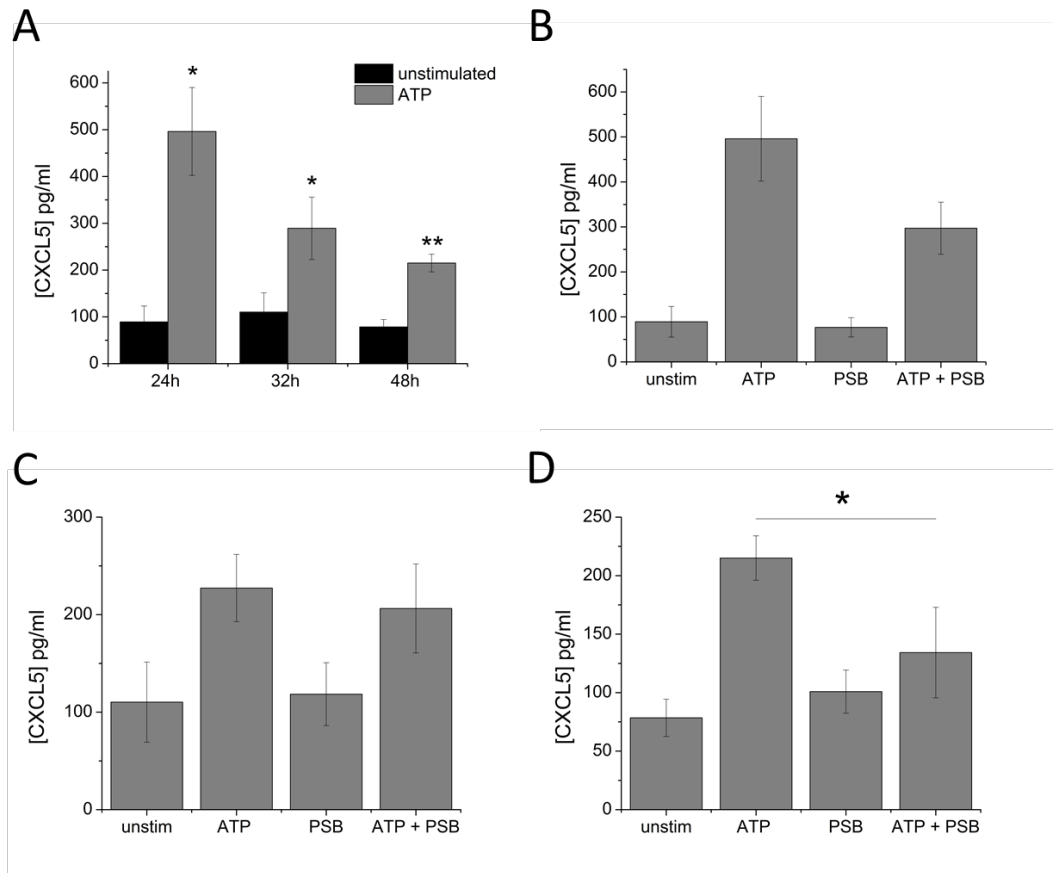
Figure 5.9. Effect of blocking P2X$_4$ activation on 100 μM ATP-induced CXCL5 synthesis in human macrophages. A) Time course study of 100 μM ATP-induced CXCL5 synthesis, measured across 3 time points (24 h, 32 h and 48 h). B-D) Effect of 10 μM PSB-12062 on 100 μM ATP-induced CXCL5 synthesis was studied across 3 different time points: B) 24 h (N=3 donors), C) 32 h (N=3 donors) and D) 48 h (N=5 donors). Asterisks include significant changes towards control (** $p<0.01$, * $p<0.05$, Student's t-test).

5.3.3.5. Involvement of other purinergic receptors in ATP-induced CXCL5 protein secretion

The contribution of $P2X_4$ receptor activation towards ATP-induced level of CXCL5 was studied in previous sections of this chapter. The role of several other purinergic receptors ($P2X_7$, $P2Y_{11}$ and $P2Y_{13}$) were also investigated. The effect of $P2X_7$ receptor activation was studied because it is highly expressed in immune cells and has been reported to be closely associated with $P2X_4$ (Guo et al., 2007), while the effect of $P2Y_{11}$ and $P2Y_{13}$ was studied as these receptors has been shown to contribute to the magnitude of ATP-evoked Ca^{2+} response in GM-MDM cells (discussed in chapter 4). The effect of selective antagonists A438079 ($P2X_7$), NF340 ($P2Y_{11}$) and MRS2211 ($P2Y_{13}$) on ATP-induced CXCL5 secretion were tested on GM-MDM cells only at one time point: 48 h. Pre-treatment of GM-MDM cells with each of the antagonists alone, in the absence of agonist, had no significant effect on the amount of endogenously secreted CXCL5. However, surprisingly, pre-treatment of GM-MDM cells with A438079 (Figure 5.10A and Figure A2; Appendix), NF340 (Figure 5.10B and Figure A3; Appendix) and MRS2211 (Figure 5.10C and Figure A4; Appendix) also had no significant effect on the ATP-induced CXCL5 secretion at 48 h, as quantified by ELISA.
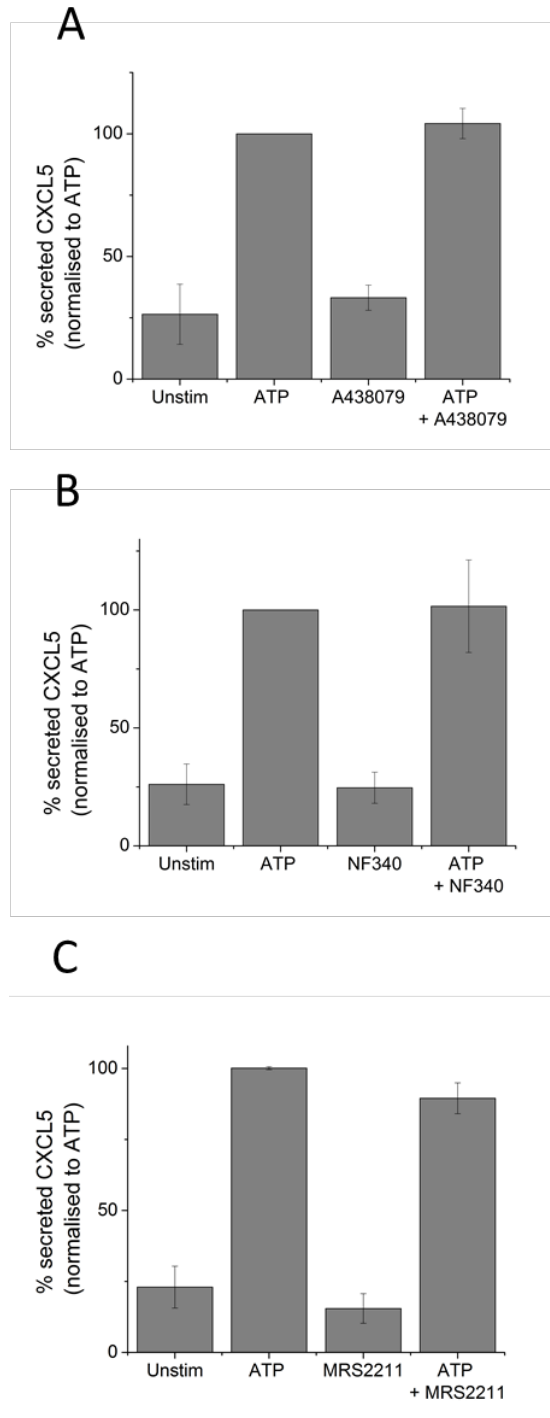
Figure 5.10. **Role of other purinergic receptors on 100 μM ATP-induced CXCL5 secretion at 48h.** The effect of selective antagonists for: A) P2X$_7$ antagonist A438079 (5 μM; N=3 donors), B) P2Y$_{11}$ antagonist NF340 (10 μM; N=3 donors) and C) P2Y$_{13}$ antagonist MRS2211 (10 μM; N=5 donors), on 100 μM ATP-induced CXCL5 secretion in GM-MDM cells.

5.4. Summary

In this chapter, the role of $P2X_4$ and other purinergic receptors on ATP-induced cytokine and chemokine level was assessed. Stimulation of GM-MDM cells using ATP positively induced the mRNA expression of various genes that include CXCL2, CXCL5, IL12β, OSM, PPBP and TGF-β2. Using RT^2 profiler PCR array to screen for 84 different genes involved in the immune system, two candidate genes (TGF-β2 and CXCL5) was selected for further study.

The activation of $P2X_4$ using 100 μM ATP caused a significant induction in the mRNA expression of TGF-β2 that peaked at 6 h. Blocking $P2X_4$ activation using PSB-12062 resulted in a significant up-regulation of ATP-induced TGF-β2 mRNA expression at 6 h, 9 h and 18 h, illustrating a potential role of $P2X_4$ in regulating the level of TGF-β2. This data corroborated a study by Kim et al. (2014) illustrating that lack of $P2X_4$ receptor expression resulted in an increased in renal fibrosis and increased expression of TGF-β level in rodent model. Despite the significant effect seen at transcriptional level, the effect of PSB-12062 on mRNA expression did not translate to protein level as no TGF-β2 protein was detected in the supernatants. The data illustrated here indicated that despite having significant effect at the transcriptional level, the lack of evidence at the protein level makes interpretation very difficult.

The second candidate gene studied in this chapter was CXCL5. Although CXCL5 has been shown to be produced by various cells such as platelets and macrophage fraction of white adipose tissue (Chavey and Fajas, 2009), no study has reported the ability of human monocyte-derived macrophages to synthesize and secrete CXCL5 in response to a DAMP signal. The activation of $P2X_4$ using ATP caused a significant induction in the mRNA expression of CXCL5 and protein secretion in a time-dependent manner that peaked at 24 h and 48 h, respectively. Pre-treatment of cells with PSB-12062 resulted in a significant inhibition of ATP-induced mRNA expression of CXCL5 at 6 h and 9 h. This was also translated at the protein level whereby 10 μM PSB-12062 treatment caused a significant inhibition of ATP-induced CXCL5 protein secretion at 32 h and 48 h. Further study also revealed that at 48 h time point, PSB-12062 was able to cause a dose-dependent inhibition of

ATP-induced CXCL5 protein secretion while IVM was able to augment ATP-induced CXCL5 secretion. Further to this, blocking $P2X_4$ activation also resulted in a reduction in ATP-induced CXCL5 synthesis at 48 h time point. Taken together, these observations illustrated that $P2X_4$ activation modulates the expression, secretion and synthesis of ATP-induced CXCL5 chemokine. Finally, one interesting observation that was made in this study was that the activation of $P2X_7$, $P2Y_{11}$ and $P2Y_{13}$ is not required for the secretion of ATP-induced CXCL5 chemokine at 48 h time point. As $P2Y_{11}$ and $P2Y_{13}$ activation plays a major role towards the peak magnitude of ATP-evoked Ca^{2+} response (described in Chapter 4), the findings in this chapter suggested that ATP-induced CXCL5 secretion is a process that may be independent of intracellular Ca^{2+} level.

Chapter 6: Discussion

6.1 Overview

Within the last decade, there has been a growing interest in identifying the role of the $P2X_4$ receptor within the immune system. It is without a doubt that, compared to other subtypes of P2 receptors, research surrounding $P2X_4$ has been significantly hampered due to the lack of commercially available selective antagonists and agonists. Targeting of other purinergic receptors such as $P2X_3$, $P2Y_2$ and $P2Y_{12}$, have allowed the discovery and clinical use of several drugs for the treatment of conditions like chronic cough, dry eye disease and acute coronary syndrome, respectively (Jacobson et al., 2012, Lau et al., 2014). Elucidating the functional role of $P2X_4$ in immune cells, such as macrophages, could therefore potentially allow the identification of new drug targets for the treatment of inflammatory conditions.

Despite its recurring expression, the role of $P2X_4$ in human macrophages is not well defined. Research in mouse macrophages, however, has revealed a regulatory role of $P2X_4$ in facilitating $P2X_7$ function. Examples of this include the involvement of $P2X_4$ in the release of inflammatory mediators such as prostaglandin E_2 (PGE_2) (Ulmann et al., 2010), and $P2X_7$-mediated autophagy (Kawano et al., 2012b). More recently, studies using a mouse macrophage cell line showed that $P2X_4$ is responsible for regulating $P2X_7$-mediated inflammation by facilitating the release of IL-1β (Kawano et al., 2012a). The interaction between $P2X_4$ and $P2X_7$ has also been shown to be important in determining macrophage phenotypic function and their ability to clear apoptotic cells following tissue injury (Gu et al., 2013). Despite these efforts, the functional roles for $P2X_4$ in human macrophages remain elusive and this emphasizes the urgent need for research within this field. Pharmacological characterization and a functional role of $P2X_4$ in human macrophages was investigated in this thesis using a combination of THP-1 differentiated macrophages (TDM) cell model and primary monocyte-derived macrophages (MDM).

Several areas studied in this thesis include:
A) The contribution of $P2X_4$ towards ATP-evoked Ca^{2+} response in THP-1 monocytes versus TDM cells (discussed in Chapter 3).

B) The contribution of P2X and P2Y receptors, with focus of $P2X_4$, towards ATP-evoked Ca^{2+} response in primary MDM cells (discussed in Chapter 4).

C) The role of $P2X_4$ activation in cytokine/chemokine mRNA expression and secretion in human primary MDM cells (discussed in Chapter 5).

6.2   Key Findings

6.2.1   THP-1 and TDM cell line model

The first part of the discussion assessed findings generated from chapter 3 which focused on verifying pharmacological tools to characterize $P2X_4$ contribution towards ATP-evoked intracellular Ca^{2+} response in THP-1 monocytes and TDM cell line model.

THP-1 and TDM cell model express a diverse repertoire of P2XRs

THP-1 and TDM cells are well established cell line models used for *in vitro* study of human monocytes and macrophages, respectively (Bosshart and Heinzelmann, 2016, Daigneault et al., 2010, Genin et al., 2015, Qin, 2012). Prior to studying intracellular Ca^{2+} responses in these cells, the expression profile of P2X receptors in THP-1 and TDM cells at the mRNA and protein level was investigated. qRT-PCR analysis detected mRNA expression of $P2X_1$, $P2X_4$, $P2X_5$, $P2X_6$ and $P2X_7$ in both cell types. mRNA expression of $P2X_2$ was detected only in THP-1 cells while $P2X_3$ was absent in both cell types. Further analysis using non-quantitative RT-PCR illustrated that both THP-1 and TDM cells express the non-functional, exon 10-less $P2X_5$, which are the predominant receptor isoform expressed in human subjects (Kotnis et al., 2010). In addition to this, qRT-PCR data illustrated that $P2X_1$ and $P2X_2$ are both down-regulated while $P2X_4$ is up regulated in TDM cells when compared to THP-1 cells. No significant differences in mRNA expression were observed for $P2X_5$, $P2X_6$ and $P2X_7$ in TDM cells compared to THP-1 cells. Further to this, immunocytochemistry was performed to detect protein expression in these cells. Using confocal imaging, protein expression of $P2X_1$, $P2X_4$, $P2X_5$ and $P2X_7$ were all detected and appeared to have a punctate distribution in both cells. $P2X_2$, $P2X_3$ and $P2X_6$ were not investigated due to the lack of available selective antibody. Although these cell lines are routinely used for the study of primary monocytes and macrophages, respectively, there are differences that may need to be considered. In this study, there was no significant difference in the mRNA expression of $P2X_7$ in THP-1 cells vs. TDM cells. However, primary monocytes have shown up-regulation of $P2X_7$ receptor mRNA upon differentiation to macrophages (Ferrari et al., 1999).

The detection of mRNA expression of $P2X_1$, $P2X_4$ and $P2X_7$ in these cell lines fits with previous reports described within the literature (Into et al., 2002, Kaufmann et al., 2005, Li and Fountain, 2012, Wang et al., 2004). However, the differential relative mRNA expression of $P2X_1$, $P2X_2$ and $P2X_4$ in the two cell types provide a novel finding. Similarly, there has been no prior literature reporting the expression of non-functional $P2X_5$ in both THP-1 and TDM cells. Although $P2X_6$ is detected in both cell types, it is unlikely to form a functional homotrimer (Barrera et al., 2005). Finally, the lack of $P2X_3$ in these cells may be explained by the fact that they are predominantly distributed in sensory neurons and smooth muscles (Burnstock and Knight, 2004).

ATP evoked an intracellular Ca^{2+} response in THP-1 and TDM cells

Intracellular Ca^{2+} signaling is considered the most prominent signaling pathway responsible for various cellular processes like proliferation, apoptosis, differentiation and motility (Berridge, 1997, Glaser et al., 2013). The mobilization of Ca^{2+} in cells can be achieved through the activation of P2X and P2Y receptors by nucleotides such as ATP (Puchalowicz et al., 2014). Although the involvement of $P2X_4$ in ATP-evoked intracellular Ca^{2+} responses in various cell types have been reported previously (Glaser et al., 2013, Li and Fountain, 2012, Pubill et al., 2001, Light et al., 2006), their contribution in THP-1 and TDM cells have not been well explored. To fill this gap, ATP dose response on THP-1 and TDM cells was initially performed in the presence of extracellular Ca^{2+} to identify a suitable concentration to maximally activate $P2X_4$ in these cells. ATP elicited a concentration-dependent increase in intracellular Ca^{2+} level in both THP-1 and TDM cells that included a rapid peak response followed by a gradual return to steady-state elevated phase in THP-1 cells and back to the baseline in TDM cells. This intracellular Ca^{2+} profile is supportive of previous studies reported in other cell types (Hashioka et al., 2014, Nobile et al., 2003, Yamamoto et al., 2000). In both THP-1 and TDM cells, 100 μM ATP caused maximum intracellular Ca^{2+} response and was chosen as the concentration used for the rest of the study. The strategy to use 100 μM ATP concentration was also supported by the fact that this concentration will maximally activate $P2X_4$ (Li and Fountain, 2012) while not sufficient to activate $P2X_7$ (Liang et al., 2015) (Chapter 3 results). As $P2X_4$ and $P2X_7$ have been demonstrated in the literature to interact closely together, it was important to avoid an agonist concentration that activates $P2X_7$ to allow characterization of $P2X_4$ (Gu et al., 2013, Kawano et al., 2012b).

The side-by-side comparison of ATP-evoked intracellular Ca^{2+} responses showed a clear difference in Ca^{2+} profiles of the two cell types. The main differences include TDM cells having a smaller magnitude of ATP-evoked Ca^{2+} response as well as a significantly faster decay response. These are novel observations, which have not been described in literature previously. Although not investigated further in this study, several factors may underlie these differences. The first possible explanation is a differential expression of P2Y receptors in the two cell types, which can be investigated by qRT-PCR and immunocytochemistry studies. A comparison of the mRNA and protein level of P2YR has never been performed in THP-1 and TDM cells and would be an interesting study to undertake to clarify this matter. Secondly, TDM cells may have a higher expression of CD39 for a more efficient breakdown of ATP. Although CD39 is well accepted as the major NTPDase expressed by monocyte/macrophage system in their cell surface (Cohen et al., 2013, Dwyer et al., 2007, Pulte et al., 2007), there has been no studies illustrating any differential expression in the two cell systems. Therefore, to clarify this matter, it may be necessary to perform a qRT-PCR analysis to see any differences in mRNA expression of CD39 in the two cell types. Further study to test the effect of selective inhibitors of CD39 (i.e. POM-1) (Bastid et al., 2015) to functionally assess this theory may also be necessary. Finally, it may be possible that TDM cells possess a better Ca^{2+} buffering capacity than THP-1 cells. Previous studies revealed that antibody/FcR generated phagocytosis in macrophages relies on an increase in cytosolic Ca^{2+} concentration (Diler et al., 2014, Lew et al., 1985). Since the process of phagocytosis relies on Ca^{2+} concentration in cells, it may be that professional phagocytes like macrophages are equipped to adapt to the changes in Ca^{2+} level better than cells that do not phagocytose (i.e. monocytes).

$P2X_4$ receptor activation, but not $P2X_1$ or $P2X_7$, contributes to U-73122- and Tg-resistant Ca^{2+} response in TDM cells

ATP is a DAMP signal that can elicit a cellular response by activating both P2X and P2Y receptors in cells (Campwala and Fountain, 2013, Tanaka et al., 2014). As the main interest of this thesis is to study the contribution of $P2X_4$ towards ATP-evoked Ca^{2+} response, pharmacological tools to block metabotropic P2Y receptor activity such as phospholipase C (PLC) inhibitor, U-73122, and SERCA pump inhibitor, Tg, were employed for intracellular Ca^{2+} measurements in THP-1 and TDM cells (Da Silva et al., 2008; Liu et al., 2000; Vial et al., 2004). An interesting revelation from

the intracellular Ca^{2+} measurements was that in THP-1 cells, a very small U-73122-resistant Ca^{2+} response remained, while Tg completely abolished ATP-evoked intracellular Ca^{2+} responses. Meanwhile, in TDM cells, both U-73122- and Tg-resistant Ca^{2+} response appeared more prominent and these responses were attenuated in the absence of extracellular Ca^{2+}, suggesting that it is dependent on Ca^{2+} influx. For this reason, the contribution of $P2X_4$ towards ATP-evoked Ca^{2+} response was investigated only in TDM cells.

In TDM cells, treatment with $P2X_4$ positive allosteric modulator, IVM, caused a significant potentiation towards the magnitude of both the U-73122- and Tg-resistant Ca^{2+} response as well as a delay in the decay kinetics. These observations are consistent with studies by Norenberg et al. (2012) illustrating the effect of IVM on $P2X_4$-mediated current. In addition to this, $P2X_4$ antagonists, 5-BDBD and PSB-12062, significantly inhibited the U-73122- and Tg-resistant Ca^{2+} response in TDM cells while $P2X_1$ antagonist, Ro0437626, and $P2X_7$ antagonist, A438079, did not appear to have any contribution towards the Ca^{2+} response. The contribution of $P2X_4$ towards the ATP-evoked Ca^{2+} response in TDM cells were further confirmed through shRNA approach whereby $P2X_4$ knockdown resulted in significant reduction of Tg-resistant Ca^{2+} response in TDM cells as well as reduced sensitivity towards IVM and PSB-12062. These results confirmed that $P2X_4$ contributes partially to the Tg-resistant Ca^{2+} response in TDM cells and clarify that IVM and PSB-12062 are useful pharmacological tools for the study of $P2X_4$. These novel findings are valuable as no studies in the past have reported the contribution of $P2X_4$ towards ATP-evoked Ca^{2+} response in TDM cells, although work in THP-1 cells has been done (Li and Fountain, 2012). Additionally, as PSB-12062 is considered a new antagonist that has not been validated in many studies, these findings demonstrated additional evidence of its reliable use in future studies concerning $P2X_4$. The reliable use of PSB-12062 can be reflected from three observations in this study so far: 1) the use of $hP2X_4$ over-expressing cell line allowed the identification that PSB-12062 is more potent in blocking ATP-evoked Ca^{2+} response than 5-BDBD, 2) PSB-12062 blocked IVM-sensitive ATP-evoked Ca^{2+} response, and 3) $P2X_4$ shRNA TDM cells illustrated reduced sensitivity towards PSB-12062 and IVM.

Dependency of ATP-evoked Tg-resistant Ca^{2+} response on known modulators of P2X$_4$ trafficking

P2X$_4$ in microglial and peripheral macrophages have been reported to be predominantly localized within lysosomal compartments, undergoing rapid constitutive recycling from the plasma membrane to intracellular compartments (Bobanovic et al., 2002, Qureshi et al., 2007, Royle et al., 2002, Toulme et al., 2006). Activation of P2X$_4$ regulates their trafficking to and from the plasma membrane in a Ca^{2+}-dependent manner and studies by Stokes and Surprenant (2009) illustrated that plasma membrane expression of P2X$_4$ is regulated by clathrin- and dynamin-dependent endocytosis. Data generated from intracellular Ca^{2+} measurements in TDM cells so far have illustrated that P2X$_4$ contributes towards the ATP-evoked Tg-resistant Ca^{2+} response. To further clarify the contribution of P2X$_4$, trafficking of lysosomal P2X$_4$ towards the plasma membrane was targeted. To study this, dynamin-dependent endocytosis inhibitor (dynasore) and lysosomal exocytosis inhibitor (vacuolin-1) was employed.

Stimulation of TDM cells with dynasore caused significant reduction in the magnitude of Tg-resistant Ca^{2+} response while significantly delaying decay response and increasing net calcium movement. These data were challenging to understand as it allowed two possible conclusions to be made. First, if P2X$_4$ contributed to the magnitude of the Tg-resistant Ca^{2+} response, the data illustrated that P2X$_4$ expression at the cell surface is likely to be very low, as dynasore treatment did not result in potentiation of the Ca^{2+} response. This speculation fits with FACS analysis, which illustrated very low expression of cell surface P2X$_4$ in TDM cells. Secondly, dynasore treatment resulted in the potentiation of net calcium movement as well as decay kinetics in the same manner as positive allosteric modulator IVM. IVM has been shown to act by preventing the internalization of P2X$_4$ from the plasma membrane (Toulme et al., 2006). This data, therefore, suggests that the ATP-evoked Tg-resistant decay response is dependent on dynamin resulting in build-up of P2X$_4$ on the plasma membrane. This is supported by studies illustrating that dynasore can rapidly enhance translocation of intracellular P2X$_4$ to the plasma membrane (Boumechache et al., 2009).

Unfortunately, the observations described above were not confirmed by experimental findings using vacuolin-1. Inhibiting lysosomal exocytosis by vacuolin-1 had no significant effect on the magnitude of both ATP-evoked Ca^{2+} response in

the presence and absence of Tg. However, vacuolin-1 had a significant, although small, inhibition towards the net calcium movement of ATP-evoked Ca^{2+} responses in TDM cells. This indicated that the Tg-resistant ATP-evoked Ca^{2+} response is likely to be independent of $P2X_4$ trafficking from lysosomes to plasma membrane. Studies within the literature have described that lysosomal $P2X_4$ are not just a reserve for regulating availability of $P2X_4$ on the plasma membrane, instead they are specifically targeted to the acidic vesicles for unique lysosome-related functions, like lysosomal trafficking (Trang and Salter, 2012). It would undoubtedly be interesting to investigate if stimulation of TDM cells with dynasore or vacuolin-1 could affect the protein expression of $P2X_4$ within the cell surface membrane through flow cytometry analysis.

6.2.2 Human primary MDM cells

The second part of the discussion assessed findings generated from chapter 4 and 5 which focused on looking at the contribution of $P2X_4$, and other P2 receptors, towards ATP-evoked intracellular Ca^{2+} response in primary monocyte-derived macrophages (MDM): GM-CSF differentiated (GM-MDM) and M-CSF differentiated (M-MDM). In addition to this, the role of $P2X_4$ activation in ATP-induced cytokine secretion was also investigated.

GM-MDM and M-MDM express various P2X and P2Y receptors at mRNA and protein level

Monocyte-derived macrophages differentiated with colony stimulating factors GM-CSF (GM-MDM) or M-CSF (M-MDM) are good *in vitro* models for the study of primary human macrophages (Fleetwood et al., 2005, Lacey et al., 2012). Within the literature, there is a tendency of using M-MDM as a model for tissue macrophages while GM-MDM as a model for dendritic cells (DCs) (Akagawa et al., 1988, Verreck et al., 2004, Martinez et al., 2006). However, a comprehensive gene analysis study and bioinformatics analysis of their transcriptome revealed that GM-MDM resembles macrophages more than DCs (Crozat et al., 2010, Lacey et al., 2012, Robbins et al., 2008). While GM-MDM and M-MDM cells are often associated with pro-inflammatory M1 macrophages and anti-inflammatory M2 macrophages, respectively, no studies have been performed to identify any differences in P2 receptor profiles within the two types of cells. Here, a side-by-side comparison of GM-MDM and M-MDM cells were studied to investigate which is a better model for the study of $P2X_4$.

qRT-PCR analysis illustrated that both GM-MDM and M-MDM cells express all P2XR apart from $P2X_2$, $P2X_3$ and $P2X_6$, as well as all P2YR apart from $P2Y_{12}$ and $P2Y_{14}$. Non-quantitative RT-PCR also further illustrated that across N=3 donors, the $P2X_5$ detected in human GM-MDM and M-MDM cells are non-functional which is supportive of findings by Kotnis et al. (2010). These observations corroborated various studies reported within the literature, particularly that in human alveolar macrophages which have been shown to express various P2 receptors but lacking $P2X_2$, $P2X_3$, $P2X_6$ and $P2Y_{12}$ receptors (Myrtek et al., 2008). qRT-PCR also revealed that although no significant differences were observed in the mRNA expression levels for P2XR in both GM-MDM and M-MDM cells, mRNA expression

of $P2Y_1$ was found to be down-regulated while $P2Y_6$ and $P2Y_{11}$ were found to be up-regulated in M-MDM cells compared to GM-MDM cells. Immunocytochemistry study confirmed the expression of P2XR ($P2X_1$, $P2X_4$, $P2X_5$ and $P2X_7$) and P2YR ($P2Y_1$, $P2Y_2$, $P2Y_6$ and $P2Y_{13}$) at a protein level in both GM-MDM and M-MDM cells. These observations are novel findings reporting mRNA and protein expression of P2 receptors in human primary macrophage models. These observations would be beneficial when choosing a macrophage model to utilize for the study of specific P2 receptors.

ATP-evoked dose-dependent Ca^{2+} response in both GM-MDM and M-MDM cells

In both GM-MDM and M-MDM cells, ATP evoked a dose-dependent increase in intracellular Ca^{2+} level in the presence and absence of extracellular Ca^{2+} with maximal response achieved at 100 μM agonist concentration. In the presence of 100 μM ATP, the Ca^{2+} profile was significantly different in the two cell types, although this was not observed at lower ATP concentrations. In GM-MDM cells, responses were biphasic with an initial rapid peak of intracellular Ca^{2+} response, which decayed back to a baseline level. However, in M-MDM cells, a biphasic Ca^{2+} response was observed with an initial rapid peak of intracellular Ca^{2+} followed by a much slower decay response that plateaued to a sustained-elevated phase. This was a striking observation which could be explained either by differential expression of P2YR or ectonucleotidases (i.e. CD39 and CD73). The latter may be a plausible reasoning in support of previous studies reported in resident M1 and M2 macrophages illustrating that M2 macrophages present increased CD39 and CD73 expression, compared to M1 macrophages (Zanin et al., 2012). Increased CD39 and CD73 will result in higher ATP and AMP hydrolysis, respectively, building up ADP levels in cells which may activate P2Y receptors in the macrophages. Although not further investigated in this study, it would be interesting to perform mRNA and protein studies to compare the expression of CD39 in GM-MDM *vs.* M-MDM cells.

$P2Y_{11}$ and $P2Y_{13}$ activation are responsible for the amplitude of ATP-evoked intracellular Ca^{2+} in GM-MDM and M-MDM cells

In the presence of 100 μM ATP, a prominent difference in the sustained phase of intracellular Ca^{2+} response was observed in M-MDM against GM-MDM cells. One of the key hypotheses for this difference is the differential expression of P2YR which

may be responsible for the slower decay phase of Ca^{2+} response, as have been described in several literatures (Govindan et al., 2010, Suplat-Wypych et al., 2010). The effect of $P2Y_1$, $P2Y_2$, $P2Y_6$, $P2Y_{11}$ and $P2Y_{13}$ antagonists were tested on ATP-evoked Ca^{2+} response in both cell types. Although ATP does not act as the main agonist for some of these P2YR, it is important to note that macrophages express CD39 enzymes, which allow the breakdown of ATP into ADP and AMP, which may then act on these receptors (Cohen et al., 2013, Dwyer et al., 2007).

In GM-MDM cells, $P2Y_{11}$ (NF340) and $P2Y_{13}$ (MRS2211) antagonists both significantly inhibited the amplitude of the ATP-evoked Ca^{2+} response. When present together, NF340 and MRS2211 did not completely attenuate the ATP-evoked intracellular Ca^{2+} response, but caused an even bigger inhibition than when present individually. None of the other P2YR antagonists had any effect on the ATP-evoked Ca^{2+} response in GM-MDM cells. In M-MDM cells, similar findings were observed. NF340 and MRS2211 caused a significant inhibition to ATP-evoked Ca^{2+} response while other P2YR had no significant effect. While $P2Y_{13}$ appear to only influence the amplitude of ATP-evoked Ca^{2+} response in M-MDM cells, $P2Y_{11}$ appear to contribute significantly to both the amplitude as well as the sustained phase of the ATP-evoked Ca^{2+} response. This observation is supported by qRT-PCR analysis illustrating an up-regulation of $P2Y_{11}$ mRNA expression in M-MDM cells compared to GM-MDM cells, although additional work to quantify protein expression would be valuable and would provide further confirmation. This observation suggests that the activation of $P2Y_{11}$ is responsible for the delayed sustained phase in ATP-evoked Ca^{2+} response in M-MDM cells. Although there has been no clear description of the P2 receptors involved in ATP-evoked Ca^{2+} response in human MDM cells, several studies have revealed that the contributions of P2 receptors vary significantly depending on cell types. In human airway epithelial cell models, P2Y receptors have been associated in eliciting a transient increase in intracellular Ca^{2+} level that is derived from intracellular stores while in rat glioma cells, P2Y receptors have been associated with sustained elevation of Ca^{2+} which occurs through the capacitive Ca^{2+} entrance mechanism typical for P2Y metabotropic receptors coupled to PLC (Suplat-Wypych et al., 2010, Zsembery et al., 2003). The latter may be supportive of the observation found in this thesis.

The conclusion so far suggests that both $P2Y_{11}$ and $P2Y_{13}$ activation is required for the amplitude of the ATP-evoked Ca^{2+} response in both GM-MDM and M-MDM cells

and that $P2Y_{11}$ contribute significantly to the decay response in M-MDM cells. These findings therefore provide novel evidence for the presence of functional $P2Y_{11}$ and $P2Y_{13}$ in human GM- and M-MDM cells as observed in their ability to evoke ATP Ca^{2+} response. Within the literature, the expression and functional characterization of P2 receptor subtypes in macrophages have been described in several cell lines. In all murine and rat macrophage cell lines, expression of multiple P2X and P2Y subtypes were seen although only $P2Y_1$, $P2Y_2$, $P2Y_4$, $P2X_4$ and $P2X_7$ receptors were demonstrated functionally through their ability in evoking ATP-mediated intracellular Ca^{2+} response (Bar et al., 2008, Bowler et al., 2003, Coutinho-Silva et al., 2005). In human alveolar macrophages, only $P2Y_1$, $P2Y_2$, $P2Y_{11}$ and $P2X_7$ have been illustrated to exhibit functional responses in inducing intracellular Ca^{2+} elevation (Myrtek et al., 2008, Jacob et al., 2013). Although there are currently no defined roles of $P2Y_{13}$ in human macrophages, a recent study revealed the potential role of $P2Y_{11}$ activation in macrophage activation. Knockdown of $P2Y_{11}$ significant suppressed polarization of macrophages towards M1-phenotype and IL-6 production (Sakaki et al., 2013b).

$P2X_4$ activation, but not $P2X_1$ or $P2X_7$, contributes to both the amplitude and sustained phase of ATP-evoked intracellular Ca^{2+} response in GM-MDM and M-MDM

Intracellular Ca^{2+} measurements have illustrated the contribution of $P2Y_{11}$ and $P2Y_{13}$ towards ATP-evoked Ca^{2+} response in both GM-MDM and M-MDM cells. Here, the contribution of P2XR ($P2X_1$, $P2X_4$ and $P2X_7$) towards ATP-evoked Ca^{2+} response was also investigated. The contribution of $P2X_5$ towards ATP-evoked Ca^{2+} response was not investigated in GM-MDM and M-MDM cells since the detected isoform corresponds to non-functional receptor while $P2X_2$, $P2X_3$ and $P2X_6$ was not investigated due to the absence of mRNA expression. In both GM-MDM and M-MDM cells, $P2X_1$ (Ro0437626) and $P2X_7$ (A438079) selective antagonists had no significant inhibitory effect towards the ATP-evoked intracellular Ca^{2+} response suggesting its limited contribution. This may be explained by the fact that 100 μM ATP concentration is not sufficient to activate $P2X_7$ (Chessell et al., 2005, Liang et al., 2015). This was also supported by ATP dose response performed on $hP2X_7$ overexpressing 1321N1 line that illustrated much higher ATP concentration is required for the activation of $P2X_7$. This data therefore did not provide evidence for a functional $P2X_1$ receptor, which corroborates with studies in human alveolar macrophages (Myrtek et al., 2008). To identify the presence of functional $P2X_7$ by

assessment of ATP-evoked Ca^{2+} response, it may be necessary to employ a higher ATP concentration. However, as this thesis focuses on characterizing $P2X_4$, it is of interest to maintain the use of 100 μM ATP concentration.

The contribution of $P2X_4$ activation towards ATP-evoked Ca^{2+} response was studied using a combination of three pharmacological tools: IVM, 5-BDBD and PSB-12062. IVM caused a significant potentiation to the amplitude of the ATP-evoked Ca^{2+} response in both GM-MDM and M-MDM cells but only delayed the sustained phase of decay response in GM-MDM cells. The effect of IVM on ATP-evoked Ca^{2+} response in GM-MDM cells corroborates previous studies illustrating the two hallmark effects of IVM on $P2X_4$-mediated currents: 1) potentiation of current and 2) delay of decay kinetic (Norenberg et al., 2012). However, it is worth noting that IVM has previously been described to also potentiate the peak of $P2X_7$-mediated current. However, the effect of IVM on delaying decay response is known to be specific to $P2X_4$. Interestingly, in M-MDM cells, IVM only had a significant effect on the amplitude of the ATP-evoked Ca^{2+} response suggesting that there is potentially minimal contribution of $P2X_4$ activation towards the sustained decay phase of the Ca^{2+} response or the possibility of IVM acting on $P2X_7$ instead. The latter seemed unlikely as the agonist concentration used in these experiments is unlikely to be sufficient to activate $P2X_7$ and A438079 had no effect on the ATP-evoked Ca^{2+} response (Chessell et al., 2005, Liang et al., 2015). The effect of $P2X_4$ antagonists, 5-BDBD and PSB-12062, was tested to provide further evidence of $P2X_4$ contribution. In GM-MDM cells, PSB-12062 significantly inhibited the magnitude and decay response of ATP-evoked Ca^{2+} response. Meanwhile, in the presence of IVM, PSB-12062 only inhibited the decay response. In M-MDM cells, PSB-12062 had a slightly different effect whereby it significantly inhibited only the magnitude of the ATP-evoked Ca^{2+} response in both presence and absence of IVM. 5-BDBD had a similar effect in both cell types whereby it caused an inhibition towards the amplitude of the ATP-evoked Ca^{2+} response. In the presence of IVM, 5-BDBD caused an inhibition towards both amplitude and decay response. These data altogether suggest that $P2X_4$ is likely to contribute to both the amplitude and the second decay phase of the ATP-evoked Ca^{2+} response. Its contribution towards the second decay phase of the Ca^{2+} response may be supported by observations that while P2YR elicit a transient Ca^{2+} response derived from intracellular store, P2XR trigger a sustained Ca^{2+} response allowing Ca^{2+} influx from extracellular space (Zsembery et al., 2003).

P2X$_4$ activation has a greater contribution to Ca^{2+} response in GM-MDM cells in comparison to M-MDM cells

The experimental study involving the characterization of P2X$_4$ in human primary monocyte-derived macrophages allowed the identification to which of the two MDM systems can serve as a better model to study functional P2X$_4$. The two macrophage systems clearly displayed differences in morphology, P2 mRNA expression profiles and most importantly, ATP-evoked Ca^{2+} response features. There are currently no reports within the literature illustrating the contribution of P2X$_4$ to ATP-evoked Ca^{2+} responses in both macrophage model. P2X$_4$ has previously been speculated to be a pro-inflammatory receptor (Li and Fountain, 2012), it is therefore important to identify if pro-inflammatory M1 macrophages, GM-MDM, would serve as a better tool to study these receptors.

As discussed previously, the utilization of P2X$_4$ specific pharmacological tools allowed the revelation that P2X$_4$ mainly contributed towards the decay phase of the ATP-evoked Ca^{2+} response, although it also had a small contribution towards the magnitude of the response. This was illustrated from Ca^{2+} measurements following the treatment of IVM, PSB-12062 and 5-BDBD. The use of PSB-12062 in the presence and absence of IVM illustrated that M-MDM cells are less sensitive towards the antagonist, compared to GM-MDM cells. The difference in sensitivities towards P2X$_4$ antagonist may be due to the level of expression of P2X$_4$ in the two cell types. Although qRT-PCR analysis illustrated no difference in P2X$_4$ mRNA expression in GM-MDM and M-MDM cells, protein expression was found to be significantly different as quantified using FACS analysis. FACS studies illustrated that M-MDM cells expresses significantly lower amount of surface and total P2X$_4$, compared to GM-MDM cells. There are currently no studies reporting the different level of protein expression of P2X$_4$ in GM-MDM and M-MDM cells and this would provide valuable knowledge to researchers interested in the study of P2X$_4$. Altogether, these findings illustrate that compared to M-MDM cells, GM-MDM cells provide a better model for the study of P2X$_4$. In addition to this, if employed at reliable concentrations, PSB-12062 and IVM are valuable pharmacological tools that can be used for the characterization of P2X$_4$.

ATP stimulation causes the induction of cytokine gene expression in GM-MDMs

To study the role of P2X$_4$ activation in cytokine and chemokine secretion, an RT profiler array was performed to screen over 84 different genes of cytokines and chemokines that are associated with inflammatory responses. In the absence of extracellular agonist, ATP, GM-MDM cells constitutively expressed all the investigated genes apart from BMP4, CCL19, CXCL11, CXCL12, IFNG, IL12A, IL17A, IL2, TNFRS11B and XCL1. Following 6h stimulation with 100 μM ATP, several genes (CXCL2, CXCL5, IL-12β, OSM, PPBP and TGFβ2) that have been associated with macrophages in the literature were found to be significantly up-regulated. Apart from PPBP, these cytokines and chemokines have been demonstrated to be important inflammatory mediators that are expressed or secreted by human macrophages.

- Tissue macrophages have been reported to synthesize CXCL2 in response to LPS stimulation. These are important chemokines for neutrophil recruitment during tissue inflammation (De Filippo et al., 2013). It has also been described that CXCL2 expression in macrophages is a process dependent on the NF-κb pathway (De Plaen et al., 2006). In addition to this, studies in mice revealed that injection of extracellular ATP intraperitoneally resulted in increased numbers of neutrophils within peritoneal cavity as well as increased levels of CXCL2 level in peritoneal lavage fluid (Kawamura et al., 2012). The increase of level of CXCL2 in mice has been demonstrated to be a process dependent on P2X$_7$ and P2Y$_2$ activation (Kawamura et al., 2012). This finding is supportive of the finding within this thesis illustrating ATP induction of CXCL2 in human GM-MDM cells.

- mRNA analysis in this thesis illustrated that ATP induced mRNA expression of IL-12β in GM-MDM cells. IL-12 is a cytokine produced primarily by APCs like macrophages and DCs (Ma et al., 2015) playing a role in activating NK cells and inducing the differentiation of naïve CD4 T lymphocytes. Our observation that ATP induced IL-12β expression in GM-MDM cells is contradictory to what was observed in a study involving peritoneal macrophages (Hasko et al., 2000). Pre-treatment with extracellular ATP was shown to reduce LPS-induced IL-12 production in macrophages as well as IL-12 (p35 and p40) mRNA expression.

- Oncostatin M (OSM) is an inflammatory cytokine belonging to IL-6 family produced by macrophages (Guihard et al., 2015). Within the literature to date, there are no studies reporting the ability of ATP stimulation to induce OSM mRNA expression in human macrophages and the data illustrated in this thesis may uncover OSM as a potential cytokine to investigate. Earlier investigation by Ganesh et al. (2012) illustrated that treatment of TDM cells with PGE_2 resulted in a dose-dependent induction of anti-inflammatory OSM. This is an extremely interesting observation as $P2X_4$ has been demonstrated to mediate PGE_2 release by tissue resident macrophages to initiate inflammatory pain. Unfortunately, in the context of this thesis, OSM was not investigated further.

It is without a doubt that one of the main limitations of this profiler array study is the use of only one time point to screen for changes in mRNA expression following ATP stimulation in GM-MDM cells. Different cytokines and chemokines genes have been shown to differ in their gene expression kinetics (Leyva-Illades et al., 2012, Sadahiro et al., 2007), however, it was not possible to screen for various time points due to difficulty in obtaining cell numbers. Altogether, IL-12β, OSM and CXCL2 are potentially interesting inflammatory mediators but were not pursued in the study of this thesis due to filtering criteria. In brief, as part of the filtering criteria, GM-MDM cells were stimulated with either PSB-12062 alone or in the presence of agonist ATP. Only genes that were unaffected by treatment with $P2X_4$ antagonist, PSB-12062, alone were investigated further and this yielded CXCL5 and TGF-β2 as potential candidates, which will be discussed more thoroughly within each section below.

Blocking $P2X_4$ increased ATP-induced TGF-β2 mRNA expression but not secretion

One candidate gene that was investigated further from the RT^2 profiler array study is one of the TGF-β isoforms, TGF-β2. Within the literature so far, there are several studies associating TGF-β and human macrophages although the involvement of purinergic receptors have not been explored in detail. TGF-β signaling is known to play a critical role in the promotion and polarization of anti-inflammatory M2 macrophages (Roszer, 2015, Gong et al., 2012). It has been reported that inflammatory macrophages, such as those found in human and murine

atherosclerotic lesions, express TGF-β1 and its receptors and that macrophage specific TGF-β1 overexpression play a role in reducing and stabilizing atherosclerotic plaques in ApoE-deficient mice (Reifenberg et al., 2012). Although the predominant isoform being explored in literature is TGF-β1, TGF-β2 has also been associated with macrophages, although to a much smaller extent. Studies in human and murine intestinal tissue samples demonstrated that TGF-β2 suppresses macrophage cytokine production and mucosal inflammatory response (Maheshwari et al., 2011).

Here, stimulation of GM-MDM cells with 100 μM ATP resulted in an increase in TGF-β2 mRNA expression, peaking at 6h. In the presence of P2X$_4$ antagonist, PSB-12062, ATP-induced TGF-β2 mRNA expression was significantly potentiated suggesting that P2X$_4$ negatively regulate the mRNA expression level of TGF-β2. The effect of PSB-12062 on ATP-induced TGF-β2 mRNA expression mimic findings by a recent study illustrating that lack of P2X$_4$ expression leads to increased renal fibrosis and increased expression of TGF-β (Kim et al., 2014). In addition to this, since P2X$_4$ has previously been described as pro-inflammatory receptor, it may be speculated that blocking P2X$_4$ resulted in increased expression of TGF-β, a known regulator for anti-inflammatory M2 macrophage activation (Li and Fountain, 2012). However, it was a surprising finding that these significant changes of mRNA expression did not translate to protein level. In fact, no TGF-β2 protein was present at a detectable level within the preconditioned supernatant across 4 independent donors. Several explanations may justify this: 1) Poor protein stability or high degradation rate of TGF-β2 proteins due to post-translational modifications; 2) post-transcriptional modifications of mRNA; 3) translation of mRNA is inhibited due to tight regulation within the cell causing no final synthesis of native protein; or 4) insufficient agonist concentration to allow the synthesis and secretion of protein. Although none of these theories have been confirmed, it has been reported that only a few primary cells and established cell lines secrete significant amounts of active TGF-β into culture medium under well-optimized conditions (Mazzieri et al., 2000). Otherwise, little, if any, soluble active TGF-β is generated by most cultured cells and therefore, the absence of detectable levels of active TGF-β in medium is not surprising. Despite undetectable levels of TGF-β in supernatants, this does not necessarily imply a lack of TGF-β activation for two reasons: 1) in certain cases

TGF-β activation takes place at the cell surface therefore generating a high local concentration of active TGF-β (Sato et al., 1990, Dennis and Rifkin, 1991, Munger et al., 1999) and 2) active TGF-β may be cleared from supernatant by binding to cell surface receptor resulting in protein levels at undetectable levels (Mazzieri et al., 2000). One potential solution for this would be to utilize a highly sensitive experimental tool to detect active TGF-β such as the use of reporter cells co-cultured with activating cells (Crawford et al., 1998).

Blocking P2X$_4$ inhibited ATP-induced CXCL5 mRNA expression, protein secretion and synthesis

Another candidate that was further investigated following the profiler array study was chemokine CXCL5. There are currently limited studies associating CXCL5 with human macrophages. A few examples include high level of expression and secretion of chemokine CXCL5 in the macrophage fraction of white adipose tissue (WAT) (Chavey and Fajas, 2009) and in monocyte-derived macrophages of normal donors that have been infected with HIV-1 (Guha et al., 2015). CXCL5 is a chemokine and adipokine that has been implicated in neutrophil recruitment and promotion of obesity by inhibiting insulin signaling (Sepuru et al., 2014). More recent studies by Li et al. (2016) showed that activation of the TLR9/MyD88/CXCL5 signaling network by resident macrophages of the heart promote the recruitment of neutrophil and that CXCL5 functions to limit macrophage foam cell formation in conditions like atherosclerosis (Rousselle et al., 2013). Despite the link between CXCL5 and human macrophages, it is unknown if MDMs can synthesize and secrete CXCL5 following stimulation with a DAMP signal, ATP, and if P2X$_4$, or any other P2 receptors, can contribute to this signaling pathway.

Stimulation of GM-MDM cells with 100 μM ATP caused a time-dependent increase in mRNA expression and protein secretion of CXCL5. These are novel findings as to date, there has been no report illustrating the ability of GM-MDM cells to synthesize and secrete CXCL5 in response to stimulation with ATP. Blocking of P2X$_4$ with PSB-12062 resulted in a significant reduction of ATP-induced CXCL5 mRNA expression and protein secretion. To further confirm the involvement of P2X$_4$ in ATP-induced CXCL5 secretion, the dose response of PSB-12062 (1, 5 and 10 μM) and IVM was tested. Lower concentrations of PSB-12062 (1 μM and 5 μM), which have been shown to be selective for P2X$_4$ over P2X$_7$, were able to still cause

a significant inhibition towards ATP-induced CXCL5 protein secretion. Reciprocally, treatment with IVM caused a significant potentiation towards ATP-induced CXCL5 secretion in GM-MDM cells at 48h time point. The effect of PSB-12062 was also tested on ATP-induced synthesis of CXCL5 in GM-MDM cells. At 32h and 48h, blocking $P2X_4$ caused a significant inhibition of ATP-induced CXCL5 synthesis. Taken together, the effect of IVM and PSB-12062 on ATP-induced CXCL5 expression and secretion is promising and may suggest a role of $P2X_4$ as a modulator of CXCL5 levels in human macrophages. These observations may corroborate with previous studies whereby *in vitro* treatment of HUVECs with atorvastatin significantly reduced IL-1β-induced CXCL5 levels in a dose-dependent manner (Zineh et al., 2008). Though no clear relationship has been associated between $P2X_4$ and CXCL5, a study by Li and Fountain (2012) illustrated suppression of $P2X_4$ activity by fluvastatin in human monocytes through depletion of cholesterol levels. It may therefore be possible that the statin is affecting the level of CXCL5 indirectly through the $P2X_4$ receptor. Despite the potentially interesting link, this was contradicted by a study illustrating that depletion of plasma membrane cholesterol did not adversely affect IL-1β secretion in response to ATP (Brough and Rothwell, 2007).

Possible interactions of $P2X_4$ and CXCL5

CXCL5 has been shown to activate ERK, JNK and p38 MAPK signaling pathways, all of which are key players in tumour growth and metastasis (Dai et al., 2016). In the context of inflammatory diseases, CXCL5 have been shown to contribute to the pathologies of cardiovascular disease, pulmonary fibrosis and rheumatoid arthritis. Analysis of bronchoalveolar lavage fluid and lung tissue revealed elevated levels of CXCL5 were identified in patients with idiopathic pulmonary fibrosis (Strieter et al., 2007). In the context of cardiovascular conditions, CXCL5 has been shown to offer an atheroprotective role by enhancing cholesterol efflux capacity in macrophages, thus regulating foam cell formation (Rousselle et al., 2013). In addition to this, treatment of HUVECs with atorvastatin *in vitro* resulted in the reduction of IL-1β-induced CXCL5 in a dose-dependent manner (Zineh et al., 2008). Finally, an increase in CXCL5 levels have been detected in synovial fluid of patients suffering from rheumatoid arthritis (Koch et al., 1994). Rat adjuvant-induced arthritis (AIA) models for the study of arthritis showed elevated CXCL5 levels in their serum with progression of arthritis when compared to control animals. Pre-treatment of rats with

anti-CXCL5 antibody resulted in a significant reduction in severity of the disease (Halloran et al., 1999), suggesting that CXCL5 play an important role in the onset and progression of rheumatoid arthritis. Although the mechanism by which $P2X_4$ receptor activation modulates expression and secretion of CXCL5 in human MDM has not been investigated in this current study, several speculations can be made.

First of all, studies by Song et al. (2013) illustrated that the pro-inflammatory chemokine CXCL5 was found to be rapidly upregulated by local presence of IL-1β and that its action was potentiated by MMP-2 and MMP-9, working synergistically to initiate neutrophil recruitment (Song et al., 2013). It is thought that the inflammatory cytokine IL-1β induces CXCL5 expression by the activation of NF-κB and CREB (Sun et al., 2008). Furthermore, evidence obtained from structural and functional studies revealed possible interactions of $P2X_4$ and $P2X_7$ and that $P2X_4$ expression facilitated $P2X_7$-dependent IL-1β release in mouse dendritic cells (Perez-Flores et al., 2015, Sakaki et al., 2013a). It may therefore be possible that $P2X_4$ receptor activation modulates ATP-induced CXCL5 secretion by regulating IL-1β levels (Figure 6). As our data here illustrated that $P2X_7$ activation had no significant effect on ATP-induced CXCL5 secretion, it may be interesting in future studies to identify if $P2X_4$ can work independently.

Secondly, the precursor of CXCL5 is made up of 114 amino acids which contain a signal peptide of 36 amino acids. The signal peptide can be cleaved to generate the mature protein containing 78 amino acids, hence the name ENA-78 (Walz et al., 1997). Upon the generation of mature protein, human CXCL5 can act as a target for several proteases such as matrix metalloproteases (MMP-1, MMP-9, MMP-12 and MMP-25), which can cleave the N-terminal region resulting in either activation or inactivation of the chemokine (Van Den Steen et al., 2003, Dean et al., 2008, Starr et al., 2012). It is unknown whether $P2X_4$ receptor can interact directly with CXCL5 or interact with proteases responsible for the generation of the mature chemokine such as cysteine cathepsins (Repnik et al., 2015). Taking the $P2X_7$ receptor as an example, it has been illustrated that their activation in macrophages in response to extracellular ATP results in the induction of NLRP3 inflammasome assembly and caspase-1-dependent processing and release of IL-1β (Brough and Rothwell, 2007, Gombault et al., 2012, Karmakar et al., 2016). This leads us to speculate that one route that $P2X_4$ can modulate chemokine CXCL5 level is through their interaction

with proteases resulting in the modulation of CXCL5 processing and release in human macrophages. However, this is a speculation made in the assumption that the CXCL5 ELISA used throughout the study selectively detects and quantifies mature CXCL5. Although the ELISA kit employed in this study was tested and validated for the detection of mature CXCL5, it is unclear if it can also detect immature CXCL5. Therefore, to further study the mechanism of interaction between $P2X_4$ and CXCL5, it may be interesting to utilize other biological assays such as western blots which will allow the distinction of the two forms of protein. Further studies will undoubtedly be required to unravel the mechanism by which $P2X_4$ regulates CXCL5 synthesis and secretion in human macrophages.
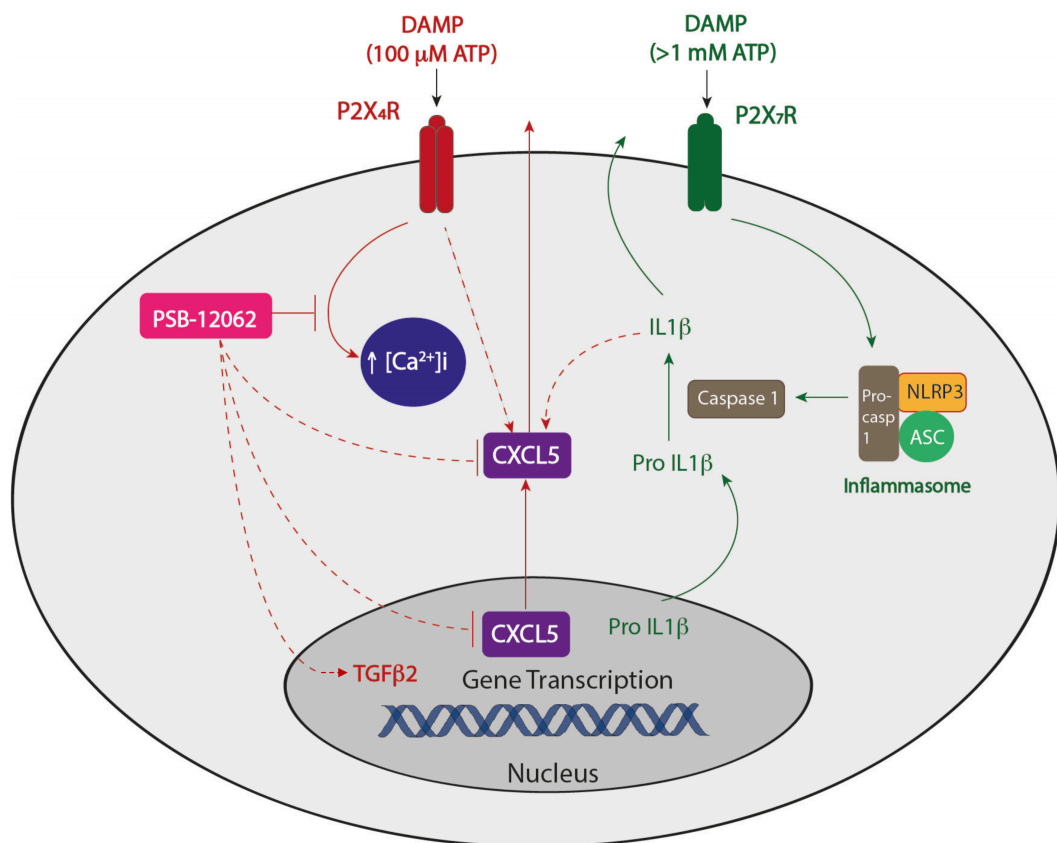
Figure 6. **Suggested downstream signaling pathway of P2X$_4$ activation following ATP stimulation in human macrophages.** In green is the speculated downstream pathway following activation of P2X$_7$ with 100 μM ATP as described in the literature. ATP activates P2X$_7$ receptor which leads to the activation of NLRP3 inflammasome and caspase-1 which can activate IL-1β. In red is the speculated downstream pathway following activation of P2X$_4$ with 100 μM ATP as hypothesized from this research. ATP activates P2X$_4$ receptor which leads to increase in intracellular Ca^{2+} level in the cell. P2X$_4$ activation modulates the expression, secretion and synthesis of CXCL5 although the pathway involved has not been identified. On the other hand, P2X$_4$ activation negatively modulates the gene expression of TGF-β2 as illustrated with the effect of selective antagonist PSB-12062. Dashed lines represent possible interaction but with unknown pathway.

ATP-induced CXCL5 protein secretion is independent of intracellular Ca^{2+} level

In addition to studying $P2X_4$ contribution towards ATP-induced CXCL5 protein secretion, several other P2 receptors were investigated based on their contribution towards ATP-evoked Ca^{2+} response. The effect of $P2Y_{11}$ (NF340) and $P2Y_{13}$ (MRS2211) antagonists were studied as they both significantly inhibited the amplitude of ATP-evoked Ca^{2+} response, while $P2X_7$ antagonist (A438079) was studied mainly because $P2X_4$ and $P2X_7$ have been described to work in close relationship (Gu et al., 2013, Kawano et al., 2012a). Treatment of cells with A438079 had no significant effect towards ATP-induced CXCL5 secretion in GM-MDM cells. This was a surprising observation as $P2X_4$ has been closely associated with $P2X_7$, especially in the context of cytokine secretion such as IL-1β. However, this is likely due to the fact that 100 μM ATP is not sufficient to cause the activation of $P2X_7$..In addition to this, treatment of GM-MDM cells with NF340 and MRS2211 had no significant effect on secretion of CXCL5 at 48h following ATP stimulation. These observations suggest that $P2Y_{11}$ and $P2Y_{13}$ are not responsible for the regulation of ATP-induced CXCL5 secretion in GM-MDM cells and that the secretion of CXCL5 may involve a pathway that is independent of intracellular Ca^{2+} level.

This observation also leads us to speculate what the mode of action of $P2X_4$ antagonist (PSB-12062) is. In the literature so far, PSB-12062 has been described as an antagonist with an allosteric nature although its binding site has not been identified. The fact that CXCL5 secretion appears to be a process independent of intracellular Ca^{2+} level, it may be that PSB-12062 permeates through the membrane and acts intracellularly. Another plausible assumption would be that $P2X_4$ is localized within intracellular compartments with CXCL5 and may interact directly, which can be investigated through co-staining of $P2X_4$ and CXCL5.

6.3   Concluding Remarks

The main purpose of this study was to characterize the contribution of $P2X_4$ towards ATP-evoked Ca^{2+} responses in the TDM cell line and primary human MDM as well as elucidating a role of $P2X_4$ activation towards cytokine and chemokine secretion in primary macrophages. In this study, TDM was used for the sole purpose of verifying the pharmacological tools commercially available for the characterization of $P2X_4$-mediated Ca^{2+} influx in macrophages. Intracellular Ca^{2+} measurements in TDM cells highlighted both IVM and PSB-12062 as valuable tools for the study of $P2X_4$ receptor. In addition to this, this thesis also allowed the demonstration that both P2XR and P2YR are responsible for ATP-evoked intracellular Ca^{2+} response in human GM-MDM and M-MDM cells. Although both MDM systems can prove to be useful tools for the study of different macrophage phenotype (i.e. pro- or anti-inflammatory), $P2X_4$ had a bigger contribution towards the ATP-evoked intracellular Ca^{2+} response in GM-MDM cells. Finally, the highlight of this study came with our observation that ATP, a DAMP signal, can induce the synthesis and secretion of chemokine CXCL5 in GM-MDM cells and that $P2X_4$ modulates this process. Although additional work will undoubtedly be required to uncover the mechanism involved in $P2X_4$-CXCL5 interaction in human macrophages, the current study has highlighted a novel role of $P2X_4$ in human macrophages and its contribution towards chemokine secretion.

6.4   Future Directions

This study has reflected the importance of $P2X_4$ towards ATP-evoked Ca^{2+} response and CXCL5 secretion in human macrophages. However, many questions remain unexplored and further studies are undoubtedly required. It is without a doubt that the next step required to follow up this finding is identifying the mechanism involved in the regulation of CXCL5 synthesis and secretion by $P2X_4$. It may be relevant to initially identify if there is a link between IL-1β and CXCL5 level in human macrophages. Further to this, it is unknown if $P2X_4$ is working with other P2 receptors to modulate ATP-evoked CXCL5 synthesis and secretion. Here, the contributions of other receptors ($P2X_7$, $P2Y_{11}$ and $P2Y_{13}$) were investigated allowing the conclusion that ATP-evoked CXCL5 secretion is potentially independent of intracellular Ca^{2+} level. It would be interesting to investigate the contributions of other ATP-activated P2 receptors such as $P2Y_2$. Finally, one of the main limitations is that this study relied on the selectivity and specificity of antagonists and modulators and knocking down $P2X_4$ in human primary macrophages would definitely provide further confirmation. Although challenging, successful transduction of lentiviral particles have been described in human macrophages (Leyva et al., 2011, Zeng et al., 2006).

Appendix: Supplementary Data

Supernatant sample	Absorbance at 490nm (OD$_{490}$)	LDH activity (μU)
Donor 32 24h unstim	0.194	13.42
Donor 32 24h PSB-12062	0.199	18.00
Donor 32 32h unstim	0.206	23.92
Donor 32 32h PSB-12062	0.210	26.75
Donor 32 48h unstim	0.201	19.25
Donor 32 48h PSB-12062	0.198	16.75
Donor 33 24h unstim	0.097	Negative value
Donor 33 24h PSB-12062	0.128	Negative value
Donor 33 32h unstim	0.101	Negative value
Donor 33 32h PSB-12062	0.072	Negative value
Donor 33 48h unstim	0.103	Negative value
Donor 33 48h PSB-12062	0.121	Negative value
Donor 34 24h unstim	0.180	Negative value
Donor 34 24h PSB-12062	0.089	Negative value
Donor 34 32h unstim	0.088	Negative value
Donor 34 32h PSB-12062	0.094	Negative value
Donor 34 48h unstim	0.089	Negative value
Donor 34 48h PSB-12062	0.084	Negative value

Table A1. **Assessing toxicity of 10 μM P2X$_4$ antagonist, PSB-12062, on 100 μM ATP-induced CXCL5 secretion at varying time points using LDH Cytotoxicity Assay.** Data are represented as individual donors (N=3 donors) across varying time points (24h, 32h and 48h). The sensitivity of LDH Cytotoxicity Assay kit allowed the measurement of any LDH activity ranging from 31.25 – 1000 μU. Unstim refers to negative control where cells are treated with vehicle (0.5% DMSO), negative value refers to no LDH activity detected due to absorbance reading obtained at 490nm being found below the minimum read-out of the standard curve.
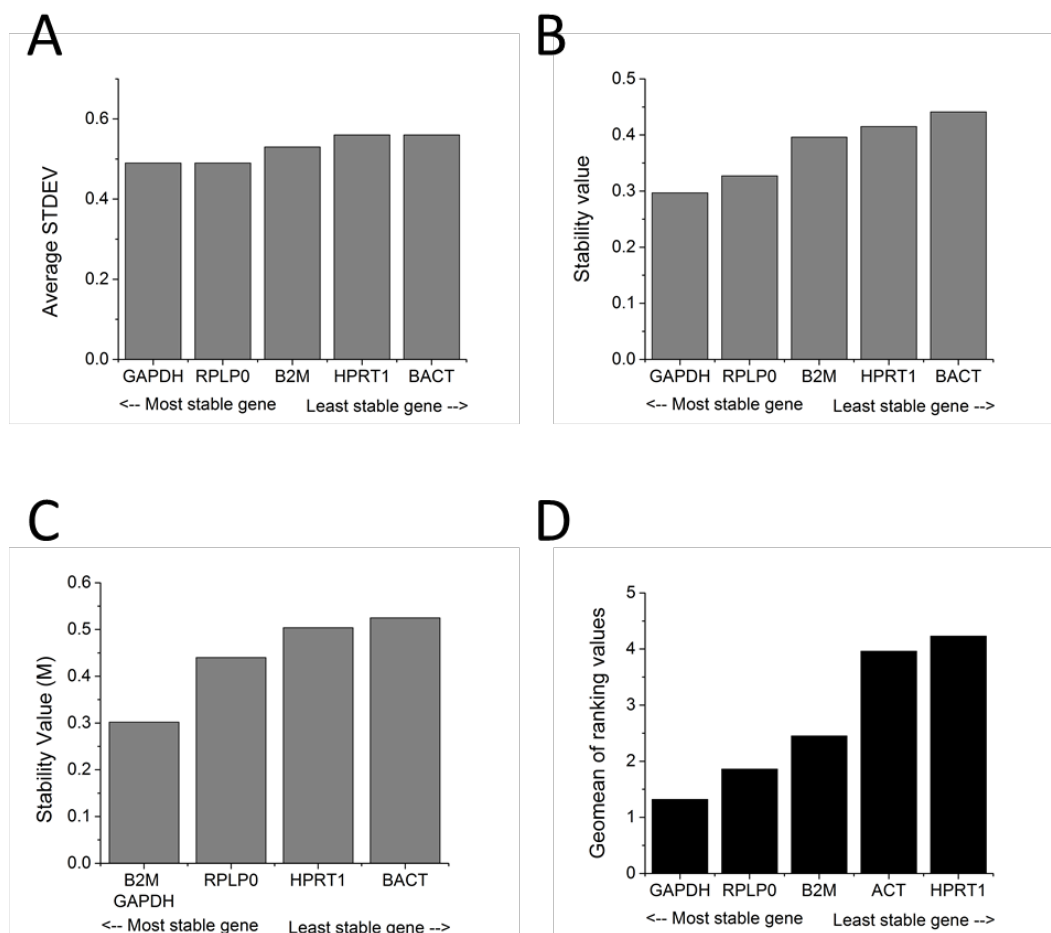
Figure A1. Gene stability ranking. Comparison of reference genes as evaluated using: A) ΔΔCt method (N=5 donors), B) NormFinder (N=5 donors), C) GeNorm (N=5 donors), and D) Overall comprehensive gene stability ranking (N=5 donors). Assessment was performed using the RefFinder online database tool. As shown on here, housekeeping genes GAPDH and RPLP0 were shown to be the most stably expressed genes in primary human GM-MDM cells. Meanwhile, ACTB and HPRT1 were found to be the least stably expressed genes by all methods. Therefore, for further gene expression studies in GM-MDM cells, GAPDH will be used as a reference gene to normalize all gene expression data.
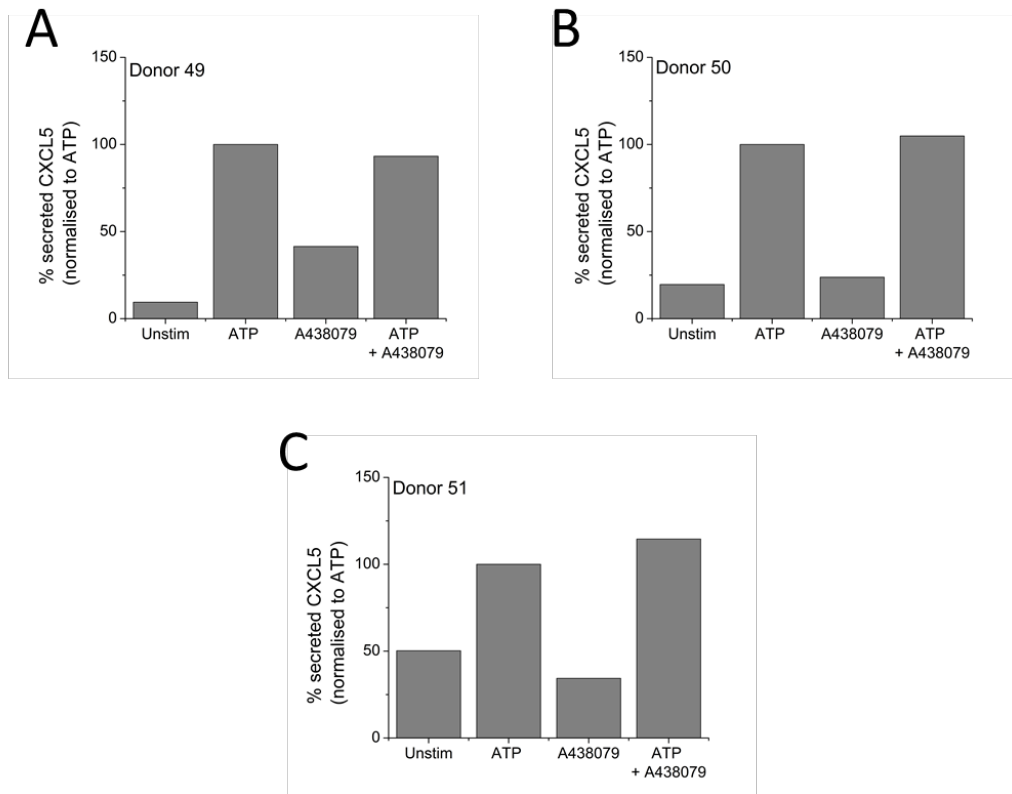
Figure A2. Effect of 10 μM P2X$_7$ antagonist, A438079, on 100 μM ATP-induced CXCL5 secretion. A – C) Effect of A438079 on ATP-induced CXCL5 secretion at 48h time point for individual donors (N=3 donors). Data is normalized to amount of secreted CXCL5 in the presence of 100 μM ATP alone. Unstim represents cells in the presence of vehicle only, as background control.
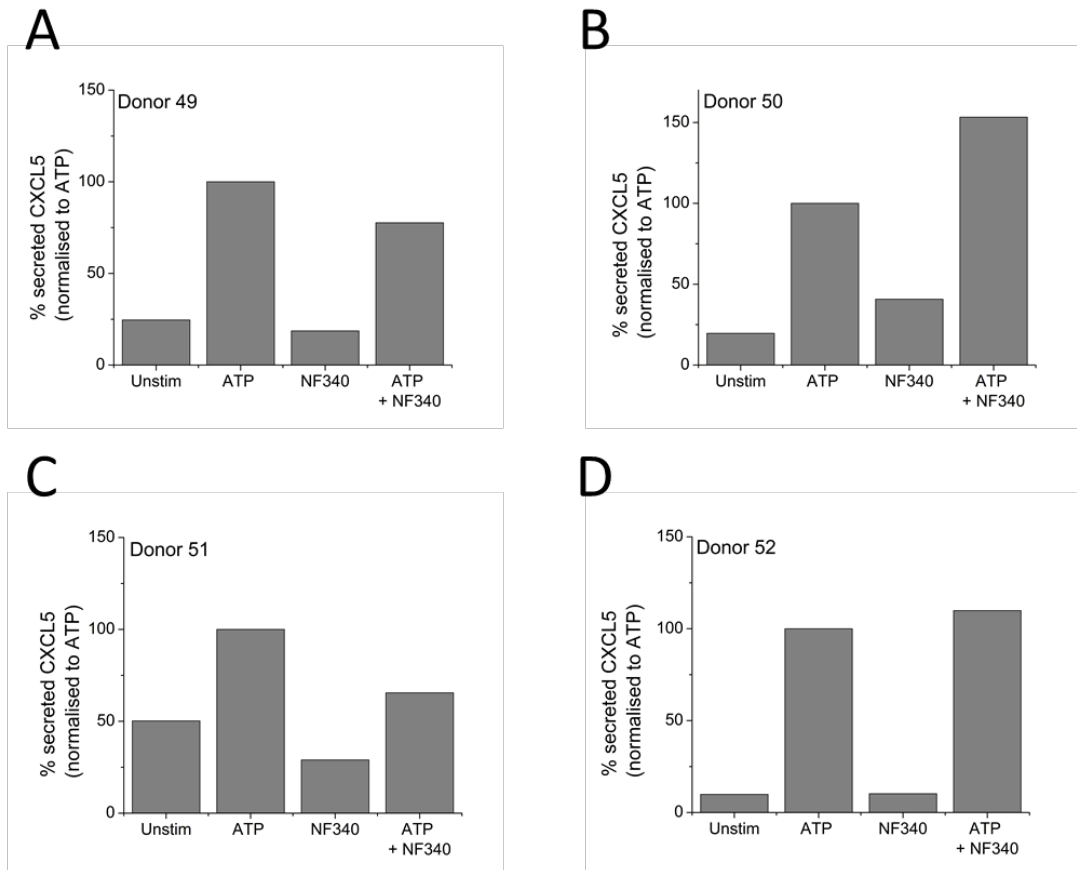
Figure A3. **Effect of 10 μM P2Y$_{11}$ antagonist, NF340, on 100 μM ATP-induced CXCL5 secretion.** A – C) Effect of NF340 on ATP-induced CXCL5 secretion at 48h time point for individual donors (N=4 donors). Data is normalized to amount of secreted CXCL5 in the presence of 100 μM ATP alone. Unstim represents cells in the presence of vehicle only, as background control.
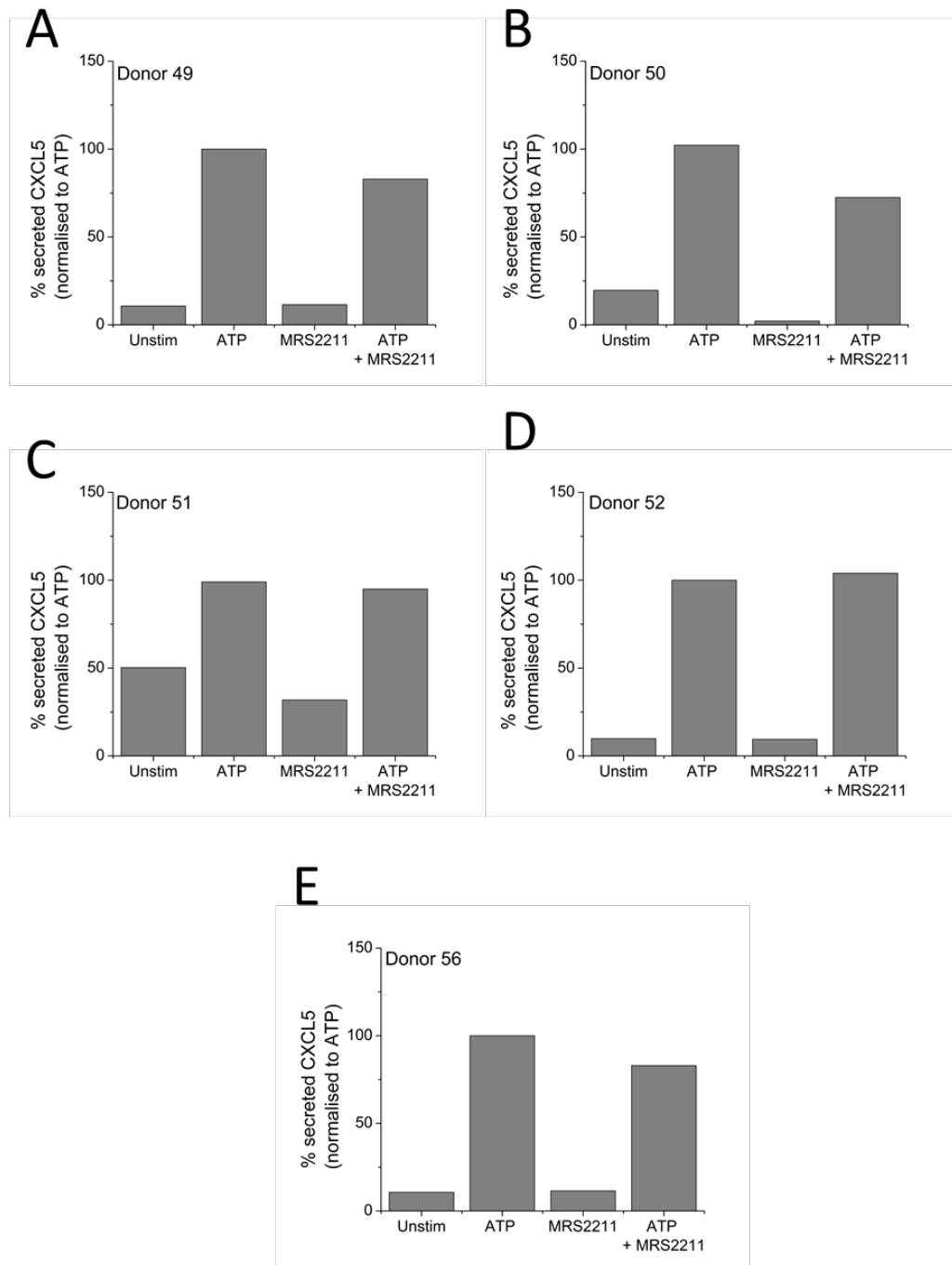
Figure A4. **Effect of 10 μM P2Y$_{13}$ antagonist, MRS2211, on 100 μM ATP-induced CXCL5 secretion.** A – C) Effect of NF340 on ATP-induced CXCL5 secretion at 48h time point for individual donors (N=5 donors). Data is normalized to amount of secreted CXCL5 in the presence of 100 μM ATP alone. Unstim represents cells in the presence of vehicle only, as background control.
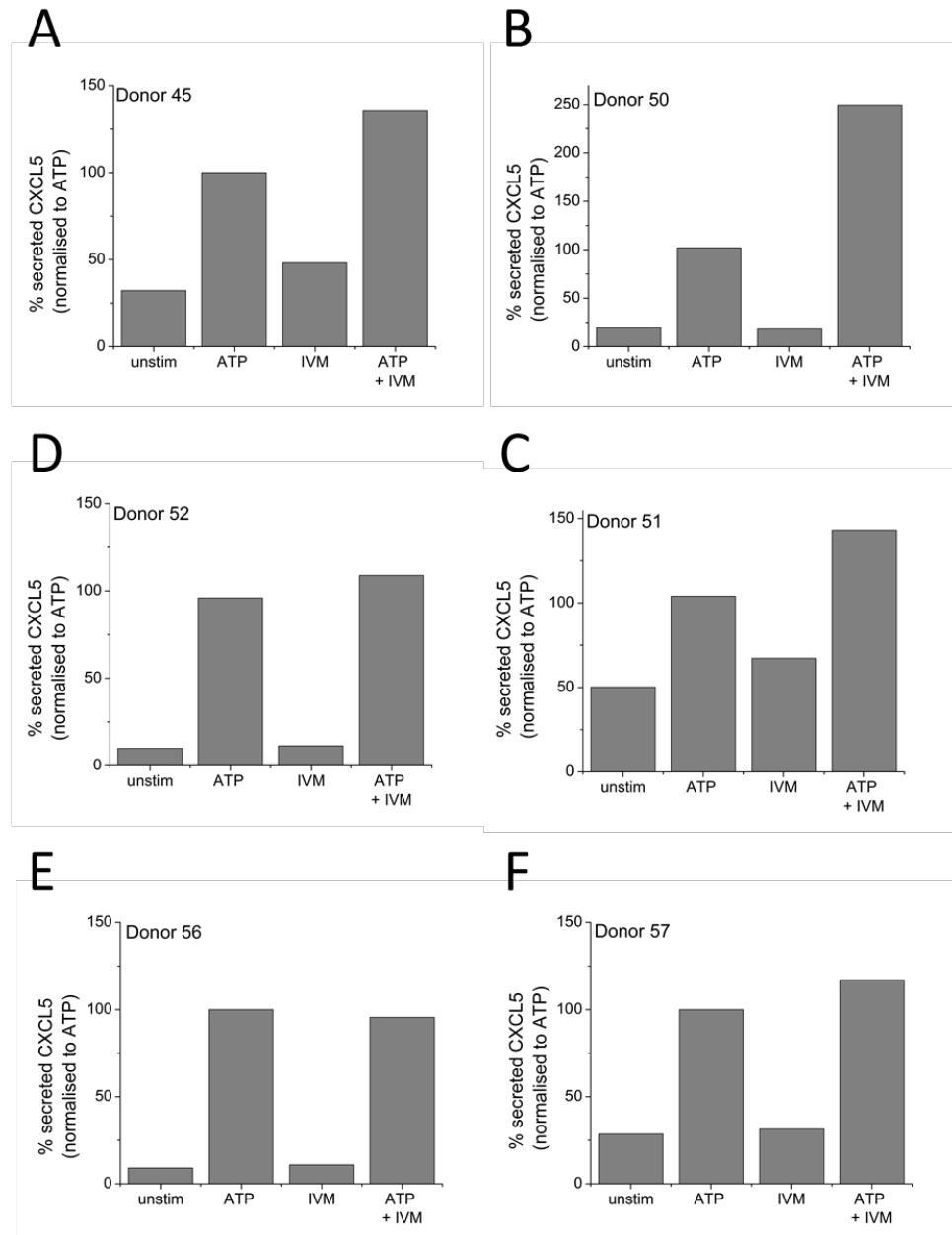
Figure A5. **Effect of 3 μM P2X$_4$ positive allosteric modulator, IVM, on 100 μM ATP-induced CXCL5 secretion.** A – C) Effect of NF340 on ATP-induced CXCL5 secretion at 48h time point for individual donors (N=6 donors). Data is normalized to amount of secreted CXCL5 in the presence of 100 μM ATP alone. Unstim represents cells in the presence of vehicle only, as background control.

References

ABBRACCHIO, M. P., BOEYNAEMS, J. M., BARNARD, E. A., BOYER, J. L., KENNEDY, C., MIRAS-PORTUGAL, M. T., KING, B. F., GACHET, C., JACOBSON, K. A., WEISMAN, G. A. & BURNSTOCK, G. 2003. Characterization of the UDP-glucose receptor (re-named here the P2Y14 receptor) adds diversity to the P2Y receptor family. *Trends Pharmacol Sci,* 24**,** 52-5.

ABBRACCHIO, M. P. & BURNSTOCK, G. 1994. Purinoceptors: are there families of P2X and P2Y purinoceptors? *Pharmacol Ther,* 64**,** 445-75.

ABBRACCHIO, M. P., BURNSTOCK, G., BOEYNAEMS, J. M., BARNARD, E. A., BOYER, J. L., KENNEDY, C., KNIGHT, G. E., FUMAGALLI, M., GACHET, C., JACOBSON, K. A. & WEISMAN, G. A. 2006. International Union of Pharmacology LVIII: update on the P2Y G protein-coupled nucleotide receptors: from molecular mechanisms and pathophysiology to therapy. *Pharmacol Rev,* 58**,** 281-341.

ABDULQAWI, R., DOCKRY, R., HOLT, K., LAYTON, G., MCCARTHY, B. G., FORD, A. P. & SMITH, J. A. 2015. P2X3 receptor antagonist (AF-219) in refractory chronic cough: a randomised, double-blind, placebo-controlled phase 2 study. *Lancet,* 385**,** 1198-205.

ACUNA-CASTILLO, C., MORALES, B. & HUIDOBRO-TORO, J. P. 2000. Zinc and copper modulate differentially the P2X4 receptor. *J Neurochem,* 74**,** 1529-37.

ADEREM, A. 2003. Phagocytosis and the inflammatory response. *J Infect Dis,* 187 Suppl 2**,** S340-5.

AKAGAWA, K. S., KAMOSHITA, K. & TOKUNAGA, T. 1988. Effects of granulocyte-macrophage colony-stimulating factor and colony-stimulating factor-1 on the proliferation and differentiation of murine alveolar macrophages. *J Immunol,* 141**,** 3383-90.

AKAZAKI, K. 1962. A concept of reticuloendothelial system. *Tohoku J Exp Med,* 76**,** 107-18.

ALLSOPP, R. C., LALO, U. & EVANS, R. J. 2010. Lipid raft association and cholesterol sensitivity of P2X1-4 receptors for ATP: chimeras and point mutants identify intracellular amino-terminal residues involved in lipid regulation of P2X1 receptors. *J Biol Chem,* 285**,** 32770-7.

ARANGO DUQUE, G. & DESCOTEAUX, A. 2014. Macrophage cytokines: involvement in immunity and infectious diseases. *Front Immunol,* 5**,** 491.

ARNOLD, L., HENRY, A., PORON, F., BABA-AMER, Y., VAN ROOIJEN, N., PLONQUET, A., GHERARDI, R. K. & CHAZAUD, B. 2007. Inflammatory monocytes recruited after skeletal muscle injury switch into antiinflammatory macrophages to support myogenesis. *J Exp Med,* 204**,** 1057-69.

ASATRYAN, L., POPOVA, M., PERKINS, D., TRUDELL, J. R., ALKANA, R. L. & DAVIES, D. L. 2010. Ivermectin antagonizes ethanol inhibition in purinergic P2X4 receptors. *J Pharmacol Exp Ther,* 334**,** 720-8.

ASE, A. R., HONSON, N. S., ZAGHDANE, H., PFEIFER, T. A. & SEGUELA, P. 2015. Identification and characterization of a selective allosteric antagonist of human P2X4 receptor channels. *Mol Pharmacol,* 87**,** 606-16.

AUFFRAY, C., FOGG, D., GARFA, M., ELAIN, G., JOIN-LAMBERT, O., KAYAL, S., SARNACKI, S., CUMANO, A., LAUVAU, G. & GEISSMANN, F. 2007. Monitoring of blood vessels and tissues by a population of monocytes with patrolling behavior. *Science,* 317**,** 666-70.

AUWERX, J. 1991. The human leukemia cell line, THP-1: a multifacetted model for the study of monocyte-macrophage differentiation. *Experientia,* 47**,** 22-31.

BABU, R. & BROWN, A. 2013. A consensus surface activation marker signature is partially dependent on human immunodeficiency virus type 1 Nef expression within productively infected macrophages. *Retrovirology,* 10**,** 155.

BAJ-KRZYWORZEKA, M., MYTAR, B., SZATANEK, R., SURMIAK, M., WEGLARCZYK, K., BARAN, J. & SIEDLAR, M. 2016. Colorectal cancer-derived microvesicles modulate differentiation of human monocytes to macrophages. *J Transl Med,* 14**,** 36.

BALASUBRAMANIAN, R., RUIZ DE AZUA, I., WESS, J. & JACOBSON, K. A. 2010. Activation of distinct P2Y receptor subtypes stimulates insulin secretion in MIN6 mouse pancreatic beta cells. *Biochem Pharmacol,* 79**,** 1317-26.

BALAZS, B., DANKO, T., KOVACS, G., KOLES, L., HEDIGER, M. A. & ZSEMBERY, A. 2013a. Investigation of the inhibitory effects of the benzodiazepine derivative, 5-BDBD on P2X4 purinergic receptors by two complementary methods. *Cell Physiol Biochem,* 32**,** 11-24.

BALAZS, Y. S., LISITSIN, E., CARMIEL, O., SHOHAM, G., SHOHAM, Y. & SCHMIDT, A. 2013b. Identifying critical unrecognized sugar-protein interactions in GH10 xylanases from Geobacillus stearothermophilus using STD NMR. *FEBS J,* 280**,** 4652-65.

BAR, I., GUNS, P. J., METALLO, J., CAMMARATA, D., WILKIN, F., BOEYNAMS, J. M., BULT, H. & ROBAYE, B. 2008. Knockout mice reveal a role for P2Y6 receptor in macrophages, endothelial cells, and vascular smooth muscle cells. *Mol Pharmacol,* 74**,** 777-84.

BARRERA, N. P., ORMOND, S. J., HENDERSON, R. M., MURRELL-LAGNADO, R. D. & EDWARDSON, J. M. 2005. Atomic force microscopy imaging demonstrates that P2X2 receptors are trimers but that P2X6 receptor subunits do not oligomerize. *J Biol Chem,* 280**,** 10759-65.

BARTH, M. W., HENDRZAK, J. A., MELNICOFF, M. J. & MORAHAN, P. S. 1995. Review of the macrophage disappearance reaction. *J Leukoc Biol,* 57**,** 361-7.

BASTID, J., REGAIRAZ, A., BONNEFOY, N., DEJOU, C., GIUSTINIANI, J., LAHEURTE, C., COCHAUD, S., LAPREVOTTE, E., FUNCK-BRENTANO, E., HEMON, P., GROS, L., BEC, N., LARROQUE, C., ALBERICI, G., BENSUSSAN, A. & ELIAOU, J. F. 2015. Inhibition of CD39 enzymatic function at the surface of tumor cells alleviates their immunosuppressive activity. *Cancer Immunol Res,* 3**,** 254-65.

BEAN, B. P., WILLIAMS, C. A. & CEELEN, P. W. 1990. ATP-activated channels in rat and bullfrog sensory neurons: current-voltage relation and single-channel behavior. *J Neurosci,* 10**,** 11-9.

BERCHTOLD, S., OGILVIE, A. L., BOGDAN, C., MUHL-ZURBES, P., OGILVIE, A., SCHULER, G. & STEINKASSERER, A. 1999. Human monocyte derived dendritic cells express functional P2X and P2Y receptors as well as ecto-nucleotidases. *FEBS Lett,* 458**,** 424-8.

BERRIDGE, M. J. 1993. Inositol trisphosphate and calcium signalling. *Nature,* 361**,** 315-25.

BERRIDGE, M. J. 1997. Elementary and global aspects of calcium signalling. *J Physiol,* 499 (Pt 2)**,** 291-306.

BERRIDGE, M. J., LIPP, P. & BOOTMAN, M. D. 2000. The versatility and universality of calcium signalling. *Nat Rev Mol Cell Biol,* 1**,** 11-21.

BEUSCHER, H. U., GUNTHER, C. & ROLLINGHOFF, M. 1990. IL-1 beta is secreted by activated murine macrophages as biologically inactive precursor. *J Immunol,* 144**,** 2179-83.

BHATT, D. L. & TOPOL, E. J. 2003. Scientific and therapeutic advances in antiplatelet therapy. *Nat Rev Drug Discov,* 2**,** 15-28.

BLAUSTEIN, M. P. & LEDERER, W. J. 1999. Sodium/calcium exchange: its physiological implications. *Physiol Rev,* 79**,** 763-854.

BOBANOVIC, L. K., ROYLE, S. J. & MURRELL-LAGNADO, R. D. 2002. P2X receptor trafficking in neurons is subunit specific. *J Neurosci,* 22**,** 4814-24.

BODIN, P. & BURNSTOCK, G. 2001. Purinergic signalling: ATP release. *Neurochem Res,* 26**,** 959-69.

BOOTMAN, M. D. 2012. Calcium signaling. *Cold Spring Harb Perspect Biol,* 4**,** a011171.

BOSSHART, H. & HEINZELMANN, M. 2016. THP-1 cells as a model for human monocytes. *Ann Transl Med,* 4**,** 438.

BOUMECHACHE, M., MASIN, M., EDWARDSON, J. M., GORECKI, D. C. & MURRELL-LAGNADO, R. 2009. Analysis of assembly and trafficking of native P2X4 and P2X7 receptor complexes in rodent immune cells. *J Biol Chem,* 284**,** 13446-54.

BOWLER, J. W., BAILEY, R. J., NORTH, R. A. & SURPRENANT, A. 2003. P2X4, P2Y1 and P2Y2 receptors on rat alveolar macrophages. *Br J Pharmacol,* 140**,** 567-75.

BRADDING, P., OKAYAMA, Y., KAMBE, N. & SAITO, H. 2003. Ion channel gene expression in human lung, skin, and cord blood-derived mast cells. *J Leukoc Biol,* 73**,** 614-20.

BRONE, B., MOECHARS, D., MARRANNES, R., MERCKEN, M. & MEERT, T. 2007. P2X currents in peritoneal macrophages of wild type and P2X4 -/- mice. *Immunol Lett,* 113**,** 83-9.

BROUGH, D., LE FEUVRE, R. A., WHEELER, R. D., SOLOVYOVA, N., HILFIKER, S., ROTHWELL, N. J. & VERKHRATSKY, A. 2003. Ca2+ stores and Ca2+ entry differentially contribute to the release of IL-1 beta and IL-1 alpha from murine macrophages. *J Immunol,* 170**,** 3029-36.

BROUGH, D. & ROTHWELL, N. J. 2007. Caspase-1-dependent processing of pro-interleukin-1beta is cytosolic and precedes cell death. *J Cell Sci,* 120**,** 772-81.

BUCHTHAL, F. & FOLKOW, B. 1948. Interaction between acetylcholine and adenosine triphosphate in normal, curarised and denervated muscle. *Acta Physiol Scand,* 15**,** 150-60.

BUELL, G., COLLO, G. & RASSENDREN, F. 1996. P2X receptors: an emerging channel family. *Eur J Neurosci,* 8**,** 2221-8.

BURKHART, C. N. 2000. Ivermectin: an assessment of its pharmacology, microbiology and safety. *Vet Hum Toxicol,* 42**,** 30-5.

BURNSTOCK, G. 1972. Purinergic nerves. *Pharmacol Rev,* 24**,** 509-81.

BURNSTOCK, G. 2006. Purinergic signalling. *British Journal of Pharmacology,* 147**,** S172-S181.

BURNSTOCK, G. 2007. Purine and pyrimidine receptors. *Cell Mol Life Sci,* 64**,** 1471-83.

BURNSTOCK, G. & BOEYNAEMS, J. M. 2014. Purinergic signalling and immune cells. *Purinergic Signal,* 10**,** 529-64.

BURNSTOCK, G. & KENNEDY, C. 1985. Is there a basis for distinguishing two types of P2-purinoceptor? *Gen Pharmacol,* 16**,** 433-40.

BURNSTOCK, G. & KNIGHT, G. E. 2004. Cellular distribution and functions of P2 receptor subtypes in different systems. *Int Rev Cytol,* 240**,** 31-304.

BURNSTOCK, G. & WILLIAMS, M. 2000. P2 purinergic receptors: modulation of cell function and therapeutic potential. *J Pharmacol Exp Ther,* 295**,** 862-9.

CAMPWALA, H. & FOUNTAIN, S. J. 2013. Constitutive and agonist stimulated ATP secretion in leukocytes. *Commun Integr Biol,* 6**,** e23631.

CARROLL, W. A., DONNELLY-ROBERTS, D. & JARVIS, M. F. 2009. Selective P2X(7) receptor antagonists for chronic inflammation and pain. *Purinergic Signal,* 5**,** 63-73.

CASELEY, E. A., MUENCH, S. P., ROGER, S., MAO, H. J., BALDWIN, S. A. & JIANG, L. H. 2014. Non-synonymous single nucleotide polymorphisms in the P2X receptor genes: association with diseases, impact on receptor functions and potential use as diagnosis biomarkers. *Int J Mol Sci,* 15**,** 13344-71.

CEKIC, C. & LINDEN, J. 2016. Purinergic regulation of the immune system. *Nat Rev Immunol,* 16**,** 177-92.

CHAVEY, C. & FAJAS, L. 2009. CXCL5 drives obesity to diabetes, and further. *Aging (Albany NY),* 1**,** 674-7.

CHAWLA, A., NGUYEN, K. D. & GOH, Y. P. 2011. Macrophage-mediated inflammation in metabolic disease. *Nat Rev Immunol,* 11**,** 738-49.

CHEN, K., ZHANG, J., ZHANG, W., ZHANG, J., YANG, J., LI, K. & HE, Y. 2013. ATP-P2X4 signaling mediates NLRP3 inflammasome activation: a novel pathway of diabetic nephropathy. *Int J Biochem Cell Biol,* 45**,** 932-43.

CHESSELL, I. P., HATCHER, J. P., BOUNTRA, C., MICHEL, A. D., HUGHES, J. P., GREEN, P., EGERTON, J., MURFIN, M., RICHARDSON, J., PECK, W. L., GRAHAMES, C. B., CASULA, M. A., YIANGOU, Y., BIRCH, R., ANAND, P. & BUELL, G. N. 2005. Disruption of the P2X7 purinoceptor gene abolishes chronic inflammatory and neuropathic pain. *Pain,* 114**,** 386-96.

CHITU, V. & STANLEY, E. R. 2006. Colony-stimulating factor-1 in immunity and inflammation. *Curr Opin Immunol,* 18**,** 39-48.

CHUA, D. & IGNASZEWSKI, A. 2009. Clopidogrel in acute coronary syndromes. *BMJ,* 338**,** b1180.

CLAPHAM, D. E. 2007. Calcium signaling. *Cell,* 131**,** 1047-58.

CLARKE, C. E., BENHAM, C. D., BRIDGES, A., GEORGE, A. R. & MEADOWS, H. J. 2000. Mutation of histidine 286 of the human P2X4 purinoceptor removes extracellular pH sensitivity. *J Physiol,* 523 Pt 3**,** 697-703.

CODDOU, C., YAN, Z., OBSIL, T., HUIDOBRO-TORO, J. P. & STOJILKOVIC, S. S. 2011. Activation and regulation of purinergic P2X receptor channels. *Pharmacol Rev,* 63**,** 641-83.

COHEN, H. B., BRIGGS, K. T., MARINO, J. P., RAVID, K., ROBSON, S. C. & MOSSER, D. M. 2013. TLR stimulation initiates a CD39-based autoregulatory mechanism that limits macrophage inflammatory responses. *Blood,* 122**,** 1935-45.

COMMUNI, D., PARMENTIER, M. & BOEYNAEMS, J. M. 1996. Cloning, functional expression and tissue distribution of the human P2Y6 receptor. *Biochem Biophys Res Commun,* 222**,** 303-8.

COUTINHO-SILVA, R., OJCIUS, D. M., GORECKI, D. C., PERSECHINI, P. M., BISAGGIO, R. C., MENDES, A. N., MARKS, J., BURNSTOCK, G. & DUNN, P. M. 2005. Multiple P2X and P2Y receptor subtypes in mouse J774, spleen and peritoneal macrophages. *Biochem Pharmacol,* 69**,** 641-55.

CRAWFORD, S. E., STELLMACH, V., MURPHY-ULLRICH, J. E., RIBEIRO, S. M., LAWLER, J., HYNES, R. O., BOIVIN, G. P. & BOUCK, N. 1998. Thrombospondin-1 is a major activator of TGF-beta1 in vivo. *Cell,* 93**,** 1159-70.

CROZAT, K., GUITON, R., GUILLIAMS, M., HENRI, S., BARANEK, T., SCHWARTZ-CORNIL, I., MALISSEN, B. & DALOD, M. 2010. Comparative genomics as a tool to reveal functional equivalences between human and mouse dendritic cell subsets. *Immunol Rev,* 234**,** 177-98.

DAEMS, W. T., KOERTEN, H. K. & SORANZO, M. R. 1976. Differences between monocyte-derived and tissue macrophages. *Adv Exp Med Biol,* 73 PT-A**,** 27-40.

DAI, Z., WU, J., CHEN, F., CHENG, Q., ZHANG, M., WANG, Y., GUO, Y. & SONG, T. 2016. CXCL5 promotes the proliferation and migration of glioma cells in autocrine- and paracrine-dependent manners. *Oncol Rep.*

DAIGNEAULT, M., PRESTON, J. A., MARRIOTT, H. M., WHYTE, M. K. & DOCKRELL, D. H. 2010. The identification of markers of macrophage differentiation in PMA-stimulated THP-1 cells and monocyte-derived macrophages. *PLoS One,* 5**,** e8668.

DALEY, J. M., BRANCATO, S. K., THOMAY, A. A., REICHNER, J. S. & ALBINA, J. E. 2010. The phenotype of murine wound macrophages. *J Leukoc Biol,* 87**,** 59-67.

DAO-UNG, P., SKARRATT, K. K., FULLER, S. J. & STOKES, L. 2015. Paroxetine suppresses recombinant human P2X7 responses. *Purinergic Signal,* 11**,** 481-90.

DAVIES, L. C., ROSAS, M., SMITH, P. J., FRASER, D. J., JONES, S. A. & TAYLOR, P. R. 2011. A quantifiable proliferative burst of tissue macrophages restores homeostatic macrophage populations after acute inflammation. *Eur J Immunol,* 41**,** 2155-64.

DAVIES, L. C. & TAYLOR, P. R. 2015. Tissue-resident macrophages: then and now. *Immunology,* 144**,** 541-8.

DE DUVE, D. 1969. The peroxisome: a new cytoplasmic organelle. *Proc R Soc Lond B Biol Sci,* 173**,** 71-83.

DE FILIPPO, K., DUDECK, A., HASENBERG, M., NYE, E., VAN ROOIJEN, N., HARTMANN, K., GUNZER, M., ROERS, A. & HOGG, N. 2013. Mast cell and macrophage chemokines CXCL1/CXCL2 control the early stage of neutrophil recruitment during tissue inflammation. *Blood,* 121**,** 4930-7.

DE PLAEN, I. G., HAN, X. B., LIU, X., HSUEH, W., GHOSH, S. & MAY, M. J. 2006. Lipopolysaccharide induces CXCL2/macrophage inflammatory protein-2 gene expression in enterocytes via NF-kappaB activation: independence from endogenous TNF-alpha and platelet-activating factor. *Immunology,* 118**,** 153-63.

DE RIVERO VACCARI, J. P., BASTIEN, D., YURCISIN, G., PINEAU, I., DIETRICH, W. D., DE KONINCK, Y., KEANE, R. W. & LACROIX, S. 2012. P2X4 receptors influence inflammasome activation after spinal cord injury. *J Neurosci,* 32**,** 3058-66.

DEAN, R. A., COX, J. H., BELLAC, C. L., DOUCET, A., STARR, A. E. & OVERALL, C. M. 2008. Macrophage-specific metalloelastase (MMP-12) truncates and inactivates ELR+ CXC chemokines and generates CCL2, -7, -8, and -13 antagonists: potential role of the macrophage in terminating polymorphonuclear leukocyte influx. *Blood,* 112**,** 3455-64.

DEL REY, A., RENIGUNTA, V., DALPKE, A. H., LEIPZIGER, J., MATOS, J. E., ROBAYE, B., ZUZARTE, M., KAVELAARS, A. & HANLEY, P. J. 2006. Knock-out mice reveal the contributions of P2Y and P2X receptors to nucleotide-induced Ca2+ signaling in macrophages. *J Biol Chem,* 281**,** 35147-55.

DELVES, P. J. & ROITT, I. M. 2000. The immune system. First of two parts. *N Engl J Med,* 343**,** 37-49.

DENNIS, P. A. & RIFKIN, D. B. 1991. Cellular activation of latent transforming growth factor beta requires binding to the cation-independent mannose 6-phosphate/insulin-like growth factor type II receptor. *Proc Natl Acad Sci U S A,* 88**,** 580-4.

DERYNCK, R., JARRETT, J. A., CHEN, E. Y., EATON, D. H., BELL, J. R., ASSOIAN, R. K., ROBERTS, A. B., SPORN, M. B. & GOEDDEL, D. V. 1985. Human transforming growth factor-beta complementary DNA sequence and expression in normal and transformed cells. *Nature,* 316**,** 701-5.

DERYNCK, R. & RHEE, L. 1987. Sequence of the porcine transforming growth factor-beta precursor. *Nucleic Acids Res,* 15, 3187.

DESAI, B. N. & LEITINGER, N. 2014. Purinergic and calcium signaling in macrophage function and plasticity. *Front Immunol,* 5**,** 580.

DI VIRGILIO, F., CHIOZZI, P., FERRARI, D., FALZONI, S., SANZ, J. M., MORELLI, A., TORBOLI, M., BOLOGNESI, G. & BARICORDI, O. R. 2001. Nucleotide receptors: an emerging family of regulatory molecules in blood cells. *Blood,* 97**,** 587-600.

DILER, E., SCHICHT, M., RABUNG, A., TSCHERNIG, T., MEIER, C., RAUSCH, F., GARREIS, F., BRAUER, L. & PAULSEN, F. 2014. The novel surfactant protein SP-H enhances the phagocytosis efficiency of macrophage-like cell lines U937 and MH-S. *BMC Res Notes,* 7**,** 851.

DING, S. & SACHS, F. 1999. Ion permeation and block of P2X(2) purinoceptors: single channel recordings. *J Membr Biol,* 172**,** 215-23.

DIXON, A. K., GUBITZ, A. K., SIRINATHSINGHJI, D. J., RICHARDSON, P. J. & FREEMAN, T. C. 1996. Tissue distribution of adenosine receptor mRNAs in the rat. *Br J Pharmacol,* 118**,** 1461-8.

DONNELLY-ROBERTS, D. L. & JARVIS, M. F. 2007. Discovery of P2X7 receptor-selective antagonists offers new insights into P2X7 receptor function and indicates a role in chronic pain states. *Br J Pharmacol,* 151**,** 571-9.

DOVI, J. V., HE, L. K. & DIPIETRO, L. A. 2003. Accelerated wound closure in neutrophil-depleted mice. *J Leukoc Biol,* 73**,** 448-55.

DRURY, A. N. & SZENT-GYORGYI, A. 1929. The physiological activity of adenine compounds with especial reference to their action upon the mammalian heart. *J Physiol,* 68**,** 213-37.

DUFFIELD, J. S., FORBES, S. J., CONSTANDINOU, C. M., CLAY, S., PARTOLINA, M., VUTHOORI, S., WU, S., LANG, R. & IREDALE, J. P. 2005. Selective depletion of macrophages reveals distinct, opposing roles during liver injury and repair. *J Clin Invest,* 115**,** 56-65.

DWYER, K. M., DEAGLIO, S., GAO, W., FRIEDMAN, D., STROM, T. B. & ROBSON, S. C. 2007. CD39 and control of cellular immune responses. *Purinergic Signal,* 3**,** 171-80.

DZIERZAK, E. & MEDVINSKY, A. 1995. Mouse embryonic hematopoiesis. *Trends Genet,* 11**,** 359-66.

EL-MOATASSIM, C. & DUBYAK, G. R. 1993. Dissociation of the pore-forming and phospholipase D activities stimulated via P2z purinergic receptors in BAC1.2F5 macrophages. Product inhibition of phospholipase D enzyme activity. *J Biol Chem,* 268**,** 15571-8.

ELIGINI, S., CRISCI, M., BONO, E., SONGIA, P., TREMOLI, E., COLOMBO, G. I. & COLLI, S. 2013. Human monocyte-derived macrophages spontaneously differentiated in vitro show distinct phenotypes. *J Cell Physiol,* 228**,** 1464-72.

ELLIOTT, M. R., CHEKENI, F. B., TRAMPONT, P. C., LAZAROWSKI, E. R., KADL, A., WALK, S. F., PARK, D., WOODSON, R. I., OSTANKOVICH, M., SHARMA, P., LYSIAK, J. J., HARDEN, T. K., LEITINGER, N. & RAVICHANDRAN, K. S. 2009. Nucleotides released by apoptotic cells act as a find-me signal to promote phagocytic clearance. *Nature,* 461**,** 282-6.

EMMELIN, N. & FELDBERG, W. 1948. Systemic effects of adenosine triphosphate. *Br J Pharmacol Chemother,* 3**,** 273-84.

ERB, L. & WEISMAN, G. A. 2012. Coupling of P2Y receptors to G proteins and other signaling pathways. *Wiley Interdisc Rev Membr Transp Signal,* 1**,** 789-803.

ERBEL, C., RUPP, G., HELMES, C. M., TYKA, M., LINDEN, F., DOESCH, A. O., KATUS, H. A. & GLEISSNER, C. A. 2013. An in vitro model to study heterogeneity of human macrophage differentiation and polarization. *J Vis Exp***,** e50332.

FADOK, V. A., BRATTON, D. L., KONOWAL, A., FREED, P. W., WESTCOTT, J. Y. & HENSON, P. M. 1998. Macrophages that have ingested apoptotic cells in vitro inhibit proinflammatory cytokine production through autocrine/paracrine mechanisms involving TGF-beta, PGE2, and PAF. *J Clin Invest,* 101**,** 890-8.

FERRARI, D., IDZKO, M., DICHMANN, S., PURLIS, D., VIRCHOW, C., NORGAUER, J., CHIOZZI, P., DI VIRGILIO, F. & LUTTMANN, W. 2000a. P2 purinergic receptors of human eosinophils: characterization and coupling to oxygen radical production. *FEBS Lett,* 486**,** 217-24.

FERRARI, D., LA SALA, A., CHIOZZI, P., MORELLI, A., FALZONI, S., GIROLOMONI, G., IDZKO, M., DICHMANN, S., NORGAUER, J. & DI VIRGILIO, F. 2000b. The P2 purinergic receptors of human dendritic cells: identification and coupling to cytokine release. *FASEB J,* 14**,** 2466-76.

FERRARI, D., LA SALA, A., PANTHER, E., NORGAUER, J., DI VIRGILIO, F. & IDZKO, M. 2006. Activation of human eosinophils via P2 receptors: novel findings and future perspectives. *J Leukoc Biol,* 79**,** 7-15.

FERRARI, D., STROH, C. & SCHULZE-OSTHOFF, K. 1999. P2X7/P2Z purinoreceptor-mediated activation of transcription factor NFAT in microglial cells. *J Biol Chem,* 274**,** 13205-10.

FLEETWOOD, A. J., COOK, A. D. & HAMILTON, J. A. 2005. Functions of granulocyte-macrophage colony-stimulating factor. *Crit Rev Immunol,* 25**,** 405-28.

FORD, A. Q., DASGUPTA, P., MIKHAILENKO, I., SMITH, E. M., NOBEN-TRAUTH, N. & KEEGAN, A. D. 2012. Adoptive transfer of IL-4Ralpha+ macrophages is sufficient to enhance eosinophilic inflammation in a mouse model of allergic lung inflammation. *BMC Immunol,* 13**,** 6.

FOUNTAIN, S. J. 2013. Primitive ATP-activated P2X receptors: discovery, function and pharmacology. *Front Cell Neurosci,* 7**,** 247.

FOUNTAIN, S. J. & BURNSTOCK, G. 2009. An evolutionary history of P2X receptors. *Purinergic Signal,* 5**,** 269-72.

FOUNTAIN, S. J. & NORTH, R. A. 2006. A C-terminal lysine that controls human P2X4 receptor desensitization. *J Biol Chem,* 281**,** 15044-9.

FREDHOLM, B. B., AP, I. J., JACOBSON, K. A., LINDEN, J. & MULLER, C. E. 2011. International Union of Basic and Clinical Pharmacology. LXXXI. Nomenclature and classification of adenosine receptors--an update. *Pharmacol Rev,* 63**,** 1-34.

FUJIWARA, N. & KOBAYASHI, K. 2005. Macrophages in inflammation. *Curr Drug Targets Inflamm Allergy,* 4**,** 281-6.

FULLER, R. & CHAVEZ, B. 2012. Ticagrelor (brilinta), an antiplatelet drug for acute coronary syndrome. *P T,* 37**,** 562-8.

GABEL, C. A. 2007. P2 purinergic receptor modulation of cytokine production. *Purinergic Signal,* 3**,** 27-38.

GANESH, K., DAS, A., DICKERSON, R., KHANNA, S., PARINANDI, N. L., GORDILLO, G. M., SEN, C. K. & ROY, S. 2012. Prostaglandin E(2) induces oncostatin M expression in human chronic wound macrophages through Axl receptor tyrosine kinase pathway. *J Immunol,* 189**,** 2563-73.

GANTNER, F., KUPFERSCHMIDT, R., SCHUDT, C., WENDEL, A. & HATZELMANN, A. 1997. In vitro differentiation of human monocytes to macrophages: change of PDE profile and its relationship to suppression of tumour necrosis factor-alpha release by PDE inhibitors. *Br J Pharmacol,* 121**,** 221-31.

GARCIA-GUZMAN, M., SOTO, F., GOMEZ-HERNANDEZ, J. M., LUND, P. E. & STUHMER, W. 1997. Characterization of recombinant human P2X4 receptor reveals pharmacological differences to the rat homologue. *Mol Pharmacol,* 51**,** 109-18.

GAUTIER, E. L., SHAY, T., MILLER, J., GRETER, M., JAKUBZICK, C., IVANOV, S., HELFT, J., CHOW, A., ELPEK, K. G., GORDONOV, S., MAZLOOM, A. R., MA'AYAN, A., CHUA, W. J., HANSEN, T. H., TURLEY, S. J., MERAD, M., RANDOLPH, G. J. & IMMUNOLOGICAL GENOME, C. 2012. Gene-expression profiles and transcriptional regulatory pathways that underlie the identity and diversity of mouse tissue macrophages. *Nat Immunol,* 13**,** 1118-28.

GEISSMANN, F., MANZ, M. G., JUNG, S., SIEWEKE, M. H., MERAD, M. & LEY, K. 2010. Development of monocytes, macrophages, and dendritic cells. *Science,* 327**,** 656-61.

GELDERMAN, K. A., HULTQVIST, M., PIZZOLLA, A., ZHAO, M., NANDAKUMAR, K. S., MATTSSON, R. & HOLMDAHL, R. 2007. Macrophages suppress T cell responses and arthritis development in mice by producing reactive oxygen species. *J Clin Invest,* 117**,** 3020-8.

GENIN, M., CLEMENT, F., FATTACCIOLI, A., RAES, M. & MICHIELS, C. 2015. M1 and M2 macrophages derived from THP-1 cells differentially modulate the response of cancer cells to etoposide. *BMC Cancer,* 15**,** 577.

GLASER, T., RESENDE, R. R. & ULRICH, H. 2013. Implications of purinergic receptor-mediated intracellular calcium transients in neural differentiation. *Cell Commun Signal,* 11**,** 12.

GOMBAULT, A., BARON, L. & COUILLIN, I. 2012. ATP release and purinergic signaling in NLRP3 inflammasome activation. *Front Immunol,* 3**,** 414.

GONG, D., SHI, W., YI, S. J., CHEN, H., GROFFEN, J. & HEISTERKAMP, N. 2012. TGFbeta signaling plays a critical role in promoting alternative macrophage activation. *BMC Immunol,* 13**,** 31.

GORDON, S. 2003. Alternative activation of macrophages. *Nat Rev Immunol,* 3**,** 23-35.

GORDON, S. & TAYLOR, P. R. 2005. Monocyte and macrophage heterogeneity. *Nat Rev Immunol,* 5**,** 953-64.

GORINI, S., CALLEGARI, G., ROMAGNOLI, G., MAMMI, C., MAVILIO, D., ROSANO, G., FINI, M., DI VIRGILIO, F., GULINELLI, S., FALZONI, S., CAVANI, A., FERRARI, D. & LA SALA, A. 2010. ATP secreted by endothelial cells blocks CX(3)CL 1-elicited natural killer cell chemotaxis and cytotoxicity via P2Y(1)(1) receptor activation. *Blood,* 116**,** 4492-500.

GORMAN, M. W., FEIGL, E. O. & BUFFINGTON, C. W. 2007. Human plasma ATP concentration. *Clin Chem,* 53**,** 318-25.

GOVINDAN, S., TAYLOR, E. J. & TAYLOR, C. W. 2010. Ca(2+) signalling by P2Y receptors in cultured rat aortic smooth muscle cells. *Br J Pharmacol,* 160**,** 1953-62.

GRIFFITHS, R. J., STAM, E. J., DOWNS, J. T. & OTTERNESS, I. G. 1995. ATP induces the release of IL-1 from LPS-primed cells in vivo. *J Immunol,* 154**,** 2821-8.

GU, B. J., BAIRD, P. N., VESSEY, K. A., SKARRATT, K. K., FLETCHER, E. L., FULLER, S. J., RICHARDSON, A. J., GUYMER, R. H. & WILEY, J. S. 2013.

A rare functional haplotype of the P2RX4 and P2RX7 genes leads to loss of innate phagocytosis and confers increased risk of age-related macular degeneration. *FASEB J,* 27**,** 1479-87.

GU, B. J., DUCE, J. A., VALOVA, V. A., WONG, B., BUSH, A. I., PETROU, S. & WILEY, J. S. 2012. P2X7 receptor-mediated scavenger activity of mononuclear phagocytes toward non-opsonized particles and apoptotic cells is inhibited by serum glycoproteins but remains active in cerebrospinal fluid. *J Biol Chem,* 287**,** 17318-30.

GU, B. J., SAUNDERS, B. M., JURSIK, C. & WILEY, J. S. 2010. The P2X7-nonmuscle myosin membrane complex regulates phagocytosis of nonopsonized particles and bacteria by a pathway attenuated by extracellular ATP. *Blood,* 115**,** 1621-31.

GUDIPATY, L., MUNETZ, J., VERHOEF, P. A. & DUBYAK, G. R. 2003. Essential role for Ca2+ in regulation of IL-1beta secretion by P2X7 nucleotide receptor in monocytes, macrophages, and HEK-293 cells. *Am J Physiol Cell Physiol,* 285**,** C286-99.

GUHA, D., KLAMAR, C. R., REINHART, T. & AYYAVOO, V. 2015. Transcriptional Regulation of CXCL5 in HIV-1-Infected Macrophages and Its Functional Consequences on CNS Pathology. *J Interferon Cytokine Res,* 35**,** 373-84.

GUIHARD, P., BOUTET, M. A., BROUNAIS-LE ROYER, B., GAMBLIN, A. L., AMIAUD, J., RENAUD, A., BERREUR, M., REDINI, F., HEYMANN, D., LAYROLLE, P. & BLANCHARD, F. 2015. Oncostatin m, an inflammatory cytokine produced by macrophages, supports intramembranous bone healing in a mouse model of tibia injury. *Am J Pathol,* 185**,** 765-75.

GUM, R. J., WAKEFIELD, B. & JARVIS, M. F. 2012. P2X receptor antagonists for pain management: examination of binding and physicochemical properties. *Purinergic Signal,* 8**,** 41-56.

GUO, C., MASIN, M., QURESHI, O. S. & MURRELL-LAGNADO, R. D. 2007. Evidence for functional P2X4/P2X7 heteromeric receptors. *Mol Pharmacol,* 72**,** 1447-56.

HALDAR, M. & MURPHY, K. M. 2014. Origin, development, and homeostasis of tissue-resident macrophages. *Immunol Rev,* 262**,** 25-35.

HALLORAN, M. M., WOODS, J. M., STRIETER, R. M., SZEKANECZ, Z., VOLIN, M. V., HOSAKA, S., HAINES, G. K., 3RD, KUNKEL, S. L., BURDICK, M. D., WALZ, A. & KOCH, A. E. 1999. The role of an epithelial neutrophil-activating peptide-78-like protein in rat adjuvant-induced arthritis. *J Immunol,* 162**,** 7492-500.

HAMILTON, J. A. 2008. Colony-stimulating factors in inflammation and autoimmunity. *Nat Rev Immunol,* 8**,** 533-44.

HANSSON, G. K. & HERMANSSON, A. 2011. The immune system in atherosclerosis. *Nat Immunol,* 12**,** 204-12.

HASHIMOTO, D., CHOW, A., NOIZAT, C., TEO, P., BEASLEY, M. B., LEBOEUF, M., BECKER, C. D., SEE, P., PRICE, J., LUCAS, D., GRETER, M., MORTHA, A., BOYER, S. W., FORSBERG, E. C., TANAKA, M., VAN ROOIJEN, N., GARCIA-SASTRE, A., STANLEY, E. R., GINHOUX, F., FRENETTE, P. S. & MERAD, M. 2013. Tissue-resident macrophages self-maintain locally throughout adult life with minimal contribution from circulating monocytes. *Immunity,* 38**,** 792-804.

HASHIOKA, S., WANG, Y. F., LITTLE, J. P., CHOI, H. B., KLEGERIS, A., MCGEER, P. L. & MCLARNON, J. G. 2014. Purinergic responses of calcium-dependent signaling pathways in cultured adult human astrocytes. *BMC Neurosci,* 15**,** 18.

HASKO, G., KUHEL, D. G., SALZMAN, A. L. & SZABO, C. 2000. ATP suppression of interleukin-12 and tumour necrosis factor-alpha release from macrophages. *Br J Pharmacol,* 129**,** 909-14.

HERNANDEZ-OLMOS, V., ABDELRAHMAN, A., EL-TAYEB, A., FREUDENDAHL, D., WEINHAUSEN, S. & MULLER, C. E. 2012. N-substituted phenoxazine and acridone derivatives: structure-activity relationships of potent P2X4 receptor antagonists. *J Med Chem,* 55**,** 9576-88.

HIBBS, R. E. & GOUAUX, E. 2011. Principles of activation and permeation in an anion-selective Cys-loop receptor. *Nature,* 474**,** 54-60.

HICKMAN, S. E., EL KHOURY, J., GREENBERG, S., SCHIEREN, I. & SILVERSTEIN, S. C. 1994. P2Z adenosine triphosphate receptor activity in cultured human monocyte-derived macrophages. *Blood,* 84**,** 2452-6.

HOGAN, P. G., LEWIS, R. S. & RAO, A. 2010. Molecular basis of calcium signaling in lymphocytes: STIM and ORAI. *Annu Rev Immunol,* 28**,** 491-533.

HUME, D. A. 2006. The mononuclear phagocyte system. *Curr Opin Immunol,* 18**,** 49-53.

IDZKO, M., DICHMANN, S., PANTHER, E., FERRARI, D., HEROUY, Y., VIRCHOW, C., JR., LUTTMANN, W., DI VIRGILIO, F. & NORGAUER, J. 2001. Functional characterization of P2Y and P2X receptors in human eosinophils. *J Cell Physiol,* 188**,** 329-36.

INTO, T., FUJITA, M., OKUSAWA, T., HASEBE, A., MORITA, M. & SHIBATA, K. 2002. Synergic effects of mycoplasmal lipopeptides and extracellular ATP on activation of macrophages. *Infect Immun,* 70**,** 3586-91.

ITALIANI, P. & BORASCHI, D. 2014. From Monocytes to M1/M2 Macrophages: Phenotypical vs. Functional Differentiation. *Front Immunol,* 5**,** 514.

ITALIANI, P., MAZZA, E. M., LUCCHESI, D., CIFOLA, I., GEMELLI, C., GRANDE, A., BATTAGLIA, C., BICCIATO, S. & BORASCHI, D. 2014. Transcriptomic profiling of the development of the inflammatory response in human monocytes in vitro. *PLoS One,* 9**,** e87680.

JACOB, F., PEREZ NOVO, C., BACHERT, C. & VAN CROMBRUGGEN, K. 2013. Purinergic signaling in inflammatory cells: P2 receptor expression, functional effects, and modulation of inflammatory responses. *Purinergic Signal,* 9**,** 285-306.

JACOBSON, K. A., BALASUBRAMANIAN, R., DEFLORIAN, F. & GAO, Z. G. 2012. G protein-coupled adenosine (P1) and P2Y receptors: ligand design and receptor interactions. *Purinergic Signal,* 8**,** 419-36.

JACOBSON, K. A., IVANOV, A. A., DE CASTRO, S., HARDEN, T. K. & KO, H. 2009. Development of selective agonists and antagonists of P2Y receptors. *Purinergic Signal,* 5**,** 75-89.

JAIME-FIGUEROA, S., GREENHOUSE, R., PADILLA, F., DILLON, M. P., GEVER, J. R. & FORD, A. P. 2005. Discovery and synthesis of a novel and selective drug-like P2X(1) antagonist. *Bioorg Med Chem Lett,* 15**,** 3292-5.

JANEWAY, C. A., TRAVERS, P., WALPORT, M. J. & SHLOMCHIK, M. J. 2001. Immunobiology : the immune system in health and disease. 5th ed ed. Edinburgh: Churchill Livingstone,.

JIANG, L. H., KIM, M., SPELTA, V., BO, X., SURPRENANT, A. & NORTH, R. A. 2003. Subunit arrangement in P2X receptors. *J Neurosci,* 23**,** 8903-10.

JONES, C. A., CHESSELL, I. P., SIMON, J., BARNARD, E. A., MILLER, K. J., MICHEL, A. D. & HUMPHREY, P. P. 2000. Functional characterization of the P2X(4) receptor orthologues. *Br J Pharmacol,* 129**,** 388-94.

JULIA, V., HESSEL, E. M., MALHERBE, L., GLAICHENHAUS, N., O'GARRA, A. & COFFMAN, R. L. 2002. A restricted subset of dendritic cells captures

airborne antigens and remains able to activate specific T cells long after antigen exposure. *Immunity,* 16**,** 271-83.

KACZMAREK-HAJEK, K., LORINCZI, E., HAUSMANN, R. & NICKE, A. 2012. Molecular and functional properties of P2X receptors--recent progress and persisting challenges. *Purinergic Signal,* 8**,** 375-417.

KAMADA, N., HISAMATSU, T., OKAMOTO, S., CHINEN, H., KOBAYASHI, T., SATO, T., SAKURABA, A., KITAZUME, M. T., SUGITA, A., KOGANEI, K., AKAGAWA, K. S. & HIBI, T. 2008. Unique CD14 intestinal macrophages contribute to the pathogenesis of Crohn disease via IL-23/IFN-gamma axis. *J Clin Invest,* 118**,** 2269-80.

KARMAKAR, M., KATSNELSON, M. A., DUBYAK, G. R. & PEARLMAN, E. 2016. Neutrophil P2X7 receptors mediate NLRP3 inflammasome-dependent IL-1beta secretion in response to ATP. *Nat Commun,* 7**,** 10555.

KAUFMANN, A., MUSSET, B., LIMBERG, S. H., RENIGUNTA, V., SUS, R., DALPKE, A. H., HEEG, K. M., ROBAYE, B. & HANLEY, P. J. 2005. "Host tissue damage" signal ATP promotes non-directional migration and negatively regulates toll-like receptor signaling in human monocytes. *J Biol Chem,* 280**,** 32459-67.

KAWAMURA, H., KAWAMURA, T., KANDA, Y., KOBAYASHI, T. & ABO, T. 2012. Extracellular ATP-stimulated macrophages produce macrophage inflammatory protein-2 which is important for neutrophil migration. *Immunology,* 136**,** 448-58.

KAWANO, A., TSUKIMOTO, M., MORI, D., NOGUCHI, T., HARADA, H., TAKENOUCHI, T., KITANI, H. & KOJIMA, S. 2012a. Regulation of P2X7-dependent inflammatory functions by P2X4 receptor in mouse macrophages. *Biochem Biophys Res Commun,* 420**,** 102-7.

KAWANO, A., TSUKIMOTO, M., NOGUCHI, T., HOTTA, N., HARADA, H., TAKENOUCHI, T., KITANI, H. & KOJIMA, S. 2012b. Involvement of P2X4 receptor in P2X7 receptor-dependent cell death of mouse macrophages. *Biochem Biophys Res Commun,* 419**,** 374-80.

KAWATE, T., MICHEL, J. C., BIRDSONG, W. T. & GOUAUX, E. 2009. Crystal structure of the ATP-gated P2X(4) ion channel in the closed state. *Nature,* 460**,** 592-8.

KEMP, P. A., SUGAR, R. A. & JACKSON, A. D. 2004. Nucleotide-mediated mucin secretion from differentiated human bronchial epithelial cells. *Am J Respir Cell Mol Biol,* 31**,** 446-55.

KEYSTONE, E. C., WANG, M. M., LAYTON, M., HOLLIS, S., MCINNES, I. B. & TEAM, D. C. S. 2012. Clinical evaluation of the efficacy of the P2X7 purinergic receptor antagonist AZD9056 on the signs and symptoms of rheumatoid arthritis in patients with active disease despite treatment with methotrexate or sulphasalazine. *Ann Rheum Dis,* 71**,** 1630-5.

KHAKH, B. S., BURNSTOCK, G., KENNEDY, C., KING, B. F., NORTH, R. A., SEGUELA, P., VOIGT, M. & HUMPHREY, P. P. 2001. International union of pharmacology. XXIV. Current status of the nomenclature and properties of P2X receptors and their subunits. *Pharmacol Rev,* 53**,** 107-18.

KHAKH, B. S., PROCTOR, W. R., DUNWIDDIE, T. V., LABARCA, C. & LESTER, H. A. 1999. Allosteric control of gating and kinetics at P2X(4) receptor channels. *J Neurosci,* 19**,** 7289-99.

KHANNA, S., BISWAS, S., SHANG, Y., COLLARD, E., AZAD, A., KAUH, C., BHASKER, V., GORDILLO, G. M., SEN, C. K. & ROY, S. 2010. Macrophage dysfunction impairs resolution of inflammation in the wounds of diabetic mice. *PLoS One,* 5**,** e9539.

KIM, H. S., OHNO, M., XU, B., KIM, H. O., CHOI, Y., JI, X. D., MADDILETI, S., MARQUEZ, V. E., HARDEN, T. K. & JACOBSON, K. A. 2003. 2-Substitution of adenine nucleotide analogues containing a bicyclo[3.1.0]hexane ring system locked in a northern conformation: enhanced potency as P2Y1 receptor antagonists. *J Med Chem,* 46**,** 4974-87.

KIM, M. J., TURNER, C. M., HEWITT, R., SMITH, J., BHANGAL, G., PUSEY, C. D., UNWIN, R. J. & TAM, F. W. 2014. Exaggerated renal fibrosis in P2X4 receptor-deficient mice following unilateral ureteric obstruction. *Nephrol Dial Transplant,* 29**,** 1350-61.

KIM, Y. C., LEE, J. S., SAK, K., MARTEAU, F., MAMEDOVA, L., BOEYNAEMS, J. M. & JACOBSON, K. A. 2005. Synthesis of pyridoxal phosphate derivatives with antagonist activity at the P2Y13 receptor. *Biochem Pharmacol,* 70**,** 266-74.

KNIGHT, G. E. & BURNSTOCK, G. 2004. The effect of pregnancy and the oestrus cycle on purinergic and cholinergic responses of the rat urinary bladder. *Neuropharmacology,* 46**,** 1049-56.

KOCH, A. E., KUNKEL, S. L., HARLOW, L. A., MAZARAKIS, D. D., HAINES, G. K., BURDICK, M. D., POPE, R. M., WALZ, A. & STRIETER, R. M. 1994. Epithelial neutrophil activating peptide-78: a novel chemotactic cytokine for neutrophils in arthritis. *J Clin Invest,* 94**,** 1012-8.

KOH, T. J. & DIPIETRO, L. A. 2011. Inflammation and wound healing: the role of the macrophage. *Expert Rev Mol Med,* 13**,** e23.

KORCOK, J., RAIMUNDO, L. N., DU, X., SIMS, S. M. & DIXON, S. J. 2005. P2Y6 nucleotide receptors activate NF-kappaB and increase survival of osteoclasts. *J Biol Chem,* 280**,** 16909-15.

KOTNIS, N. A., PARASU, N., FINLAY, K., JURRIAANS, E. & GHERT, M. 2011. Chronology of the radiographic appearances of the calcium sulphate-calcium phosphate synthetic bone graft composite following resection of bone tumours--a preliminary study of the normal post-operative appearances. *Skeletal Radiol,* 40**,** 563-70.

KOTNIS, S., BINGHAM, B., VASILYEV, D. V., MILLER, S. W., BAI, Y., YEOLA, S., CHANDA, P. K., BOWLBY, M. R., KAFTAN, E. J., SAMAD, T. A. & WHITESIDE, G. T. 2010. Genetic and functional analysis of human P2X5 reveals a distinct pattern of exon 10 polymorphism with predominant expression of the nonfunctional receptor isoform. *Mol Pharmacol,* 77**,** 953-60.

KRAUSGRUBER, T., BLAZEK, K., SMALLIE, T., ALZABIN, S., LOCKSTONE, H., SAHGAL, N., HUSSELL, T., FELDMANN, M. & UDALOVA, I. A. 2011. IRF5 promotes inflammatory macrophage polarization and TH1-TH17 responses. *Nat Immunol,* 12**,** 231-8.

KRUGER, M., VAN DE WINKEL, J. G., DE WIT, T. P., COOREVITS, L. & CEUPPENS, J. L. 1996. Granulocyte-macrophage colony-stimulating factor down-regulates CD14 expression on monocytes. *Immunology,* 89**,** 89-95.

LACEY, D. C., ACHUTHAN, A., FLEETWOOD, A. J., DINH, H., ROINIOTIS, J., SCHOLZ, G. M., CHANG, M. W., BECKMAN, S. K., COOK, A. D. & HAMILTON, J. A. 2012. Defining GM-CSF- and macrophage-CSF-dependent macrophage responses by in vitro models. *J Immunol,* 188**,** 5752-65.

LACY, P. 2015. Editorial: secretion of cytokines and chemokines by innate immune cells. *Front Immunol,* 6**,** 190.

LAHMAR, Q., KEIRSSE, J., LAOUI, D., MOVAHEDI, K., VAN OVERMEIRE, E. & VAN GINDERACHTER, J. A. 2016. Tissue-resident versus monocyte-

derived macrophages in the tumor microenvironment. *Biochim Biophys Acta,* 1865**,** 23-34.

LANGRISH, C. L., MCKENZIE, B. S., WILSON, N. J., DE WAAL MALEFYT, R., KASTELEIN, R. A. & CUA, D. J. 2004. IL-12 and IL-23: master regulators of innate and adaptive immunity. *Immunol Rev,* 202**,** 96-105.

LAU, O. C., SAMARAWICKRAMA, C. & SKALICKY, S. E. 2014. P2Y2 receptor agonists for the treatment of dry eye disease: a review. *Clin Ophthalmol,* 8**,** 327-34.

LE, K. T., BABINSKI, K. & SEGUELA, P. 1998. Central P2X4 and P2X6 channel subunits coassemble into a novel heteromeric ATP receptor. *J Neurosci,* 18**,** 7152-9.

LEITINGER, N. & SCHULMAN, I. G. 2013. Phenotypic polarization of macrophages in atherosclerosis. *Arterioscler Thromb Vasc Biol,* 33**,** 1120-6.

LEW, D. P., ANDERSSON, T., HED, J., DI VIRGILIO, F., POZZAN, T. & STENDAHL, O. 1985. Ca2+-dependent and Ca2+-independent phagocytosis in human neutrophils. *Nature,* 315**,** 509-11.

LEWIS, C., NEIDHART, S., HOLY, C., NORTH, R. A., BUELL, G. & SURPRENANT, A. 1995. Coexpression of P2X2 and P2X3 receptor subunits can account for ATP-gated currents in sensory neurons. *Nature,* 377**,** 432-5.

LEY, K. 2014. The second touch hypothesis: T cell activation, homing and polarization. *F1000Res,* 3**,** 37.

LEYVA, F. J., ANZINGER, J. J., MCCOY, J. P., JR. & KRUTH, H. S. 2011. Evaluation of transduction efficiency in macrophage colony-stimulating factor differentiated human macrophages using HIV-1 based lentiviral vectors. *BMC Biotechnol,* 11**,** 13.

LEYVA-ILLADES, D., CHERLA, R. P., LEE, M. S. & TESH, V. L. 2012. Regulation of cytokine and chemokine expression by the ribotoxic stress response elicited by Shiga toxin type 1 in human macrophage-like THP-1 cells. *Infect Immun,* 80**,** 2109-20.

LI, J. & FOUNTAIN, S. J. 2012. Fluvastatin suppresses native and recombinant human P2X4 receptor function. *Purinergic Signal,* 8**,** 311-6.

LI, W., HSIAO, H. M., HIGASHIKUBO, R., SAUNDERS, B. T., BHARAT, A., GOLDSTEIN, D. R., KRUPNICK, A. S., GELMAN, A. E., LAVINE, K. J. & KREISEL, D. 2016. Heart-resident CCR2+ macrophages promote neutrophil extravasation through TLR9/MyD88/CXCL5 signaling. *JCI Insight,* 1.

LI, Z., LIANG, D. & CHEN, L. 2008. Potential therapeutic targets for ATP-gated P2X receptor ion channels. *Assay Drug Dev Technol,* 6**,** 277-84.

LIANG, X., SAMWAYS, D. S., WOLF, K., BOWLES, E. A., RICHARDS, J. P., BRUNO, J., DUTERTRE, S., DIPAOLO, R. J. & EGAN, T. M. 2015. Quantifying Ca2+ current and permeability in ATP-gated P2X7 receptors. *J Biol Chem,* 290**,** 7930-42.

LIGHT, A. R., WU, Y., HUGHEN, R. W. & GUTHRIE, P. B. 2006. Purinergic receptors activating rapid intracellular Ca increases in microglia. *Neuron Glia Biol,* 2**,** 125-138.

LINK, T. M., PARK, U., VONAKIS, B. M., RABEN, D. M., SOLOSKI, M. J. & CATERINA, M. J. 2010. TRPV2 has a pivotal role in macrophage particle binding and phagocytosis. *Nat Immunol,* 11**,** 232-9.

LIU, X., WANG, N., ZHU, Y., YANG, Y., CHEN, X., FAN, S., CHEN, Q., ZHOU, H. & ZHENG, J. 2016. Inhibition of Extracellular Calcium Influx Results in Enhanced IL-12 Production in LPS-Treated Murine Macrophages by Downregulation of the CaMKKbeta-AMPK-SIRT1 Signaling Pathway. *Mediators Inflamm,* 2016**,** 6152713.

LIU, Y. C., ZOU, X. B., CHAI, Y. F. & YAO, Y. M. 2014. Macrophage polarization in inflammatory diseases. *Int J Biol Sci,* 10**,** 520-9.

LUSTER, A. D. 1998. Chemokines--chemotactic cytokines that mediate inflammation. *N Engl J Med,* 338**,** 436-45.

MA, X., YAN, W., ZHENG, H., DU, Q., ZHANG, L., BAN, Y., LI, N. & WEI, F. 2015. Regulation of IL-10 and IL-12 production and function in macrophages and dendritic cells. *F1000Res,* 4.

MAHESHWARI, A., KELLY, D. R., NICOLA, T., AMBALAVANAN, N., JAIN, S. K., MURPHY-ULLRICH, J., ATHAR, M., SHIMAMURA, M., BHANDARI, V., APRAHAMIAN, C., DIMMITT, R. A., SERRA, R. & OHLS, R. K. 2011. TGF-beta2 suppresses macrophage cytokine production and mucosal inflammatory responses in the developing intestine. *Gastroenterology,* 140**,** 242-53.

MALLAT, Z., GOJOVA, A., MARCHIOL-FOURNIGAULT, C., ESPOSITO, B., KAMATE, C., MERVAL, R., FRADELIZI, D. & TEDGUI, A. 2001. Inhibition of transforming growth factor-beta signaling accelerates atherosclerosis and induces an unstable plaque phenotype in mice. *Circ Res,* 89**,** 930-4.

MAMEDOVA, L. K., JOSHI, B. V., GAO, Z. G., VON KUGELGEN, I. & JACOBSON, K. A. 2004. Diisothiocyanate derivatives as potent, insurmountable antagonists of P2Y6 nucleotide receptors. *Biochem Pharmacol,* 67**,** 1763-70.

MANTOVANI, A., SOZZANI, S., LOCATI, M., ALLAVENA, P. & SICA, A. 2002. Macrophage polarization: tumor-associated macrophages as a paradigm for polarized M2 mononuclear phagocytes. *Trends Immunol,* 23**,** 549-55.

MARQUEZ-KLAKA, B., RETTINGER, J., BHARGAVA, Y., EISELE, T. & NICKE, A. 2007. Identification of an intersubunit cross-link between substituted cysteine residues located in the putative ATP binding site of the P2X1 receptor. *J Neurosci,* 27**,** 1456-66.

MARTINEZ, F. O. & GORDON, S. 2014. The M1 and M2 paradigm of macrophage activation: time for reassessment. *F1000Prime Rep,* 6**,** 13.

MARTINEZ, F. O., GORDON, S., LOCATI, M. & MANTOVANI, A. 2006. Transcriptional profiling of the human monocyte-to-macrophage differentiation and polarization: new molecules and patterns of gene expression. *J Immunol,* 177**,** 7303-11.

MARTINEZ, F. O., SICA, A., MANTOVANI, A. & LOCATI, M. 2008. Macrophage activation and polarization. *Front Biosci,* 13**,** 453-61.

MASSAGUE, J. 2000. How cells read TGF-beta signals. *Nat Rev Mol Cell Biol,* 1**,** 169-78.

MASSAGUE, J. & CHEN, Y. G. 2000. Controlling TGF-beta signaling. *Genes Dev,* 14**,** 627-44.

MAZZIERI, R., MUNGER, J. S. & RIFKIN, D. B. 2000. Measurement of active TGF-beta generated by cultured cells. *Methods Mol Biol,* 142**,** 13-27.

MCGARAUGHTY, S., CHU, K. L., NAMOVIC, M. T., DONNELLY-ROBERTS, D. L., HARRIS, R. R., ZHANG, X. F., SHIEH, C. C., WISMER, C. T., ZHU, C. Z., GAUVIN, D. M., FABIYI, A. C., HONORE, P., GREGG, R. J., KORT, M. E., NELSON, D. W., CARROLL, W. A., MARSH, K., FALTYNEK, C. R. & JARVIS, M. F. 2007. P2X7-related modulation of pathological nociception in rats. *Neuroscience,* 146**,** 1817-28.

MEIS, S., HAMACHER, A., HONGWISET, D., MARZIAN, C., WIESE, M., ECKSTEIN, N., ROYER, H. D., COMMUNI, D., BOEYNAEMS, J. M., HAUSMANN, R., SCHMALZING, G. & KASSACK, M. U. 2010. NF546 [4,4'-(carbonylbis(imino-3,1-phenylene-carbonylimino-3,1-(4-methyl-phenylene)-car bonylimino))-bis(1,3-xylene-alpha,alpha'-diphosphonic acid) tetrasodium salt] is a non-nucleotide P2Y11 agonist and stimulates release of interleukin-

8 from human monocyte-derived dendritic cells. *J Pharmacol Exp Ther,* 332**,** 238-47.

MELGERT, B. N., TEN HACKEN, N. H., RUTGERS, B., TIMENS, W., POSTMA, D. S. & HYLKEMA, M. N. 2011. More alternative activation of macrophages in lungs of asthmatic patients. *J Allergy Clin Immunol,* 127**,** 831-3.

MESTAS, J. & LEY, K. 2008. Monocyte-endothelial cell interactions in the development of atherosclerosis. *Trends Cardiovasc Med,* 18**,** 228-32.

MESZAROS, A. J., REICHNER, J. S. & ALBINA, J. E. 1999. Macrophage phagocytosis of wound neutrophils. *J Leukoc Biol,* 65**,** 35-42.

MESZAROS, A. J., REICHNER, J. S. & ALBINA, J. E. 2000. Macrophage-induced neutrophil apoptosis. *J Immunol,* 165**,** 435-41.

MEYERHOF, W., MULLER-BRECHLIN, R. & RICHTER, D. 1991. Molecular cloning of a novel putative G-protein coupled receptor expressed during rat spermiogenesis. *FEBS Lett,* 284**,** 155-60.

MILLER, K. J., MICHEL, A. D., CHESSELL, I. P. & HUMPHREY, P. P. 1998. Cibacron blue allosterically modulates the rat P2X4 receptor. *Neuropharmacology,* 37**,** 1579-86.

MILLS, C. D. 2012. M1 and M2 Macrophages: Oracles of Health and Disease. *Crit Rev Immunol,* 32**,** 463-88.

MILLS, C. D., KINCAID, K., ALT, J. M., HEILMAN, M. J. & HILL, A. M. 2000. M-1/M-2 macrophages and the Th1/Th2 paradigm. *J Immunol,* 164**,** 6166-73.

MILLS, C. D. & LEY, K. 2014. M1 and M2 macrophages: the chicken and the egg of immunity. *J Innate Immun,* 6**,** 716-26.

MOGENSEN, T. H. 2009. Pathogen recognition and inflammatory signaling in innate immune defenses. *Clin Microbiol Rev,* 22**,** 240-73, Table of Contents.

MOORE, K. J., SHEEDY, F. J. & FISHER, E. A. 2013. Macrophages in atherosclerosis: a dynamic balance. *Nat Rev Immunol,* 13**,** 709-21.

MOORE, K. J. & TABAS, I. 2011. Macrophages in the pathogenesis of atherosclerosis. *Cell,* 145**,** 341-55.

MOREIRA, A. P., CAVASSANI, K. A., HULLINGER, R., ROSADA, R. S., FONG, D. J., MURRAY, L., HESSON, D. P. & HOGABOAM, C. M. 2010. Serum amyloid P attenuates M2 macrophage activation and protects against fungal spore-induced allergic airway disease. *J Allergy Clin Immunol,* 126**,** 712-721 e7.

MORRIS, D. L., CHO, K. W., DELPROPOSTO, J. L., OATMEN, K. E., GELETKA, L. M., MARTINEZ-SANTIBANEZ, G., SINGER, K. & LUMENG, C. N. 2013. Adipose tissue macrophages function as antigen-presenting cells and regulate adipose tissue CD4+ T cells in mice. *Diabetes,* 62**,** 2762-72.

MOSSER, D. M. & EDWARDS, J. P. 2008. Exploring the full spectrum of macrophage activation. *Nat Rev Immunol,* 8**,** 958-69.

MUKAIDA, N. 2003. Pathophysiological roles of interleukin-8/CXCL8 in pulmonary diseases. *Am J Physiol Lung Cell Mol Physiol,* 284**,** L566-77.

MULLER, C. E. 2015. Medicinal chemistry of P2X receptors: allosteric modulators. *Curr Med Chem,* 22**,** 929-41.

MUNGER, J. S., HUANG, X., KAWAKATSU, H., GRIFFITHS, M. J., DALTON, S. L., WU, J., PITTET, J. F., KAMINSKI, N., GARAT, C., MATTHAY, M. A., RIFKIN, D. B. & SHEPPARD, D. 1999. The integrin alpha v beta 6 binds and activates latent TGF beta 1: a mechanism for regulating pulmonary inflammation and fibrosis. *Cell,* 96**,** 319-28.

MURAI, M., TUROVSKAYA, O., KIM, G., MADAN, R., KARP, C. L., CHEROUTRE, H. & KRONENBERG, M. 2009. Interleukin 10 acts on regulatory T cells to maintain expression of the transcription factor Foxp3 and suppressive function in mice with colitis. *Nat Immunol,* 10**,** 1178-84.

MURRAY, P. J. & WYNN, T. A. 2011a. Obstacles and opportunities for understanding macrophage polarization. *J Leukoc Biol,* 89**,** 557-63.

MURRAY, P. J. & WYNN, T. A. 2011b. Protective and pathogenic functions of macrophage subsets. *Nat Rev Immunol,* 11**,** 723-37.

MYLONAS, K. J., NAIR, M. G., PRIETO-LAFUENTE, L., PAAPE, D. & ALLEN, J. E. 2009. Alternatively activated macrophages elicited by helminth infection can be reprogrammed to enable microbial killing. *J Immunol,* 182**,** 3084-94.

MYRTEK, D., MULLER, T., GEYER, V., DERR, N., FERRARI, D., ZISSEL, G., DURK, T., SORICHTER, S., LUTTMANN, W., KUEPPER, M., NORGAUER, J., DI VIRGILIO, F., VIRCHOW, J. C., JR. & IDZKO, M. 2008. Activation of human alveolar macrophages via P2 receptors: coupling to intracellular $Ca2+$ increases and cytokine secretion. *J Immunol,* 181**,** 2181-8.

NAGATA, K., IMAI, T., YAMASHITA, T., TSUDA, M., TOZAKI-SAITOH, H. & INOUE, K. 2009. Antidepressants inhibit P2X4 receptor function: a possible involvement in neuropathic pain relief. *Mol Pain,* 5**,** 20.

NATHAN, C. & DING, A. 2010. Nonresolving inflammation. *Cell,* 140**,** 871-82.

NELSON, D. W., GREGG, R. J., KORT, M. E., PEREZ-MEDRANO, A., VOIGHT, E. A., WANG, Y., GRAYSON, G., NAMOVIC, M. T., DONNELLY-ROBERTS, D. L., NIFORATOS, W., HONORE, P., JARVIS, M. F., FALTYNEK, C. R. & CARROLL, W. A. 2006. Structure-activity relationship studies on a series of novel, substituted 1-benzyl-5-phenyltetrazole P2X7 antagonists. *J Med Chem,* 49**,** 3659-66.

NEURATH, M. F. 2014. Cytokines in inflammatory bowel disease. *Nat Rev Immunol,* 14**,** 329-42.

NICKE, A., KERSCHENSTEINER, D. & SOTO, F. 2005. Biochemical and functional evidence for heteromeric assembly of P2X1 and P2X4 subunits. *J Neurochem,* 92**,** 925-33.

NOBILE, M., MONALDI, I., ALLOISIO, S., CUGNOLI, C. & FERRONI, S. 2003. ATP-induced, sustained calcium signalling in cultured rat cortical astrocytes: evidence for a non-capacitative, P2X7-like-mediated calcium entry. *FEBS Lett,* 538**,** 71-6.

NORENBERG, W., SOBOTTKA, H., HEMPEL, C., PLOTZ, T., FISCHER, W., SCHMALZING, G. & SCHAEFER, M. 2012. Positive allosteric modulation by ivermectin of human but not murine P2X7 receptors. *Br J Pharmacol,* 167**,** 48-66.

NORTH, R. A. 2002. Molecular physiology of P2X receptors. *Physiol Rev,* 82**,** 1013-67.

NORTH, R. A. 2016. P2X receptors. *Philosophical Transactions of the Royal Society B-Biological Sciences,* 371.

NORTH, R. A. & JARVIS, M. F. 2013. P2X receptors as drug targets. *Mol Pharmacol,* 83**,** 759-69.

OSTROVSKAYA, O., ASATRYAN, L., WYATT, L., POPOVA, M., LI, K., PEOPLES, R. W., ALKANA, R. L. & DAVIES, D. L. 2011. Ethanol is a fast channel inhibitor of P2X4 receptors. *J Pharmacol Exp Ther,* 337**,** 171-9.

OWEN, J. L. & MOHAMADZADEH, M. 2013. Macrophages and chemokines as mediators of angiogenesis. *Front Physiol,* 4**,** 159.

PARK, E. K., JUNG, H. S., YANG, H. I., YOO, M. C., KIM, C. & KIM, K. S. 2007. Optimized THP-1 differentiation is required for the detection of responses to weak stimuli. *Inflamm Res,* 56**,** 45-50.

PARKIN, J. & COHEN, B. 2001. An overview of the immune system. *Lancet,* 357**,** 1777-89.

PARWARESCH, M. R. & WACKER, H. H. 1984. Origin and kinetics of resident tissue macrophages. Parabiosis studies with radiolabelled leucocytes. *Cell Tissue Kinet,* 17**,** 25-39.

PELEGRIN, P. & SURPRENANT, A. 2006. Pannexin-1 mediates large pore formation and interleukin-1beta release by the ATP-gated P2X7 receptor. *EMBO J,* 25**,** 5071-82.

PEREZ-FLORES, G., LEVESQUE, S. A., PACHECO, J., VACA, L., LACROIX, S., PEREZ-CORNEJO, P. & ARREOLA, J. 2015. The P2X7/P2X4 interaction shapes the purinergic response in murine macrophages. *Biochem Biophys Res Commun,* 467**,** 484-90.

PEREZ-SEN, R., QUEIPO, M. J., MORENTE, V., ORTEGA, F., DELICADO, E. G. & MIRAS-PORTUGAL, M. T. 2015. Neuroprotection Mediated by P2Y13 Nucleotide Receptors in Neurons. *Comput Struct Biotechnol J,* 13**,** 160-8.

PERREGAUX, D. & GABEL, C. A. 1994. Interleukin-1 beta maturation and release in response to ATP and nigericin. Evidence that potassium depletion mediated by these agents is a necessary and common feature of their activity. *J Biol Chem,* 269**,** 15195-203.

PIKE, L. J. 2004. Lipid rafts: heterogeneity on the high seas. *Biochem J,* 378**,** 281-92.

PONOMAREV, E. D., VEREMEYKO, T., BARTENEVA, N., KRICHEVSKY, A. M. & WEINER, H. L. 2011. MicroRNA-124 promotes microglia quiescence and suppresses EAE by deactivating macrophages via the C/EBP-alpha-PU.1 pathway. *Nat Med,* 17**,** 64-70.

POZZAN, T., RIZZUTO, R., VOLPE, P. & MELDOLESI, J. 1994. Molecular and cellular physiology of intracellular calcium stores. *Physiol Rev,* 74**,** 595-636.

PRIEL, A. & SILBERBERG, S. D. 2004. Mechanism of ivermectin facilitation of human P2X4 receptor channels. *J Gen Physiol,* 123**,** 281-93.

PUBILL, D., DAYANITHI, G., SIATKA, C., ANDRES, M., DUFOUR, M. N., GUILLON, G. & MENDRE, C. 2001. ATP induces intracellular calcium increases and actin cytoskeleton disaggregation via P2x receptors. *Cell Calcium,* 29**,** 299-309.

PUCHALOWICZ, K., TARNOWSKI, M., BARANOWSKA-BOSIACKA, I., CHLUBEK, D. & DZIEDZIEJKO, V. 2014. P2X and P2Y receptors-role in the pathophysiology of the nervous system. *Int J Mol Sci,* 15**,** 23672-704.

PULTE, E. D., BROEKMAN, M. J., OLSON, K. E., DROSOPOULOS, J. H., KIZER, J. R., ISLAM, N. & MARCUS, A. J. 2007. CD39/NTPDase-1 activity and expression in normal leukocytes. *Thromb Res,* 121**,** 309-17.

PY, B. F., JIN, M., DESAI, B. N., PENUMAKA, A., ZHU, H., KOBER, M., DIETRICH, A., LIPINSKI, M. M., HENRY, T., CLAPHAM, D. E. & YUAN, J. 2014. Caspase-11 controls interleukin-1beta release through degradation of TRPC1. *Cell Rep,* 6**,** 1122-8.

QIN, Z. 2012. The use of THP-1 cells as a model for mimicking the function and regulation of monocytes and macrophages in the vasculature. *Atherosclerosis,* 221**,** 2-11.

QU, Y., FRANCHI, L., NUNEZ, G. & DUBYAK, G. R. 2007. Nonclassical IL-1 beta secretion stimulated by P2X7 receptors is dependent on inflammasome activation and correlated with exosome release in murine macrophages. *J Immunol,* 179**,** 1913-25.

QURESHI, O. S., PARAMASIVAM, A., YU, J. C. & MURRELL-LAGNADO, R. D. 2007. Regulation of P2X4 receptors by lysosomal targeting, glycan protection and exocytosis. *J Cell Sci,* 120**,** 3838-49.

RAOUF, R., CHABOT-DORE, A. J., ASE, A. R., BLAIS, D. & SEGUELA, P. 2007. Differential regulation of microglial P2X4 and P2X7 ATP receptors following LPS-induced activation. *Neuropharmacology,* 53**,** 496-504.

REIFENBERG, K., CHENG, F., ORNING, C., CRAIN, J., KUPPER, I., WIESE, E., PROTSCHKA, M., BLESSING, M., LACKNER, K. J. & TORZEWSKI, M. 2012. Overexpression of TGF-ss1 in macrophages reduces and stabilizes atherosclerotic plaques in ApoE-deficient mice. *PLoS One,* 7**,** e40990.

REPNIK, U., STARR, A. E., OVERALL, C. M. & TURK, B. 2015. Cysteine Cathepsins Activate ELR Chemokines and Inactivate Non-ELR Chemokines. *J Biol Chem,* 290**,** 13800-11.

ROBBINS, S. H., WALZER, T., DEMBELE, D., THIBAULT, C., DEFAYS, A., BESSOU, G., XU, H., VIVIER, E., SELLARS, M., PIERRE, P., SHARP, F. R., CHAN, S., KASTNER, P. & DALOD, M. 2008. Novel insights into the relationships between dendritic cell subsets in human and mouse revealed by genome-wide expression profiling. *Genome Biol,* 9**,** R17.

ROBINSON, L. E. & MURRELL-LAGNADO, R. D. 2013. The trafficking and targeting of P2X receptors. *Front Cell Neurosci,* 7**,** 233.

ROBSON, S. C., SEVIGNY, J. & ZIMMERMANN, H. 2006. The E-NTPDase family of ectonucleotidases: Structure function relationships and pathophysiological significance. *Purinergic Signal,* 2**,** 409-30.

ROSZER, T. 2015. Understanding the Mysterious M2 Macrophage through Activation Markers and Effector Mechanisms. *Mediators Inflamm,* 2015**,** 816460.

ROUSSELLE, A., QADRI, F., LEUKEL, L., YILMAZ, R., FONTAINE, J. F., SIHN, G., BADER, M., AHLUWALIA, A. & DUCHENE, J. 2013. CXCL5 limits macrophage foam cell formation in atherosclerosis. *J Clin Invest,* 123**,** 1343-7.

ROYLE, S. J., BOBANOVIC, L. K. & MURRELL-LAGNADO, R. D. 2002. Identification of a non-canonical tyrosine-based endocytic motif in an ionotropic receptor. *J Biol Chem,* 277**,** 35378-85.

ROYLE, S. J., QURESHI, O. S., BOBANOVIC, L. K., EVANS, P. R., OWEN, D. J. & MURRELL-LAGNADO, R. D. 2005. Non-canonical YXXGPhi endocytic motifs: recognition by AP2 and preferential utilization in P2X4 receptors. *J Cell Sci,* 118**,** 3073-80.

RYU, S. Y., PEIXOTO, P. M., WON, J. H., YULE, D. I. & KINNALLY, K. W. 2010. Extracellular ATP and P2Y2 receptors mediate intercellular Ca(2+) waves induced by mechanical stimulation in submandibular gland cells: Role of mitochondrial regulation of store operated Ca(2+) entry. *Cell Calcium,* 47**,** 65-76.

SADAHIRO, A., DIOGO, C. L., OSHIRO, T. M. & SHIKANAI-YASUDA, M. A. 2007. Kinetics of IFN-gamma, TNF-alpha, IL-10 and IL-4 production by mononuclear cells stimulated with gp43 peptides, in patients cured of paracoccidioidomycosis. *Rev Soc Bras Med Trop,* 40**,** 156-62.

SAKAKI, H., FUJIWAKI, T., TSUKIMOTO, M., KAWANO, A., HARADA, H. & KOJIMA, S. 2013a. P2X4 receptor regulates P2X7 receptor-dependent IL-1beta and IL-18 release in mouse bone marrow-derived dendritic cells. *Biochem Biophys Res Commun,* 432**,** 406-11.

SAKAKI, H., TSUKIMOTO, M., HARADA, H., MORIYAMA, Y. & KOJIMA, S. 2013b. Autocrine regulation of macrophage activation via exocytosis of ATP and activation of P2Y11 receptor. *PLoS One,* 8**,** e59778.

SATO, Y., TSUBOI, R., LYONS, R., MOSES, H. & RIFKIN, D. B. 1990. Characterization of the activation of latent TGF-beta by co-cultures of

endothelial cells and pericytes or smooth muscle cells: a self-regulating system. *J Cell Biol,* 111**,** 757-63.

SCHRIJVERS, D. M., DE MEYER, G. R., HERMAN, A. G. & MARTINET, W. 2007. Phagocytosis in atherosclerosis: Molecular mechanisms and implications for plaque progression and stability. *Cardiovasc Res,* 73**,** 470-80.

SEGUELA, P., HAGHIGHI, A., SOGHOMONIAN, J. J. & COOPER, E. 1996. A novel neuronal P2x ATP receptor ion channel with widespread distribution in the brain. *J Neurosci,* 16**,** 448-55.

SEPURU, K. M., POLURI, K. M. & RAJARATHNAM, K. 2014. Solution structure of CXCL5--a novel chemokine and adipokine implicated in inflammation and obesity. *PLoS One,* 9**,** e93228.

SIEWEKE, M. H. & ALLEN, J. E. 2013. Beyond stem cells: self-renewal of differentiated macrophages. *Science,* 342**,** 1242974.

SIM, J. A. & NORTH, R. A. 2010. Amitriptyline does not block the action of ATP at human P2X4 receptor. *Br J Pharmacol,* 160**,** 88-92.

SIM, J. A., PARK, C. K., OH, S. B., EVANS, R. J. & NORTH, R. A. 2007. P2X1 and P2X4 receptor currents in mouse macrophages. *Br J Pharmacol,* 152**,** 1283-90.

SINDRILARU, A., PETERS, T., WIESCHALKA, S., BAICAN, C., BAICAN, A., PETER, H., HAINZL, A., SCHATZ, S., QI, Y., SCHLECHT, A., WEISS, J. M., WLASCHEK, M., SUNDERKOTTER, C. & SCHARFFETTER-KOCHANEK, K. 2011. An unrestrained proinflammatory M1 macrophage population induced by iron impairs wound healing in humans and mice. *J Clin Invest,* 121**,** 985-97.

SLUYTER, R., BARDEN, J. A. & WILEY, J. S. 2001. Detection of P2X purinergic receptors on human B lymphocytes. *Cell Tissue Res,* 304**,** 231-6.

SMITH, A. M., RAHMAN, F. Z., HAYEE, B., GRAHAM, S. J., MARKS, D. J., SEWELL, G. W., PALMER, C. D., WILDE, J., FOXWELL, B. M., GLOGER, I. S., SWEETING, T., MARSH, M., WALKER, A. P., BLOOM, S. L. & SEGAL, A. W. 2009. Disordered macrophage cytokine secretion underlies impaired acute inflammation and bacterial clearance in Crohn's disease. *J Exp Med,* 206**,** 1883-97.

SOLLE, M., LABASI, J., PERREGAUX, D. G., STAM, E., PETRUSHOVA, N., KOLLER, B. H., GRIFFITHS, R. J. & GABEL, C. A. 2001. Altered cytokine production in mice lacking P2X(7) receptors. *J Biol Chem,* 276**,** 125-32.

SONG, J., WU, C., ZHANG, X. & SOROKIN, L. M. 2013. In vivo processing of CXCL5 (LIX) by matrix metalloproteinase (MMP)-2 and MMP-9 promotes early neutrophil recruitment in IL-1beta-induced peritonitis. *J Immunol,* 190**,** 401-10.

SOTO, F., GARCIA-GUZMAN, M., GOMEZ-HERNANDEZ, J. M., HOLLMANN, M., KARSCHIN, C. & STUHMER, W. 1996a. P2X4: an ATP-activated ionotropic receptor cloned from rat brain. *Proc Natl Acad Sci U S A,* 93**,** 3684-8.

SOTO, F., GARCIA-GUZMAN, M., KARSCHIN, C. & STUHMER, W. 1996b. Cloning and tissue distribution of a novel P2X receptor from rat brain. *Biochem Biophys Res Commun,* 223**,** 456-60.

SPERLAGH, B., HASKO, G., NEMETH, Z. & VIZI, E. S. 1998. ATP released by LPS increases nitric oxide production in raw 264.7 macrophage cell line via P2Z/P2X7 receptors. *Neurochem Int,* 33**,** 209-15.

SPRENT, J. 1995. Antigen-presenting cells. Professionals and amateurs. *Curr Biol,* 5**,** 1095-7.

STANLEY, E. R., BERG, K. L., EINSTEIN, D. B., LEE, P. S., PIXLEY, F. J., WANG, Y. & YEUNG, Y. G. 1997. Biology and action of colony--stimulating factor-1. *Mol Reprod Dev,* 46**,** 4-10.

STARR, A. E., BELLAC, C. L., DUFOUR, A., GOEBELER, V. & OVERALL, C. M. 2012. Biochemical characterization and N-terminomics analysis of leukolysin, the membrane-type 6 matrix metalloprotease (MMP25): chemokine and vimentin cleavages enhance cell migration and macrophage phagocytic activities. *J Biol Chem,* 287**,** 13382-95.

STOKES, L., SCURRAH, K., ELLIS, J. A., CROMER, B. A., SKARRATT, K. K., GU, B. J., HARRAP, S. B. & WILEY, J. S. 2011. A loss-of-function polymorphism in the human P2X4 receptor is associated with increased pulse pressure. *Hypertension,* 58**,** 1086-92.

STOKES, L. & SURPRENANT, A. 2007. Purinergic P2Y2 receptors induce increased MCP-1/CCL2 synthesis and release from rat alveolar and peritoneal macrophages. *J Immunol,* 179**,** 6016-23.

STOKES, L. & SURPRENANT, A. 2009. Dynamic regulation of the P2X4 receptor in alveolar macrophages by phagocytosis and classical activation. *Eur J Immunol,* 39**,** 986-95.

STOUT, R. D., JIANG, C., MATTA, B., TIETZEL, I., WATKINS, S. K. & SUTTLES, J. 2005. Macrophages sequentially change their functional phenotype in response to changes in microenvironmental influences. *J Immunol,* 175**,** 342-9.

STRIETER, R. M., GOMPERTS, B. N. & KEANE, M. P. 2007. The role of CXC chemokines in pulmonary fibrosis. *J Clin Invest,* 117**,** 549-56.

SUN, H., CHUNG, W. C., RYU, S. H., JU, Z., TRAN, H. T., KIM, E., KURIE, J. M. & KOO, J. S. 2008. Cyclic AMP-responsive element binding protein- and nuclear factor-kappaB-regulated CXC chemokine gene expression in lung carcinogenesis. *Cancer Prev Res (Phila),* 1**,** 316-28.

SUPLAT-WYPYCH, D., DYGAS, A. & BARANSKA, J. 2010. 2', 3'-O-(4-benzoylbenzoyl)-ATP-mediated calcium signaling in rat glioma C6 cells: role of the P2Y(2) nucleotide receptor. *Purinergic Signal,* 6**,** 317-25.

SURESH, A. & SODHI, A. 1991. Production of interleukin-1 and tumor necrosis factor by bone marrow-derived macrophages: effect of cisplatin and lipopolysaccharide. *Immunol Lett,* 30**,** 93-100.

SURPRENANT, A. 1996. Functional properties of native and cloned P2X receptors. *Ciba Found Symp,* 198**,** 208-19; discussion 219-22.

SURPRENANT, A. & NORTH, R. A. 2009. Signaling at purinergic P2X receptors. *Annu Rev Physiol,* 71**,** 333-59.

TABAS, I. & GLASS, C. K. 2013. Anti-inflammatory therapy in chronic disease: challenges and opportunities. *Science,* 339**,** 166-72.

TAKAHASHI, K., NAITO, M. & TAKEYA, M. 1996. Development and heterogeneity of macrophages and their related cells through their differentiation pathways. *Pathol Int,* 46**,** 473-85.

TANAKA, K., CHOI, J., CAO, Y. & STACEY, G. 2014. Extracellular ATP acts as a damage-associated molecular pattern (DAMP) signal in plants. *Front Plant Sci,* 5**,** 446.

TAVIAN, M. & PEAULT, B. 2005. Embryonic development of the human hematopoietic system. *Int J Dev Biol,* 49**,** 243-50.

TAYLOR, A. W. 2009. Review of the activation of TGF-beta in immunity. *J Leukoc Biol,* 85**,** 29-33.

TIAN, M., ABDELRAHMAN, A., WEINHAUSEN, S., HINZ, S., WEYER, S., DOSA, S., EL-TAYEB, A. & MULLER, C. E. 2014. Carbamazepine derivatives with P2X4 receptor-blocking activity. *Bioorg Med Chem,* 22**,** 1077-88.

TONETTI, M., STURLA, L., BISTOLFI, T., BENATTI, U. & DE FLORA, A. 1994. Extracellular ATP potentiates nitric oxide synthase expression induced by

lipopolysaccharide in RAW 264.7 murine macrophages. *Biochem Biophys Res Commun,* 203**,** 430-5.

TORRES, G. E., EGAN, T. M. & VOIGT, M. M. 1999. Hetero-oligomeric assembly of P2X receptor subunits. Specificities exist with regard to possible partners. *J Biol Chem,* 274**,** 6653-9.

TOULME, E., SOTO, F., GARRET, M. & BOUE-GRABOT, E. 2006. Functional properties of internalization-deficient P2X4 receptors reveal a novel mechanism of ligand-gated channel facilitation by ivermectin. *Mol Pharmacol,* 69**,** 576-87.

TRANG, T. & SALTER, M. W. 2012. P2X4 purinoceptor signaling in chronic pain. *Purinergic Signal,* 8**,** 621-8.

TRINCHIERI, G. 2003a. The choices of a natural killer. *Nat Immunol,* 4**,** 509-10.

TRINCHIERI, G. 2003b. Interleukin-12 and the regulation of innate resistance and adaptive immunity. *Nat Rev Immunol,* 3**,** 133-46.

TSUDA, M., SHIGEMOTO-MOGAMI, Y., KOIZUMI, S., MIZOKOSHI, A., KOHSAKA, S., SALTER, M. W. & INOUE, K. 2003. P2X4 receptors induced in spinal microglia gate tactile allodynia after nerve injury. *Nature,* 424**,** 778-83.

ULMANN, L., HIRBEC, H. & RASSENDREN, F. 2010. P2X4 receptors mediate PGE2 release by tissue-resident macrophages and initiate inflammatory pain. *EMBO J,* 29**,** 2290-300.

UNANUE, E. R., BELLER, D. I., CALDERON, J., KIELY, J. M. & STADECKER, M. J. 1976. Regulation of immunity and inflammation by mediators from macrophages. *Am J Pathol,* 85**,** 465-78.

VACCA, F., GIUSTIZIERI, M., CIOTTI, M. T., MERCURI, N. B. & VOLONTE, C. 2009. Rapid constitutive and ligand-activated endocytic trafficking of P2X receptor. *J Neurochem,* 109**,** 1031-41.

VAN DEN STEEN, P. E., WUYTS, A., HUSSON, S. J., PROOST, P., VAN DAMME, J. & OPDENAKKER, G. 2003. Gelatinase B/MMP-9 and neutrophil collagenase/MMP-8 process the chemokines human GCP-2/CXCL6, ENA-78/CXCL5 and mouse GCP-2/LIX and modulate their physiological activities. *Eur J Biochem,* 270**,** 3739-49.

VAN FURTH, R., COHN, Z. A., HIRSCH, J. G., HUMPHREY, J. H., SPECTOR, W. G. & LANGEVOORT, H. L. 1972. The mononuclear phagocyte system: a new classification of macrophages, monocytes, and their precursor cells. *Bull World Health Organ,* 46**,** 845-52.

VAN WILGENBURG, B., BROWNE, C., VOWLES, J. & COWLEY, S. A. 2013. Efficient, long term production of monocyte-derived macrophages from human pluripotent stem cells under partly-defined and fully-defined conditions. *PLoS One,* 8**,** e71098.

VERKHRATSKY, A., KRISHTAL, O. A. & BURNSTOCK, G. 2009. Purinoceptors on neuroglia. *Mol Neurobiol,* 39**,** 190-208.

VERRECK, F. A., DE BOER, T., LANGENBERG, D. M., HOEVE, M. A., KRAMER, M., VAISBERG, E., KASTELEIN, R., KOLK, A., DE WAAL-MALEFYT, R. & OTTENHOFF, T. H. 2004. Human IL-23-producing type 1 macrophages promote but IL-10-producing type 2 macrophages subvert immunity to (myco)bacteria. *Proc Natl Acad Sci U S A,* 101**,** 4560-5.

VOLKMAN, A. 1976. Disparity in origin of mononuclear phagocyte populations. *J Reticuloendothel Soc,* 19**,** 249-68.

WALDO, S. W., LI, Y., BUONO, C., ZHAO, B., BILLINGS, E. M., CHANG, J. & KRUTH, H. S. 2008. Heterogeneity of human macrophages in culture and in atherosclerotic plaques. *Am J Pathol,* 172**,** 1112-26.

WALZ, A., SCHMUTZ, P., MUELLER, C. & SCHNYDER-CANDRIAN, S. 1997. Regulation and function of the CXC chemokine ENA-78 in monocytes and its role in disease. *J Leukoc Biol,* 62**,** 604-11.

WANG, L., JACOBSEN, S. E., BENGTSSON, A. & ERLINGE, D. 2004. P2 receptor mRNA expression profiles in human lymphocytes, monocytes and CD34+ stem and progenitor cells. *BMC Immunol,* 5**,** 16.

WARNY, M., ABOUDOLA, S., ROBSON, S. C., SEVIGNY, J., COMMUNI, D., SOLTOFF, S. P. & KELLY, C. P. 2001. P2Y(6) nucleotide receptor mediates monocyte interleukin-8 production in response to UDP or lipopolysaccharide. *J Biol Chem,* 276**,** 26051-6.

WATANABE, N., SUZUKI, J. & KOBAYASHI, Y. 1996. Role of calcium in tumor necrosis factor-alpha production by activated macrophages. *J Biochem,* 120**,** 1190-5.

WIKTOR-JEDRZEJCZAK, W., BARTOCCI, A., FERRANTE, A. W., JR., AHMED-ANSARI, A., SELL, K. W., POLLARD, J. W. & STANLEY, E. R. 1990. Total absence of colony-stimulating factor 1 in the macrophage-deficient osteopetrotic (op/op) mouse. *Proc Natl Acad Sci U S A,* 87**,** 4828-32.

WILKIN, F., STORDEUR, P., GOLDMAN, M., BOEYNAEMS, J. M. & ROBAYE, B. 2002. Extracellular adenine nucleotides modulate cytokine production by human monocyte-derived dendritic cells: dual effect on IL-12 and stimulation of IL-10. *Eur J Immunol,* 32**,** 2409-17.

WYNN, T. A. & BARRON, L. 2010. Macrophages: master regulators of inflammation and fibrosis. *Semin Liver Dis,* 30**,** 245-57.

WYNN, T. A., CHAWLA, A. & POLLARD, J. W. 2013. Macrophage biology in development, homeostasis and disease. *Nature,* 496**,** 445-55.

XIANG, Z., LV, J., JIANG, P., CHEN, C., JIANG, B. & BURNSTOCK, G. 2006. Expression of P2X receptors on immune cells in the rat liver during postnatal development. *Histochem Cell Biol,* 126**,** 453-63.

YAMAMOTO, K., KORENAGA, R., KAMIYA, A., QI, Z., SOKABE, M. & ANDO, J. 2000. P2X(4) receptors mediate ATP-induced calcium influx in human vascular endothelial cells. *Am J Physiol Heart Circ Physiol,* 279**,** H285-92.

YAMAMOTO, S., SHIMIZU, S., KIYONAKA, S., TAKAHASHI, N., WAJIMA, T., HARA, Y., NEGORO, T., HIROI, T., KIUCHI, Y., OKADA, T., KANEKO, S., LANGE, I., FLEIG, A., PENNER, R., NISHI, M., TAKESHIMA, H. & MORI, Y. 2008. TRPM2-mediated Ca^{2+}influx induces chemokine production in monocytes that aggravates inflammatory neutrophil infiltration. *Nat Med,* 14**,** 738-47.

YEGUTKIN, G. G. 2008. Nucleotide- and nucleoside-converting ectoenzymes: Important modulators of purinergic signalling cascade. *Biochim Biophys Acta,* 1783**,** 673-94.

ZANIN, R. F., BRAGANHOL, E., BERGAMIN, L. S., CAMPESATO, L. F., FILHO, A. Z., MOREIRA, J. C., MORRONE, F. B., SEVIGNY, J., SCHETINGER, M. R., DE SOUZA WYSE, A. T. & BATTASTINI, A. M. 2012. Differential macrophage activation alters the expression profile of NTPDase and ecto-5'-nucleotidase. *PLoS One,* 7**,** e31205.

ZEMKOVA, H., BALIK, A., JINDRICHOVA, M. & VAVRA, V. 2008. Molecular structure of purinergic P2X receptors and their expression in the hypothalamus and pituitary. *Physiol Res,* 57 Suppl 3**,** S23-38.

ZEMKOVA, H., TVRDONOVA, V., BHATTACHARYA, A. & JINDRICHOVA, M. 2014. Allosteric modulation of ligand gated ion channels by ivermectin. *Physiol Res,* 63 Suppl 1**,** S215-24.

ZENG, L., PLANELLES, V., SUI, Z., GARTNER, S., MAGGIRWAR, S. B., DEWHURST, S., YE, L., NERURKAR, V. R., YANAGIHARA, R. & LU, Y.

2006. HIV-1-based defective lentiviral vectors efficiently transduce human monocytes-derived macrophages and suppress replication of wild-type HIV-1. *J Gene Med,* 8**,** 18-28.

ZHANG, X. & MOSSER, D. M. 2008. Macrophage activation by endogenous danger signals. *J Pathol,* 214**,** 161-78.

ZIEGLER-HEITBROCK, H. W. & ULEVITCH, R. J. 1993. CD14: cell surface receptor and differentiation marker. *Immunol Today,* 14**,** 121-5.

ZINEH, I., BEITELSHEES, A. L., WELDER, G. J., HOU, W., CHEGINI, N., WU, J., CRESCI, S., PROVINCE, M. A. & SPERTUS, J. A. 2008. Epithelial neutrophil-activating peptide (ENA-78), acute coronary syndrome prognosis, and modulatory effect of statins. *PLoS One,* 3**,** e3117.

ZSEMBERY, A., BOYCE, A. T., LIANG, L., PETI-PETERDI, J., BELL, P. D. & SCHWIEBERT, E. M. 2003. Sustained calcium entry through P2X nucleotide receptor channels in human airway epithelial cells. *J Biol Chem,* 278**,** 13398-408.